University of Alberta
Department of Civil &
Environmental Engineering

Structural Engineering Report No. 280

Strength of Welded Joints Under Combined Shear and Out-of-Plane Bending

by

Yu Kay Kwan

and

Gilbert Y. Grondin

November, 2008

Strength of Welded Joints under Combined Shear and Out-of-Plane Bending

by

Yu Kay Kwan
and
Gilbert Y. Grondin

Structural Engineering Report 280

Department of Civil and Environmental Engineering
University of Alberta

Edmonton, Alberta

November 2008

ABSTRACT

The test results from three experimental programs reveal that the current design equations in the North American structural steel design standards (CSA-S16-01 and AISC Specifications) for eccentrically loaded welds can be very conservative for joints with out-of-plane eccentricity. An alternative approach for the calculation of welded joint strength is proposed, and the resulting strength predictions are compared to the current design standards.

A total of 14 strength prediction models were evaluated. A reliability analysis was conducted to assess the current North American design equations for welded joints subjected to combined shear and out-of-plane bending. The model consisting of a modified version of the instantaneous center of rotation approach developed by Dawe and Kulak (1972) was found to provide the target safety index of 4.27 with a resistance factor of 0.67. A simple closed form model was developed and is proposed as a substitute for the more complex instantaneous center of rotation model. The proposed closed form model provides a safety index of 4.0 with a resistance factor of 0.67.

ACKNOWLEDGMENTS

The project presented in this report is part of a collaborative project between the University of Alberta and the University of California, Davis. Funding for the part of the project presented here was provided by the American Institute of Steel Construction and the Natural Sciences and Engineering Research Council of Canada (NSERC). The feedback and comments provided by Dr. Amit Kanvinde of UC Davis are acknowledged with thanks.

TABLE OF CONTENTS

LIST OF TABLES

LIST OF FIGURES

LIST OF SYMBOLS

A_{throat}	-	Theoretical throat area based on average measured leg dimensions
$A_{,fracture}$	-	Throat area based on average measured fracture throat size
A_w	-	Weld throat area
a	-	Load eccentricity ratio
COV	-	Coefficient of variation
C'	-	Coefficient tabulated in Appendix D
D	-	Weld size
d	-	Weld (leg) size
e	-	Load eccentricity
F_u	-	Ultimate strength of plate or weld
F_y	-	Yield strength of plate or weld
$f(\rho)$	-	Normalized force in a weld element
H_B	-	Normal force in the compression zone
L	-	Characteristic length of weld group
M_p	-	Plastic moment
MTD	-	Measured throat dimension
P_{max}	-	Experimentally observed maximum strength
P_m	-	Load carrying capacity of joint in flexural compression zone
P_v	-	Shear capacity of fillet weld in flexural compression zone

P_{ult}, P_u, P_r	-	Predicted maximum strength
$P_{u,fract}$	-	Predicted maximum strength based on fracture surface
P_0, P_{ro}	-	Resistance of joint with no eccentricity
P_{r53}	-	Resistance of joint with $a/Q = 0.53$
$P_{0.4}$	-	Resistance of joint with $a = 0.40$
Q	-	Non-dimensional factor
Q_u	-	Non-dimensional factor equals to the ratio of the base metal strength to the weld metal strength
R	-	Force in a weld element
R_u	-	Normalized location of the center of rotation (neutral axis)
R_{ult}	-	Ultimate force (predicted capacity) of a weld element
R_0	-	Resultant force in a weld element loaded longitudinally ($\theta = 0^o$)
R_θ	-	Load capacity of the fillet weld when loaded at an angle θ to the weld axis
$(R_i)_v$	-	Vertical force component
$(R_i)_h$	-	Horizontal force component
r_o	-	Distance between instantaneous center and the longitudinal axis of the line of weld
s_1, s_2	-	Fillet weld leg dimensions
t	-	Plate bearing thickness (root notch length)
V_B	-	Vertical force in the compression zone

V_G	-	Coefficient of variation for the measured-to-nominal weld Dimension
V_{M1}	-	Coefficient of variation for the measured-to-nominal ultimate tensile strength of the filler metal
V_{M2}	-	Coefficient of variation for the measured-to-predicted ultimate shear strength of the filler metal
V_P	-	Coefficient of variation for the test-to-predicted weld Capacity
V_p	-	Plastic shear
V_R	-	Coefficient of variation for the resistance of the weld
V_r	-	Measured capacity of the transverse weld
V_θ, V_0	-	Ultimate strength of a fillet weld loaded in shear at θ and $\theta = 0°$, respectively
w	-	Weld segment leg size
X_u, F_{EXX}	-	Ultimate tensile strength of weld metal
y_o	-	Distance of neutral axis to the extreme compression fibre
α_R	-	Coefficient of separation
β	-	Safety index (reliability index)
Δ	-	Elongation (deformation) of weld
Δ_f	-	Fracture elongation of weld; Observed shear leg weld deformation at fracture
Δ_{max}	-	Ultimate deformation of weld element
Δ_u	-	Elongation of weld at ultimate strength; Average normalized extreme tension end weld deformation
ε	-	Average true strain

θ	-	Angle between weld axis and loading direction
λ	-	Regression coefficient used to characterize fillet weld Response
μ	-	Regression coefficient used to characterize fillet weld response
ρ	-	Normalized weld deformation of the weld element
ρ_G	-	Bias coefficient for the theoretical weld dimension
ρ_{M1}	-	Bias coefficient for the ultimate tensile strength of the filler metal
ρ_{M2}	-	Bias coefficient for the ultimate shear strength of the filler metal
ρ_P	-	Mean test-to-predicted weld capacity
ρ_R	-	Bias coefficient for resistance of the weld
σ_u	-	Tensile strength of the plate
σ_y	-	Static yield strength of the plate
τ_u	-	Measured ultimate shear strength for a longitudinal weld
ϕ	-	Resistance factor

Chapter 1

Introduction

1.1 GENERAL

Fillet welded joints are widely used in civil engineering construction due to their relatively high strength and the ease of surface preparation required for such welds. In many joint configurations used in practice in-plane or out-of-plane eccentricity is unavoidable, creating more complex stress conditions in the joint than concentrically loaded joints where the welds are generally subjected to shear in only one direction. Design methods that account for load eccentricity on welded joints have been developed for both in-plane and out-of-plane eccentricity (Dawe and Kulak, 1974; Tide, 1980).

In welded joints that are subjected to in-plane eccentricity (Figure 1.1a) the weld is free to deform over its entire length. In the case of welds subjected to out-of-plane eccentricity as shown in Figure 1.1b, the part of the weld in the compression zone is not free to deform because of direct bearing between the connected plates. This fundamental difference between the in-plane and out-of-plane eccentric loading has been recognized in the derivation of an ultimate limit state formulation for the strength of eccentric joints (Dawe and Kulak, 1974). The method of instantaneous centre, originally developed for bolted joints and welded joints with in-plane eccentricity, was modified for out-of-plane eccentricity to account for the bearing of the plate in the compression zone at ultimate load. The method proposed by Dawe and Kulak was adopted in the CISC Handbook of Steel Construction for the versions pre dating the ninth (current) edition. A closed form procedure proposed by Beaulieu and Picard (1985), which was adjusted to correlate well with the previous design tables, was used to derive the current design table. The approach used in the AISC Steel Construction Manual (2005) treats the joint with out-of-plane eccentricity as a joint with in-plane eccentricity, thus ignoring load transfer by bearing on the compression side of the joint (Tide, 1980).

1.2 BACKGROUND

Eccentrically loaded fillet-welded connections with combined shear and out-of-plane bending have received limited attention. An experimental investigation by Dawe and Kulak (1972) included eight test specimens that consisted of a wide-flange section with its end welded to an end plate by fillet welds along the outer side of each flange. The test configuration involved loading the wide flange sections in minor axis bending to determine the joint strength. The key variables investigated included the length of weld, the eccentricity of the load and the size of the wide flange section. Two nominal weld lengths (203 mm (8 in.) and 305 mm (12 in.)) and four load eccentricities (ranging from 203 mm (8 in.) to 508 mm (20 in.)) were considered. Since the specimens were loaded in the minor axis orientation, the effective bearing width was twice the flange thickness of the wide-flange section. Using this interpretation, five nominal bearing widths (ranging

from 21.8 mm (0.86 in.) to 38.6 mm (1.52 in.)) were investigated. All specimens were fabricated from ASTM A36 steel and used 1/4 in. welds deposited with AWS E60 electrodes.

An experimental program was later conducted by Warren (1984) and Beaulieu and Picard (1985) and included 24 fillet welded plate connections loaded eccentrically out-of-plane. The main variables investigated in this study included the weld size (nominally 6, 8, 10 and 12 mm) the load eccentricity (ranging from 75 mm to 375 mm) and the bearing width (20 mm and 40 mm). All specimens were fabricated from ASTM A36 steel, and the welds (all approximately 250 mm long) were made with AWS E480 (E70) electrodes. Weld failure, plate rupture and plate buckling were the various failure modes observed in the experimental program.

A series of tests on 60 fillet weld cruciform shape specimens were recently tested with out-of-plane eccentricity at UC Davis (Gomez *et al*., 2008). All specimens were fabricated using ASTM A572 Grade 50 steel and the test welds were made with E70 (480) flux cored electrodes. The parameters examined experimentally were: root notch length (31.4 mm (1.25 in.), 44.5 mm (1.75 in.) and 63.5 mm (2.50 in.)), weld metal toughness classification, magnitude of eccentricity (76.2 mm (3 in.), 139.7 mm (5.5 in.) and 216 mm (8.5 in.)) and nominal weld size (8 mm (5/16 in.) and 12 mm (1/2 in.)).

In addition to the experimental programs, joint strength prediction methods were developed. Dawe and Kulak (1972) proposed a method based on the method of instantaneous center of rotation, accounting for moment transfer through plate bearing and weld tension. The model was later adopted by CISC for design, but a strength reduction factor was added to the model in addition to the resistance factor used for design of concentrically loaded welded joints. Although the model proposed by Dawe and Kulak is a rational and comprehensive approach, it involves an iterative procedure that makes it difficult to implement without the use of a computer program or special design tables. Simpler, closed form solutions were proposed by Neis (1980), but these models never received broad acceptance. Picard and Beaulieu (1991) proposed a closed form design model similar to one of the models proposed earlier by Neis and expanded to account for joints with small eccentricity. This approach was recently adopted by the CISC in the ninth edition of the Handbook of Steel Construction.

The earlier work of Dawe and Kulak was based on load versus deformation behaviour for fillet welds derived from small weld specimen tests conducted by Butler and Kulak (1971). Later, Lesik and Kennedy (1990) proposed a different set of equations to describe the fillet weld ultimate capacity, deformation and response under loading applied at various orientations.

The current design tables for welded joints under combined shear and out-of-plane moment used in Canadian design practice is based on the closed-form solution proposed by Picard and Beaulieu (1991), which is based on the load-deformation relationships of Lesik and Kennedy (1990). The design tables used by the American Institute of Steel Construction (AISC) are based on the instantaneous centre of rotation method proposed

by Butler *et al.* (1972) along with the load-deformation relationship derived by Lesik and Kennedy (1990).

Prior to the test results from Gomez *et al*. (2008), the experimental research on welded joints subjected to combined shear and out-of-plane bending was limited and, hence, the strength prediction models could not be evaluated over a wide range of parameters. Therefore, several assumptions were made to arrive at analytical models using weld load versus deformation relationships derived from tests on concentrically loaded lapped specimens. As a result, none of the design methods consider the potentially detrimental effect of the root notch existing between two fillet weld lines on the strength and ductility of the welds. The effect of other parameters such as plate thickness, weld dimension, load eccentricity, the ratio of load eccentricity to weld length and weld metal toughness must also be investigated. In order to address these issues an investigation of the effect of the above parameters will be conducted using the results from three test programs. The applicability of the current design standards for joints with out-of-plane eccentricity will be assessed using a reliability analysis. Such an assessment was not conducted in the earlier research of Dawe and Kulak (1972) and Beaulieu and Picard (1985).

1.3 OBJECTIVES AND SCOPE

The objectives of this study are to:

1. collect and document available test data from welded joints loaded under combined shear and out-of-plane bending;
2. investigate the effects of geometric parameters and toughness requirement on the strength of fillet welds loaded perpendicular to the root notch;
3. use the test results from available test programs to assess the existing strength prediction models, including the model implemented in the CISC Handbook of Steel Construction and the AISC Manual of Steel Construction;
4. conduct a reliability analysis to assess the level of safety of the most promising design models and determine the resistance factor required to provide the desired level of safety; and
5. make recommendations for a design approach that is both easy to implement and offers the required level of safety.

Test results from three experimental programs (Dawe and Kulak, 1972, Beaulieu and Picard, 1985 and Gomez *et al*., 2008) are compared with capacities predicted using existing analytical models (Butler and Kulak, 1971; Dawe and Kulak, 1972; Neis, 1980; Lesik and Kennedy, 1990 and Picard and Beaulieu, 1991) and the current design table in the CISC handbook of steel construction (CISC, 2006). A reliability analysis was conducted to assess the level of safety and resistance factor provided by the current design tables in CISC design handbook. Upon examining all analytical models, a new design model will be developed if they are found to be inadequate.

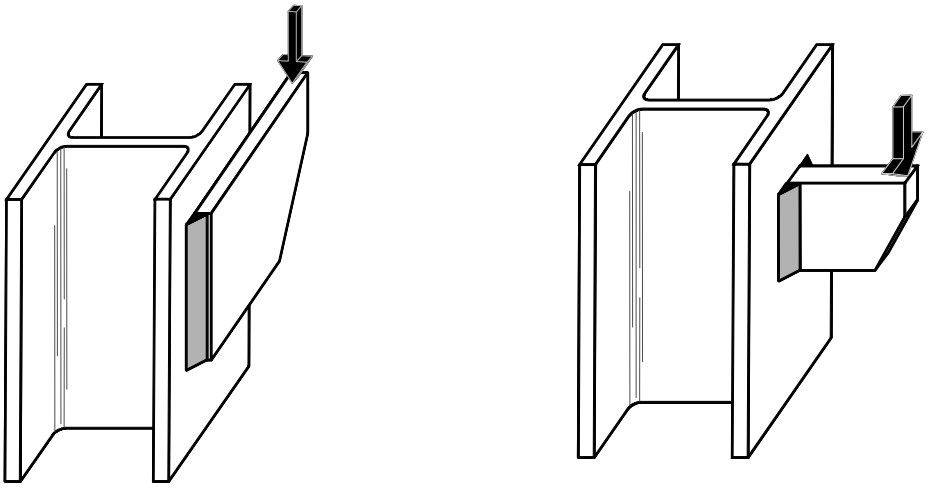

(a) In-plane eccentricity (b) Out-of-plane eccentricity

Figure 1.1 – Eccentrically loaded welded joints

Chapter 2

Literature Review

2.1 INTRODUCTION

Before Limit States Design (LSD) rules were adopted, the design of eccentrically loaded welded joints was based on a simple elastic analysis where it was assumed that the weld element furthest from the centre of gravity of the weld group controlled the capacity of the welded joint. Although this elastic analysis approach was expedient, it was not appropriate for a LSD design approach since it represented only the first yield of the weld group rather than its ultimate capacity. With the introduction of limit states design, new design methods that attempted to predict the ultimate capacity of the weld group were introduced. This chapter presents a brief summary of various analytical models that have been proposed since the early 1970's for the prediction of the ultimate capacity of welded joints with out-of-plane eccentricity. A detailed development of these analytical models is presented in Chapter 4. First, a review of available test data on eccentrically loaded welded joints is presented.

2.2 BEHAVIOUR OF FILLET WELDS UNDER LOAD

2.2.1 Butler and Kulak (1971)

Early investigations on transverse fillet welds (Ligtenburg, 1968) indicated that transverse fillet welds in tension (where the loading is applied perpendicular to the weld axis) were approximately 60% stronger than longitudinal fillet welds (welds where the line of axis of the applied load is parallel to the axis of the weld). Similar findings have been reported by others (Higgins and Preece, 1969; Clark, 1971).

Butler and Kulak (1971) conducted a series of 23 tests on specimens with 6.35 mm (1/4 in.) fillet welds loaded in tension at 0^o, 30^o, 60^o and 90^o to the weld axis. The purpose of their test was to establish the effect of load direction behaviour to the load-deformation response of fillet welds. The test specimens were prepared using E60XX electrodes, CSA-G40.12 steel plate and the shielded metal arc welding (SMAW) process, with a specified yield stress of 300 MPa (44 ksi) and a minimum tensile strength of 430 MPa (62 ksi). Based on the test results, Butler and Kulak concluded that the increase in loading angle improved the strength yet reduced the weld deformation capacity. Hence, an empirical equation was developed to predict the load capacity as a function of the direction of the applied load to the weld axis,

$$R_{ult} = \frac{10 + \theta}{0.92 + 0.0603\theta} \qquad [2.1]$$

where R_{ult} is the predicted capacity of a fillet weld of orientation θ (expressed in degrees) given in kips/inch. Another empirical equation was also proposed to predict the loads versus deformation response for various loading angles. This equation is described as the follows:

$$\Delta_{\max} = 0.225(\theta + 5)^{-0.47} \quad [2.2]$$

$$R = R_{ult}(1 - e^{-\mu\Delta})^{\lambda} \quad [2.3]$$

$$\mu = 75e^{0.0114\theta} \quad [2.4]$$

$$\lambda = 0.4e^{0.0146\theta} \quad [2.5]$$

Equation 2.2 defines the ultimate deformation of fillet welds (in inches) as a function of the angle θ between the line of action of the applied force and the axis of the weld. The relationship between the weld force R (kips/inch) and deformation Δ is given by Equation 2.3. The constants μ and λ are regression coefficients used to fit Equation 2.3 to test data.

2.2.2 Lesik and Kennedy (1990)

Lesik and Kennedy (1990) extended the work of Miazga and Kennedy (1989). They formulated a simplified version of the strength equation by using the method of instantaneous center (IC) of rotation to calculate the strength of fillet welds loaded eccentrically in-plane in various directions and proposed a load versus deformation relationship for welds loaded at an angle θ to the axis of the weld of the following form:

$$R_{\theta} = 0.67 X_u A_w \left(1.0 + 0.5\sin^{1.5}\theta\right) f(\rho) \quad [2.6]$$

$$\frac{\Delta_u}{d} = 0.209(\theta + 2)^{-0.32} \quad [2.7]$$

$$\frac{\Delta_f}{d} = 1.087(\theta + 6)^{-0.65} \quad [2.8]$$

$$f(\rho) = 8.234\rho; \quad 0 < \rho \le 0.0325 \quad [2.9]$$

$$f(\rho) = -13.29\rho + 457.32\rho^{\frac{1}{2}} - 3385.9\rho^{\frac{1}{3}} + 9054.29\rho^{\frac{1}{4}} - 9952.13\rho^{\frac{1}{5}} + 3840.71\rho^{\frac{1}{6}}; \quad \rho > 0.0325 \qquad [2.10]$$

$$\rho = \frac{\Delta}{\Delta_u} \qquad [2.11]$$

where in Equation 2.6, R_θ is the load capacity of the fillet weld when loaded at an angle θ to the weld axis, A_w is the weld area calculated at the throat, X_u is the nominal tensile strength of the filler metal and ϕ is the resistance factor. The leading constant 0.67 is the shear stress transformation factor adopted in S16-01. This constant is taken as 0.60 in the AISC LRFD specification (AISC, 2005). This equation represents an empirical relationship between the angle of the load and the weld strength and it is shown to have a good agreement with the theoretical relationship developed by Miazga and Kennedy. It gives 50% higher prediction on weld strength when the specimen is subjected to a load in the longitudinal direction than in the transverse direction. Equation 2.7 and Equation 2.8 predict the deformations of the fillet weld at ultimate capacity and fracture, respectively. The deformations have been normalized by the weld size, *d*. Equation 2.9 and Equation 2.10 are used to predict the variation of load as a function of normalized deformation, ρ, taken as the ratio of weld deformation, Δ, to the ultimate deformation, Δ_u, obtained from Equation 2.7. The load versus deformation relationship described by Equations 2.9 and 2.10 was obtained using a nonlinear regression analysis of test data. This work of Lesik and Kennedy was recently confirmed by Callele *et al*. (2005).

Figure 2.1 presents the comparison of load deformation curves of specimens loaded at varies angles predicted by Butler & Kulak (1971) and Lesik & Kennedy (1990). When comparing the weld strength of specimens loaded at each angle, the predictions by Butler and Kulak are about 50 percent higher than using the model proposed by Lesik and Kennedy. Figure 2.2 R_θ/R_o for the three different angles of loading predicted by Butler & Kulak and Lesik & Kennedy. By taking the ratio of the weld strength at an angle θ to the strength of a longitudinal weld ($\theta = 0^o$), similar predictions are observed from the two models. Note that both models show that the increase in strength results in a reduction of ductility as the loading direction changes from longitudinal ($\theta = 0^o$) to transverse ($\theta = 90^o$).

2.3 EXPERIMENTAL PROGRAMS ON JOINTS LOADED WITH OUT-OF-PLANE ECCENTRICITY

2.3.1 University of Alberta (Dawe and Kulak, 1972)

A series of eight test specimens consisting of full-size eccentricity loaded fillet weld connections were tested by Dawe and Kulak (1972) to investigate the behaviour of weld groups subjected to shear and out-of-plane bending. The test results were used to validate

an analysis procedure presented in section 2.2. Each test specimen was made of a wide flange section with a 12.7 mm (1/2 in.) load plate welded to one end. The test end of the specimen was attached to a 19.1 mm (3/4 in.) reaction plate by one line of a fillet weld along the outer side of each flange. The reaction plate of the test specimen was bolted to the flange of a stub column. A vertical load was then applied to the test specimen through the load plate until failure of the welded joint.

The test variables were: length of weld, load eccentricity and thickness of the connected plate. The nominal weld length for the first six specimens was approximately 203.2 mm (8.0 in.) and the load eccentricity and the wide flange depth varied from 203.2 mm to 508.0 mm (8 in. to 20 in.) and 13.2 mm to 19.3 mm (0.52 in. to 0.76 in.), respectively. The weld length for the last two specimens was increased to 304.8 mm (12 in.) and the plate thickness remained constant at 15.7 mm (0.62 in.). The load eccentricity was varied from 381.0 mm (15 in.) and 508.0 mm (20 in.), resulting in eccentricity ratios (ratio of load eccentricity to weld length) from 1.03 to 2.56. The steel used in the connections was ASTM A36 and all test welds were made with E60XX shielded metal arc electrodes with nominal leg dimension of 6.34 mm (1/4 in.). To ensure weld uniformity throughout the test program, all welding on the specimens was performed by the same welder using electrodes from the same lot. The weld returns on the specimens were later removed to ensure uniform weld lengths. No filler metal material tests were conducted to determine the strength of the weld metal.

A model was developed to predict the strength of eccentrically loaded weld groups that are not free to rotate in the compression zone of the connection. A comparison of the predicted welded joint capacities with the test results indicated that their proposed model predicted the test capacity much more reliably than the elastic models in prevalent use at that time.

2.3.2 Université Laval (Beaulieu and Picard, 1985; Werren, 1984)

Werren (1984) and Beaulieu and Picard (1985) conducted a test program to expand the earlier work of Dawe and Kulak to include test specimens with smaller eccentricity ratios (0.3 to 1.5) than those investigated by Dawe and Kulak. Their experimental program included the testing of 24 specimens. The specimens tested were made up of assemblies consisting of a reaction column with a rectangular plate bracket at each end, representing a total of 24 eccentrically loaded plate connections. The specimens were fabricated using plates with thickness either 20 mm (0.788 in.) or 40 mm (1.576 in.). The weld length, L, used in each specimen was 250 mm (10 in.) and load eccentricities, e, were in the range of 75 mm to 375 mm (3 in. to 15 in.) corresponding to eccentricity ratios, a, of 0.3 and 1.5, respectively. Nominal fillet weld sizes of 6 mm (1/4 in.) and 12 mm (7/16 in.) were used for specimens with plate thickness of 20 mm (0.788 in.) (Type A specimens). Type B specimens consisted of plate thickness of 40 mm (1.576 in.) and nominal fillet weld sizes of 8 mm (5/16 in.) and 10 mm (3/8 in.). The grade of steel used for the plates was not identified, but the results of coupon tests were reported.

In addition to tests on joints with eccentric shear, double lapped splices where tested to determine the strength of welds loaded transverse to the weld axis and parallel to the

weld axis. The test specimens made use of 6 mm (1/4 in.) welds of 480 MPa (70 ksi) nominal strength and were used to confirm the load versus deformation relationships proposed by Butler and Kulak. No direct material tests were conducted on the weld metal.

The test results were compared with the theoretical ultimate loads obtained from the methods by Dawe and Kulak (1972) and Neis (1980). It is demonstrated that the method of instantaneous centre proposed by Dawe and Kulak was accurate for any value of load eccentricity as long as the welds are continuous all around the welded plate. One of the models proposed by Neis was found to be accurate for an eccentricity ratio of greater than 0.5. For smaller values of load eccentricity, it was found that the same model was accurate as long as a limit on the compression stress of 0.85 times the material yield strength was adopted. For values of $F_y\, t/X_u\, D$ smaller than 1.5, the plate was found to be the critical element of the connection.

2.3.3 University of California, Davis (Gomez *et al.*, 2008)

A total of 60 tests on welded joints under combined shear and out-of-plane bending were conducted at UC Davis (Gomez *et al.,* 2008). The experimental program comprised twenty cruciform specimens replicated three times each. All steel plates used for the tests were ASTM A572 Grade 50 steel. The test welds, prepared with E70XX (480XX) electrodes, had two nominal leg dimensions, namely, 12.7 mm (1/2 in.) and 7.9 mm (5/16 in.). The eccentricity in each specimen was designed to be different and it was achieved by varying the length of the test specimens. The test specimens were prepared with the combination of the following test variables: plate thicknesses of 31.8, 44.5 and 63.5 mm (1.25 in., 1.75 in., 2.5 in.), load eccentricities of 76.2, 139.7 and 215.9 mm (3 in., 5.5 in., 8.5 in.) and two filler metals were selected: E70T-7 (no toughness rating) and E70T7-K2 (toughness rated as defined by AWS A5.29 (AWS, 2005)). All welding was performed using the flux cored arc welding (FCAW) process. Three weld passes were used for the 12.7 mm (1/2 in.) welds, while only one pass was used for the 7.9 mm (5/16 in.) welds. The specimens were tested by three-point bending under continuous monotonic loading until failure.

The results of the experimental program indicated that the strength and ductility of welded joints under combined shear and out-of-plane bending is not significantly affected by the root notch length.

2.4 THEORETICAL STUDIES ON ECCENTRICALLY LOADED WELDED JOINTS

A number of theoretical models have been proposed for the prediction of the strength of welded joints subjected to a combination of shear and out-of-plane eccentricity. These models are briefly reviewed in the following. A detailed description of each model is presented in Chapter 4.

2.4.1 Butler, Pal and Kulak (1972)

A series of 13 tests were conducted by Butler, Pal and Kulak (1972) on eccentrically loaded fillet welded connections to study the behaviour of weld groups subjected to a combination of direct shear and moment. Based on the test results, the researcher developed the method of instantaneous center of rotation. It is a theoretical method to predict the ultimate capacity of eccentrically loaded welded connections in which the weld is free to deform throughout its depth. This method contains the parameters of the direction of the applied load and the actual load-deformation response of elemental lengths of the fillet weld. The following assumptions had been made for predicting the ultimate capacities of a fillet welded connection that is eccentrically loaded:

1. All the segments in the weld group rotate about an instantaneous centre of rotation.
2. The deformation which occurs at any point in the weld group varies linearly with the distance from the instantaneous centre and acts in a direction perpendicular to a radius from that point.
3. The ultimate capacity of a connection is reached when the ultimate strength and rupture deformation of any element of weld are reached.
4. The ultimate strength of a fillet weld subjected to a tension-induced shear is equivalent to an identical weld loaded in compression-induced shear.
5. The line of action of the load is parallel to the principal axis of the weld group.

2.4.2 Dawe and Kulak (1972)

Dawe and Kulak (1972) proposed an iterative procedure for determining the ultimate strength of welded joints with out-of-plane eccentricity based on the method of instantaneous centre of rotation earlier developed by Crawford and Kulak (1971) for bolted connections and adapted by Butler, Pal and Kulak (1972) for welded joints with in-plane eccentricity. The empirical relationships of the load versus deformation response of individual weld elements as proposed by Butler and Kulak (1971) were adopted. The approach proposed by Dawe and Kulak is based on the following assumptions:

1. The ultimate capacity of a connection is reached when a critical weld element reaches its ultimate deformation.
2. The load-induced resisting force of each weld element acts through the center gravity of that element.
3. The deformation of each weld element varies linearly with its distance from the instantaneous center and takes place in a direction perpendicular to its radius of rotation.
4. The connecting plates in the compression zone of the connection are in direct bearing at the time when the ultimate load is reached.
5. Although Dawe and Kulak investigated various bearing stress distributions in the compression zone, a linearly variable bearing stress distribution with a maximum

stress equal to the yield strength of the plates in bearing was proposed. The proposed model was validated by comparison of predicted strength with the measured capacity of test specimens. A modified version of this model was later adopted by the Canadian Institute of Steel Construction for design of welded joints subjected to shear and out-of-plane bending.

2.4.3 Neis (1980)

Neis (1980) proposed simplified closed-form models in an attempt to find a suitable replacement for the more complex model proposed by Dawe and Kulak (1972). Seven models were developed; all with the maximum stress in the weld assumed to have reached the rupture stress at the extreme fibre on the tension side of the welded joint. The weld capacity was taken as the capacity of a transverse weld ($\theta = 90^o$) as predicted by the model proposed by Butler and Kulak (1971). Various stress distributions were investigated, both in the tension and in the compression zones of the connection.

2.4.4 Beaulieu and Picard (1985)

After a review of the simplified models proposed by Neis (1980), Beaulieu and Picard proposed a simple model that gave good correlation with the more complex model of Dawe and Kulak and the test data from Dawe and Kulak and new test data derived as part of their research program. Although the original prediction model proposed by Beaulieu and Picard was based on the weld metal strength predicted by Butler and Kulak (1971), the proposed model was later adapted to the weld strength predicted by Lesik and Kennedy (1990) (Picard and Beaulieu, 1991). This latter model was adopted by the Canadian Institute of Steel Construction for their current edition of the Steel Design Handbook (CISC, 2006).

2.5 CRUCIFORM JOINTS

The analytical methods presented in the previous section were all based on the assumption that the steel toughness (base metal and weld metal) is adequate to develop the same weld strength in joints with in-plane eccentricity as joints with out-of-plane eccentricity where the primary stress is applied perpendicular to the root notch. However, a study by Ng *et al*. (2002) featured a limited number of specimens with the root notch perpendicular to the direction of loading. A comparison of test results from cruciform specimens with test results from double lapped splice specimens with transverse welds indicated that the strength of fillet welds is affected slightly by the root notch, whereas the ductility is significantly reduced. With reference to welded joints with out-of-plane eccentricity, tests indicate that the effect of the weld root notch on all aspects of the load versus deformation response maybe critical for the accurate characterization of the strength of joints, especially joints subjected to out-of-plane bending. However, this observation is not supported by recent tests conducted at UC Davis (Gomez *et al*., 2008).

2.6 CONCLUSIONS

A limited number of test results for welded joints with shear and out-of-plane bending have been conducted by two different sources. Neither sources reported the filler metal material properties. The material properties in both cases were assumed to be similar to those reported by Butler and Kulak (1971) who reported the results of tests conducted on lapped joints to determine the effect of load direction on the strength of fillet welds. A comparison of the weld strength material model proposed by Butler and Kulak (1971) with later results from Lesik and Kennedy (1990) indicated that the model from Butler and Kulak predicts significantly higher strength for all load orientations. The ratio of weld strength at various angles of loading to the longitudinal weld strength is similar for the Butler and Kulak and the Lesik and Kennedy models.

An examination of several prediction models has indicated that although the model presented by Dawe and Kulak (1972) is the most rational since it accounts directly for the load versus deformation behaviour of the welds, its complexity makes it difficult to implement in design practice. Several closed form models have been proposed as a replacement to the iterative procedure of Dawe and Kulak. These models present the distinct advantage of being simple to use. The work or Dawe and Kulak (1972) and Beaulieu and Picard (1985) was not accompanied by a reliability analysis to determine the level of safety provided by their design procedures. A reliability analysis of the current design approaches is desirable to determine whether the level of safety is adequate.

In order to evaluate properly the various strength prediction models for welded joints subjected to combined shear and out-of-plane bending, a direct characterization of the weld metal used for the preparation of the welded joints is required. The effect of root notch size on strength and ductility should be further investigated. The work described in the following includes a review of a recent investigation of the root notch size effect on cruciform tension joints as well as joints loaded under combined shear and out-of-plane bending. The material properties of the weld metal used in these tests were established from all-weld metal coupon tests. The entire test data collected in this chapter will be used to evaluate several strength prediction models proposed by various researchers and modifications of these strength prediction models.

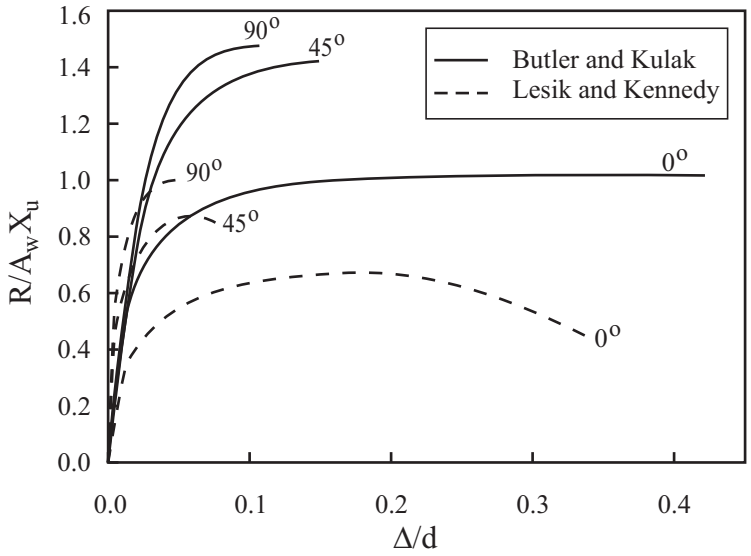

Figure 2.1 – Load versus deformation curves for fillet welds
(Modified from Butler and Kulak 1971 and Lesik and Kennedy 1990)

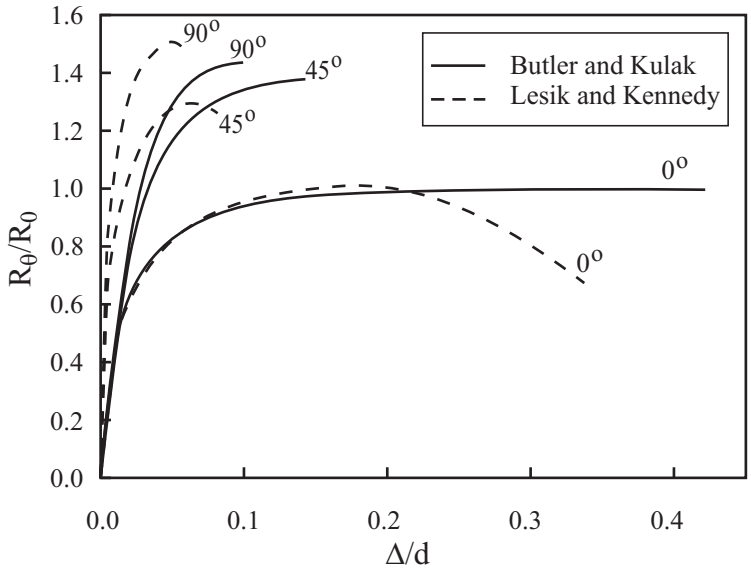

Figure 2.2 – Normalized load verse deformation curves for fillet welds
(Modified from Butler and Kulak 1971 and Lesik and Kennedy 1990)

Chapter 3

Collection of Test Data

3.1 INTRODUCTION

The primary objective of this chapter is to present test data on welded joints loaded with out-of-plane eccentricity. Three main sources of test results are reviewed, namely, a test program by Dawe and Kulak (1972), a test program by Beaulieu and Picard (1985) and a recent test program by Gomez *et al.* (2008). Researchers from some of the test programs have reported the welding electrode strength designation used for the preparation of the test specimens, but have not conducted ancillary tests to determine the actual weld metal strength. It is therefore important to conduct a review of the literature to collect information about the strength distribution for the grades of filler metal used in these test programs so that the strength of the weld metal for the tested specimens can be estimated more accurately. This chapter first presents a review of ancillary test results for various grades of welding electrodes. The second part of the chapter reports test results on welded joints loaded with out-of-plane eccentricity.

3.2 ANCILLARY TEST RESULTS

The actual tensile strength of the AWS E60 (E410) weld electrode used for the preparation of Dawe and Kulak's (1972) specimens was not reported. Weld strength data for AWS E60 (E410) electrode were therefore collected from various sources and are presented in Table 3.1. Data were obtained from three sources, although the majority of the data (94 %) was obtained from a single source. The mean strength of the data collected is 462 MPa and the coefficient of variation, *COV*, is 0.063.

The 1985 test program by Beaulieu and Picard on welded joints with out-of-plane eccentricity made use of AWS E70 (E480) welding electrode. Although a series of lapped splice specimens with transverse and longitudinal welds was tested, no direct measurement of the weld metal strength was reported. Therefore, weld strength data for E70 (E480) electrode was collected and a summary of the data set is presented in Table 3.2. A comparison between Tables 3.1 and 3.2 indicates that the measured to nominal strength ratio for E60 (E410) electrode is slightly lower than for E70 (E480) electrode.

In order to correlate weld metal test data to the test data from Beaulieu and Picard (1985), only the weld electrodes that would have been available on the market during their research period was considered, namely, the tensile strength of welding electrodes tested in the period from 1978 to 1987 are taken into consideration. For this set of data the mean ratio of measured to nominal tensile strength is approximately 1.154 and the coefficient of variation is 0.090. The weld metal tensile strength used in the calculation of joint capacity was therefore taken as 552 MPa.

Alternatively, the tensile strength of the weld metal can be predicted by comparing the test results of tests on joints with transverse welds and joints with longitudinal welds reported by Beaulieu and Picard (1985) with similar tests conducted at the University of Alberta by Ng *et al.* (2002) and Callele *et al.* (2005), for which all-welded metal coupon tests were conducted. The measured tensile strength of weld for Beaulieu and Picard can be predicted based on a relationship establish by the ratios of predicted tensile strength on transverse weld specimens and the measured tensile strength on the all-welded coupon test specimens.

The tensile strength of filler metal can be predicted from the results of tests on joints with a transverse weld, X_u,

$$X_u = \frac{V_r}{(0.67)(1.5)A_w L} \qquad [3.1]$$

Where V_r is the measured capacity of the transverse weld, A_w is the theoretical throat area calculated from the specified or measured leg size, and L is the length of weld. Based on equation 3.1, the predicted tensile strength of the filler metal used for the test joints with transverse weld tested by Beaulieu and Picard (1985) and by Ng *et al*. (2002) are 759 MPa (7.9 mm weld sizes) and 903 MPa (6.4 and 12.7 mm weld sizes), respectively. It should be noted that the predicted tensile strength from the latter is calculated respective to the average of two weld sizes. The mean measured tensile strength for 32 all-weld metal coupons tested at University of Alberta in the first four phases of this program is 552 MPa. Assuming that the same strength ratio exists for the all-weld metal coupons as for the transverse weld specimens the filler metal strength for the test program presented by Beaulieu and Picard (1985) is estimated to be 463 MPa.

Four all-weld metal coupons (two from E70T7-K2 filler metal and two from E70T-7 filler metal) and 12 standard Charpy V-notch coupons (six from E70T7-K2 filler metal and six from E70T-7 filler metal) were tested to determine the material tensile properties and fracture toughness of the UC Davis (Gomez *et al.*, 2008) specimens. Each coupon was fabricated in accordance with Clause 8 of ANSI/AWS A5.20 (AWS, 2005). The results of the Charpy impact tests and the tension coupon tests are presented in Tables 3.3 and 3.4, respectively.

3.3 TESTS ON WELDED JOINTS WITH OUT-OF-PLANE ECCENTRICITY

3.3.1 Tests from University of Alberta (Dawe and Kulak, 1972, 1974)

Dawe and Kulak (1972) conducted eight tests on welded joints with out-of-plane eccentricity as described in Chapter 2. The specimens consisted of a wide flange section with a 12.7 mm (1/2 in.) load plate welded to one end as shown in Figure 3.1. The other end of the specimen was connected to a 19.1 mm (3/4 in.) reaction plate by two lines of fillet weld on the exterior sides of each flange. ASTM A36 steel was used for the test specimens and AWS-E60 filler metal was used for the welds. In order to prevent load transfer through bearing of the web with the reaction plate, the web of each section was

shortened by 25.4 mm (1 in.) from the end. The specimens were bolted to the flange of a reaction column and loaded quasi-statically to failure.

The test parameters and measured specimen strength are presented in Table 3.5. The types of section used are W10x39, W10x33, W10x66 and W12x65. The test parameters include load eccentricity, weld dimensions, flange thickness, the static yield strength and tensile strength of the plate, σ_y and σ_u, and measured weld capacity. The reported weld length and size are the average of both weld segments. Since the tensile strength of section was not reported by Dawe and Kulak (1972), there is a need to investigate the relationship of ultimate tensile strength and yield strength of the W-shape sections by considering the ratio between these two parameters. From Schmidt and Bartlett (2002), the bias coefficient of ultimate tensile strength for W-shape sections is 1.13 with nominal tensile strength of 448 MPa (65 ksi). The bias coefficient of yield strength is 1.11 with nominal yield strength of 345 MPa (50 ksi). By using these values, the ratio of ultimate tensile strength to yield strength is 1.323. As presented in Table 3.5, the ultimate tensile strength listed is 1.323 times the yield strength of the plate.

3.3.2 Tests from Université Laval (Beaulieu and Picard, 1985)

A total of 24 eccentrically loaded plate connections, as shown in Figure 3.2, were tested. According to the test records, five failure modes were observed. The specimens were failed by one of the following modes: weld rupture in tension, shear failure of weld, plate rupture in tension, plate shear failure or failure by excessive twisting. In reality, it is not easy to identify the distinctions between tension and shear failure. Therefore, both weld rupture in tension and shear failure of weld are considered to be weld failure for simplicity. Similarly, plate rupture in tension and plate shear failure are considered as plate failure. For the purpose of this research, the specimens failed by excessive twisting are ignored. This reduces the specimen quantity to 22. The load eccentricities, E, considered in the tests were in the range of 75 to 375 mm, corresponding to eccentricity ratios, a, from 0.3 to 1.5 for a weld length, L, of 250 mm. The plate thicknesses, t, were 20 and 40 mm. Nominal fillet weld sizes of 6.4 and 12.7 mm were selected for specimens of type A (t = 20 mm.) and weld sizes of 7.9 and 9.5 mm were selected for type B (t = 40 mm). The measured dimensions of the specimens and test results are presented in Table 3.6. The specimens are designated by type (A or B), weld size (6.4, 7.9, 9.5, or 12.7 mm), eccentricity and test specimen numbers. The weld length reported in the table is an average of both welds in a test specimen.

3.3.3 Tests from University of California Davis (Gomez *et al.*, 2008)

A total of 60 test specimens were tested by Gomez *et al.* (2008) at UC Davis and a summary of the test results are presented in Table 3.7. Twenty cruciform type specimens were fabricated in assemblies sufficiently large to contain three test specimens. Three test specimens were cut from each assembly. The specimens were tested eccentricity was varied by varying the length, L, of the specimen. Triplicate tests were conducted to obtain a good estimate of variation within each set of variables. The specimens were tested under three-point bending under quasi-static loading to failure in the test set up shown in Figure 3.3. They were loaded in displacement control with an average loading rate of

about 0.44 kN/second. The test variables were the plate thickness (31.8, 44.5 and 63.5 mm), load eccentricity (76.2, 139.7 and 215.9 mm), weld size (7.9 and 12.7 mm), and weld electrode classification (toughness and non-toughness rated E70XX (E480XX) electrode). It was observed that the failures for most specimens with eccentricities of 139.7 and 215.9 mm (5.5 and 8.5 in.) were moderate and the weld rupture involved a gradual "un-zipping" of the specimen that was initiated at the bottom end of the weld (tension face). For other specimens with smaller eccentricities, they demonstrated sudden shear failure that entirely severed the test welds.

3.4 COMPARISONS BETWEEN THE TEST PROGRAMS

3.4.1 Loading Protocols and Test Setups

As described in the previous section, the test setups used by Dawe and Kulak (1972) and Beaulieu and Picard (1985) were similar. The test setup used in UC Davis (Gomez *et al.,* 2008) achieved a similar loading condition as the two other test programs, but with a substantially simpler test setup. The loading condition achieved in all three test programs is similar, namely, a combination of shear and bending moment on the welded joint.

The eccentricity ratio (ratio of load eccentricity to weld length) used by Dawe and Kulak, Beaulieu and Picard and UC Davis (Gomez *et al.*, 2008) are listed in Table 3.8. An examination of Tables 3.5 to 3.8 and Figure 3.4 indicates that a higher ultimate joint capacity is obtained for the specimens with higher eccentricity ratio. The eccentricity ratio for all specimens from the three data sets varied within different ranges. Dawe and Kulak (1972) used an eccentricity ratio varying from 1.03 to 2.56. Beaulieu and Picard (1985) used a range of eccentricity ratio between 0.30 and 1.51, whereas UC Davis (Gomez *et al.*, 2008) used values varying from 0.73 to 2.23. A comparison between the specimens from Dawe and Kulak with those from Beaulieu and Picard indicates that the latter tend to have lower eccentricity ratios than those of Dawe and Kulak. The specimens from UC Davis (Gomez *et al.*, 2008) cover a broader range of eccentricity ratio, although they do not go as high as those tested by Dawe and Kulak or as low as those tested by Beaulieu and Picard. The loading protocol used in the three test programs was not identical. Dawe and Kulak used quasi-static loading and UC Davis applied a slow and continuous monotonic load. The loading protocol used in the Beaulieu and Picard tests is not described (Warren, 1984).

3.4.2 Results of Bend Tests

The results of bend tests from three sources and their predicted capacities using the current CISC approach (CISC, 2006), AISC approach (AISC, 2005) and a modified version of Model 1 are presented in Tables 3.9 to 3.12. The detailed descriptions for the models are presented in Chapter 4. The modified Model 1 is based on the instantaneous centre of rotation approach proposed by Dawe and Kulak with the weld load versus deformation model of Butler and Kulak (1971) modified by multiplying the solution from Model 1 by a factor of 0.67. This corresponds to the approach used in the eighth edition and earlier editions of the CISC Handbook of Steel Construction (CISC, 2004). It should be noted that the tabulated capacities presented in Tables 3.9 to 3.12 all have a resistance

factor of 1.0 so that the predicted values can be compared directly with the test results. Tables 3.9 and 3.11 show that the two predictions (the modified Model 1 and the eighth edition of the CISC design handbook) are close. The small discrepancies between the predictions using the modified Model 1 and the 8th edition of the of the CISC Handbook (CISC, 2004) can be attributed to the small differences between the actual material strengths, which are used in the modified Model 1 approach, and the material strength used to derive the CISC design table. The CISC design table was developed for a E480XX electrode with a nominal tensile strength of 480 MPa. The test data reviewed earlier indicated that the actual tensile strengths are different from the nominal tensile strength used in the design table. Therefore, a correction factor is used to adjust the predicted capacity obtained from the CISC design table. The factor is taken as the ratio of the actual tensile strength to the nominal tensile strength of the weld metal. However, the instantaneous centre method developed by Dawe and Kulak clearly shows that the strength of the joint is not a linear function of the strength of the weld metal. The linear correction factor therefore gives a non-conservative prediction of the capacity. This effect is manifest when considering data from UC Davis (Gomez *et al.*, 2008) since the actual tensile strength reported is significantly higher from the nominal tensile strength used in the design table. Second, the plate thicknesses on numerous specimens from UC Davis (Gomez *et al.*, 2008) exceed the maximum thickness presented in the design table. Although the design table suggests using the maximum available plate thickness when the plate thickness used is larger than the maximum tabulated plate thickness, this approach will lead to conservative strength predictions. However, this effect overshadows the effect of the tensile strength difference for the UC Davis test results. Although the CISC Handbook of Steel Construction provides a sufficient number of plate thickness for design purpose, interpolation was still required for all of the predicted test results obtained from the design table. The use of linear interpolation and extrapolation may provide inaccurate predictions.

The capacity predicted using the three approaches for the Dawe and Kulak specimens are presented in Table 3.9. It is observed that this approach predicts the test results conservatively, with mean test-to-predicted values of 1.173, 1.270 and 1.316 for the current CISC (the ninth edition), AISC and modified Model 1 approaches, respectively. Tables 3.10 and 3.11 show that all the approaches provide conservative predictions for the specimens from Beaulieu and Picard (1985) based on an estimated weld metal tensile strength of 552 MPa and 463 MPa, respectively. The weld metal strength of 552 MPa yields mean test-to-predicted values of 1.321, 1.480 and 1.472 and the weld metal strength of 463 MPa yields the mean test-to-predicted values of 1.575, 1.584 and 1.626 when using current the CISC, AISC and modified Model 1, respectively. Table 3.12 presents the test and predicted capacities for the UC Davis specimens. The current CISC, AISC and the modified Model 1 approaches give mean test-to-predicted values of 1.946, 2.268 and 2.301, respectively. On average, the specimens tested at UC Davis show higher joint strengths than the specimens from the earlier test programs. The large difference between the UC Davis test results and the earlier test results prompted a comparison between an earlier research program conducted at the University of Alberta (Ng *et al.,* 2002) to ensure that the specimens fabricated for the UC Davis test program were consistent with other test results.

The current CISC approach (CISC, 2006) results in a COV for the test-to-predicted value for the Dawe and Kulak test results of 10% and values of 11% and 14% for the Beaulieu and Picard and UC Davis test specimens, respectively. The current AISC (2005) approach results in COV values of 12%, 20% and 17% for the Dawe and Kulak, the Beaulieu and Picard, and the UC Davis test programs, respectively. The modified Model 1 gives COV values of 11%, 14% and 17% for the same three test programs. Due to the high values of COV observed for all the models examined here, the test-to-predicted values obtained from the three approaches are plotted as function of various parameters in Figures 3.5 to 3.7 to investigate possible shortcomings of the prediction models in order to improve the models. The parameters considered are plate thickness, eccentricity, weld length, weld size and eccentricity ratio.

Figure 3.5a shows a plot of test-to-predicted ratio versus plate thickness for modified Model 1. As expected, the data points do not show any trend. This is expected because Model 1 already accounts for plate thickness. An examination of Figure 3.6a shows an increasing trend in the test-to-predicted ratio as the plate thickness increases. This indicates that the model implemented in the AISC design table does not account for the effect of plate thickness adequately. In fact, the AISC method does not account for the plate thickness at all. Figure 3.7a shows no definite trend between the test-to-predicted ratio based on the current CISC design approach and plate thickness. This indicates that the current approach accounts for plate thickness appropriately.

Figures 3.5b, 3.6b and 3.7b investigate possible trend between test-to-predicted ratio and weld size. The data points from all the sources show large scatter and no apparent effect of weld size on the test-to-predicted ratio.

The effect of weld length on the test-to-predicted ratio is illustrated in Figures 3.5c, 3.6c and 3.7c. No clear trend is found for any of the approaches. Figures 3.5d, 3.6d and 3.7d show that test-to-predicted values reduce as the load eccentricity increases. However, plots of test-to-predicted ratios as a function of the eccentricity ratio, a/L, presented in figures 3.5e, 3.6e, and 3.7e show no trend between the two parameters. It is therefore concluded that the eccentricity effect, expressed as a ratio of load eccentricity to weld length, accounts for the load eccentricity effect appropriately. Figures 3.5f, 3.6f and 3.7f, show plots of test-to-predicted ratios as a function of filler metal classification. These plots indicate that weld toughness may have an effect on the strength of eccentrically loaded welded joints. However, such effect is not considered in the approaches investigated in this chapter.

Of all the parameters investigated in figures 3.5 to 3.7, only the weld metal toughness seems to have a significant effect that is ignored by all of the models investigated. Plate thickness is a parameter that has a significant effect on joint capacity. The AISC model is the only model investigated that does not include the effect of plate thickness in its formulation. The instantaneous centre of rotation method proposed by Dawe and Kulak and the current CISC design approach seem to account for plate thickness appropriately.

3.5 COMPARISON OF MATERIAL PROPERTIES

An examination of test data on eccentrically loaded welded joints from three sources seems to indicate that the joints used in the UC Davis (Gomez *et al.*, 2008) test program have a significantly higher capacity than those tested by Dawe and Kulak (1972) and Beaulieu and Picard (1985). In order to determine whether the UC Davis (Gomez *et al.*, 2008) specimens had unusually high weld strength, the test results from the cruciform specimens were compared with recent test results obtained from the first phase of this research program on welded joints (Ng *et al.* 2002). Both series of tests made use of welding electrodes of the same classification and were accompanied by tension tests on all-weld metal coupons and Charpy V-notch tests at -29°C, 21°C and 100°C to characterize the weld metal properties.

3.5.1 Cruciform Specimen Tests at U of Alberta (2002)

Five different electrode classifications were investigated, namely, E7014, E70T-4, E70T-7, E70T7-K2, and E71T8-K6. Only the test specimens fabricated with E70T-4, E70T-7 and E70T7-K2 electrodes are considered here since these filler metal designations, or equivalent, were also used in the UC Davis (Gomez *et al.*, 2008) test program. E70T-4 and E70T-7 electrodes have no specified toughness requirement whereas E70T7-K2 electrodes have a specified toughness requirement of 27 J (20 ft-lb) at -29°C (-20°F). The weld metal tension coupons and Charpy V-notch impact specimens were machined from a standard groove welded assembly fabricated in accordance to Clause 8 of ANSI/AWS A5.20 (AWS 2005) for flux cored arc welded specimens. A total of nine specimens were fabricated for all-weld-metal tension coupon tests: one set of five specimens from E70T-4 and two sets of two specimens were from E70T-7 and E70T7-K2. A total of 42 Charpy impact V notch specimens were prepared for testing at different temperatures: two sets of 18 specimens each from E70T-4 and E70T-7 electrodes and one set of six specimens from E70T7-K2 electrode. Cruciform specimens with a single pass 6.4 mm (1/4 in.) welds were welded using an automated welding track. In every case, three nominally identical specimens were cut from a single assembly and milled to a width of 76 mm (3 in.). Six specimens were fabricated in a cruciform configuration and two welds from each specimen were reinforced to ensure failure would occur at two test welds to measure the weld joint capacity. The specimens were loaded to failure by applied quasi-static and static readings were taken at multiple points during the tests.

3.5.2 Cruciform Specimen Tests at UC Davis (Gomez *et al.*, 2008)

Two filler metal classifications (E70T7-K2 and E70T-7) and two weld sizes of 12.7 mm and 7.9 mm (1/2 in. and 5/16 in.) were tested. A total of 24 cruciform specimens were tested in direct tension. Two all-weld-metal tension coupons were tested for each classification. Six specimens for each classification were prepared for Charpy V-Notch tests at three different temperatures as per the ANSI/AWS A5.20 and A5.29 (2005) standards. Three test specimens, approximately 101.6 mm (4 in.) wide, were cut from each assembly of three plates (A572 Grade 50) welded in a cruciform configuration. Three weld passes were performed for the specimens with 12.7 mm (1/2 in.) welds and

only one pass was performed for the specimens with 7.9 mm (5/16 in.) welds. As for the test configuration used for the specimens at U of Alberta, one side of the cruciform joint had been reinforced to ensure failure on the side of the test welds. The specimens were loaded monotonically and continuously until failure.

3.5.3 Comparison of Test Results

Although the test program conducted by Ng *et al*. (2002) included five different welding electrodes, only the E70T-4 and E70T7-K2 electrode were used for the fabrication of cruciform specimens. However, E70T-7 and E70T7-K2 were tested at UC Davis (Gomez *et al.*, 2008). E70T-4 and E70T-7 welding electrodes do not have toughness requirement. In addition, based on the Charpy V-Notch impact test results presented in Table 3.13, both electrodes show similar CVN energy. Therefore, it is considered appropriate to compare E70T-4 to E70T-7 directly.

3.5.3.1 Charpy V-notch Impact Test

Table 3.13 presents the results from the Charpy V-notch impact tests from the U of Alberta and from UC Davis. As expected, the toughness rated E70T7-K2 filler metal generally demonstrated much higher impact energy than those non-toughness rated filler metals at all three temperatures. The electrodes with no toughness requirement, E70T-4 and E70T-7, have similar toughness values at -29^{o}C (-20^{o}F) and 100^{o}C (212^{o}F), but the E70T-7 electrode showed a higher toughness than the E70T-4 electrode at 21^{o}C (70^{o}F). All the toughness rated filler metals E70T7-K2 from UC Davis (Gomez *et al.*, 2008) met the requirements.

3.5.3.2 All-Weld-Metal Tension Coupon Test

A total of 13 all-weld-metal tension coupon tests were conducted in two test programs and a summary of the measured and average static yield strength and static tensile strength is presented in Table 3.14. Both coupons made with non-toughness rated filler metal E70T-4 at U of Alberta and E70T-7 at UC Davis (Gomez *et al.*, 2008) met the tensile strength of the required range of 480 MPa (70 ksi) to 650 MPa (95 ksi). A comparison of the E70T-7 electrodes from the U of Alberta and the UC Davis (Gomez *et al.*, 2008) test programs indicates that the latter has yield strength and a tensile strength from 10 to 15 percent higher than the strength values from the U of Alberta filler metal. The static tensile strength of the E70T-7 electrode from UC Davis (Gomez *et al.*, 2008) is approximately 20% greater than the tensile strength of the E70T-4 electrode from U of Alberta. The coupons made with the toughness rated E70T7-K2 electrode used at U of Alberta exhibited a static tensile strength in the required range of 480 MPa (70 ksi) to 620 MPa (90 ksi). However, the same classification of filler metal used in the UC Davis test program exceeded the upper limit of 620 MPa (90 ksi). In addition, all coupons met the required minimum static yield strength of 400 MPa (58 ksi), except the E70T-4 coupons used in U of Alberta with static yield strength of 354 MPa (51.3 ksi). Two filler coupons, E70T-4 and E70T7-K2, from U of Alberta have mean elongations of 22.3% and 24.6% respectively. They both met the AWS elongation specifications as 22% for E70T-4 and 20% for E70T7-K2.

3.5.3.3 Tension Test for Cruciform Specimen

The tests on cruciform specimens conducted by Ng *et al.* (2002) were conducted under quasi-static loading (i.e. static values of loading were obtained at regular intervals during the tests) whereas the UC Davis tests were conducted under "dynamic" loading (i.e. the specimens were loaded continuously, although very slowly, until failure). Observations from the University of Alberta showed "dynamic" tension gave higher load readings; however, the difference between the two loading procedures is very small.

The measured ultimate joint capacity and the test-to-predicted ratio using CISC approach for welds loaded transverse to their axis are presented in Table 3.15. The predicted capacity using the CISC (2006) strength equation is given as:

$$V_r = 0.67\,\phi\,A_W\,X_u\left(1.0+0.5\sin^{1.5}\theta\right) \qquad [3.2]$$

where ϕ is the resistance factor, A_w is the theoretical throat area as a function of leg size, X_u is the minimum specified tensile strength of filler metal and θ is the angle of loading with respect to the weld axis.

For all the cases, the predicted capacity is determined by using the measured tensile strength of the weld metal and the resistance factor is taken as 1.0. A_w is the effective throat area of the weld (calculated from the measured leg dimensions, but neglecting the root penetration and weld reinforcement), X_u was determined using the measured strength for the all-weld-metal tension coupon tests for the given electrode classification, and θ is 90^o.

The CISC design equation which is used on the E70T-4 and E70T7-K2 data sets from Ng *et al.* (2002) provides significantly conservative prediction of the weld capacity. However, the equation gives predictions closer to the tested weld capacities for UC Davis (Gomez *et al.*, 2008) E70T-7 and E70T7-K2 data sets. The mean test-to-predicted values for the Ng *et al.* (2002) data vary from 1.554 to 1.744 as shown in Table 3.15. On the other hand, the mean test-to-predicted values for the UC Davis (Gomez *et al.*, 2008) test data are reduced to 0.865 to 0.983. It is apparent that the UC Davis (Gomez *et al.*, 2008) specimens provide lower capacity than the earlier U of Alberta specimens.

Figure 3.8 presents a plot of capacity predicted using the CISC equation versus the measured test capacity for the cruciform test specimens discussed above. The solid line represents a test-to-predicted value of unity. The data points that appear below the solid line are considered to be conservative while the data points that appear above the line are considered as non-conservative predictions. In Figure 3.9, it shows that the root notch distances have no affect on the test to predicted ratio based on the test data from UC Davis (when root notches equal to 31.8 mm (1.25 in.) and 63.5 mm (2.5 in.)). However, the test-to-predict value is slightly affected when comparing with the test data from U of Alberta (when root notch used is 19.0 mm (0.75 in.)). It indicates that the test-to-predicted value for U of Alberta is higher than UC Davis and also shows it is in the conservative region as observed in Figure 3.8. An overview of the weld stress, calculated

on the throat dimension calculated from the measured leg size, as a function of electrode classification and the test program is presented in Figure 3.10. The mean test result is represented by a solid diamond and the range of test results is represented by a vertical bar. The lower variation in test results observed in the U of Alberta test results compared to the UC Davis results is attributed to the much smaller sample size used in the U of Alberta test program. It is observed that the weld stresses for the electrodes used by Ng *et al.* (2002) are significantly higher than those used in the UC Davis test program.

3.6 CONCLUSIONS

Test results from welded joints loaded under out-of-plane eccentricity obtained from the test programs of Dawe and Kulak (1972), Beaulieu and Picard (1985) and UC Davis (Gomez *et al.*, 2008) were presented and compared. Based on the three approaches discussed (the current CISC and AISC approaches and a modified version of Model 1), the predicted weld capacities are close to the test results presented by Dawe and Kulak and Beaulieu and Picard. However, all three approaches provide very conservative predictions of the UC Davis test data. Therefore, an investigation of the test data from the UC Davis program was conducted by comparing test results from their program with a limited number of test results from cruciform specimens and material tests from Ng *et al.* (2002). Also, the COVs of the approaches are found to be around 10% to 14%, 12% to 17% and 11% to 17% for current CISC, AISC and modified Model 1, respectively. A comparison of the all-weld-metal tension coupons and Charpy V-notch impact test results obtained from U of Alberta and UC Davis (Gomez *et al.*, 2008) indicated that the material properties from the two test programs are similar. The filler metals used in the UC Davis (Gomez *et al.*, 2008) test program were found to meet the strength and toughness requirements of AWS A5.20 and A5.29 standards. Also, the tested fillet weld capacities of cruciform specimens from UC Davis are well predicted by using design equation in CISC approach. By comparing the root notch distance with test-to-predicated ratios from UC Davis and U of Alberta, the data shows that the root notch has no significant affect to the test-to-predicted ratio. The effect of loading rate was found to be negligible when test results from U of Alberta were compared with those from UC Davis. In conclusion, the over-predicted weld capacities by the current CISC, AISC and modified Model 1 approaches on UC Davis combined shear and moment test results are not caused by the dissimilarity in material properties of the specimens and the method of loading.

Table 3.1 - Material Factor Specific for E60 (E410)

Source of Data	Sample size, N	Nominal tensile strength, (MPa) X_u	Mean tensile strength, (MPa) σ_u	Ratio of Measured to Nominal strength $\rho_{(410)}$	Coefficient of Variation V
Swannell and Skewes (1979)	2	414	537.9	1.302	0.020
Fisher *et al.* (1978)	127	414	455.2	1.099	0.039
Mansell and Yadav (1982)	6	414	558.6	1.349	0.027
All Sources	**135**	**414**	**462.1**	**1.113**	**0.063**

Table 3.2 - Material Factor Specific for E70 (E480)

Source of Data	Sample size, N	Nominal tensile strength, (MPa) X_u	Mean tensile strength, (MPa) σ_u	Ratio of Measured to Nominal strength $\rho_{(480)}$	Coefficient of Variation V
Bowman and Quinn (1994)	3	483	475.9	0.986	0.029
Callele *et al.* (2005)†	32	483	552.4	1.151	0.084
Miazga and Kennedy (1986)	3	483	537.9	1.120	0.014
Pham (1981)	3	483	500.0	1.042	0.044
UC Davis (2008)	4	483	671.0	1.398	0.002
Fisher *et al.* (1978)	40	483	598.6	1.239	0.114
	128	483	589.0	1.219	0.056
	138	483	516.6	1.069	0.036
Gagnon and Kennedy (1987)	10	483	580.0	1.208	0.036
All Sources	**361**	483	**557.9**	**1.155**	**0.092**

† Including all weld metal tension coupon tests from Phases 1 through 4.

Table 3.3 - Charpy V-Notch Impact Test Results (UC Davis (Gomez *et al.*, 2008))

Source of Data	Filler Metal	Test	CVN Energy (J)		
			-29°C	21°C	100°C
UC Davis	E70T-7	1	7.5	25.8	55.6
		2	8.1	24.4	55.6
		Mean	**7.8**	**25.1**	**55.6**
	E70T7-K2	1	40.7	75.9	119.3
		2	31.2	84.1	119.3
		Mean	**36.0**	**80.0**	**119.3**

Table 3.4 - Weld Metal Tension Coupon Test Results (UC Davis (Gomez *et al.*, 2008))

Source of Data	Filler Metal	Test	Static Yield Strength, F_y (MPa)	Static Tensile Strength, X_u (MPa)
UC Davis	E70T-7	1	522.8	669.7
		2	529.7	670.3
		Mean	**526.2**	**670.0**
	E70T7-K2	1	570.3	672.4
		2	572.4	671.7
		Mean	**571.7**	**672.4**

Table 3.5 – Test Specimen Data from Dawe and Kulak (1972)

Specimen number	Type of Section	Load eccentricity, e, (mm)	Average weld dimensions, (mm)		Flange thickness, t (mm)	Static yield of base metal, σ_y, (MPa)	Tensile strength of base plate, σ_u, (MPa)	Test capacity, (kN)
			Length, L	Effective leg size, D_e				
A-1	W10X39	203.2	197.4	7.9	26.4	299	396	278
A-2	W10X39	304.8	199.6	7.9	26.4	299	396	173
A-3	W10X39	406.4	199.9	7.6	26.4	289	382	103
A-4	W10X39	508.0	198.4	7.6	26.9	289	382	87
A-5	W10X33	406.4	199.1	7.6	21.8	263	348	105
A-6	W10X66	406.4	201.2	8.1	38.6	265	351	145
A-7	W12X65	381.0	301.2	7.4	31.5	271	359	265
A-8	W12X65	508.0	299.7	7.9	31.5	271	359	220

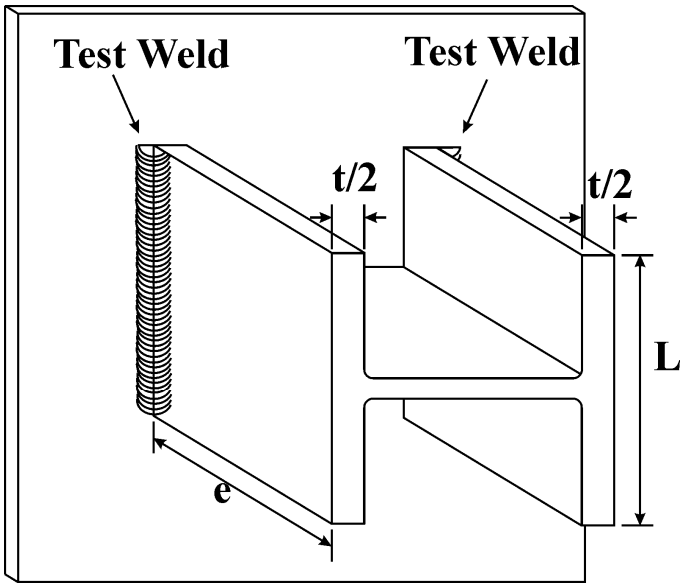

Table 3.6 – Test Specimen Data from Beaulieu and Picard (1985)

Specimen number	Load eccentricity (mm)	Weld dimensions (mm)			Plate thickness, t (mm)	σ_y (MPa)	σ_u (MPa)	Test Capacity (kN)	Actual Failure Mode
		Length	Leg size, D_{e1}	Leg size, D_{e2}					
A-6-375-1	375	249.8	8.0	7.4	19.7	287	489	226	Weld
A-6-375-2[1]	375	246.8	12.4	12.5	19.7	287	489	366	Twist
A-12-375-1[2]	375	250.8	13.3	14.0	19.7	287	489	275	Weld
A-12-375-2	375	250.8	14.3	12.9	19.7	287	489	304	Plate
A-6-125-1	125	251.8	8.3	7.7	19.7	287	489	702	Weld
A-6-125-2	125	251.9	7.5	8.2	19.7	287	489	630	Weld
A-12-125-1	125	249.6	14.1	13.9	19.7	287	489	733	Plate
A-12-125-2[1]	125	252.3	13.6	12.8	19.7	287	489	939	Twist
A-6-75-1	75	251.9	10.8	9.9	19.7	287	489	1190	Plate
A-6-75-2	75	251.3	8.1	7.9	19.7	287	489	1093	Weld
A-12-75-1	75	248.9	11.9	13.6	19.7	287	489	1071	Plate
A-12-75-2	75	251.4	13.7	12.6	19.7	287	489	1131	Plate
B-8-375-1	375	249.0	12.9	11.3	40.7	317	493	416	Weld
B-8-375-2	375	251.5	10.9	12.6	40.7	317	493	427	Weld
B-10-375-1	375	248.9	11.7	12.1	40.7	317	493	273	Weld
B-10-375-2	375	248.8	12.9	11.1	40.7	317	493	485	Weld
B-8-125-1	125	250.9	10.4	11.0	40.7	317	493	1047	Weld
B-8-125-2	125	250.9	9.9	11.2	40.7	317	493	1274	Weld
B-10-125-1	125	250.7	10.4	10.5	40.7	317	493	1183	Weld
B-10-125-2	125	248.2	11.4	11.0	40.7	317	493	1109	Weld
B-8-75-1	75	248.8	9.2	9.1	40.7	317	493	1487	Weld
B-8-75-2	75	248.4	8.6	8.8	40.7	317	493	1393	Weld
B-10-75-1[2]	75	246.0	12.4	12.7	40.7	317	493	1696	Weld
B-10-75-2[2]	75	248.8	12.8	11.7	40.7	317	493	1594	Weld

[1]Test stopped due to torsion of plate

[2]Weld returns removed

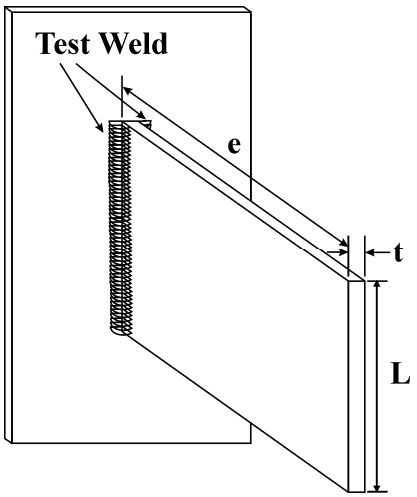

Table 3.7 – Summary of Test Results from Gomez *et al*. (2008)

Specimen tag	Load eccentricity, (mm)	Weld Dimensions, (mm)				Plate thickness, t (mm)	σ_y (MPa)	σ_u (MPa)	Test Capacity (kN)
		Length, L_1	Leg size, D_{e1}	Length, L_2	Leg size, D_{e2}				
B_125_A516_55_1	139.7	98.5	10.9	98.4	9.4	32.0	384	494	197
B_125_A516_55_2	139.7	99.2	10.4	99.4	9.8	31.9	384	494	239
B_125_A516_55_3	139.7	97.0	10.4	99.7	10.5	31.9	384	494	233
B_125_A12_55_1	139.7	96.9	15.1	101.6	15.0	32.1	384	494	326
B_125_A12_55_2	139.7	100.6	15.7	99.4	14.4	32.7	384	494	321
B_125_A12_55_3	139.7	100.8	15.0	101.6	14.8	32.2	384	494	316
B_175_A516_3_1	76.2	99.8	9.2	100.6	9.0	44.5	384	494	173
B_175_A516_3_2	76.2	101.1	9.5	101.2	9.1	44.5	384	494	134
B_175_A516_3_3	76.2	103.6	9.0	103.3	9.3	44.5	384	494	149
B_175_A12_3_1	76.2	98.2	14.5	98.3	13.5	44.9	384	494	231
B_175_A12_3_2	76.2	101.6	14.0	101.5	14.2	44.8	384	494	228
B_175_A12_3_3	76.2	96.9	14.2	99.3	14.7	44.8	384	494	236
B_175_A516_55_1	139.7	103.3	9.9	103.1	8.7	44.7	384	494	386
B_175_A516_55_2	139.7	102.9	9.9	103.0	8.7	44.5	384	494	452
B_175_A516_55_3	139.7	99.7	9.6	101.0	9.2	44.7	384	494	420
B_175_A12_55_1	139.7	103.8	15.5	103.6	14.9	45.6	384	494	533
B_175_A12_55_2	139.7	96.4	14.4	97.1	14.2	45.7	384	494	529
B_175_A12_55_3	139.7	99.5	14.6	98.7	15.0	45.2	384	494	551
B_175_A516_85_1	215.9	98.3	11.3	98.8	9.9	44.5	384	494	276
B_175_A516_85_2	215.9	96.7	10.6	97.0	10.8	44.5	384	494	261
B_175_A516_85_3	215.9	99.5	9.5	99.1	11.6	44.6	384	494	259
B_175_A12_85_1	215.9	103.0	15.0	103.4	14.7	45.0	384	494	274
B_175_A12_85_2	215.9	103.4	14.4	103.2	14.8	45.0	384	494	265
B_175_A12_85_3	215.9	101.9	15.7	103.2	15.9	44.9	384	494	280
B_250_A516_55_1	139.7	103.7	11.4	105.7	9.2	64.1	384	494	204
B_250_A516_55_2	139.7	101.0	11.2	101.2	9.3	64.0	384	494	208
B_250_A516_55_3	139.7	104.4	10.3	104.5	9.8	64.4	384	494	205
B_250_A12_55_1	139.7	100.2	14.8	101.7	14.8	64.3	384	494	386
B_250_A12_55_2	139.7	105.1	15.0	106.0	14.2	64.2	384	494	310
B_250_A12_55_3	139.7	104.6	13.9	104.2	14.3	64.0	384	494	347
B_125_B516_55_1	139.7	96.0	10.7	96.0	11.0	32.3	384	494	400
B_125_B516_55_2	139.7	97.7	10.7	97.2	10.9	32.4	384	494	341
B_125_B516_55_3	139.7	95.3	9.8	95.5	11.5	32.3	384	494	354
B_125_B12_55_1	139.7	102.3	15.3	100.9	14.6	32.3	384	494	682
B_125_B12_55_2	139.7	100.2	14.8	100.3	13.7	32.8	384	494	778

Table 3.7 – Cont'd

Specimen tag	Load eccentricity, (mm)	Weld Dimensions, (mm)				Plate thickness, t (mm)	σ_y (MPa)	σ_u (MPa)	Test Capacity (kN)
		Length, L_1	Leg size, D_{e1}	Length, L_2	Leg size, D_{e2}				
B_125_B12_55_3	139.7	104.2	15.2	104.2	15.7	32.3	384	494	676
B_175_B516_3_1	76.2	101.0	9.4	101.9	11.1	45.0	384	494	441
B_175_B516_3_2	76.2	104.9	9.6	104.0	9.9	44.9	384	494	400
B_175_B516_3_3	76.2	103.6	10.1	103.1	9.5	45.1	384	494	385
B_175_B12_3_1	76.2	103.4	14.7	103.8	14.9	45.0	384	494	364
B_175_B12_3_2	76.2	102.5	14.7	102.7	14.8	45.2	384	494	375
B_175_B12_3_3	76.2	103.0	14.3	103.7	14.3	45.3	384	494	439
B_175_B516_55_1	139.7	101.4	13.1	103.1	9.5	44.7	384	494	263
B_175_B516_55_2	139.7	102.0	13.1	102.6	8.4	44.6	384	494	266
B_175_B516_55_3	139.7	102.5	9.7	102.9	8.6	44.8	384	494	254
B_175_B12_55_1	139.7	101.7	14.6	102.3	15.1	45.6	384	494	224
B_175_B12_55_2	139.7	99.4	16.4	96.9	14.1	45.4	384	494	255
B_175_B12_55_3	139.7	100.2	13.5	96.9	15.7	45.4	384	494	270
B_175_B516_85_1	215.9	103.4	10.9	103.9	10.4	45.4	384	494	734
B_175_B516_85_2	215.9	101.0	10.7	101.0	10.4	44.5	384	494	713
B_175_B516_85_3	215.9	100.6	11.0	101.3	10.2	44.7	384	494	690
B_175_B12_85_1	215.9	103.5	15.6	103.5	14.2	45.2	384	494	859
B_175_B12_85_2	215.9	101.6	15.1	101.3	15.5	46.0	384	494	889
B_175_B12_85_3	215.9	96.3	15.9	97.3	16.2	45.2	384	494	824
B_250_B516_55_1	139.7	100.1	9.8	104.0	9.5	64.5	384	494	346
B_250_B516_55_2	139.7	100.7	10.1	101.2	10.2	64.4	384	494	342
B_250_B516_55_3	139.7	100.7	10.8	98.6	9.9	64.1	384	494	339
B_250_B12_55_1	139.7	101.7	14.8	101.5	16.7	64.5	384	494	491
B_250_B12_55_2	139.7	99.1	15.4	100.3	17.1	64.8	384	494	498
B_250_B12_55_3	139.7	97.8	15.1	99.6	16.2	64.5	384	494	492

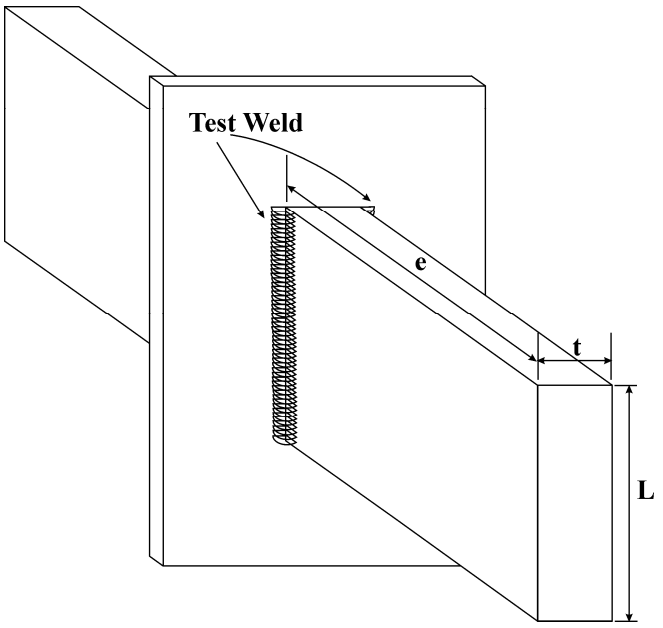

Table 3.8 – Specimen Eccentricity Ratio used by Dawe and Kulak, Picard and Beaulieu and UC Davis (Gomez *et al*., 2008)

Dawe and Kulak (1972)		Beaulieu and Picard (1985)		UC Davis	
Specimen number	Eccentricity ratio, a	Specimen number	Eccentricity ratio, a	Specimen tag	Eccentricity ratio, a
A-1	1.03	A-6-375-1	1.50	B_125_A516_55_1	1.42
A-2	1.53	A-6-125-1	0.50	B_125_A516_55_2	1.41
A-3	2.03	A-6-125-2	0.50	B_125_A516_55_3	1.42
A-4	2.56	B-8-375-1	1.51	B_125_A12_55_1	1.41
A-5	2.04	B-8-375-2	1.49	B_125_A12_55_2	1.40
A-6	2.02	B-10-375-1	1.51	B_125_A12_55_3	1.38
A-7	1.26	B-10-375-2	1.51	B_175_A516_3_1	0.76
A-8	1.69	B-8-125-1	0.50	B_175_A516_3_2	0.75
		B-8-125-2	0.50	B_175_A516_3_3	0.74
		B-10-125-2	0.50	B_175_A12_3_1	0.78
		B-10-125-1	0.50	B_175_A12_3_2	0.75
		A-6-75-2	0.30	B_175_A12_3_3	0.78
		B-8-75-1	0.30	B_175_A516_55_1	1.35
		B-8-75-2	0.30	B_175_A516_55_2	1.36
		B-10-75-1	0.30	B_175_A516_55_3	1.39
		B-10-75-2	0.30	B_175_A12_55_1	1.35
		A-6-75-1	0.30	B_175_A12_55_2	1.44
		A-12-75-1	0.30	B_175_A12_55_3	1.41
		A-12-75-2	0.30	B_175_A516_85_1	2.19
		A-12-375-1	1.50	B_175_A516_85_2	2.23
		A-12-375-2	1.50	B_175_A516_85_3	2.17
		A-12-125-1	0.50	B_175_A12_85_1	2.09
				B_175_A12_85_2	2.09
				B_175_A12_85_3	2.11
				B_250_A516_55_1	1.33
				B_250_A516_55_2	1.38
				B_250_A516_55_3	1.34
				B_250_A12_55_1	1.38
				B_250_A12_55_2	1.32
				B_250_A12_55_3	1.34
				B_125_B516_55_1	1.46
				B_125_B516_55_2	1.43
				B_125_B516_55_3	1.46
				B_125_B12_55_1	1.38
				B_125_B12_55_2	1.39
				B_125_B12_55_3	1.34
				B_175_B516_3_1	0.75
				B_175_B516_3_2	0.73
				B_175_B516_3_3	0.74
				B_175_B12_3_1	0.74
				B_175_B12_3_2	0.74
				B_175_B12_3_3	0.74

Table 3.8 – Cont'd

UC Davis	
Specimen number	Eccentricity ratio, a
B_175_B516_55_1	1.37
B_175_B516_55_2	1.37
B_175_B516_55_3	1.36
B_175_B12_55_1	1.37
B_175_B12_55_2	1.42
B_175_B12_55_3	1.42
B_175_B516_85_1	2.08
B_175_B516_85_2	2.14
B_175_B516_85_3	2.14
B_175_B12_85_1	2.09
B_175_B12_85_2	2.13
B_175_B12_85_3	2.23
B_250_B516_55_1	1.37
B_250_B516_55_2	1.38
B_250_B516_55_3	1.40
B_250_B12_55_1	1.38
B_250_B12_55_2	1.40
B_250_B12_55_3	1.42

Table 3.9 –Predicted Welded Joint Capacity on Test Results from University of Alberta (Dawe and Kulak, 1972)

Specimen number	Measured ultimate load, (kN)	AISC Approach		Modified Model 1		9th edition CISC		8th edition CISC Handbook
		Predicted capacity (kN)	Test-to-predicted ratio	Predicted capacity (kN)	Test-to-predicted ratio	Predicted capacity (kN)	Test-to-predicted ratio	Predicted capacity (kN)
A-1	278	200	1.388	185	1.498	180	1.545	191
A-2	173	139	1.248	127	1.369	123	1.413	130
A-3	103	102	1.009	92	1.114	89	1.151	94.
A-4	87	80	1.078	74	1.178	71	1.222	75
A-5	105	101	1.039	75	1.391	77	1.370	76
A-6	145	110	1.319	115	1.264	107	1.357	110
A-7	265	235	1.128	236	1.123	223	1.188	—*
A-8	220	188	1.170	180	1.224	172	1.281	176
Mean of ratios			**1.173**		**1.270**		**1.316**	
Coefficient of variation, V			**0.116**		**0.109**		**0.100**	

—* Resistance not listed in design table because weld size is smaller than minimum required for plate thickness.

Table 3.10 – Predicted Welded Joint Capacity on Test Results from Université Laval (Beaulieu and Picard, 1985) using X_u = 552 MPa

Specimen number	Measured ultimate load (kN)	AISC Approach		Modified Model 1		9th edition CISC		8th edition CISC Handbook
		Predicted capacity (kN)	Test-to-predicted ratio	Predicted capacity (kN)	Test-to-predicted ratio	Predicted capacity (kN)	Test-to-predicted ratio	Predicted capacity (kN)
A-12-375-1	275	376	0.732	153	1.798	172	1.595	192
A-6-125-1	702	588	1.194	413	1.699	438	1.604	488
A-6-125-2	630	575	1.096	411	1.532	434	1.451	—*
A-6-375-1	226	210	1.077	134	1.682	141	1.602	—*
A-6-75-2	1093	786	1.390	678	1.613	768	1.422	776
B-10-125-1	1183	759	1.560	782	1.514	766	1.545	881
B-10-125-2	1109	798	1.390	787	1.409	778	1.426	894
B-10-375-1	273	322	0.845	273	1.000	269	1.013	314
B-10-375-2	485	325	1.493	273	1.778	269	1.799	315
B-10-75-1	1696	1195	1.419	1300	1.304	1274	1.331	1464
B-10-75-2	1594	1190	1.339	1316	1.211	1276	1.249	1471
B-8-125-1	1047	779	1.345	790	1.326	777	1.349	892
B-8-125-2	1274	768	1.658	786	1.621	771	1.652	886
B-8-375-1	416	328	1.269	274	1.518	271	1.534	316
B-8-375-2	427	325	1.314	277	1.542	273	1.565	319
B-8-75-1	1487	886	1.679	1131	1.314	1016	1.463	1210
B-8-75-2	1393	838	1.663	1071	1.301	972	1.432	1169
Mean of ratios			**1.321**		**1.480**		**1.472**	
Coefficient of variation, V			**0.204**		**0.146**		**0.121**	

–* Resistance not listed in design table because weld size is smaller than minimum required for plate thickness.

Table 3.11 –Predicted Welded Joint Capacity on Test Results from Université Laval (Beaulieu and Picard, 1985) using X_u = 463 MPa

Specimen number	Measured ultimate load (kN)	AISC Approach		Modified Model 1		9th edition CISC		8th edition CISC Handbook
		Predicted capacity (kN)	Test-to-predicted ratio	Predicted capacity (kN)	Test-to-predicted ratio	Predicted capacity (kN)	Test-to-predicted ratio	Predicted capacity (kN)
A-12-375-1	275	315	0.872	148	1.857	164	1.679	161
A-6-125-1	702	493	1.423	394	1.783	407	1.724	409
A-6-125-2	630	482	1.306	391	1.609	404	1.561	—*
A-6-375-1	226	176	1.284	128	1.764	131	1.725	—*
A-6-75-2	1093	660	1.656	640	1.706	672	1.626	657
B-10-125-1	1183	636	1.859	726	1.630	695	1.702	739
B-10-125-2	1109	669	1.656	734	1.511	708	1.565	750
B-10-375-1	273	270	1.008	256	1.063	246	1.109	264
B-10-375-2	485	272	1.779	256	1.890	246	1.969	264
B-10-75-1	1696	1003	1.691	1199	1.414	1115	1.521	1228
B-10-75-2	1594	999	1.597	1211	1.317	1115	1.430	1233
B-8-125-1	1047	653	1.604	735	1.426	706	1.484	748
B-8-125-2	1274	644	1.976	730	1.745	701	1.818	743
B-8-375-1	416	275	1.513	258	1.614	248	1.679	266
B-8-375-2	427	272	1.566	260	1.640	249	1.715	268
B-8-75-1	1487	743	2.001	994	1.496	885	1.681	1015
B-8-75-2	1393	703	1.982	951	1.464	846	1.646	980
Mean of ratios			**1.575**		**1.584**		**1.626**	
Coefficient of variation, V			**0.204**		**0.133**		**0.113**	

–* Resistance not listed in design table because weld size is smaller than minimum required for plate thickness.

Table 3.12 –Predicted Welded Joint Capacity on Test results from University of California, Davis (Gomez *et al.*, 2008)

Specimen tag	Measured ultimate load (kN)	AISC Approach		Modified Model 1		9th edition CISC		8th edition CISC Handbook
		Predicted capacity (kN)	Test-to-predicted ratio	Predicted capacity (kN)	Test-to-predicted ratio	Predicted capacity (kN)	Test-to-predicted ratio	Predicted capacity (kN)
B_125_A12_55_1	326	211	1.547	123	2.655	128	2.546	175
B_125_A12_55_2	321	214	1.500	126	2.540	135	2.369	180
B_125_A12_55_3	316	217	1.455	128	2.472	136	2.327	183
B_125_A516_55_1	197	140	1.406	108	1.818	109	1.803	151
B_125_A516_55_2	239	142	1.678	110	2.166	111	2.152	152
B_125_A516_55_3	233	144	1.622	109	2.138	109	2.141	152
B_175_A12_3_1	682	339	2.011	276	2.468	278	2.452	364
B_175_A12_3_2	778	363	2.141	295	2.633	298	2.609	388
B_175_A12_3_3	676	350	1.933	278	2.431	278	2.431	365
B_175_A12_55_1	400	232	1.725	174	2.297	177	2.260	225
B_175_A12_55_2	341	191	1.783	149	2.279	150	2.276	193
B_175_A12_55_3	354	207	1.707	157	2.254	160	2.214	205
B_175_A12_85_1	231	147	1.567	110	2.099	111	2.073	144
B_175_A12_85_2	228	145	1.572	110	2.081	111	2.056	144
B_175_A12_85_3	236	155	1.523	110	2.137	112	2.100	146
B_175_A516_3_1	533	229	2.332	244	2.181	230	2.323	312
B_175_A516_3_2	529	237	2.228	251	2.107	237	2.230	321
B_175_A516_3_3	551	244	2.254	261	2.110	247	2.233	333
B_175_A516_55_1	274	141	1.941	144	1.906	135	2.025	184
B_175_A516_55_2	265	140	1.894	143	1.860	134	1.980	183
B_175_A516_55_3	280	135	2.072	137	2.047	128	2.187	174
B_175_A516_85_1	173	96	1.808	89	1.949	85	2.034	114
B_175_A516_85_2	134	93	1.431	86	1.549	83	1.612	111
B_175_A516_85_3	149	97	1.532	90	1.644	87	1.710	116
B_250_A12_55_1	386	214	1.801	206	1.875	195	1.977	213
B_250_A12_55_2	452	231	1.954	224	2.019	212	2.126	232
B_250_A12_55_3	420	218	1.924	207	2.031	205	2.052	225
B_250_A516_55_1	276	160	1.723	187	1.470	168	1.639	198
B_250_A516_55_2	261	149	1.754	175	1.492	158	1.651	183
B_250_A516_55_3	259	156	1.656	186	1.391	168	1.544	195

Table 3.12 – Cont'd

Specimen tag	Measured ultimate load (kN)	AISC Approach		Modified Model 1		9th edition CISC		8th edition CISC Handbook
		Predicted capacity (kN)	Test-to-predicted ratio	Predicted capacity (kN)	Test-to-predicted ratio	Predicted capacity (kN)	Test-to-predicted ratio	Predicted capacity (kN)
B_125_B12_55_1	364	220	1.657	129	2.819	139	2.625	185
B_125_B12_55_2	375	204	1.838	126	2.986	133	2.826	180
B_125_B12_55_3	439	239	1.839	137	3.205	147	2.990	193
B_125_B516_55_1	224	142	1.578	106	2.117	108	2.081	148
B_125_B516_55_2	255	146	1.746	109	2.333	111	2.290	152
B_125_B516_55_3	270	139	1.950	104	2.595	105	2.563	145
B_175_B12_3_1	859	396	2.168	313	2.748	317	2.708	411
B_175_B12_3_2	889	387	2.295	308	2.890	312	2.852	403
B_175_B12_3_3	824	381	2.164	309	2.665	311	2.649	404
B_175_B12_55_1	441	219	2.013	167	2.643	169	2.619	218
B_175_B12_55_2	400	210	1.903	156	2.568	160	2.494	203
B_175_B12_55_3	385	201	1.913	155	2.487	159	2.423	202
B_175_B12_85_1	263	149	1.772	111	2.374	113	2.341	145
B_175_B12_85_2	266	146	1.821	109	2.447	111	2.408	141
B_175_B12_85_3	254	140	1.818	99	2.562	101	2.511	130
B_175_B516_3_1	734	264	2.785	264	2.777	252	2.913	337
B_175_B516_3_2	713	264	2.701	274	2.601	262	2.723	349
B_175_B516_3_3	690	262	2.633	270	2.554	258	2.677	343
B_175_B516_55_1	386	168	2.301	151	2.554	145	2.653	196
B_175_B516_55_2	310	160	1.936	147	2.104	142	2.191	192
B_175_B516_55_3	347	137	2.527	141	2.452	132	2.624	181
B_175_B516_85_1	204	106	1.918	100	2.043	95	2.137	127
B_175_B516_85_2	208	100	2.077	93	2.228	90	2.321	120
B_175_B516_85_3	205	100	2.037	94	2.183	90	2.284	120
B_250_B12_55_1	491	232	2.120	214	2.298	206	2.378	221
B_250_B12_55_2	498	231	2.159	209	2.384	201	2.474	213
B_250_B12_55_3	492	217	2.268	201	2.446	192	2.561	208
B_250_B516_55_1	346	143	2.414	174	1.989	153	2.258	182
B_250_B516_55_2	342	147	2.331	174	1.962	157	2.181	182
B_250_B516_55_3	339	146	2.319	172	1.978	157	2.167	178
Mean of ratios			**1.946**		**2.268**		**2.301**	
Coefficient of variation, V			**0.167**		**0.167**		**0.142**	

Table 3.13 – Charpy V-Notch Impact Test Results

Source of Data	Filler Metal	Test	CVN Energy (J)		
			-29°C	21°C	100°C
Ng *et al.* (2002)	E70T-4	1	7.1	8.0	31.0
		2	7.1	8.0	27.0
		3	8.9	15.0	56.9
		4	8.0	18.0	47.0
		5	5.0	19.0	72.0
		6	5.0	15.0	76.1
		Mean	**6.8**	**13.8**	**51.7**
	E70T-7	1	7.1	16.0	48.9
		2	5.0	15.0	56.0
		3	11.0	24.0	62.0
		4	5.0	30.0	75.0
		5	7.1	19.0	43.0
		6	7.1	20.1	48.9
		Mean	**7.1**	**20.6**	**55.7**
	E70T7-K2	1	34.0	75.0	165.0
		2	14.0	88.9	180.1
		Mean	**24.0**	**82.0**	**172.5**
Gomez *et al*. (2008)	E70T-7	1	7.5	25.8	55.6
		2	8.1	24.4	55.6
		Mean	**7.8**	**25.1**	**55.6**
	E70T7-K2	1	40.7	75.9	119.3
		2	31.2	84.1	119.3
		Mean	**35.9**	**80.0**	**119.3**

Table 3.14 – Weld Metal Tension Coupon Test Results

Source of Data	Filler Metal	Test	Static Yield Strength, F_y (MPa)	Static Tensile Strength, X_u (MPa)
Ng *et al.* (2002)	E70T-4	1	315	513
		2	312	513
		3	376	557
		4	383	557
		Mean	**354**	**535**
	E70T-7	1	465	609
		2	471	600
		Mean	**468**	**605**
	E70T7-K2	1	530	592
		2	523	591
		Mean	**526**	**592**
Gomez *et al.* (2008)	E70T7	1	523	670
		2	530	670
		Mean	**526**	**670**
	E70T7-K2	1	570	672
		2	572	672
		Mean	**571**	**672**

Table 3.15 – Comparison of Cruciform Test Results with Prediction by Current CISC Method

Source of data	Filler metal	Nominal leg size (mm)	Root notch (mm)	Total A_w (mm^2)	Measured capacity P_{max} (kN)	CSA			
						Predicted capacity, P_u (kN)	Test / predicted	Mean ratio	COV
Ng *et al.* (2002)	E70T-4	6.4	19	678	672	364	1.845	1.744	0.065
				694	658	373	1.766		
				690	600	370	1.620		
	E70T7-K2	6.4	19	699	650	416	1.564	1.554	0.031
				691	655	411	1.596		
				693	618	412	1.501		
Gomez *et al.* (2008)	E70T-7	12.7	32	1962	1212	1319	0.919	0.865	0.109
				2303	1224	1548	0.790		
				2154	1234	1448	0.852		
			64	2173	1201	1461	0.822		
				2128	1375	1431	0.961		
				2442	1324	1641	0.807		
		7.9	32	1329	874	893	0.978		
				1416	871	952	0.915		
				1531	915	1029	0.889		
			64	1454	616	977	0.631		
				1365	841	918	0.916		
				1334	809	897	0.902		
	E70T7-K2	12.7	32	2264	1441	1527	0.944	0.983	0.065
				2309	1529	1557	0.982		
				2294	1447	1547	0.935		
			64	2284	1656	1540	1.076		
				2307	1591	1555	1.023		
				2088	1522	1408	1.081		
		7.9	32	1421	917	958	0.956		
				1485	891	1002	0.889		
				1622	1058	1094	0.967		
			64	1473	1060	993	1.067		
				1572	1002	1060	0.945		
				1387	869	936	0.929		

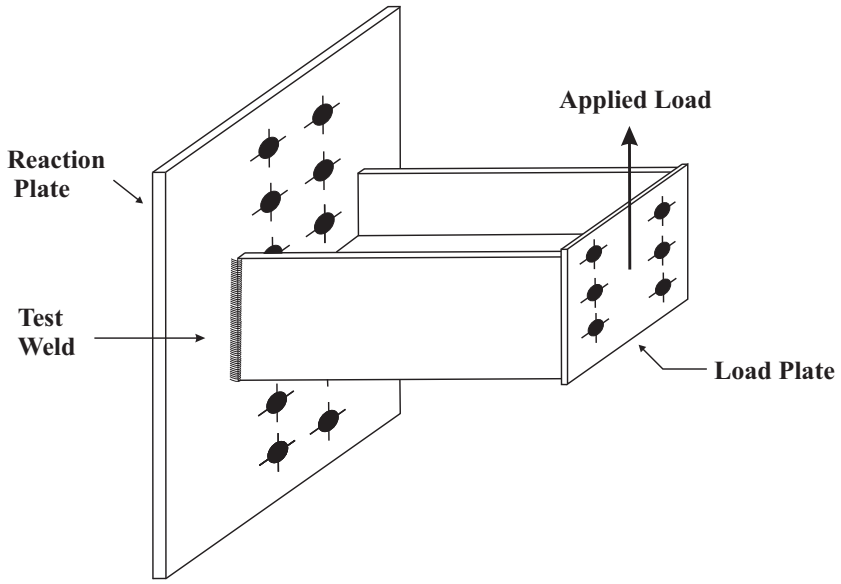

Figure 3.1 – Typical test specimen used in Dawe and Kulak (1972) test program

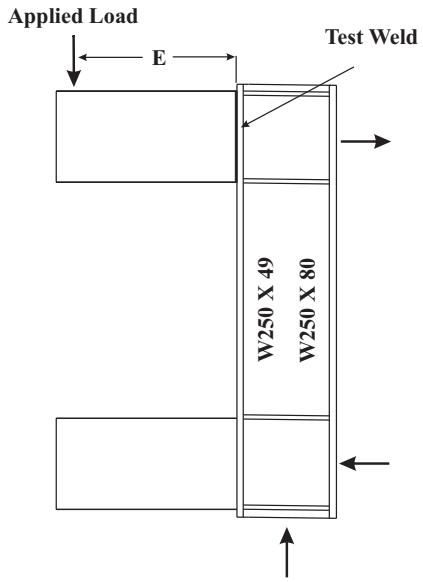

Figure 3.2 – Typical test specimen used in Beaulieu and Picard (1985) test program

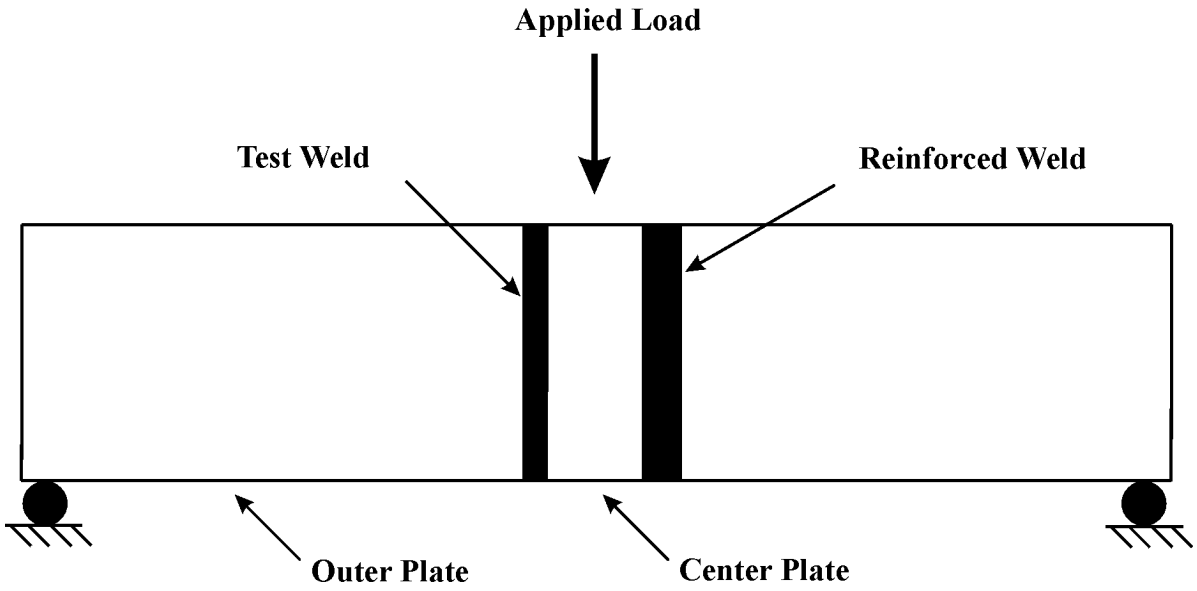

Figure 3.3 – Typical test specimen used in the Gomez *et al.* (2008) test program

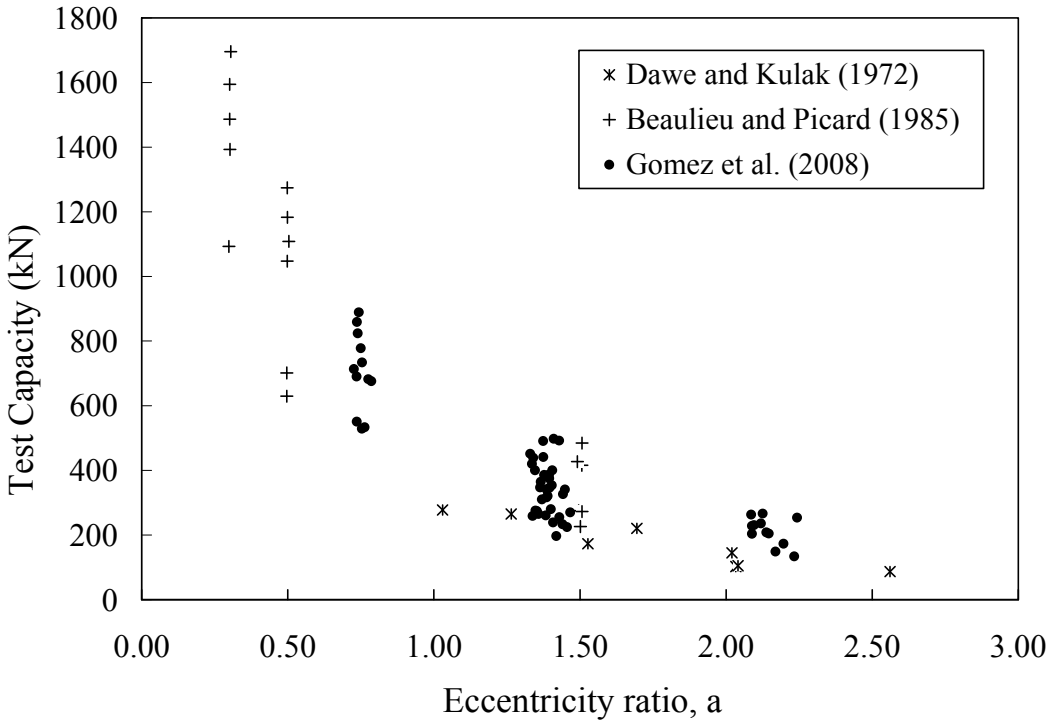

Figure 3.4 – Test capacity versus eccentricity ratio

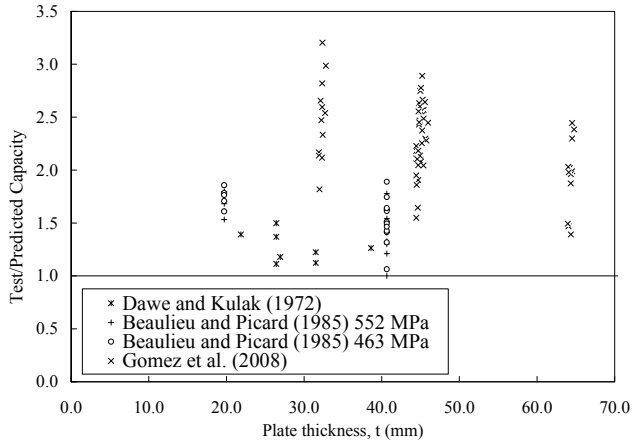

a) Test-to-predicted ratio versus plate thickness

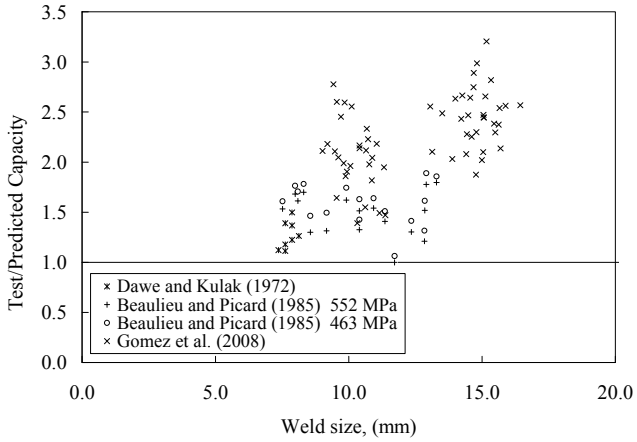

b) Test-to-predicted ratio versus weld size

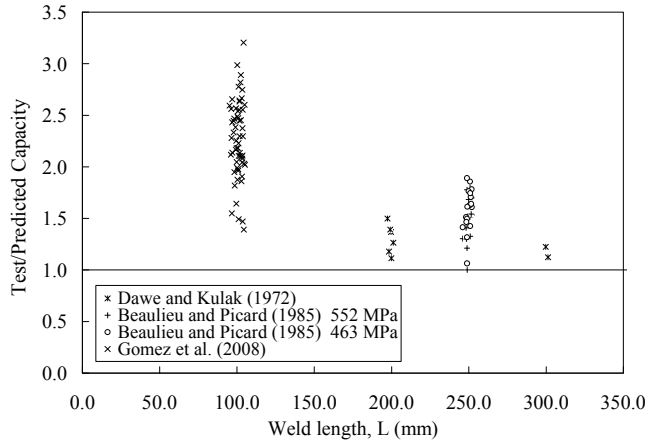

c) Test-to-predicted ratio versus weld length

Figure 3.5 – Modified Model 1 – Test Parameters vs. Test-to-Predicted Ratios

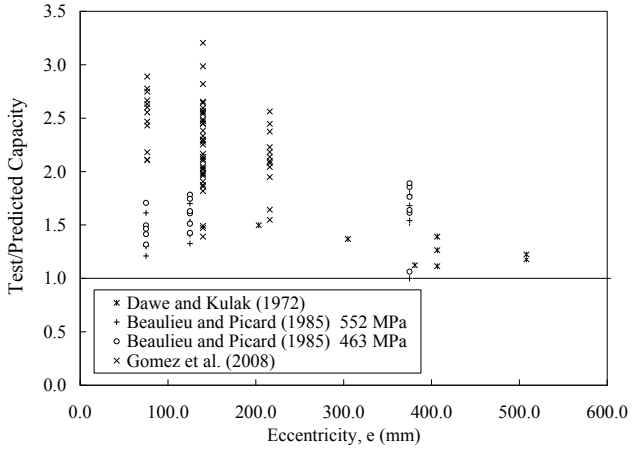

d) Test-to-predicted ratio versus eccentricity

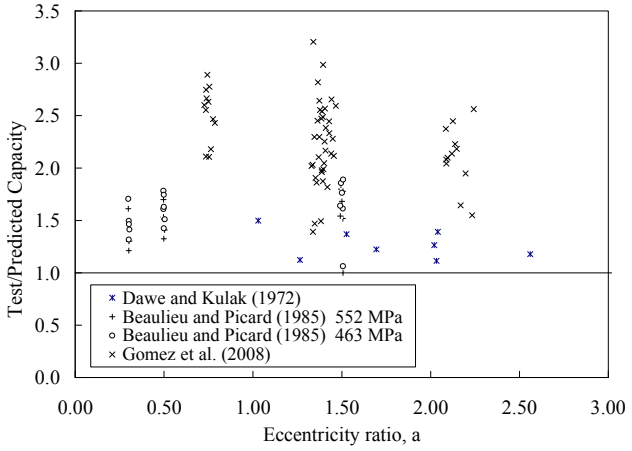

e) Test-to-predicted ratio versus eccentricity ratio

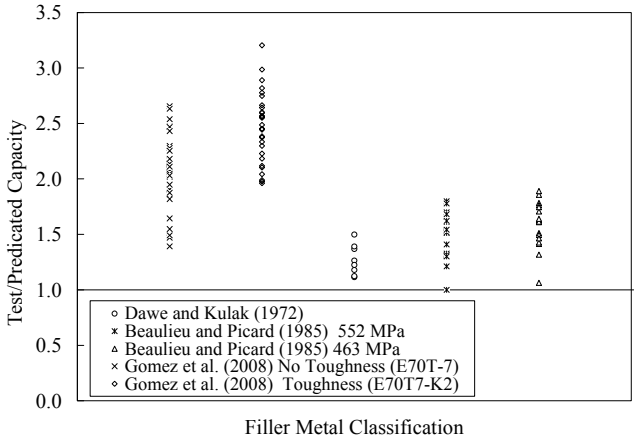

f) Test-to-predicted ratio versus filler metal classification

Figure 3.5 – (cont'd)

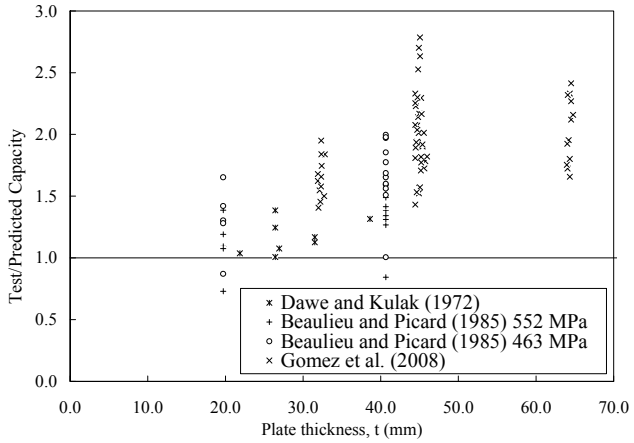

a) Test-to-predicted ratio versus plate thickness

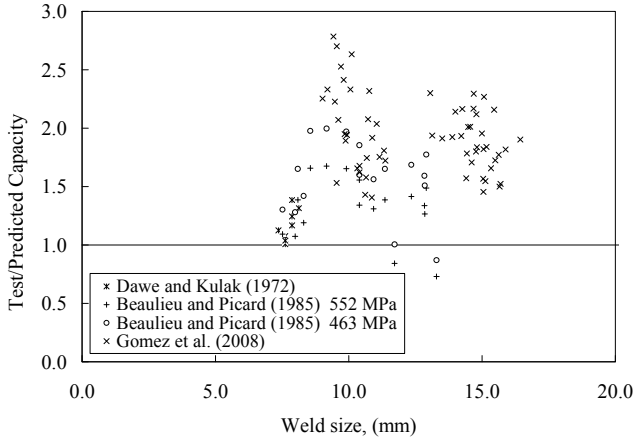

b) Test-to-predicted ratio versus weld size

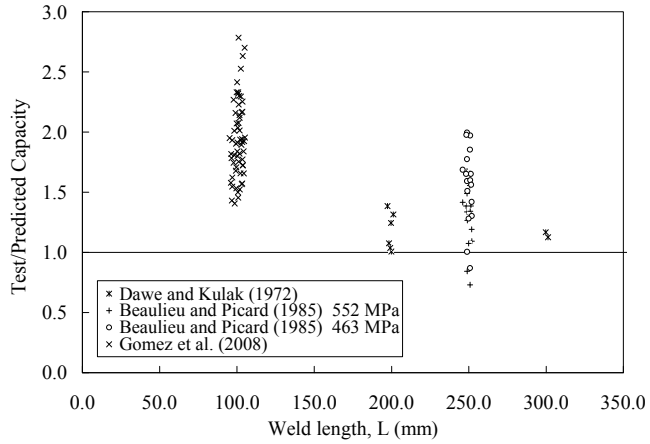

c) Test-to-predicted ratio versus weld length

Figure 3.6 –AISC Approach – Test Parameters vs. Test-to-Predicted Ratios

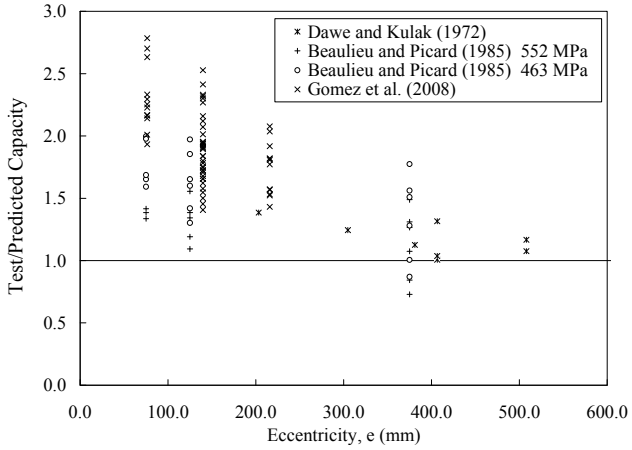

d) Test-to-predicted ratio versus eccentricity

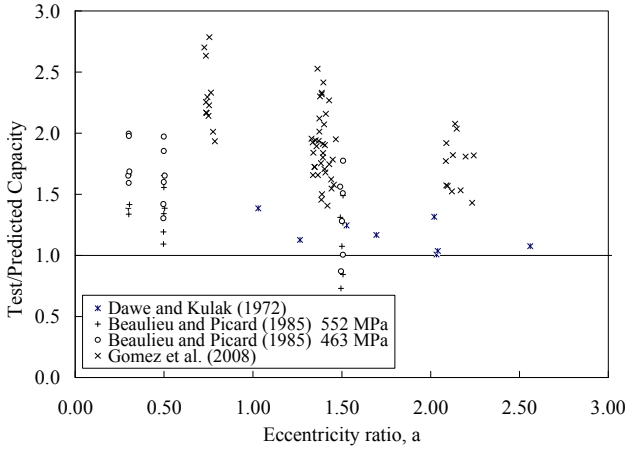

e) Test-to-predicted ratio versus eccentricity ratio

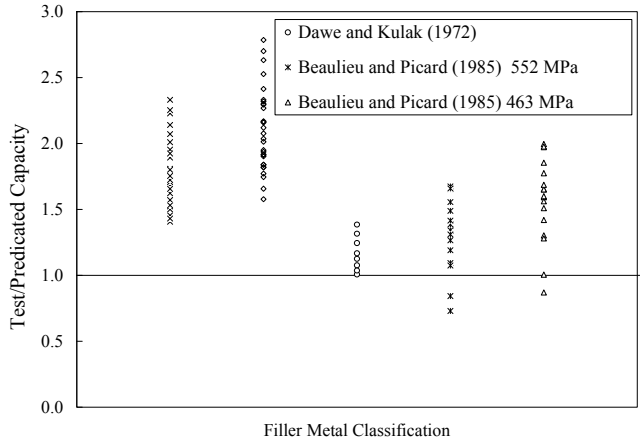

f) Test-to-predicted ratio versus filler metal classification

Figure 3.6 – (cont'd)

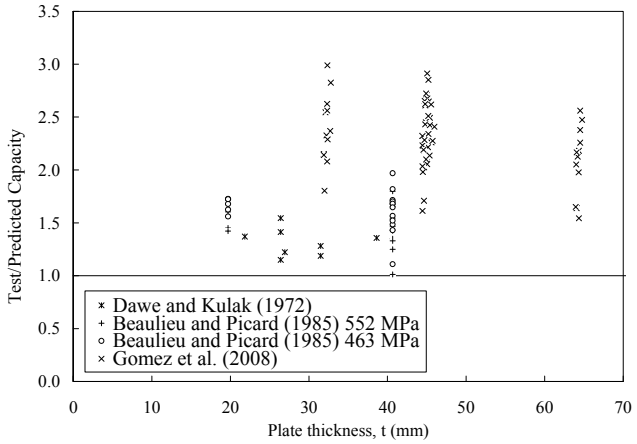

a) Test-to-predicted ratio versus plate thickness

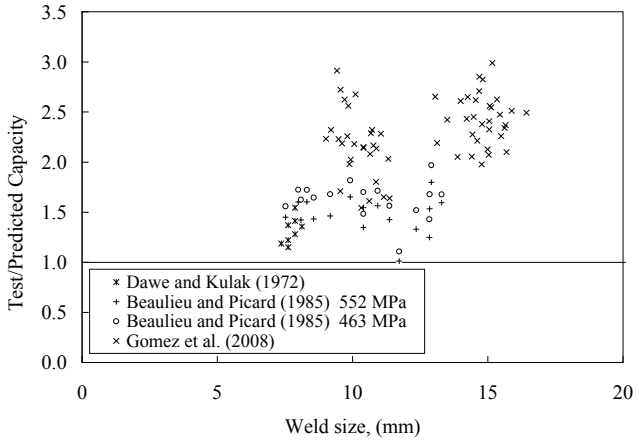

b) Test-to-predicted ratio versus weld size

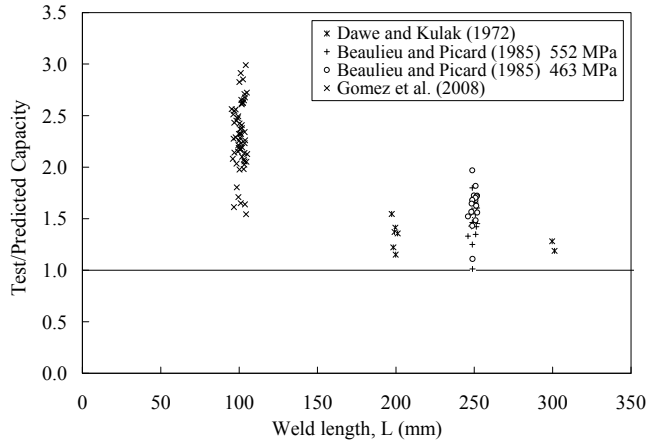

c) Test-to-predicted ratio versus weld length

Figure 3.7 –Ninth Edition of CISC Handbook – Test Parameters vs. Test-to-Predicted Ratios

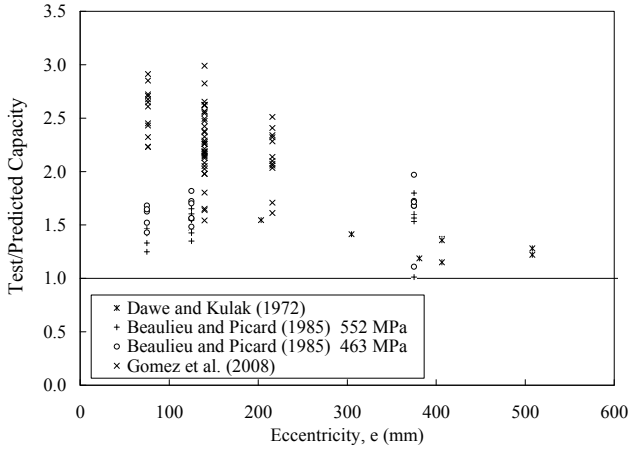

d) Test-to-predicted ratio versus eccentricity

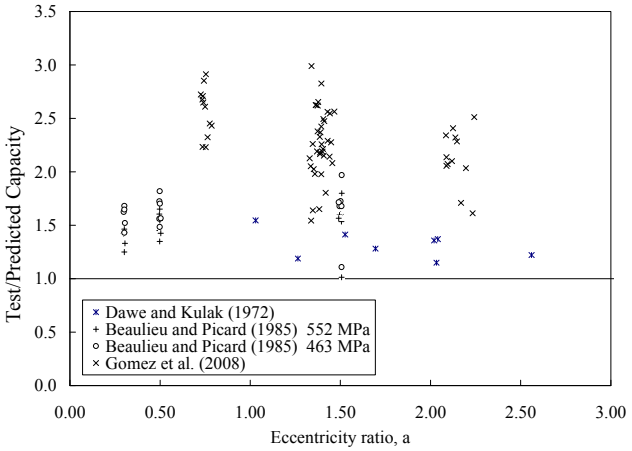

e) Test-to-predicted ratio versus eccentricity ratio

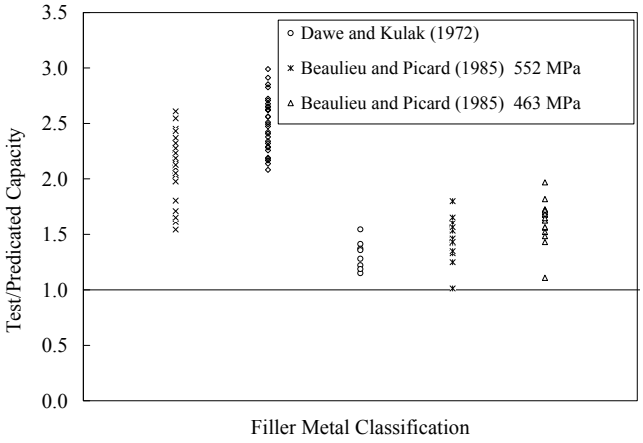

f) Test-to-predicted ratio versus filler metal classification

Figure 3.7 – (cont'd)

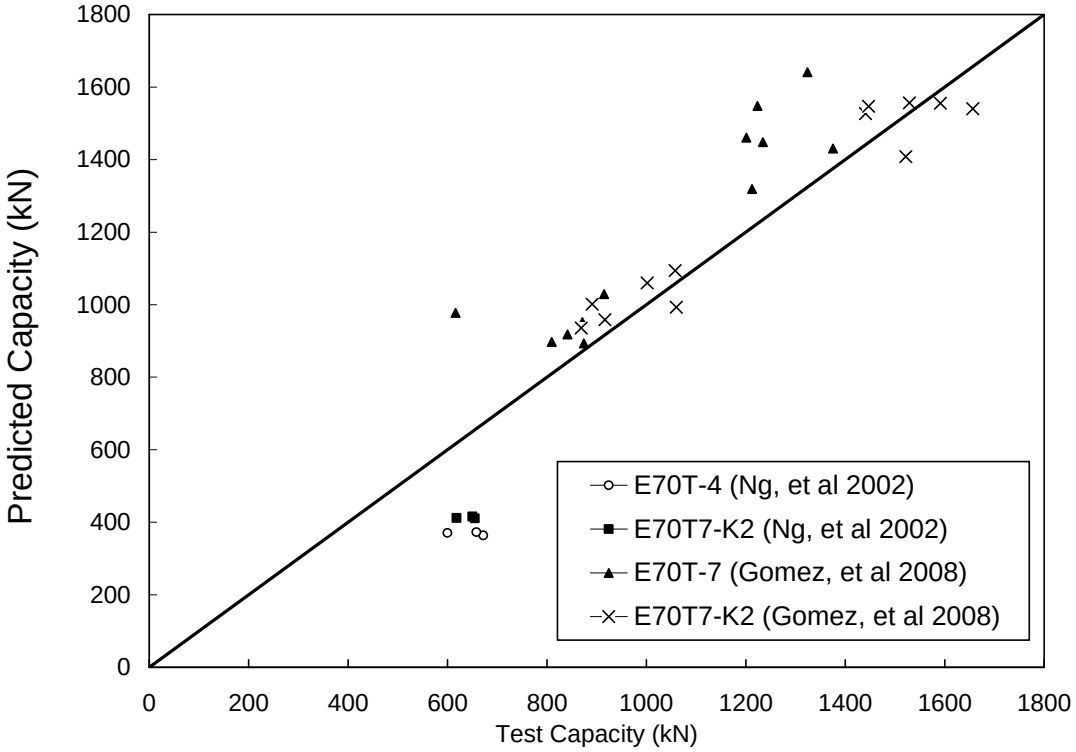

Figure 3.8 – Predicted capacity of cruciform specimens using CISC approach

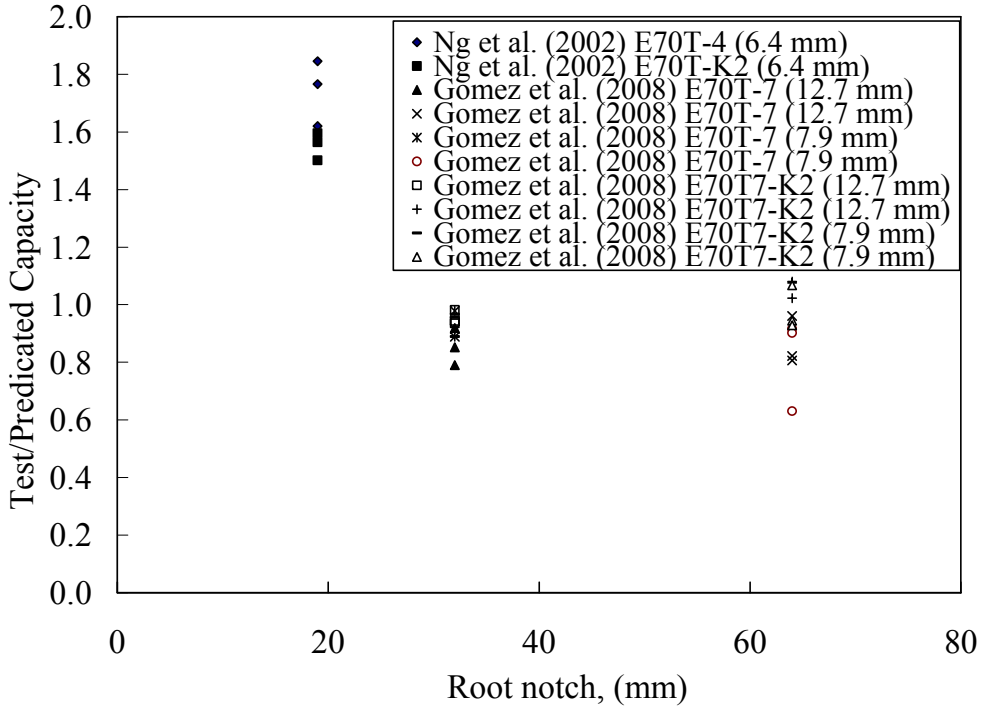

Figure 3.9 – Test-to-predicted ratio versus root notch of cruciform specimens

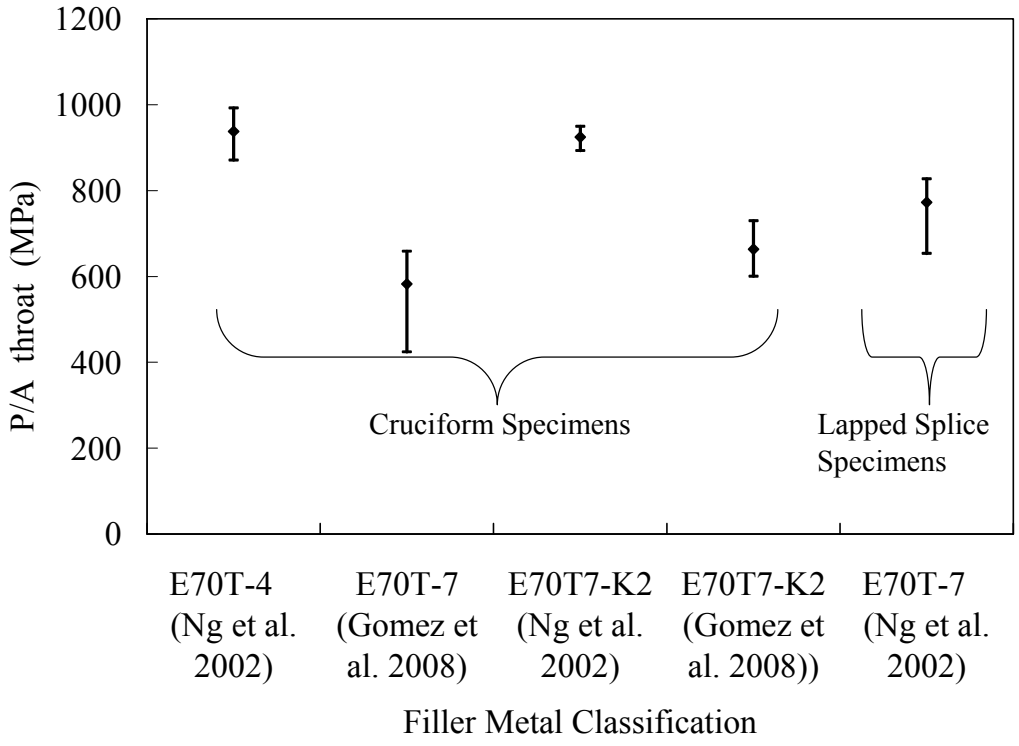

Figure 3.10 – Effect of filler metal classification on fillet weld behaviour

Chapter 4

Analysis and Discussion

4.1 INTRODUCTION

Several strength calculation models have been presented for welded joints with combined out-of-plane bending and shear (Dawe and Kulak, 1972; Neis, 1980; Beaulieu and Picard, 1985). These models, modified versions of these models, and the models used in current North American design practice (AISC, 2005; CISC, 2006) are presented in detail in this chapter. This represents a total of 14 different prediction models, which are evaluated by comparing the capacities predicted by these models with test results from three different sources. The most promising models are then evaluated using a reliability analysis to assess the level of safety provided by each one of them.

4.2 DESCRIPTION OF EXISTING ANALYTICAL MODELS

The majority of the strength prediction models investigated are models proposed to replace the procedure proposed by Dawe and Kulak (1972), which requires an iterative procedure to determine the capacity of welded joints. A review of the various prediction models is first presented. These models will then be assessed by comparing the predicted capacity with test results obtained from three different sources, namely, the test program by Dawe and Kulak (1972), by Beaulieu and Picard (1985), and the recent tests conducted at UC Davis (Gomez *et al.,* 2008) as reported in Chapter 3.

4.2.1 Model 1 – Instantaneous Centre of Rotation Approach Proposed by Dawe and Kulak (1972) with the Load versus Deformation Model of Butler and Kulak (1969)

Dawe and Kulak (1972) proposed an iterative procedure based on the method of instantaneous centre of rotation to predict the ultimate strength of welded joints with out-of-plane eccentricity. The method, illustrated in Figure 4.1, makes use of the instantaneous centre of rotation in the tension zone of the connection and assumes load transfer in the compression zone by bearing of the connected plates. A triangular stress distribution was assumed in the compression zone, with the maximum stress taken as the yield strength of the steel plates. Since the normal force in the compression zone (H_B in Figure 4.1) is carried by bearing of the two plates, the weld in that zone is assumed to carry a vertical force V_B corresponding to the strength of the weld loaded at an angle $\theta = 0°$.

In the original work of Dawe and Kulak, the load versus deformation behaviour of the weld segments in the tension zone followed the model proposed by Butler and Kulak (1969) as presented in Chapter 2.

4.2.2 Model 2 – Modified Dawe and Kulak's Instantaneous Centre of Rotation Approach with the Load versus Deformation Model of Butler and Kulak

Although Dawe and Kulak suggested that a triangular stress block is the most appropriate stress distribution in the compression zone, a rectangular stress block will be investigated since the rectangular stress block is a better representation of the ultimate limit state (full capacity of the connection). The rectangular stress block can develop only if sufficient ductility is available in the tension zone to allow stress redistribution after yielding. The iterative procedure of Dawe and Kulak is therefore investigated with the database of test results presented later in this chapter. The load versus deformation behaviour for the weld still remains that proposed by Butler and Kulak (1969).

4.2.3 Model 3 – Dawe and Kulak's Instantaneous Centre of Rotation Approach with the Load versus Deformation Model of Lesik and Kennedy

The third model consists of the instantaneous centre of rotation approach presented by Dawe and Kulak (1972), with the exception that the load versus deformation behaviour for the welds is the one proposed by Lesik and Kennedy (1990) as presented in Chapter 2. The triangular stress block proposed by Dawe and Kulak for the compression zone is adopted for Model 3.

4.2.4 Model 4 – Modified Dawe and Kulak's Instantaneous Centre of Rotation Approach with the Load versus Deformation Model of Lesik and Kennedy

This model is similar to Model 3 except that it uses a rectangular stress block in the compression zone of the welded joint.

4.2.5 Model 5 – Current AISC Approach

The current method used in the 13th edition of the AISC steel design handbook is based on the instantaneous centre of rotation method and assumes that the compression side of the welded joint transfers forces through the weld only, with no transfer of force in bearing. The method therefore reverts to the instantaneous centre of rotation method originally proposed for joints with in-plane load eccentricity (refer to Figure 4.2). Therefore, this method is identical to the case illustrated in Figure 4.3 where two parallel lines of weld are loaded with in-plane eccentricity.

The load versus deformation relationship for the weld segments proposed by Lesik and Kennedy and presented in Chapter 2 (Equations 2.6 to 2.11) was adopted for the derivation of the design tables in the AISC steel design handbook.

The value of k shown in Figure 4.3 defines the distance between two vertical weld segments as a fraction of the weld length, L. When an eccentric load is applied to a weld

group, each element is subjected to strains proportional to their distance from the instantaneous centre, which is determined iteratively. Since the AISC approach assumes that no load transfer takes place by bearing in the compression zone, the value of k is effectively taken as 0 (Figure 4.4).

4.2.6 Model 6 – Modified AISC Approach with Load versus Deformation Model of Butler and Kulak

This method adopts the load versus deformation model for the welds proposed by Butler and Kulak (1969) as presented in the previous section (Equation 2.1 to Equation 2.5). All other aspects of the model are identical to Model 5.

4.2.7 Model 7 – Models proposed by Neis (1980)

Neis (1980) presented several models to predict the ultimate capacity of welded joints loaded in combined shear and out-of-plane bending. His models offered considerable simplification compared to the iterative procedure proposed by Dawe and Kulak. This simplification resulted in a closed form solution for welded joints with an eccentricity ratio, a, greater than or equal to 0.4. The stress distribution in the weld at rupture is based on the load versus deformation behaviour proposed by Butler and Kulak (1969) for a weld loaded perpendicular to its axis (θ = 90^o). A total of seven different stress distributions, consisting of various combinations of stress block geometries and bearing stress intensities in the compression zone, were investigated. The investigated stress distributions are illustrated in Figure 4.5 and the details of each model are discussed in the following.

4.2.7.1 Case 1

Neis' first case consists of a parabolic stress distribution in the tension zone with the maximum stress at the extreme fibre equal to $1.476\,X_u$. The constant 1.476 reflects the increase in strength of a weld segment loaded perpendicular to the axis of the weld as proposed by Butler and Kulak (1969). A triangular bearing stress distribution is assumed in the compression zone. The limiting bearing stress at the extreme fibre of the plate is equal to the yield strength of the plate, F_y. The capacity of the welded joint, P_u, loaded with an eccentricity e, is given as a function of a non-dimensional factor, Q, as follows:

$$P_u = \frac{F_y t L (1 + 0.2739Q)}{3\,a\,(1 + 0.3093Q)^2} \qquad [4.1]$$

$$Q = \frac{F_y t}{X_u D} \qquad [4.2]$$

$$a = \frac{e}{L} \qquad [4.3]$$

where t is the thickness of the plate, X_u is the tensile strength of the filler metal, L is the length of the weld and D is the weld size.

4.2.7.2 Case 2

The model proposed for Case 2 assumes the same stress distributions as Case 1 except the limiting bearing stress in the compression zone is set to the tensile strength, F_u, of the plates in bearing. The capacity of the eccentrically loaded joint is given as:

$$P_u = \frac{F_u\, t\, L\,(1 + 0.2739 Q_u)}{3\, a\,(1 + 0.3093 Q_u)^2} \qquad [4.4]$$

$$Q_u = \frac{F_u\, t}{X_u\, D} \qquad [4.5]$$

where Q_u is a non-dimensional factor equal to the ratio of the base metal strength to the weld metal strength.

4.2.7.3 Case 3

In this model a triangular stress distribution is adopted in the tension and the compression zones. The maximum stress in the tension zone is taken as $1.476\, X_u$ and F_u in the compression zone. The resulting predicted capacity is given as:

$$P_u = \frac{F_u\, t\, L}{3\, a\,(1 + 0.4791 Q_u)} \qquad [4.6]$$

4.2.7.4 Case 4

As for Case 1, Neis suggested a parabolic stress distribution in the tension zone with a maximum stress of $1.476\, X_u$ at the extreme fibre. The stress in the compression zone is represented by a rectangular stress block with a magnitude equal to the yield strength of the plate, F_y. The joint capacity is given as:

$$P_u = \frac{F_y\, t\, L\,(1 + 0.7304 Q)}{2\, a\,(1 + 0.6186 Q)^2} \qquad [4.7]$$

where Q is as defined by Equation 4.2.

4.2.7.5 Case 5

This case represents the upper bound of all the cases investigated by Neis. The stresses are assumed to be constant along the weld length in both tension and compression zones.

Neis suggested using $1.414\,X_u$ as the tensile stress and the yield strength of the plate, F_y, as the compressive stress. The joint capacity predicted from this model is given as:

$$P_u = \frac{F_y\,t\,L}{a\,(2+Q)} \qquad [4.8]$$

where Q is as defined by Equation 4.2.

4.2.7.6 Case 6

This case was proposed for thick plates ($2.09 < Q \leq 3.5$) where the ultimate strength of welded joint is reached as the rupture of the weld may occur before yielding of the plate. Neis proposed linear stress distributions in the tension and compression zones. The maximum stresses in the extreme fibre in tension and compression zones are taken as $1.476\,X_u$ and F_y, respectively. The capacity of the welded joint is given as:

$$P_u = \frac{F_y\,t\,L}{3\,a\,(1+0.479Q)} \qquad [4.9]$$

4.2.7.7 Case 7

Case 7 was proposed for the thin plates ($0.6 \leq Q \leq 2.09$) where the plate material yields before the weld deforms sufficiently to rupture. The central portion of the cross-section is assumed to carry the shear load and is taken as $0.577\,F_y$ based on the Hencky-von Mises yield condition. Constant stress distribution is assumed along the weld length. In the tension and compression zone, the stress is taken as F_y. The resulting connection capacity is expressed as:

$$P_u = 0.577 F_y\,t\,L\left(\sqrt{1+1.332\,a^2} - 1.154\,a\right) \qquad [4.10]$$

4.2.8 Model 8 – Model Proposed by Picard and Beaulieu (1991) (CISC Approach)

Picard and Beaulieu (1991) presented the results of an experimental investigation of welded joints with out-of-plane eccentricity and an evaluation of the model proposed by Dawe and Kulak and the models presented by Neis. Using an approach similar to that proposed by Neis (1980) a new model that agreed well with the more complex procedure of Dawe and Kulak was proposed. The new model is based on the stress distribution shown in Figure 4.6 where the stress in the tension zone is based on the load versus deformation behaviour proposed by Lesik and Kennedy (1990) for a weld loaded perpendicular to its axis ($\theta = 90^o$) and the stress in the compression zone, resulting from bearing of the steel plates, is equal to the yield strength of the connected plates. The model proposed by Beaulieu and Picard also assumes that the weld area on the tension side of the joint is equal to the leg area rather than the throat area. This closed form solution is based on the assumption that the moment on the welded joint is sufficiently large to make the shear contribution negligible. Therefore, the use of this model was

limited to values of eccentricity factor, a, greater than 0.4. For smaller values of a, it was recommended that a parabolic interpolation between P_0 (the resistance of the joint with no eccentricity) and $P_{0.4}$ (the resistance of the joint with $a = 0.40$) be used. This model was adopted by CISC in the latest edition of the CISC Handbook of Steel Construction (CISC, 2006). The predicted welded joint capacity is therefore given as:

$$P_u = \frac{0.5F_y tL}{a(Q+2)} \qquad a \geq 0.40 \text{ and } t \leq 40\text{mm} \qquad [4.11]$$

where

$$Q = \frac{F_y t}{X_u D}$$

$$P_u = P_0 + \frac{a^2(P_{0.4} - P_0)}{0.16} \qquad a < 0.40 \text{ and } t \leq 40\text{mm} \qquad [4.12]$$

where $P_0 = 2(0.67)0.7071X_u DL$ and $P_{0.4} = P_u$ calculated using Equation 4.11 for $a = 0.4$

The reduction factor of 0.5 in the Equation 4.11 was proposed to give results in very close agreement with the design table provided in the previous edition of the CISC Handbook.

4.3 EVALUATION OF THE EXISTING MODELS

A total of 14 analytical models are available for the prediction of the weld capacities of specimens from three different sources: Dawe and Kulak (1972), Beaulieu and Picard (1985) and UC Davis (Gomez *et al.,* 2008). A comparison of the test results with the joint capacities predicted using the models presented above are summarized in Table 4.1.

As detailed in Appendix A, the models that are based on the instantaneous centre of rotation method, Models 1 to 6, are applicable to all ranges of load eccentricity. However, the cases considered in Model 7 are limited to joints loaded with a large eccentricity ($a > 0.4$). Model 8, which was proposed by Beaulieu and Picard, contains two equations to cover the full range of load eccentricity. All the test specimens from Dawe and Kulak had a large eccentricity and hence all eight specimens are considered in the models. Out of the 22 welded joints tested by Beaulieu and Picard (1985), 17 failed in the weld. These 17 test results are used to assess Models 1 to 6 and 8. Only 11 test results from the Beaulieu and Picard test program are used to assess all cases of Model 7 since only these specimens satisfied the eccentricity requirement for Model 7 ($a > 0.4$). All the 60 test results from UC Davis (Gomez *et al.,* 2008) were loaded with a load eccentricity ratio greater than 0.4 and none failed in the plate. Therefore, all the test results from the UC Davis (Gomez *et al.,* 2008) test program were compared with the 14 different models.

4.3.1 Prediction of test results

The test results from various test programs were compared with the current prediction methods used in AISC, CISC and modified Model 1 and the results of these comparisons were presented in Chapter 3. In these comparisons the weld shear strength was taken as 0.6 times the tensile strength of the weld metal for the AISC approach and 0.67 times the tensile strength of the weld metal for the CISC approach (9^{th} edition of the CISC steel design handbook) (see Equation 2.6). In order to conduct a reliability analysis for the various prediction models, all the sources of variation must be accounted for. One of these sources of variation is the shear strength of the weld metal, explicitly used in all the models based on the Lesik and Kennedy weld strength model. The shear strength is expressed as a constant (shear factor), taken as 0.6 in the AISC specification (AISC, 2005) or 0.67 in Canadian standard CSA-S16 (CSA, 2001), times the tensile strength, X_u. Therefore, the bias coefficient and coefficient of variation (COV) for the shear strength can be evaluated by assessing these two statistical parameters for the tensile strength and the shear factor (0.6 for the AISC approach and 0.67 for the CISC approach). When evaluating the professional factor (ratio of test capacity to the predicted capacity using measured dimensions and material properties) required for the reliability analysis, the actual shear strength of the weld metal must be used. A shear factor representative of the actual shear strength of the weld metal is therefore required. As explained in detail in section 4.5, the ratio of shear strength to tensile strength for weld metal was evaluated from tests conducted by Deng *et al.* (2003). The shear factor is found to be 0.78. This shear factor is used in the calculation of the predicted test capacity rather than the nominal value of 0.6 currently used in AISC (2005) or 0.67 used in CSA (2001). The discrepancy between the actual shear factor (0.78) and the design shear factor (0.6 for the AISC design approach and 0.67 for the CISC design approach) will be accounted for in the reliability analysis through the introduction of a second material factor.

4.3.2 Comparison of test results with predicted capacity

The mean test-to-predicted ratio and the COV are used as a measure of the ability of each model to predict the test capacities. Because Beaulieu and Picard did not measure the weld metal tensile strength directly, the predicted values for their test specimens were calculated using two values of tensile strength for the weld metal, namely, 463 MPa, which was deduced from the results of their tests on lapped joints with transverse or longitudinal welds, and 552 MPa, obtained from material test results published by Fisher *et al*. (1978), Pham (1981), Miazga and Kennedy (1986) and Gagnon and Kennedy (1987). As indicated in Chapter 3, the tensile strength for the weld metal used in the test program by Dawe and Kulak was taken as 462 MPa based on weld metal tests on similar electrode designation reported by other researchers. For all the 14 models investigated, the professional factor ranges from 1.044 to 1.934 and the coefficient of variation varies from 0.225 to 0.259.

Table 4.1 indicates that the UC Davis (Gomez *et al.,* 2008) test data lead to a higher professional factor than those of Dawe and Kulak and Beaulieu and Picard. However, an

investigation of the various test programs presented in Chapter 3 indicated that the difference in capacities observed in the UC Davis (Gomez *et al.,* 2008) test specimens is neither caused by the dissimilarity in material properties of the specimens nor the method of loading. The difference is believed to be caused by changes in the filler metal properties over time.

The COV for the pooled data is relatively large at values of 0.225 to 0.259 for all models investigated. However, Table 4.1 indicates that the COV within individual test programs is significantly lower. In an attempt to identify the source of variation of the test-to-predicted ratio, its value was plotted against various geometric parameters such as plate thickness, eccentricity, weld length, weld size, eccentricity ratio and filler metal classification. The plots were used to determine whether a trend exists between the test-to-predicted ratio and any of these parameters.

4.3.2.1 Model 1 – Dawe and Kulak's Instantaneous Centre of Rotation Approach with the Load versus Deformation Model of Butler and Kulak

Model 1 provides conservative predictions. However, the predicted capacities of Dawe and Kulak's data set are higher than the measured capacities. The mean test-to-predicted ratio for this test program is 0.851. The COV for the data sets from Dawe and Kulak, Beaulieu and Picard and UC Davis (Gomez *et al.,* 2008) vary from 11 to 17%, with a COV of about 26% for the pooled data.

The effect of various geometric parameters and filler metal classification are examined independently in Figure 4.7. Although the variability in the test-to-predicted ratio is large there is a visibly noticeable tendency of the test-to-predicted value to decrease as the weld length increases, and to be larger for filler metals with toughness requirement. No trend is apparent between the test-to-predicted ratio and the other parameters presented in Figure 4.7. However, because of the large scatter in the test-to-predicted values, the observed trend is statistically insignificant. The fact that weld size, plate thickness and load eccentricity and eccentricity ratio do not show any correlation with the test-to-predicted ratio indicates that these parameters are accounted for suitably in the prediction model. Although there seems to be a weld length effect, this effect disappears when plotted as the ratio of eccentricity to weld length, thus indicating that the weld length parameter is also accounted for suitably in the model. The model, however, does not account for weld toughness. It seems from this analysis that weld toughness might have an effect on the strength of eccentrically loaded welded joints. None of the models investigated here account for the weld metal toughness.

4.3.2.2 Model 2 – Modified Dawe and Kulak's Instantaneous Centre of Rotation Approach with the Load versus Deformation Model of Butler and Kulak

Because this model assumes a rectangular stress block in the compression zone of the joint rather than the triangular stress block assumed in Model 1, this model predicts a higher capacity than Model 1. It generally overestimates the capacity of the specimens tested by Dawe and Kulak and Beaulieu and Picard, but provides a generally conservative estimate of the test results from UC Davis (Gomez *et al.,* 2008). The test-to-predicted

ratio for the three test programs varies from 0.671 to 1.175 with an overall average of 1.065. The COV varies from 0.10 to 0.14, with an overall value of 24%.

The plots of test-to-predicted ratio versus geometric parameters and filler metal toughness requirement are shown in Figures 4.8a to 4.8f. The plots have similar appearance to the plots for Model 1, showing similar trend with a change in weld length and filler metal toughness requirement. It should be noted that scatter in the test-to-predicted values for Model 2 is smaller than the scatter observed for Model 1. Nevertheless, the observed trend between the test-to-predicted ratio and the weld length is still statistically insignificant at a level of significance of 5%.

4.3.2.3 Model 3 – Dawe and Kulak's Instantaneous Centre of Rotation Approach with the Load versus Deformation Model of Lesik and Kennedy

Compared to Model 1, the Lesik and Kennedy load versus deformation curves implemented in Model 3 gives a more conservative prediction of joint capacity and leads to slightly less scatter.

From Figures 4.9a to 4.9c similar trends to those observed for the earlier two models are also observed for Model 3. Both the weld length and the toughness requirement show up as influential, although this influence is statistically insignificant.

4.3.2.4 Model 4 – Modified Dawe and Kulak's Instantaneous Centre of Rotation Approach with the Load versus Deformation Model of Lesik and Kennedy

As expected, since the model is based on Model 3, but modified with a rectangular stress block, it is less conservative for all three sources of data as shown in Table 4.1. Model 4 overestimates the joint capacity for the specimens tested by Dawe and Kulak, with a mean professional factor of 0.760 and a COV of 0.10. The model provides generally conservative predictions of the test results from the UC Davis (Gomez *et al.,* 2008) test program, but over predicts the capacity of the test specimens from Dawe and Kulak considerably.

Once again, the same trends observed in the previous models are observed for Model 4. Figures 4.10a to 4.10f show that the weld length and toughness requirement seem to have an effect on the joint strength, however, this effect is statistically insignificant.

4.3.2.5 Model 5 – Current AISC Approach

A discussion of the current AISC approach was presented in Chapter 3. Table 4.1 and Figures 4.11a to 4.11f present the test-to-predicted ratios for this model and the effect of various geometric parameters on the test-to-predicted ratio. The mean test-to-predicted ratio for all the test specimens examined is 1.38.

Figure 4.11a indicates that, in contrast to the previously examined models, the test-to-predicted ratio for the AISC model increases with an increase in plate thickness, indicating that the plate thickness should be incorporated into the prediction model.

Figure 4.11c indicates that there is also an influence of the weld length. As for the other models, the effect of weld size and load eccentricity on the test-to-predicted ratio is negligible.

4.3.2.6 Model 6 – Modified AISC Approach with Load–Deformation Model of Butler and Kulak

This model is a modified version of the AISC approach where the load versus weld deformation relationship of Lesik and Kennedy is replaced by the load versus deformation relationship proposed by Butler and Kulak. As for the AISC model, load transfer in the compression side of the connection is assumed to be through the weld only.

Table 4.1 shows that the predicted capacities are conservative for the test specimens from the UC Davis (Gomez *et al.,* 2008) test program only. The model over-estimates the joint capacity of the specimens from Dawe and Kulak and Beaulieu and Picard, giving professional factors of 0.735 and 0.938, respectively. The COV for the tests from Dawe and Kulak is 0.11 and 0.19 for the test program by Beaulieu and Picard. The model gives conservative prediction for the joints tested at UC Davis (Gomez *et al.,* 2008), with a mean professional factor of 1.215 and COV of 16%. The overall professional factor is 1.114 and COV is 22%.

Plots of test-to-predicted ratio versus geometric parameters are presented in Figures 4.12a to 4.12f. The plots have comparable behaviours as observed for Model 5, however, the data points show less dispersion than in Model 5.

4.3.2.7 Model 7 – Models proposed by Neis (1980)

Neis (1980) proposed seven different models with varying stress distributions and magnitudes. Test-to-predicted ratios for all seven models, designated as Case 1 to Case 7, were calculated and the results are presented below.

Case 1

The overall test-to-predicted ratio for all the combined test programs predicted by Neis Model Case 1 is 1.337 and the COV is 0.23. The test-to-predicted ratio and COV for each individual data set are presented in Table 4.1 where they are ranging from 0.827 to 1.459 and 0.10 to 0.16, respectively. A comparison with Models 1 and 2 indicates that the results from Case 1 model lie between the two models.

In Figures 4.13a to 4.13f, the test-to-predicted ratios are plotted against the plate thickness, weld size, weld length, eccentricity, eccentricity ratio and filler metal classification. It is observed that the parameters of plate thickness, weld size and load eccentricity and eccentricity ratio do not have any direct relationships to the test-to-predicted ratio as the data points are dispersed randomly in the plots. However, as for Models 1 to 6 there seems to be a weak correlation with weld length and weld metal classification.

Case 2

The mean test-to-predicted value and its COV for the all the test data collected are 1.117 and 25%, respectively. As for Case 1, this model over-predicts the weld capacities for the specimens tested by Dawe and Kulak and Beaulieu and Picard, with mean test-to-predicted values of 0.63 and 0.81, respectively.

Since Case 2 the tensile strength of the steel plate rather than the yield strength in the compression zone, the model is expected to yield a higher predicted capacity than the model in Case 1. This is demonstrated by the lower test-to-predicted values, which are significantly below 1.0 for the specimens from the early test programs. Plots of test-to-predicted ratios versus various parameters presented in Figures 4.14a to 4.14f show similar trends as were observed for the model of Case 1.

Case 3

The test-to-predicted ratios tabulated in Table 4.1 for the specimens of all three test programs range from 0.808 to 1.467. The COV ranges from 0.10 to 0.14 and it increases to 0.23 when all the test results are pooled together. This case is basically a modification of Case 2 as a triangular stress block is assumed in the tension zone instead of the parabolic stress block used in Case 2.

The test-to-predicted ratios are plotted against the geometric parameters such as plate thickness, weld size, weld length, eccentricity, eccentricity ratio and filler metal classification in Figures 4.15a to 4.15f. The scatter in the test data is similar to that observed in the previous models proposed by Neis. It is concluded that the plate thickness, weld size and weld length are not factors that directly influence test-to-predicted ratios.

Case 4

For this case, the triangular stress block used for Case 1 is replaced by a rectangular stress block, resulting in a higher predicted capacity. The overall test-to-predicted ratio is 1.071 and it is on the lower range as comparing with other models and cases. The test-to-predicted ratios for three data sets are 0.670 for Dawe and Kulak and 0.833 for Beaulieu and Picard and 1.168 for UC Davis (Gomez *et al.,* 2008). The respective COVs are 10%, 13% and 14% and the overall COV is 22%.

Comparisons between test-to-predicted ratio on the weld capacities and the geometric parameters of specimen have been made and reported in Figures 4.16a to 4.16f. The data points appear in narrow bands in all plots as contrast to the plots for Case 1 in Neis' Model (Figures 4.13a to 4.13f).

Case 5

The parabolic stress blocks adopted in the tension and compression zone is replaced by the parabola stress block in the tension zone. The predicted weld capacity would further

increase as the extra resistance is provided in the tension zone. The test-to-predicted ratio values and the COVs for all data sets are presented in Table 4.1 and they are ranging from 0.658 to 1.148 and 10% to 14%, respectively. The lowest test-to-predicted ratio is also found in this case, it is reported as 1.053 and its COV is 22%.

Figures 4.17a to 4.17f show the plots that compare the test-to-predicted ratio to the geometric parameters. The data points are further condensed as comparing with the plots for Case 4 (Figures 4.16a to 4.16f). As similar to Case 4, the plate thickness, weld size and weld size have made no effects on the test-to-predicted ratios.

Combined Case 6 and Case 7

The Q parameters for the specimens being tested are ranging from 0.73 to 3.66. Case 6 is formulated for thick connecting plates with large values of Q, between 2.09 and 3.5. Case 7 is formulated for thin connecting plates with small values of Q, between 0.6 and 2.09. The combined Case 6 and Case 7, cover the full test program. The test-to-predicted weld capacity ratios and COVs by using Model 7 Case 6 and Case 7 are presented in Table 4.1. The test-to-predicted ratios for 3 data sets are ranging from 0.937 to 1.556 where the overall is 1.446. The COVs are ranging from 12% to 17% with an overall COV of 22%. These combined cases give higher predicted capacity than the other cases.

The test-to-predicted ratio is made comparison to the geometric parameters, and the plots are presented in Figures 4.18a to 4.18f. The effects occur in all plots and the overall appearances of plots remain unchanged.

4.3.2.8 Model 8 – Model Proposed by Picard and Beaulieu (1991)

This model was adopted in the ninth edition of the CISC Handbook of Steel Construction (CISC 2006). The original model proposed by Beaulieu and Picard provides the most promising predictions on the weld capacity from all the models using Lesik and Kennedy load deformation relationship. In the later stage of their derivation of a simplified closed form model, Beaulieu and Picard applied a reduction factor of 0.5 to their original model to get good agreement with the previous CISC design table, which was based on Model 1 by Dawe and Kulak. As mentioned above, this model contains two equations to account for specimens subject to small eccentricity ratio ($a < 0.4$) and large eccentricity ratio ($a \geq 0.4$). Only five specimens fall in the category of small eccentricity and they are all from the test program presented by Beaulieu and Picard. As shown in Table 4.1, the test-to-predicted ratio is 1.403 and COV is 0.064. A total of 80 specimens from all three test programs satisfy the requirement for large eccentricity. The test-to-predicted ratio for these test specimens from Dawe and Kulak, Beaulieu and Picard and UC Davis (Gomez *et al.,* 2008) are 1.215, 1.524 and 2.134, respectively. The COVs are 10%, 13% and 15%, respectively. The overall test-to-predicted ratio and COV for all the test specimens with large eccentricity are 1.951 and 22%, respectively.

The comparisons between the geometric parameters and test-to-predicted ratio of weld capacity are presented in Figures 4.19a to 4.19f. Figure 4.19a shows that Model 8 gives a

slightly higher test-to-predicted ratio for the UC Davis specimens with plate thickness of 31.8 mm compared to the values predicted using the model currently used in the ASIC Steel Construction Manual (Model 5) (see Figure 4.11a). The other data points are similar in both plots. However, the trends observed for the two models are reversed: the AISC model shows an upward trend as plate thickness increases whereas Model 8 shows a downward trend. In Figure 4.19b, the data points predicted by Model 8 for weld size less than 12.7 mm. are similar to the data points in Figure 4.11b for Model 5. For the specimens with weld size larger than 12.7 mm, Model 8 gives higher test-to-predicted ratio and is found to be more conservative than Model 5. The data points shown in Figure 4.19c for test-to-predicted ratio versus weld length are dispersed as randomly as in Figure 4.11c for Model 5. Once again, the test-to-predicted value seems to be influenced by the weld metal classification as shown in Figure 4.19f.

4.4 SEGREGATION OF TEST SPECIMENS IN ACCORDANCE TO TOUGHNESS REQUIREMENT

The welded joint specimens tested at UC Davis (Gomez *et al.,* 2008) and prepared with the toughness rated filler metal E70T7-K2 showed higher weld strengths than those with non toughness rated filler metal. Because the higher strength of these test specimens tend to increase the overall test-to-predicted value. When the test specimens with toughness rated filler metal are combined with the other specimens the COV for the overall data set also increases. It was necessary to consider the specimens with toughness and without toughness requirements separately in the reliability analysis. The data set that gives the lower resistance factor should be adopted for design. Only the test program conducted at UC Davis (Gomez *et al.,* 2008) reported the filler metal classification for the specimens. Although the classification of the filler metals used in the Dawe and Kulak (1972) and Beaulieu and Picard (1985) test programs were not reported, they were all considered as filler metals with no toughness requirement.

Although 14 different strength prediction models are evaluated, the models that are based on the load versus deformation behaviour proposed by Lesik and Kennedy (1990), namely, Models 4, 5 and 8, will be receiving more attention for the following three reasons: 1) the load versus deformation model for fillet welds proposed by Lesik and Kennedy has received general acceptance in North American design codes; 2) the equation proposed by Lesik and Kennedy was developed based on various weld sizes whereas Butler and Kulak's model was developed based on tests conducted on 6.4 mm (1/4 in.) welds only (Ng *et al.* (2002) found that smaller fillet welds tend to provide significantly higher unit strength than larger welds); 3) Models 4, 5 and 8 all show promising predictions when considering all available test results.

The test-to-predicted ratios for the specimens prepared with weld with no toughness requirement and those prepared with toughness requirement are presented in Tables 4.2 and 4.3, respectively. Thus, the effect of filler metal classification is eliminated. The resulting test-to-predicted ratios for the specimens with no toughness requirement show a mean value closer to 1.0 and a lower COV.

4.5 RELIABILITY ANALYSIS

The level of safety is assessed for each of the proposed strength prediction models. The traditional target safety index, β, is usually taken as 3.0 for ductile structures but can be as high as 4.0 to 4.5 for parts of structures that require a reduced probability of failure, such as connections. The safety index is directly related to the probability of failure (ratio of resistance to demand under loading R/D $\leq$ 1.0) as shown in Figure 4.20. Using a log-normal distribution for the frequency distribution of R/D, the safety index represents the distance between the mean value of the natural log of R/D and a value ln(R/D) = 0.0, measured in terms of the standard deviation of ln(R/D). The safety index for each model is unique as the procedure to obtain the joint capacity varies between models. It can be determined by using the equation for the resistance factor, ϕ, which was originally proposed by Galambos and Ravindra (1978):

$$\phi = C\rho_R \exp(-\beta\alpha_R V_R) \qquad [4.13]$$

The separation variable, α_R, is set to 0.55 as proposed by Galambos and Ravindra. C is an adjustment factor for modifying the resistance factor for cases where β adopts a value other than 3.0. An equation for C, derived using a procedure proposed by Fisher *et al*. (1978) for welded and bolted connections, is adopted to calculate the adjustment factor for a live to dead load ratio of 3.0:

$$C = 0.0078\beta^2 - 0.156\beta + 1.400 \qquad [4.14]$$

It should be noted that the above equation is applicable for a range of safety index from 1.5 to 6.0. For values of β greater than 6.0, the probability of failure is so low that any refinement in the resistance factor is unwarranted.

The bias coefficient for the resistance, ρ_R, represents the ratio of the expected mean resistance to the nominal resistance and V_R is a function of the variability in the parameters that define the strength. These statistical parameters can be obtained as:

$$\rho_R = \rho_G \rho_M \rho_P \qquad [4.15]$$

and the associated coefficient of variation, V_R, is given as:

$$V_R^2 = V_G^2 + V_M^2 + V_P^2 \qquad [4.16]$$

where the geometric parameter, ρ_G, is the ratio of mean-to-nominal relevant geometric properties such as the throat area, and V_G is the associated coefficient of variation. It can be calculated as the mean value of the ratio of the measured throat dimension (*MTD*) to 0.707 times the nominal weld leg size, namely,

$$\rho_G = Mean\left(\frac{MTD}{0.707 \times (\text{nominal weld leg size})}\right) \qquad [4.17]$$

Due to the difference in reported test data, *MTD* was calculated differently for the Dawe and Kulak, the Beaulieu and Picard and the UC Davis (Gomez *et al.,* 2008) test programs. Dawe and Kulak reported only the average of the tension and shear leg sizes. Beaulieu and Picard also reported only the average of the shear and tension leg sizes although both legs were reportedly measured at several locations (Werren, 1984). Therefore, *MTD* for this test data is calculated as:

$$MTD = 0.707 \times \frac{s_1 + s_2}{2} \qquad [4.18]$$

where s_1 and s_2 are the two weld leg sizes. For the data from UC Davis (Gomez *et al.,* 2008), the two leg sizes were measured and reported. In here, MTD is taken as the minimum throat dimension, obtained from the measured size of the two weld leg:

$$MTD = \frac{s_1 \times s_2}{\sqrt{s_1^2 + s_2^2}} \qquad [4.19]$$

It should also be noted that, both Equations 4.18 and 4.19 neglect the reinforcement at the weld face and the variability of weld root penetration.

The material ratio, ρ_M, is the mean-to-nominal ratio of the relevant material property. As explained in section 4.3.1, the relevant material property is the shear strength of the weld metal. However, in design practice the shear strength is taken as the tensile strength times a shear factor. Therefore, ρ_M is a function of two parameters, ρ_{M1} and ρ_{M2}. The factor ρ_{M1} addresses the variation in the weld metal tensile strength, yielding strength or tensile strength of the plate, while ρ_{M2} addresses the variation in the conversion from the tensile strength to shear strength. Thus, the material ratio and its coefficient of variation are represented by the following equations:

$$\rho_M = \rho_{M1}\rho_{M2} \qquad [4.20]$$

$$V_M^2 = V_{M1}^2 + V_{M2}^2 \qquad [4.21]$$

The various strength prediction models examined in this study involve either weld material strength or plate material strength or the combination of both. Therefore, the first material bias coefficient, ρ_{M1}, can be approximately taken as the mean value of the measured to nominal weld metal tensile strength, the measured to nominal static yield strength of the plate, or the ratio of tensile strength of the plate.

The mean value of the measured to nominal weld metal tensile strength is expressed as:

$$\rho_{M1} = \text{Mean}\left(\frac{\text{Measured Tensile Strength, } \sigma_u}{\text{Specified Tensile Strength, } X_u}\right) \qquad [4.22]$$

where σ_u is determined from all-weld-metal tension coupons.

The mean value of the measured to nominal static yield strength of the plate is expresses as:

$$\rho_{M1} = \text{Mean}\left(\frac{\text{Measured Static Yield Strength, } \sigma_y}{\text{Specified Static Yield Strength, } F_y}\right) \quad [4.23]$$

The mean value of the measured to nominal ultimate tensile strength of the plate:

$$\rho_{M1} = \text{Mean}\left(\frac{\text{Mean Ultimate Tensile Strength, } \sigma_u}{\text{Specified Ultimate Tensile Strength, } F_u}\right) \quad [4.24]$$

The second material bias coefficient, ρ_{M2}, accounts for the relationship between the tensile strength and the shear strength. For the shear factor used in the AISC Specification (AISC, 2005), it is expressed as:

$$\rho_{M2} = \text{Mean}\left(\frac{\text{Measured Shear Strength, } \tau_u / \text{Measured Tensile Strength, } \sigma_u}{0.60}\right) \quad [4.25a]$$

and for the shear factor used in the CISC Handbook of Steel Construction (CISC, 2006), expressed as:

$$\rho_{M2} = \text{Mean}\left(\frac{\text{Measured Shear Strength, } \tau_u / \text{Measured Tensile Strength, } \sigma_u}{0.67}\right) \quad [4.25b]$$

The second material bias coefficient is only incorporated in the models that adopted the Lesik and Kennedy (1988) load versus deformation relationship (Models 4 and 5) and the Beaulieu and Picard approach (Model 8). The measured shear strength to tensile strength ratio is obtained from longitudinal weld test specimens. The shear strength, τ_u, based on the fracture surface area, $A_{fracture}$ which accounts for the additional area due to root penetration and weld face reinforcement. These specimens are only presented by Deng *et al.* (2003). V_{M1} and V_{M2} are the associated coefficients of variation of ρ_{M1} and ρ_{M2}, respectively.

The professional factor, ρ_P, accounts for variation between the test and predicted capacities by taking the ratio of observed test capacity to the predicted capacity:

$$\rho_P = \text{Mean}\left(\frac{\text{Test Capacity}}{\text{Predicted Capacity}}\right) \quad [4.26]$$

V_P is the associated coefficient of variation for the test-to-predicted ratios. The predicted capacity is calculated using any of the prediction models with the measured values of the relevant material and geometric properties and the resistance factor, ϕ, equal to 1.0.

4.5.1 Summary of Test Data from Different Sources

4.5.1.1 Geometric Factor, ρ_G

The bias coefficient, ρ_G, and the coefficient of variation, V_G, for the mean-to-nominal throat dimension based on the work collected by Li *et al*. (2007) are summarized in Table 4.4. Additional data from the Beaulieu and Picard and the UC Davis (Gomez *et al.,* 2008) test programs were also added to the values reported by Li *et al*. The table includes the results based on two methods to measure the weld dimensions: measured throat dimension and measured leg size. The mean ratios of the geometric factor (ρ_G) and associated coefficient of variation (V_G) are obtained by pooling the respective factor from each data group. The mean value of ρ_G was found to be 1.07 and the coefficient of variation, V_G, 0.154.

Tables 4.5 to 4.8 provide the leg size measurements at the shear face, the tensile face and the throat dimension measured at 45^o from any shear or tensile face. It also presents the calculated measured throat dimension (*MTD*) and the bias coefficient (ρ_G) for the specimens tested at UC Davis (Gomez *et al.,* 2008). The same parameters for the specimens tested by Beaulieu and Picard are also presented in Tables 4.9 to 4.12. It should be noted that the *MTD* for the Beaulieu and Picard specimens and the UC Davis (Gomez *et al.,* 2008) specimens are calculated using Equations 4.18 and 4.19, respectively.

4.5.1.2 Material Factor, ρ_{M1}

The material factor (ρ_{M1}) and its corresponding coefficient of variation (V_{M1}) collected from the several sources are summarized in Tables 4.13 to 4.15. For the model that assumes no transfer of load by plate bearing in the compression zone (Model 5), the material factor (ρ_{M1}) is simply taken as a function tensile strength of the electrode only. Table 4.13 presents the values of ρ_{M1} compiled from various sources by Li *et al*. (2007) and augmented here by the values measured for the test program presented in Chapter 3. However, a modification has been made to the material factor for the models that assume load transfer by bearing in the compression zone. In order to simplify the statistical analysis, for Models 4 and 8, ρ_{M1} is taken as either a function of the nominal tensile strength of the weld or the nominal static yield strength of the plates, whichever provides the most conservative result. The correct value should lie between the two values of bias coefficient. Two independent bias coefficients for the resistance (ρ_R) and associated COV were calculated; one based on the value of ρ_{M1} for the tensile strength of the filler metal and one based on the yield strength of the plate steel.

4.5.1.3 Material Factor, ρ_{M2}

Table 4.16 presents a summary of the material factor (ρ_{M2}) and its associated coefficient of variation (V_{M2}) as collected from Deng *et al.* (2003). This parameter is a function of the shear strength (τ_u) of the filler metal as calculated according to Equation 4.25 and the shear coefficient used in the design equation to relate the shear resistance to the tensile strength. This material factor is only applicable to the models based on the load-

deformation relationship proposed by Lesik and Kennedy (Models 4 and 5) and the approach proposed by Beaulieu and Picard (Model 8).

4.5.1.4 Professional Factor, ρ_P

The professional factor, ρ_P, and the associated coefficient of variation, V_P, for the welded joint with out-of-plane eccentricity for the various strength prediction models presented earlier are summarized in Tables 4.2 and 4.3 for specimens with filler metals with no toughness requirement and with toughness requirement, respectively. The actual weld shear strength (τ_u), which is used to replace $0.67 \times F_{EXX}$ in Equation 2.6 when evaluating the professional factor was not evaluated for the weld metal used in the reported test programs. Therefore, the ratio of shear strength to tensile strength of 0.78, calculated from the test results of Deng *et al.* (2003) and reported in Table 4.16, was used to calculate the shear strength of the weld metal from the reported (or assessed in the case of the test programs from Dawe and Kulak and Beaulieu and Picard) tensile strength of the weld metal. The detailed calculations of the professional factor for the various prediction models are presented in Appendix B. It should be noted that the predicted strength for the specimens from Beaulieu and Picard was calculated for two different values of weld metal strength (463 MPa and 552 MPa), as explained in Chapter 3.

4.6 LEVEL OF SAFETY PROVIDED BY EXISTING MODELS

Test results from three independent test programs are used to conduct a reliability analysis to determine the level of safety provided by three selected models for design of welded joints with out-of-plane eccentricity. These models are Model 4, which makes use of the method proposed by Dawe and Kulak (modified with a rectangular stress block in the compression zone) with the weld metal behaviour proposed by Lesik and Kennedy, Model 5 currently implemented in the AISC Steel Construction Manual, and Model 8 proposed by Beaulieu and Picard as a substitute for the more complex instantaneous centre approach. The results of the analysis and the resistance factors for different values of safety index are presented in Tables 4.17 and 4.18 for filler metal with no toughness requirement and filler metal with toughness requirement, respectively.

Table 4.17 shows that the difference in the calculated value of safety index less than 2% when ρ_{M1} is based on the tensile strength of the weld metal versus the base metal. This difference is considered negligible. For a resistance factor, ϕ, of 0.75, the safety index for Model 5 varies from 4.56 to 4.93. For a resistance factor, ϕ, of 0.67, the safety index for Models 4 and 8 varies from 4.27 to 6.77. All three models are found to be conservative, although the method of instantaneous centre of rotation provides a value close to the target value of 4.0. A safety index of 4.0 is obtained with a resistance factor of 0.72 for Model 4 and 0.87 for Model 5.

A comparison of Table 4.17 with Table 4.18 indicates that the level of safety provided by filler metals with toughness requirement provide a higher level of safety than the filler metals with no toughness requirement. This reflects the earlier observation that the strength of filler metals with toughness requirement seem to be higher than filler metals

of the same nominal tensile strength with no toughness requirement. The safety index varies from 6.48 to 6.60 for Model 4, 6.60 for Model 5 and from 9.30 to 9.56 for Model 8. Once again, whether the reliability analysis is based on the material factor for the tensile strength of the weld metal or the yield strength of the base metal does not make a significant difference. Since only the UC Davis (Gomez *et al.,* 2008) test program included test specimens with weld metal with toughness requirement, there are no data for joints with small eccentricity ratio.

4.7 PROPOSED NEW MODEL

Based on the reliability analysis presented in the previous section, it is found that Model 8 provides the most conservative weld strength predictions. The method of instantaneous centre of rotation with a rectangular stress block and weld metal deformation characteristics proposed by Lesik and Kennedy provide the desired level of safety with a resistance factor of 0.72. The method currently used by AISC lies between the other two models.

Although Model 4 is presents a rational approach and produces the desired level of safety, it is a model that is relatively difficult to implement since it requires an iterative approach and the use of a computer program to calculate the strength of welded joints. A simple closed form solution, similar to that proposed by Beaulieu and Picard is more desirable. However, close examination of Model 8 reveals a few problems with the model. The first one is an inconsistency with the calculation of the weld strength on the tension side of the connection since it is based on the leg size rather than the throat size of the weld. Earlier work in welded joint research program (Ng *et al*., 2002) indicated that fillet weld strengths should be calculated based on the throat area for any angle of loading. Therefore, it is necessary to modify the model that accounts for the throat area on the tension side. The second problem is the inclusion of an arbitrary reduction factor of 0.5 in Equation 4.11. This was done to obtain values similar to earlier CISC Handbook (eighth and earlier editions) values. The earlier CISC Handbook used Model 1, which is based on the load versus weld deformation behaviour proposed by Butler and Kulak, and a triangular stress block in the compression zone. In addition, the method as implemented in the earlier editions of the CISC Handbook incorporated a reduction factor of 0.67 on the strength of the weld metal. The reason for this reduction factor is not clear, although it was referred to as a shear factor by Lesik and Kennedy (1990). Therefore, it is not surprising that Model 8, which was developed to produce values in good agreement with the CISC Handbook of Steel Construction, provides a high level of safety. A modified version of Model 8 is therefore proposed as a substitute to the more complex Model 4.

The proposed new model (Model 9) is represented by three equations to cover the typical range of welded joints loaded eccentrically (joints with large and small eccentricity and joint with thick and thin plates). The derivation of the equations is detailed in Appendix C.

4.7.1 Thick Plate Connection (Weld Failure)

4.7.1.1 For a/Q > 0.53

For values of eccentricity ratio, *a*, to strength ratio *Q* (defined by Equation 4.2) greater than 0.53, Appendix C demonstrates that failure of the joint will be governed by bending rather than shear. Figure 4.21 illustrates the assumed stress distribution in the joint at weld failure. From this stress distribution, the welded joint capacity for connections with thick plate can be expressed as:

$$P_r = \frac{0.711 F_y t L}{a(Q + 1.421)} \qquad [4.27]$$

where all the parameters are as defined earlier.

4.7.1.2 For a/Q ≤ 0.53

As eccentricity is reduced, shear failure becomes the dominant failure mode of the welded joint. For this situation, the stress distribution shown in Figure 4.22 is used to predict the combine shear and moment capacities. The derived expression for the capacity of the joint for the assumed stress distribution is quite complex, as shown in Appendix C. A simpler approach using a simplified equation obtained by using a linear interpolation between P_{ro} and P_{r53} is proposed:

$$P_r = P_{ro}\left(1 - 1.89\left(a/Q\right)\right) + 1.89\left(a/Q\right) P_{r53} \qquad [4.28]$$

where

$$P_{ro} = 2(0.67)(0.707) D X_u L \qquad [4.29]$$

and P_{r53} is obtained using Equation 4.27 for an eccentricity ratio *a* that yields a value of *a/Q* of 0.53 for the applicable value of *Q*.

The derivation of proposed Equations 4.27 and 4.28 is based on a shear factor of 0.67 as presented in Appendix C. However, the professional factor presented in Table 4.19 is based on the actual shear strength of the weld metal rather than the nominal value of 0.67 times the tensile strength. Therefore, Equations 4.27 and 4.28 should be expressed in terms of the weld shear strength, τ_u, which is equal to the empirical value of the shear factor, 0.78, times the measured tensile strength of the weld metal. Equations 4.27 and 4.28 can be re-written in terms of the measured shear strength τ_u as follows:

$$P_r = \frac{1.061 F_y t \tau_u D L}{a\left(F_y t + 2.121 \tau_u D\right)} \qquad \frac{a}{Q} > 0.53 \qquad [4.30]$$

$$P_r = P_{ro}\left(1-1.89\left(a/Q\right)\right)+1.89\left(a/Q\right)P_{r53} \qquad \frac{a}{Q} \le 0.53 \qquad [4.31]$$

where

$$P_{ro} = 2(0.707)\tau_u\, D\; L \qquad [4.32]$$

$$P_{r53} = \frac{1.061 F_y\, t\, \tau_u\, D\, L}{0.53Q(F_y\, t + 2.121\tau_u\, D)} \qquad [4.33]$$

where Q was defined in Equation 4.11. Equation 4.33 was obtained by substituting Equation 4.32 into Equation 4.30.

4.7.2 Thin Plate Connection (Plate Failure)

For failure in the plate (thin plate behaviour), a simple interaction equation presented by Chen and Han (1988), based on a lower bound approach, is proposed. The equation considers strictly material strength failure. Failure by possible plate instability is beyond the scope of this research project. Appendix C shows that the interaction equation can be solved for the capacity P_r of the joint. The following equation for the plate capacity is obtained:

$$P_r = \frac{2V_p\left(\sqrt{a^2L^2V_p{}^2 + 3M_p{}^2} - aLV_p\right)}{3M_p} \qquad [4.34]$$

where,

$$M_p = \frac{1}{4}tL^2F_u \qquad [4.35]$$

$$V_p = \frac{1}{2}tLF_u \qquad [4.36]$$

Although the interaction equation presented by Chen and Han (1988) is based on the plastic moment, the yield strength was substituted by the tensile strength in the plastic moment and plastic shear calculations. This was found to yield more accurate prediction of the test results since plate rupture rather than plate yielding was observed as the failure mode in the limited number of test specimens that failed in this mode. The test-to-predicted values for the proposed model (Model 9) are presented in Table 4.19. The specimens are grouped according to the filler metal toughness requirement. For filler metals with no toughness requirement the values of the test-to-predicted ratio are further divided according the failure mode (weld failure and plate failure). A total of 31 specimens from three data sets fall into the group that represents weld failure with large eccentricity ($a/Q > 0.53$). The mean test-to-predicted value is 1.01 and its coefficient of

variation is 22%. A total of 24 specimens meet the requirement for small eccentricity ratio ($a/Q \leq 0.53$). The mean test-to-predicted value and coefficient of variation for this group are 1.07 and 22%, respectively. Lastly, only five test specimens from the Beaulieu and Picard test program failed by plate rupture. The mean test-to-predicted ratio and the coefficient of variation for these five specimens are 1.03 and 16%, respectively.

The same categories are used for specimens used weld metal with toughness requirement. Only the specimens from UC Davis (Gomez *et al.,* 2008) are considered since only the UC Davis (Gomez *et al.,* (2008) test program incorporated test specimens with filler metal of this grade. The test program included 20 specimens with a high eccentricity ratio. The mean test-to-predicted ratio for this set of data is 1.35 and its COV is 8%. Ten specimens fall into the low eccentricity ratio group. The mean test-to-predicted value and COV are 1.26 and 19%, respectively.

A comparison of the data presented in Table 4.19 for Model 9 with the data presented in Tables 4.2 and 4.3 for Models 4, 5 and 8, shows that the proposed model gives the best predictions of the test results with the professional factor closest to 1.0 of all the models investigated. However, the coefficient of variation is still relatively high.

A summary of reliability analysis conducted for Model 9 is presented in Tables 4.20 and 4.21. The current resistance factor of 0.67 provides a minimum safety index of 3.98 for the weld failure mode and 4.8 for the mode of plate failure for joints welded with filler metal with no toughness requirement. It is noted that the minimum value of safety index is obtained when the weld metal tensile strength for the Beaulieu and Picard test program is assumed to be 552 MPa. The reader is reminded that this value is based weld metal tensile strengths reported by other researchers for welding electrodes of that era. The tests on concentric lap splices conducted by Beaulieu and Picard indicated that the weld metal strength was substantially lower than 552 MPa (463 MPa). Using the lower strength filler metal as a basis for predicting the test capacities, the resulting safety index is 4.13 for failure in the weld.

As expected, the safety index for filler metal with toughness requirement is higher than the value for weld metal with no toughness requirement. The minimum value of β observed in Table 4.21 is 5.1 for joints with small eccentricity and 6.3 for joints with large eccentricity.

4.8 CONCLUSIONS

A total of 92 test results from three independent test programs were examined and analyzed using 14 strength prediction models. A detailed assessment of three of these models was presented in this chapter. It was observed that filler metals with toughness requirement yield higher test-to-predicted ratio than the specimens with filler metal with no toughness requirement. The test specimens were therefore separated into two groups according to weld metal classification and analyzed using Models 4, 5 and 8. Unlike other current models, these three models are developed using the most recent load deformation relationship proposed by Lesik and Kennedy (1990). Based on a reliability

analysis, the safety index provided by Models 5 and 8 are significantly higher than target value of 4.0. Although Model 4 provides an acceptable level of safety, the computation procedure is complicated and time consuming. Moreover, none of the existing models with Lesik and Kennedy load versus deformation relationship consider plate fracture, which could become critical as the plate thickness is reduced. Therefore, a simpler, closed form, model that is applicable to both weld and plate failure modes is proposed. This model provides reliable prediction and satisfactory safety index ($\beta = 4.0$) with a resistance factor of 0.67.

Table 4.1 – Summary of Professional Factor, ρ_P, for Existing Models

	Source of Data	Sample Size	Professional factor	Coefficient of Variation
		n	ρ_p	V_p
Model 1	Dawe and Kulak (1972)	8	0.851	0.109
	Beaulieu and Picard (1985) **463 MPa** / 552 MPa	17	**1.061** / 0.992	**0.133** / 0.146
	Gomez et al. (2008)	60	1.520	0.167
	All Sources	85	**1.365** / 1.351	**0.244** / 0.256
Model 2	Dawe and Kulak (1972)	8	0.671	0.101
	Beaulieu and Picard (1985) **463 MPa** / 552 MPa	17	**0.863** / 0.779	**0.114** / 0.114
	Gomez et al. (2008)	60	1.175	0.144
	All Sources	85	**1.065** / 1.048	**0.218** / 0.237
Model 3	Dawe and Kulak (1972)	8	0.909	0.104
	Beaulieu and Picard (1985) **463 MPa** / 552 MPa	17	**1.213** / 1.094	**0.120** / 0.114
	Gomez et al. (2008)	60	1.603	0.150
	All Sources	85	**1.460** / 1.436	**0.218** / 0.236
Model 4	Dawe and Kulak (1972)	8	0.760	0.103
	Beaulieu and Picard (1985) **463 MPa** / 552 MPa	17	**1.065** / 0.938	**0.157** / 0.137
	Gomez et al. (2008)	60	1.326	0.142
	All Sources	85	**1.221** / 1.195	**0.207** / 0.225
Model 5	Dawe and Kulak (1972)	8	0.900	0.116
	Beaulieu and Picard (1985) **463 MPa** / 552 MPa	17	**1.208** / 1.014	**0.204** / 0.204
	Gomez et al. (2008)	60	1.493	0.167
	All Sources	85	**1.380** / 1.341	**0.221** / 0.246
Model 6	Dawe and Kulak (1972)	8	0.735	0.114
	Beaulieu and Picard (1985) **463 MPa** / 552 MPa	17	**0.938** / 0.787	**0.187** / 0.187
	Gomez et al. (2008)	60	1.215	0.162
	All Sources	85	**1.114** / 1.084	**0.222** / 0.251
Model 8 (a<0.4)	Beaulieu and Picard (1985) **463 MPa** / 552 MPa	5	**1.403** / 1.226	**0.064** / 0.062
	All Sources	5	**1.403** / 1.226	**0.064** / 0.062
Model 8 (a≥0.4)	Dawe and Kulak (1972)	8	1.215	0.101
	Beaulieu and Picard (1985) **463 MPa** / 552 MPa	12	**1.524** / 1.411	**0.129** / 0.131
	Gomez et al. (2008)	60	2.134	0.147
	All Sources	80	**1.951** / 1.934	**0.222** / 0.234

Table 4.1 – Cont'd

	Source of Data	Sample Size	Professional factor	Coefficient of Variation
		n	ρ_p	V_p
Model 7 Case 1	Dawe and Kulak (1972)	8	0.827	0.104
	Beaulieu and Picard (1985) **463 MPa** / 552 MPa	11	**1.042** / 0.974	**0.138** / 0.142
	Gomez et al. (2008)	60	1.459	0.155
	All Sources	79	**1.337** / 1.327	**0.227** / 0.236
Model 7 Case 2	Dawe and Kulak (1972)	8	0.627	0.108
	Beaulieu and Picard (1985) **463 MPa** / 552 MPa	11	**0.806** / 0.738	**0.137** / 0.135
	Gomez et al. (2008)	60	1.240	0.144
	All Sources	79	**1.117** / 1.108	**0.247** / 0.259
Model 7 Case 3	Dawe and Kulak (1972)	8	0.808	0.098
	Beaulieu and Picard (1985) **463 MPa** / 552 MPa	11	**0.967** / 0.873	**0.143** / 0.139
	Gomez et al. (2008)	60	1.467	0.135
	All Sources	79	**1.330** / 1.317	**0.230** / 0.245
Model 7 Case 4	Dawe and Kulak (1972)	8	0.670	0.099
	Beaulieu and Picard (1985) **463 MPa** / 552 MPa	11	**0.833** / 0.765	**0.134** / 0.135
	Gomez et al. (2008)	60	1.168	0.140
	All Sources	79	**1.071** / 1.061	**0.217** / 0.229
Model 7 Case 5	Dawe and Kulak (1972)	8	0.658	0.100
	Beaulieu and Picard (1985) **463 MPa** / 552 MPa	11	**0.819** / 0.754	**0.134** / 0.135
	Gomez et al. (2008)	60	1.148	0.142
	All Sources	79	**1.053** / 1.044	**0.218** / 0.229
Model 7 Case 6 and Case 7	Dawe and Kulak (1972)	8	0.937	0.122
	Beaulieu and Picard (1985) **463 MPa** / 552 MPa	11	**1.218** / 1.049	**0.157** / 0.246
	Gomez et al. (2008)	60	1.556	0.169
	All Sources	79	**1.446** / 1.422	**0.220** / 0.243

Table 4.2 – Summary of Professional Factor, ρ_P, for Specimens with Filler Metals with No Toughness Requirement

	Source of Data	Sample Size	Test/Predicted	Coefficient of Variation
		n	ρ_p	V_p
Model 4	Dawe and Kulak (1972)	8	0.760	0.103
	Beaulieu and Picard (1985) **463 MPa** / 552 MPa	17	**1.065** / 0.938	**0.157** / 0.137
	Gomez et al. (2008)	30	1.213	0.128
	All Sources	55	**1.101** / 1.062	**0.196** / 0.210
Model 5	Dawe and Kulak (1972)	8	0.900	0.116
	Beaulieu and Picard (1985) **463 MPa** / 552 MPa	17	**1.208** / 1.014	**0.204** / 0.204
	Gomez et al. (2008)	30	1.371	0.143
	All Sources	55	**1.252** / 1.192	**0.207** / 0.230
Model 8 (a<0.4)	Beaulieu and Picard (1985) **463 MPa** / 552 MPa	5	**1.403** / 1.226	**0.064** / 0.062
	All Sources	5	**1.403** / 1.226	**0.064** / 0.062
Model 8 (a≥0.4)	Dawe and Kulak (1972)	8	1.215	0.101
	Beaulieu and Picard (1985) **463 MPa** / 552 MPa	12	**1.524** / 1.411	**0.129** / 0.131
	Gomez et al. (2008)	30	1.952	0.139
	All Sources	50	**1.731** / 1.704	**0.215** / 0.228

Table 4.3 – Summary of Professional Factor, ρ_P, for Specimens with Filler Metal with Toughness Requirement

	Source of Data	Sample Size	Test/Predicted	Coefficient of Variation
		n	ρ_p	V_p
Model 4	Gomez et al. (2008)	30	1.440	0.102
Model 5	Gomez et al. (2008)	30	1.615	0.147
Model 8 (a>0.4)	Gomez et al. (2008)	30	2.317	0.103

Table 4.4 – Summary of Geometric Factor ρ_G from Various Sources (Li *et al*., 2007)

Weld Dimension Measurement Method	Source of Data	Nominal leg size	Sample Size	Ratio of Measured to Nominal	Coefficient of Variation
		(mm)	n	ρ_G	V_G
Measured Throat Dimension	Bornscheuer and Feder (1966)	5.7	18	0.957	0.090
		11.3	6	0.938	0.048
		17.0	5	0.921	0.020
	Ligtenberg (1968)	4.2	97	1.230	0.168
		5.0	67	1.121	0.163
		5.7	91	1.109	0.171
		6.4	13	1.071	0.096
		7.1	302	1.056	0.155
		8.5	145	1.039	0.147
		10.6	41	0.986	0.098
		11.3	87	0.997	0.100
		14.1	31	0.996	0.124
	Kato and Morita (1969)	5.0	8	1.057	0.065
		7.0	1	1.041	0.000
		10.0	3	1.009	0.021
		12.0	1	0.953	0.000
		15.0	6	1.014	0.005
		20.0	3	0.960	0.079
		22.0	1	0.929	0.000
		30.0	1	1.000	0.000
		40.0	2	0.940	0.090
	Clark (1971)	7.9	18	0.985	0.065
	Pham (1981)	5.0	17	1.072	0.102
		10.0	6	1.058	0.051
		16.0	3	1.030	0.054
	All Specimens with Measured Throat Dimension	**N.A.**	**973**	**1.065**	**0.159**

Table 4.4 – Cont'd

Weld Dimension Measurement Method	Source of Data	Nominal leg size	Sample Size	Ratio of Measured to Nominal	Coefficient of Variation
		(mm)	n	ρ_G	V_G
Measured Leg Size	Butler and Kulak (1969)	6.4	31	1.138	0.069
	Dawe and Kulak (1972)	6.4	43	1.158	0.075
	Swannell (1979b)	6.4	21	1.070	0.031
	Pham (1983a,b)	6.0	22	1.346	0.060
		10.0	23	1.118	0.106
		16.0	23	1.072	0.081
	Beaulieu and Picard (1985)	6.0	12	1.510	0.206
		8.0	12	1.311	0.135
		10.0	12	1.172	0.076
		12.0	12	1.116	0.053
	Miazga and Kennedy (1986)	5.0	21	1.040	0.026
		9.0	21	1.030	0.027
	Bowman and Quinn (1994)	6.4	8	1.182	0.082
		9.5	4	1.128	0.040
		12.7	6	1.087	0.030
	Ng *et al*. (2002)	6.4	126	1.026	0.102
		12.7	78	0.954	0.073
	Deng *et al*. (2003)	12.7	54	0.836	0.053
	Callele *et al*. (2005)	7.9	48	1.118	0.061
		12.7	180	0.981	0.082
	Li *et al.* (2007)	12.7	24	0.914	0.055
	Gomez *et al.* (2008) (tensile data)	7.9	24	1.266	0.075
		12.7	24	1.234	0.081
	Gomez *et al.* (2008) (bending data)	7.9	60	1.175	0.050
		12.7	60	1.277	0.094
	All Specimens with Measured Throat Dimension	**N.A.**	**949**	**1.076**	**0.149**
All Sources		**N.A.**	**1922**	**1.070**	**0.154**

Table 4.5 – Geometric Factor ρ_G for Tensile Specimens from UC Davis (Gomez *et al.*, 2008) (Leg size = 12.7 mm)

Specimen	Nominal Leg Size (mm)	Weld	Tension Leg Size (mm)	Shear Leg Size (mm)	45° Meas. (mm)	MTD (mm)	Ratio ρ_G
T_125_A12_1	12.7	Front	11.7	18.0	9.9	9.8	1.096
		Back	11.6	15.8	10.5	9.4	1.042
T_125_A12_2	12.7	Front	17.6	18.7	9.2	12.8	1.425
		Back	13.2	16.9	10.5	10.4	1.161
T_125_A12_3	12.7	Front	13.1	17.3	9.5	10.4	1.160
		Back	13.4	19.8	11.6	11.1	1.237
T_125_B12_1	12.7	Front	15.1	20.4	7.0	12.1	1.350
		Back	13.5	17.5	10.9	10.7	1.189
T_125_B12_2	12.7	Front	15.1	19.2	9.2	11.9	1.322
		Back	15.3	16.7	10.8	11.3	1.257
T_125_B12_3	12.7	Front	15.5	17.4	7.9	11.6	1.289
		Back	14.0	18.3	10.6	11.1	1.241
T_250_A12_1	12.7	Front	13.7	22.1	11.1	11.6	1.295
		Back	12.8	18.6	11.9	10.5	1.174
T_250_A12_2	12.7	Front	12.5	19.7	10.4	10.5	1.172
		Back	12.3	17.3	9.5	10.0	1.119
T_250_A12_3	12.7	Front	16.5	22.5	10.8	13.3	1.481
		Back	13.5	19.0	10.1	11.0	1.224
T_250_B12_1	12.7	Front	13.4	20.5	9.2	11.2	1.249
		Back	13.5	18.3	11.2	10.9	1.209
T_250_B12_2	12.7	Front	14.3	18.5	10.3	11.3	1.260
		Back	15.1	18.8	12.2	11.8	1.310
T_250_B12_3	12.7	Front	12.3	18.7	9.5	10.3	1.148
		Back	13.5	18.5	11.4	10.9	1.215
All Specimens			Mean Ratio				**1.234**
			Coefficient of Variation, V				**0.081**

Table 4.6 – Geometric Factor ρ_G for Tensile Specimens from UC Davis (Gomez *et al.*, 2008) (Leg size = 7.9 mm)

Specimen	Nominal Leg Size (mm)	Weld	Tension Leg Size (mm)	Shear Leg Size (mm)	45° Meas. (mm)	MTD (mm)	Ratio ρ_G
T_125_A516_1	7.9	Front	7.7	11.5	7.1	6.4	1.138
		Back	8.5	11.8	7.1	6.9	1.225
T_125_A516_2	7.9	Front	8.2	11.9	6.4	6.8	1.204
		Back	8.6	12.0	7.7	7.0	1.241
T_125_A516_3	7.9	Front	9.3	11.5	6.7	7.2	1.284
		Back	8.8	13.1	7.4	7.3	1.302
T_125_B516_1	7.9	Front	8.7	13.3	7.3	7.3	1.301
		Back	10.3	9.5	8.1	7.0	1.247
T_125_B516_2	7.9	Front	8.9	13.3	7.9	7.4	1.319
		Back	10.5	9.3	7.8	7.0	1.244
T_125_B516_3	7.9	Front	9.3	12.7	7.8	7.5	1.342
		Back	11.3	12.3	8.7	8.3	1.480
T_250_A516_1	7.9	Front	7.9	12.2	8.8	6.6	1.185
		Back	8.7	12.8	5.6	7.2	1.285
T_250_A516_2	7.9	Front	7.1	12.3	5.6	6.1	1.092
		Back	8.7	12.7	6.6	7.2	1.282
T_250_A516_3	7.9	Front	7.3	13.5	5.8	6.4	1.147
		Back	8.1	12.9	7.6	6.9	1.223
T_250_B516_1	7.9	Front	10.3	11.2	8.7	7.6	1.352
		Back	7.9	12.1	7.9	6.6	1.182
T_250_B516_2	7.9	Front	10.3	11.9	8.1	7.8	1.390
		Back	10.4	12.1	8.1	7.9	1.405
T_250_B516_3	7.9	Front	9.4	13.1	8.7	7.6	1.363
		Back	7.9	11.1	7.9	6.5	1.151
All Specimens			Mean Ratio				**1.266**
			Coefficient of Variation, V				**0.075**

Table 4.7 – Geometric Factor ρ_G for Bending Specimens from UC Davis (Gomez *et al.*, 2008) (Leg size = 12.7 mm)

Specimen	Nominal Leg Size (mm)	Weld	Tension Leg Size (mm)	Shear Leg Size (mm)	45° Meas. (mm)	MTD (mm)	Ratio ρ_G
B_125_A12_55_1	12.7	Front	13.2	18.2	9.6	10.7	1.191
		Back	12.7	19.2	10.7	10.6	1.180
B_125_A12_55_2	12.7	Front	13.6	19.2	11.0	11.1	1.233
		Back	12.9	16.4	10.1	10.2	1.131
B_125_A12_55_3	12.7	Front	13.1	18.3	10.8	10.6	1.185
		Back	12.9	17.7	10.5	10.4	1.163
B_125_B12_55_1	12.7	Front	13.7	17.8	9.9	10.8	1.208
		Back	13.4	16.1	10.2	10.3	1.148
B_125_B12_55_2	12.7	Front	12.9	17.8	11.0	10.5	1.166
		Back	12.2	16.1	9.8	9.7	1.081
B_125_B12_55_3	12.7	Front	14.6	15.8	9.3	10.7	1.194
		Back	14.5	17.3	11.3	11.1	1.237
B_175_A12_3_1	12.7	Front	12.0	19.4	10.4	10.2	1.140
		Back	12.2	15.3	9.4	9.5	1.064
B_175_A12_3_2	12.7	Front	11.9	18.0	10.1	9.9	1.102
		Back	13.1	15.7	10.2	10.0	1.117
B_175_A12_3_3	12.7	Front	12.3	17.5	9.7	10.1	1.120
		Back	13.3	16.8	11.1	10.4	1.160
B_175_A12_55_1	12.7	Front	13.6	18.6	10.9	11.0	1.220
		Back	12.8	18.4	9.7	10.5	1.170
B_175_A12_55_2	12.7	Front	13.0	16.5	10.9	10.2	1.136
		Back	12.5	16.9	9.7	10.0	1.116
B_175_A12_55_3	12.7	Front	13.4	16.1	10.9	10.3	1.150
		Back	13.2	17.9	10.8	10.6	1.183
B_175_A12_85_1	12.7	Front	14.1	16.2	11.1	10.6	1.184
		Back	14.1	15.3	10.2	10.4	1.156
B_175_A12_85_2	12.7	Front	13.4	15.6	11.0	10.2	1.135
		Back	13.4	16.9	10.8	10.5	1.168
B_175_A12_85_3	12.7	Front	14.2	17.8	10.5	11.1	1.236
		Back	14.1	18.6	11.1	11.2	1.250
B_175_B12_3_1	12.7	Front	13.7	16.0	10.4	10.4	1.156
		Back	13.1	17.8	11.1	10.6	1.175
B_175_B12_3_2	12.7	Front	12.9	17.5	11.0	10.4	1.157
		Back	13.3	17.0	9.9	10.5	1.165
B_175_B12_3_3	12.7	Front	13.3	15.4	10.5	10.1	1.123
		Back	12.5	17.2	11.0	10.1	1.129
B_175_B12_55_1	12.7	Front	12.8	17.2	11.0	10.3	1.146
		Back	13.2	18.0	11.0	10.7	1.186
B_175_B12_55_2	12.7	Front	14.2	20.3	10.8	11.6	1.294
		Back	12.2	17.4	9.4	10.0	1.112

Table 4.7 – Cont'd

Specimen	Nominal Leg Size (mm)	Weld	Tension Leg Size (mm)	Shear Leg Size (mm)	45° Meas. (mm)	MTD (mm)	Ratio ρ_G
B_175_B12_85_1	12.7	Front	13.4	19.4	11.2	11.0	1.230
		Back	12.9	16.1	9.8	10.1	1.120
B_175_B12_85_2	12.7	Front	14.4	15.8	9.6	10.6	1.185
		Back	13.7	18.1	9.8	10.9	1.219
B_175_B12_85_3	12.7	Front	14.7	17.5	9.9	11.2	1.251
		Back	14.1	19.5	10.3	11.4	1.273
B_250_A12_55_1	12.7	Front	12.2	20.1	9.7	10.4	1.163
		Back	12.9	17.9	10.1	10.4	1.163
B_250_A12_55_2	12.7	Front	12.6	19.5	9.4	10.6	1.181
		Back	12.0	18.3	9.6	10.0	1.119
B_250_A12_55_3	12.7	Front	11.5	18.9	9.7	9.8	1.093
		Back	12.7	16.7	10.9	10.1	1.125
B_250_B12_55_1	12.7	Front	12.5	19.2	10.0	10.5	1.164
		Back	14.7	19.9	10.6	11.8	1.319
B_250_B12_55_2	12.7	Front	13.4	18.8	10.7	10.9	1.217
		Back	15.1	20.2	11.0	12.1	1.349
B_250_B12_55_3	12.7	Front	13.3	17.7	10.7	10.7	1.187
		Back	13.8	20.4	11.5	11.4	1.275
All Specimens			Mean Ratio				**1.176**
			Coefficient of Variation, V				**0.049**

Table 4.8 – Geometry Factor ρ_G for Bending Specimens from UC Davis (Gomez *et al.*, 2008) (Leg size = 7.9 mm)

Specimen	Nominal Leg Size (mm)	Weld	Tension Leg Size (mm)	Shear Leg Size (mm)	45° Meas. (mm)	MTD (mm)	Ratio ρ_G
B_125_A516_55_1	7.9	Front	9.5	13.1	7.3	7.7	1.370
		Back	8.5	10.7	6.3	6.7	1.189
B_125_A516_55_2	7.9	Front	9.0	12.8	7.7	7.4	1.311
		Back	9.0	10.9	7.7	7.0	1.239
B_125_A516_55_3	7.9	Front	9.2	12.3	7.2	7.4	1.311
		Back	9.4	12.1	8.1	7.4	1.318
B_125_B516_55_1	7.9	Front	9.4	12.6	8.1	7.5	1.342
		Back	9.7	13.1	8.3	7.8	1.390
B_125_B516_55_2	7.9	Front	9.2	13.1	9.0	7.5	1.345
		Back	9.6	13.0	7.8	7.7	1.379
B_125_B516_55_3	7.9	Front	8.6	11.9	7.6	7.0	1.240
		Back	10.2	13.6	7.6	8.2	1.453
B_175_A516_3_1	7.9	Front	7.8	11.9	6.6	6.5	1.160
		Back	7.6	11.9	6.1	6.4	1.139
B_175_A516_3_2	7.9	Front	7.9	12.6	7.1	6.7	1.195
		Back	7.6	11.8	6.1	6.4	1.142
B_175_A516_3_3	7.9	Front	7.9	10.7	6.3	6.4	1.136
		Back	7.8	12.4	6.6	6.6	1.175
B_175_A516_55_1	7.9	Front	8.7	12.0	8.0	7.0	1.252
		Back	7.2	11.9	6.5	6.2	1.099
B_175_A516_55_2	7.9	Front	8.8	11.4	7.6	7.0	1.245
		Back	7.4	11.0	6.3	6.2	1.097
B_175_A516_55_3	7.9	Front	8.1	12.4	7.3	6.8	1.211
		Back	8.0	11.5	7.0	6.5	1.165
B_175_A516_85_1	7.9	Front	10.3	12.7	7.1	8.0	1.426
		Back	8.7	11.9	7.0	7.0	1.248
B_175_A516_85_2	7.9	Front	9.4	12.4	6.8	7.5	1.338
		Back	9.4	13.1	6.7	7.6	1.360
B_175_A516_85_3	7.9	Front	9.6	9.5	6.8	6.8	1.203
		Back	10.1	14.0	7.9	8.2	1.464
B_175_B516_3_1	7.9	Front	8.1	11.7	7.7	6.7	1.188
		Back	9.3	14.4	9.0	7.8	1.393
B_175_B516_3_2	7.9	Front	8.4	11.5	7.2	6.8	1.204
		Back	8.3	13.0	7.7	7.0	1.243
B_175_B516_3_3	7.9	Front	8.8	12.1	8.0	7.1	1.274
		Back	7.9	12.7	7.7	6.7	1.200
B_175_B516_55_1	7.9	Front	10.6	18.5	8.4	9.2	1.645
		Back	8.2	11.7	7.1	6.7	1.200
B_175_B516_55_2	7.9	Front	10.5	19.6	8.7	9.3	1.654
		Back	6.6	13.5	7.2	5.9	1.060

Table 4.8 – Cont'd

Specimen	Nominal Leg Size (mm)	Weld	Tension Leg Size (mm)	Shear Leg Size (mm)	45° Meas. (mm)	MTD (mm)	Ratio ρ_G
B_175_B516_85_1	7.9	Front	9.8	12.4	7.9	7.7	1.371
		Back	9.1	12.5	8.5	7.4	1.313
B_175_B516_85_2	7.9	Front	9.8	12.0	9.3	7.6	1.351
		Back	10.1	10.8	8.2	7.4	1.312
B_175_B516_85_3	7.9	Front	9.7	13.2	5.9	7.8	1.392
		Back	8.9	12.2	9.1	7.2	1.279
B_250_A516_55_1	7.9	Front	9.8	14.2	8.2	8.0	1.433
		Back	7.6	12.4	6.5	6.5	1.154
B_250_A516_55_2	7.9	Front	9.3	14.7	8.1	7.9	1.406
		Back	7.8	12.3	7.2	6.6	1.171
B_250_A516_55_3	7.9	Front	8.6	13.8	7.7	7.3	1.300
		Back	8.2	13.0	7.3	6.9	1.235
B_250_B516_55_1	7.9	Front	8.9	11.1	8.4	6.9	1.236
		Back	8.3	11.7	7.2	6.7	1.203
B_250_B516_55_2	7.9	Front	9.1	11.4	8.4	7.1	1.268
		Back	8.9	12.2	7.7	7.2	1.279
B_250_B516_55_3	7.9	Front	10.0	11.7	8.5	7.6	1.357
		Back	8.4	12.6	7.3	7.0	1.246
All Specimens			Mean Ratio				**1.281**
			Coefficient of Variation, V				**0.093**

Table 4.9 – Geometric Factor ρ_G for Specimens from Beaulieu and Picard (Leg size = 6 mm)

Specimen	Nominal Leg Size (mm)	Weld	De (mm)	MTD (mm)	Ratio ρ_G
A-6-375-1	6	Front	8.0	5.6	1.332
		Back	7.4	5.2	1.230
A-6-375-2	6	Front	12.4	8.8	2.067
		Back	12.5	8.9	2.088
A-6-125-1	6	Front	8.3	5.9	1.385
		Back	7.7	5.5	1.290
A-6-125-2	6	Front	7.5	5.3	1.253
		Back	8.2	5.8	1.363
A-6-75-1	6	Front	10.8	7.6	1.792
		Back	9.9	7.0	1.652
A-6-75-2	6	Front	8.1	5.7	1.348
		Back	7.9	5.6	1.320
All Specimens			Mean Ratio		**1.510**
			Coefficient of Variation, V		**0.206**

Table 4.10 – Geometric Factor ρ_G for Specimens from Beaulieu and Picard (Leg size = 12 mm)

Specimen	Nominal Leg Size (mm)	Weld	De (mm)	MTD (mm)	Ratio ρ_G
A-12-375-1	12	Front	13.3	9.4	1.108
		Back	14.0	9.9	1.167
A-12-375-2	12	Front	14.3	10.1	1.190
		Back	12.9	9.1	1.078
A-12-125-1	12	Front	14.1	10.0	1.176
		Back	13.9	9.8	1.161
A-12-125-2	12	Front	13.6	9.6	1.134
		Back	12.8	9.0	1.065
A-12-75-1	12	Front	11.9	8.4	0.988
		Back	13.6	9.6	1.130
A-12-75-2	12	Front	13.7	9.7	1.138
		Back	12.6	8.9	1.053
All Specimens			Mean Ratio		**1.116**
			Coefficient of Variation, V		**0.053**

Table 4.11 – Geometric Factor ρ_G for Specimens from Beaulieu and Picard (Leg size = 8 mm)

Specimen	Nominal Leg Size (mm)	Weld	De (mm)	MTD (mm)	Ratio ρ_G
B-8-375-1	8	Front	12.9	9.1	1.606
		Back	11.3	8.0	1.413
B-8-375-2	8	Front	10.9	7.7	1.366
		Back	12.6	8.9	1.574
B-8-125-1	8	Front	10.4	7.4	1.300
		Back	11.0	7.8	1.373
B-8-125-2	8	Front	9.9	7.0	1.239
		Back	11.2	7.9	1.403
B-8-75-1	8	Front	9.2	6.5	1.146
		Back	9.1	6.5	1.143
B-8-75-2	8	Front	8.6	6.1	1.070
		Back	8.8	6.2	1.100
All Specimens			Mean Ratio		**1.311**
			Coefficient of Variation, V		**0.135**

Table 4.12 – Geometric Factor ρ_G for Specimens from Beaulieu and Picard (Leg size = 10 mm)

Specimen	Nominal Leg Size (mm)	Weld	De (mm)	MTD (mm)	Ratio ρ_G
B-10-375-1	10	Front	11.7	8.3	1.172
		Back	12.1	8.5	1.209
B-10-375-2	10	Front	12.9	9.1	1.291
		Back	11.1	7.8	1.107
B-10-125-1	10	Front	10.4	7.4	1.040
		Back	10.5	7.4	1.047
B-10-125-2	10	Front	11.4	8.0	1.136
		Back	11.0	7.8	1.100
B-10-75-1	10	Front	12.4	8.7	1.235
		Back	12.7	9.0	1.274
B-10-75-2	10	Front	12.8	9.1	1.284
		Back	11.7	8.3	1.174
All Specimens			Mean Ratio		**1.172**
			Coefficient of Variation, V		**0.076**

Table 4.13 – Summary of Material Factor ρ_{M1} for tensile strength of the weld

Source of Data	Sample size,	Nominal tensile strength, (MPa)	Mean tensile strength, (MPa)	Ratio of Measured to Nominal	Coefficient of Variation
	n	X_u	σ_u	ρ_{M1}	V_{M1}
Miazga and Kennedy (1986)	3	480	537.7	1.120	0.014
Gagnon and Kennedy (1987)	10	480	579.9	1.208	0.036
Swannell and Skewes (1979)	2	410	538.8	1.314	0.020
Fisher et al. (1978)	127	414	455.1	1.099	0.039
	138	483	516.4	1.069	0.036
	136	552	606.1	1.098	0.049
	16	621	690.9	1.113	0.043
	72	758	806	1.063	0.040
	128	483	588.8	1.219	0.056
	40	483	598.5	1.239	0.114
Pham (1981)	3	480	500	1.042	0.044
Mansell and Yadav (1982)	6	410	558	1.361	0.027
Bowman and Quinn (1994)	3	483	475.8	0.985	0.029
Callele et al. (2005)†	32	480	552.3	1.151	0.084
Gomez *et al.* (2008)	4	480	671	1.398	0.002
All Sources	**720**	**N.A.**	**N.A.**	**1.127**	**0.082**

† Including all weld metal tension coupon tests from phases 1 through 4.

Table 4.14 – Summary of Material Factor ρ_{M1} for static yield strength of the plate

Source of Data	Thickness (mm)	Sample size,	Nominal static yield strength, (MPa)	Mean static yield strength, (MPa)	Ratio of Measured to Nominal	Coefficient of Variation
	t	n	F_y	σ_y	ρ_{M1}	V_{M1}
Schmidt and Bartlett (2002)	10-19.9	1231	350	388.5	1.110	0.054
	20-29.9	239	350	388.5	1.110	0.053
	30-39.9	157	350	406	1.160	0.063
	40-49.9	186	350	420	1.200	0.055
All Sources		**1813**	**N.A.**	**N.A.**	**1.124**	**0.061**

Table 4.15 – Summary of Material Factor ρ_{M1} for ultimate tensile strength of the plate

Source of Data	Thickness (mm)	Sample size,	Nominal ultimate tensile strength, (MPa)	Mean ultimate tensile strength, (MPa)	Ratio of Measured to Nominal	Coefficient of Variation
	t	n	F_u	σ_u	ρ_{M1}	V_{M1}
Schmidt and Bartlett (2002)	10-19.9	1231	450	535.5	1.190	0.034
	20-29.9	239	450	544.5	1.210	0.029
	30-39.9	157	450	562.5	1.250	0.040
	40-49.9	186	450	594	1.320	0.037
All Sources		**1813**	**N.A.**	**N.A.**	**1.211**	**0.048**

Table 4.16 – Summary of Material Factor ρ_{M2} (Deng *et al.*, 2003)

Weld Dimension Measurement Method	Specimen Designation	AWS Classification	$P/A_{fracture}$, τ_u (MPa)	Tensile Strength, σ_u (MPa)	τ_u / σ_u	$0.60\,\sigma_u$ (MPa)	ρ_{M2} (0.60)	$0.67\,\sigma_u$ (MPa)	ρ_{M2} (0.67)
Fracture Surface Area	L1-1	E70T-4	—	631	—	378.6	—	422.8	—
			—	631	—	378.6	—	422.8	—
			503	631	0.798	378.6	1.330	422.8	1.191
			506	631	0.802	378.6	1.337	422.8	1.197
	L1-2	E70T-4	494	631	0.782	378.6	1.304	422.8	1.167
			421	631	0.668	378.6	1.113	422.8	0.997
			—	631	—	378.6	—	422.8	—
			—	631	—	378.6	—	422.8	—
	L1-3	E70T-4	468	631	0.742	378.6	1.237	422.8	1.108
			464	631	0.735	378.6	1.225	422.8	1.097
			—	631	—	378.6	—	422.8	—
			—	631	—	378.6	—	422.8	—
	L2-1	E70T-7	—	605	—	363.0	—	405.4	—
			437	605	0.722	363.0	1.203	405.4	1.078
			—	605	—	363.0	—	405.4	—
			—	605	—	363.0	—	405.4	—
	L2-2	E70T-7	—	605	—	363.0	—	405.4	—
			—	605	—	363.0	—	405.4	—
			—	605	—	363.0	—	405.4	—
			515	605	0.851	363.0	1.418	405.4	1.270
	L2-3	E70T-7	—	605	—	363.0	—	405.4	—
			—	605	—	363.0	—	405.4	—
			475	605	0.785	363.0	1.309	405.4	1.172
			—	605	—	363.0	—	405.4	—
	L3-1	E71T8-K6	413	493	0.837	295.8	1.395	330.3	1.250
			374	493	0.758	295.8	1.263	330.3	1.131
			393	493	0.797	295.8	1.328	330.3	1.189
			355	493	0.720	295.8	1.201	330.3	1.075
	L3-2	E71T8-K6	—	493	—	295.8	—	330.3	—
			379	493	0.768	295.8	1.281	330.3	1.147
			—	493	—	295.8	—	330.3	—
			—	493	—	295.8	—	330.3	—
	L3-3	E71T8-K6	443	493	0.899	295.8	1.499	330.3	1.342
			—	493	—	295.8	—	330.3	—
			—	493	—	295.8	—	330.3	—
			—	493	—	295.8	—	330.3	—
All Specimens			Mean Ratio		**0.778**		**1.296**		**1.161**
			Coefficient of Variation, V				**0.075**		**0.075**

Table 4.17 – Reliability Analysis for Models 4, 5 and 8 and Filler Metal with No Toughness Requirement

Model		Model 4 (Modified Dawe & Kulak I.C. Approach w/ Lesik & Kennedy)	Model 8 (Beaulieu and Picard Approach) (a < 0.4)	Model 8 (Beaulieu and Picard Approach) (a ≥ 0.4)	Model		Model 5 (AISC Approach w/ Lesik & Kennedy)
ρ_G		1.070	1.070	1.070	ρ_G		1.070
V_G		0.154	0.154	0.154	V_G		0.154
ρ_{M1} (X_u)		1.127	1.127	1.127	ρ_{M1} (X_u)		1.127
V_{M1} (X_u)		0.082	0.082	0.082	V_{M1} (X_u)		0.082
ρ_{M1} (F_y)		1.124	1.124	1.124	ρ_{M1} (F_y)		—
V_{M1} (F_y)		0.061	0.061	0.061	V_{M1} (F_y)		—
ρ_{M2}		1.161	1.161	1.161	ρ_{M2}		1.296
V_{M2}		0.075	0.075	0.075	V_{M2}		0.075
$\rho_{p\ (463\ MPa)}$		1.101	1.403	1.731	$\rho_{p\ (463\ MPa)}$		1.252
$V_{p\ (463\ MPa)}$		0.196	0.064	0.215	$V_{p\ (463\ MPa)}$		0.207
$\rho_{p\ (552\ MPa)}$		1.062	1.226	1.704	$\rho_{p\ (552\ MPa)}$		1.192
$V_{p\ (552\ MPa)}$		0.210	0.062	0.228	$V_{p\ (552\ MPa)}$		0.230
ρ_R (X_u) 463 MPa		1.541	1.964	2.423	ρ_R (X_u) 463 MPa		1.957
V_R (X_u) 463 MPa		0.273	0.200	0.287	V_R (X_u) 463 MPa		0.281
ρ_R (F_y) 463 MPa		1.537	1.959	2.417	ρ_R (F_y) 463 MPa		—
V_R (F_y) 463 MPa		0.267	0.193	0.282	V_R (F_y) 463 MPa		—
ρ_R (X_u) 552 MPa		1.487	1.716	2.386	ρ_R (X_u) 552 MPa		1.863
V_R (X_u) 552 MPa		0.283	0.200	0.297	V_R (X_u) 552 MPa		0.298
ρ_R (F_y) 552 MPa		1.483	1.712	2.379	ρ_R (F_y) 552 MPa		—
V_R (F_y) 552 MPa		0.278	0.192	0.292	V_R (F_y) 552 MPa		—
β (X_u) 463 MPa	$\Phi = 0.67$	4.51	6.63	6.18	β (X_u) 463 MPa	$\Phi = 0.75$	4.93
Φ	β = 4.5	0.67	1.02	1.02	Φ	β = 4.5	0.84
Φ	β = 4.0	0.76	1.14	1.16	Φ	β = 4.0	0.95
β (F_y) 463 MPa	$\Phi = 0.67$	4.55	6.77	6.25	β (F_y) 463 MPa	$\Phi = 0.75$	—
Φ	β = 4.5	0.68	1.04	1.03	Φ	β = 4.5	—
Φ	β = 4.0	0.77	1.15	1.17	Φ	β = 4.0	—
β (X_u) 552 MPa	$\Phi = 0.67$	4.27	5.93	5.98	β (X_u) 552 MPa	$\Phi = 0.75$	4.56
Φ	β = 4.5	0.63	0.90	0.98	Φ	β = 4.5	0.76
Φ	β = 4.0	0.72	1.00	1.12	Φ	β = 4.0	0.87
β (F_y) 552 MPa	$\Phi = 0.67$	4.31	6.05	6.04	β (F_y) 552 MPa	$\Phi = 0.75$	—
Φ	β = 4.5	0.64	0.91	0.99	Φ	β = 4.5	—
Φ	β = 4.0	0.72	1.13	—	Φ	β = 4.0	—

Table 4.18 – Reliability Analysis for Models 4, 5 and 8 and Filler Metal with Toughness Requirement

Model		Model 4 (Modified Dawe & Kulak I.C. Approach w/ Lesik & Kennedy)	Model 8 (Beaulieu and Picard Approach) (a ≥ 0.4)	Model		Model 5 (AISC Approach w/ Lesik & Kennedy)
ρ_G		1.070	1.070	ρ_G		1.070
V_G		0.154	0.154	V_G		0.154
$\rho_{M1}(X_u)$		1.127	1.127	$\rho_{M1}(X_u)$		1.127
$V_{M1}(X_u)$		0.082	0.082	$V_{M1}(X_u)$		0.082
$\rho_{M1}(Fy)$		1.124	1.124	$\rho_{M1}(Fy)$		—
$V_{M1}(Fy)$		0.061	0.061	$V_{M1}(Fy)$		—
ρ_{M2}		1.161	1.161	ρ_{M2}		1.296
V_{M2}		0.075	0.075	V_{M2}		0.075
ρ_p		1.440	2.317	ρ_p		1.615
V_p		0.102	0.103	V_p		0.147
$\rho_R(X_u)$		2.016	3.244	$\rho_R(X_u)$		2.524
$V_R(X_u)$		0.216	0.216	$V_R(X_u)$		0.240
$\rho_R(F_y)$		2.011	3.235	$\rho_R(F_y)$		—
$V_R(F_y)$		0.208	0.209	$V_R(F_y)$		—
$\beta(X_u)$	$\Phi = 0.67$	6.48	9.30	$\beta(X_u)$	$\Phi = 0.75$	6.60
Φ	$\beta = 4.5$	1.01	1.63	Φ	$\beta = 4.5$	1.19
Φ	$\beta = 4.0$	1.13	1.82	Φ	$\beta = 4.0$	1.34
$\beta(F_y)$	$\Phi = 0.67$	6.60	9.56	$\beta(F_y)$	$\Phi = 0.75$	—
Φ	$\beta = 4.5$	1.03	1.65	Φ	$\beta = 4.5$	—
Φ	$\beta = 4.0$	1.14	1.84	Φ	$\beta = 4.0$	—

Table 4.19 – Summary of Professional Factor, ρ_P, for Model 9

			Source of Data	Sample Size	Mean Test/Predicted	Coefficient of Variation
				n	ρ_p	V_p
Model 9 No toughness requirement	Weld Failure	$a/Q >$ 0.53	Dawe and Kulak (1972)	6	0.721	0.076
			Beaulieu and Picard (1985) **463 MPa** / 552 MPa	**6** / 6	**0.906** / 0.829	**0.174** / 0.173
			Gomez *et al.* (2008)	19	1.153	0.097
			All Sources	**31** / 31	**1.022** / 1.007	**0.205** / 0.217
		$a/Q \leq$ 0.53	Dawe and Kulak (1972)	2	0.667	0.194
			Beaulieu and Picard (1985) **463 MPa** / 552 MPa	**11** / 11	**1.181** / 1.026	**0.153** / 0.140
			Gomez *et al.* (2008)	11	1.032	0.245
			All Sources	**24** / 24	**1.070** / 0.999	**0.235** / 0.219
	Plate Failure	all a values	Dawe and Kulak (1972)	—	—	—
			Beaulieu and Picard (1985) **463 MPa** / 552 MPa	**5**./ 5	**1.027** / 1.027	**0.155** / 0.155
			Gomez *et al.* (2008)	—	—	—
			All Sources	**5**./ 5	**1.027** / 1.027	**0.155** / 0.155
Model 9 With toughness requirement	Weld Failure	$a/Q >$ 0.53	Dawe and Kulak (1972)	—	—	—
			Beaulieu and Picard (1985) **463 MPa** / 552 MPa	—	—	—
			Gomez *et al.* (2008)	20	1.350	0.084
			All Sources	20	1.350	0.084
		$a/Q \leq$ 0.53	Dawe and Kulak (1972)	—	—	—
			Beaulieu and Picard (1985) **463 MPa** / 552 MPa	—	—	—
			Gomez *et al.* (2008)	10	1.260	0.193
			All Sources	10	1.260	0.193
	Plate Failure	all a values	Dawe and Kulak (1972)	—	—	—
			Beaulieu and Picard (1985) **463 MPa** / 552 MPa	—	—	—
			Gomez *et al.* (2008)	—	—	—
			All Sources	—	—	—

Table 4.20 – Reliability Analysis for Model 9 and Filler Metal with No Toughness Requirement

Thick Plate (Weld Failure)				Thin Plate(Plate Failure)		
Parameter		Model 9 (a/Q > 0.53)	Model 9 (a/Q ≤ 0.53)	Parameter		Model 9 (all a values)
ρ_G		1.070	1.070	—		—
V_G		0.154	0.154	—		—
ρ_{M1} (X_u)		1.127	1.127	—		—
V_{M1} (X_u)		0.082	0.082	—		—
ρ_{M1} (F_y)		1.124	1.124	ρ_{M1} (F_u)		1.210
V_{M1} (F_y)		0.061	0.061	V_{M1} (F_u)		0.048
ρ_{M2}		1.161	1.161	—		—
V_{M2}		0.075	0.075	—		—
$\rho_{p\ (463\ MPa)}$		1.022	1.070	$\rho_{p\ (463\ MPa)}$		1.027
$V_{p\ (463\ MPa)}$		0.205	0.235	$V_{p\ (463\ MPa)}$		0.155
$\rho_{p\ (552\ MPa)}$		1.007	0.999	$\rho_{p\ (552\ MPa)}$		1.027
$V_{p\ (552\ MPa)}$		0.217	0.219	$V_{p\ (552\ MPa)}$		0.155
ρ_R (X_u) *463 MPa*		1.431	1.498	—		—
V_R (X_u) *463 MPa*		0.279	0.302	—		—
ρ_R (F_y) *463 MPa*		1.427	1.494	ρ_R (F_u) *463 MPa*		1.243
V_R (F_y) *463 MPa*		0.274	0.297	V_R (F_u) *463 MPa*		0.162
ρ_R (X_u) *552 MPa*		1.410	1.399	—		—
V_R (X_u) *552 MPa*		0.288	0.290	—		—
ρ_R (F_y) *552 MPa*		1.406	1.395	ρ_R (F_u) *552 MPa*		1.243
V_R (F_y) *552 MPa*		0.283	0.285	V_R (F_u) *552 MPa*		0.162
β (X_u) 463 MPa	*Φ = 0.67*	4.15	4.13	β (X_u) 463 MPa	*Φ = 0.67*	—
Φ	β = 4.5	0.61	0.61	*Φ*	β = 4.5	—
Φ	β = 4.0	0.70	0.69	*Φ*	β = 4.0	—
β (F_y) 463 MPa	*Φ = 0.67*	4.19	4.16	β (F_y) 463 MPa	*Φ = 0.67*	4.82
Φ	β = 4.5	0.62	0.61	*Φ*	β = 4.5	0.71
Φ	β = 4.0	0.70	0.70	*Φ*	β = 4.0	0.78
β (X_u) 552 MPa	*Φ = 0.67*	4.02	3.98	β (X_u) 552 MPa	*Φ = 0.67*	—
Φ	β = 4.5	0.59	0.58	*Φ*	β = 4.5	—
Φ	β = 4.0	0.67	0.67	*Φ*	β = 4.0	—
β (F_y) 552 MPa	*Φ = 0.67*	4.05	4.01	β (F_y) 552 MPa	*Φ = 0.67*	4.82
Φ	β = 4.5	0.60	0.59	*Φ*	β = 4.5	0.71
Φ	β = 4.0	0.68	0.67	*Φ*	β = 4.0	0.78

Table 4.21 – Reliability Analysis for Model 9 and Filler Metal with Toughness Requirement

Parameter		Thick Plate (Weld Failure)	
		Model 9 (a/Q > 0.53)	Model 9 (a/Q ≤ 0.53)
ρ_G		1.070	1.070
V_G		0.154	0.154
ρ_{M1} (X_u)		1.127	1.127
V_{M1} (X_u)		0.082	0.082
ρ_{M1} (F_y)		1.124	1.124
V_{M1} (F_y)		0.061	0.061
ρ_{M2}		1.161	1.161
V_{M2}		0.075	0.075
ρ_p		1.350	1.260
V_p		0.084	0.193
ρ_R (X_u)		1.890	1.764
V_R (X_u)		0.208	0.271
ρ_R (F_y)		1.885	1.759
V_R (F_y)		0.200	0.265
β (X_u)	Φ = 0.67	6.29	5.08
Φ	β = 4.5	0.97	0.77
Φ	β = 4.0	1.08	0.88
β (F_y)	Φ = 0.67	6.41	5.13
Φ	β = 4.5	0.98	0.78
Φ	β = 4.0	1.09	0.88

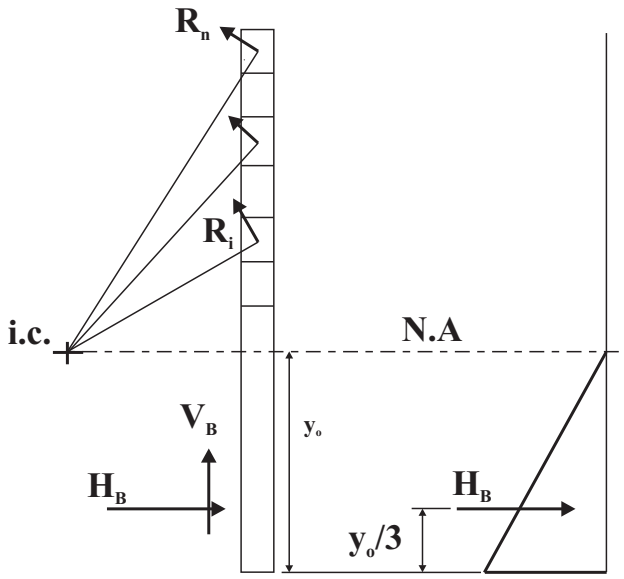

Figure 4.1 – Force distribution in weld loaded in shear and bending

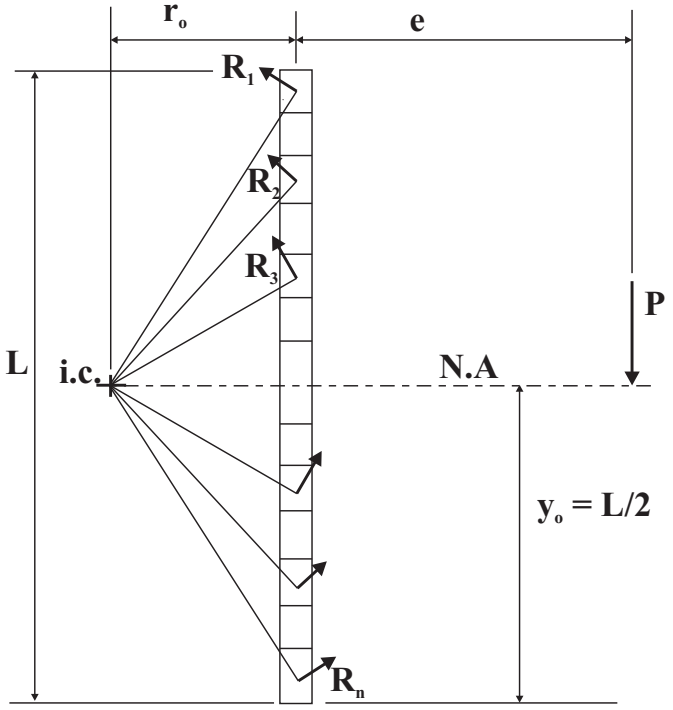

Figure 4.2 – Eccentrically loaded fillet weld (AISC Approach)

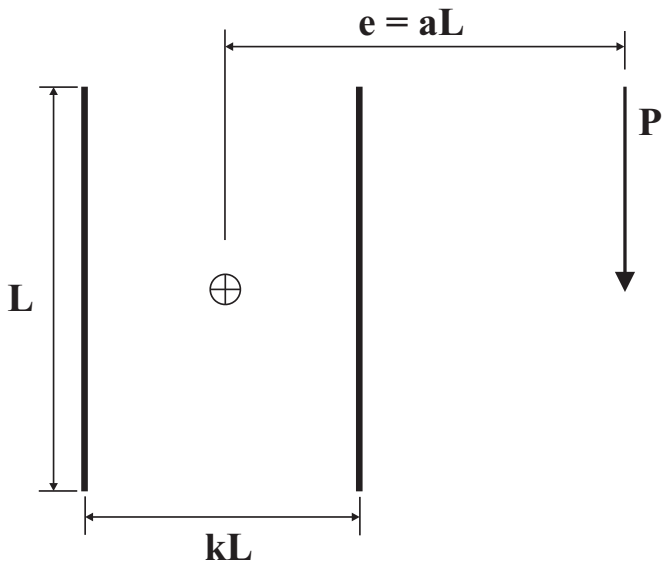

Figure 4.3 – In-plane eccentricity

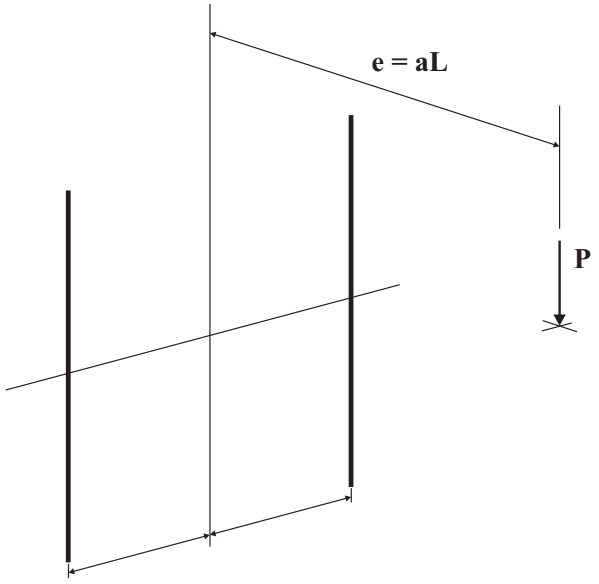

Figure 4.4 – Out-of-plane eccentricity

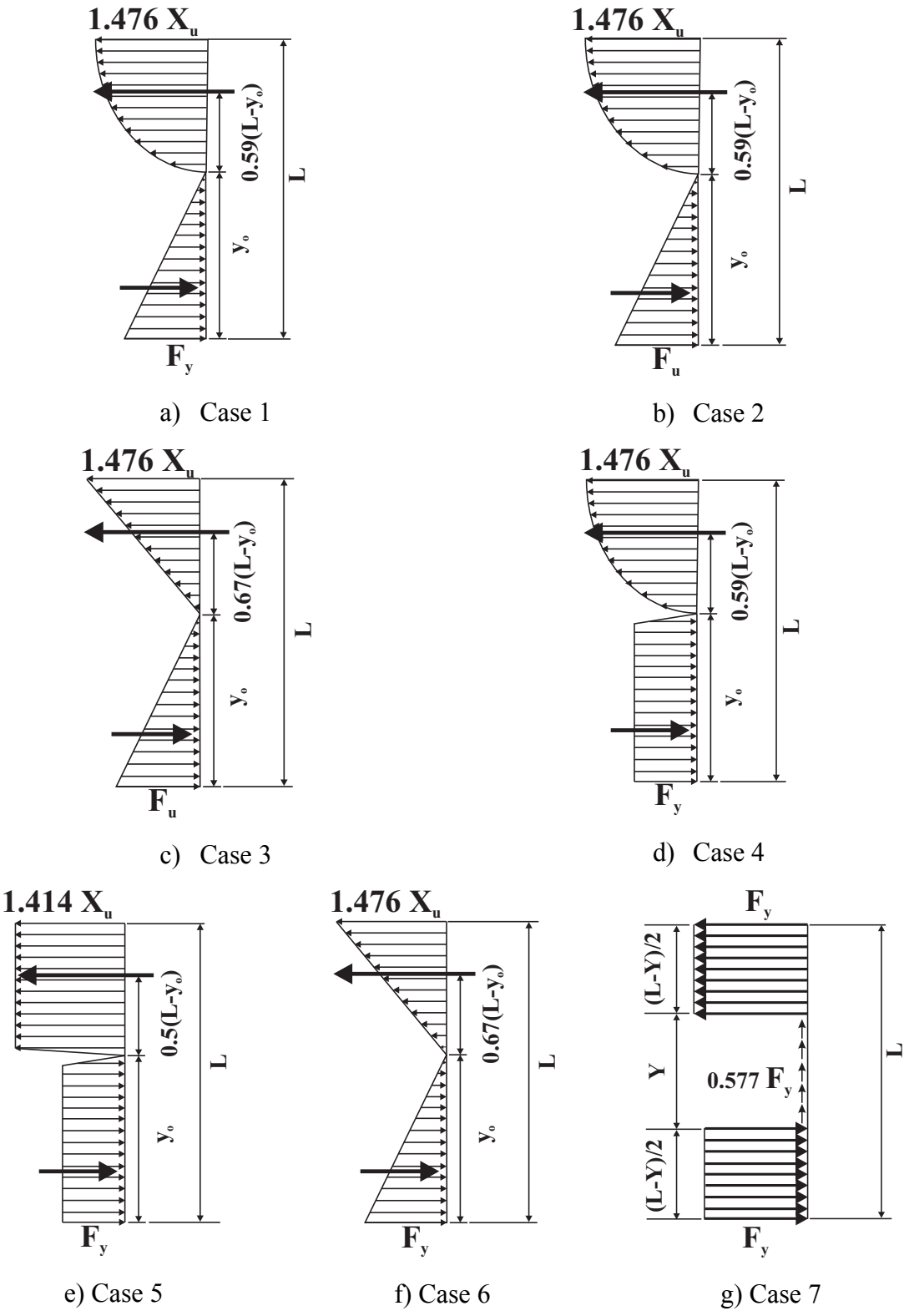

Figure 4.5 – Stress distributions proposed by Neis (1980)

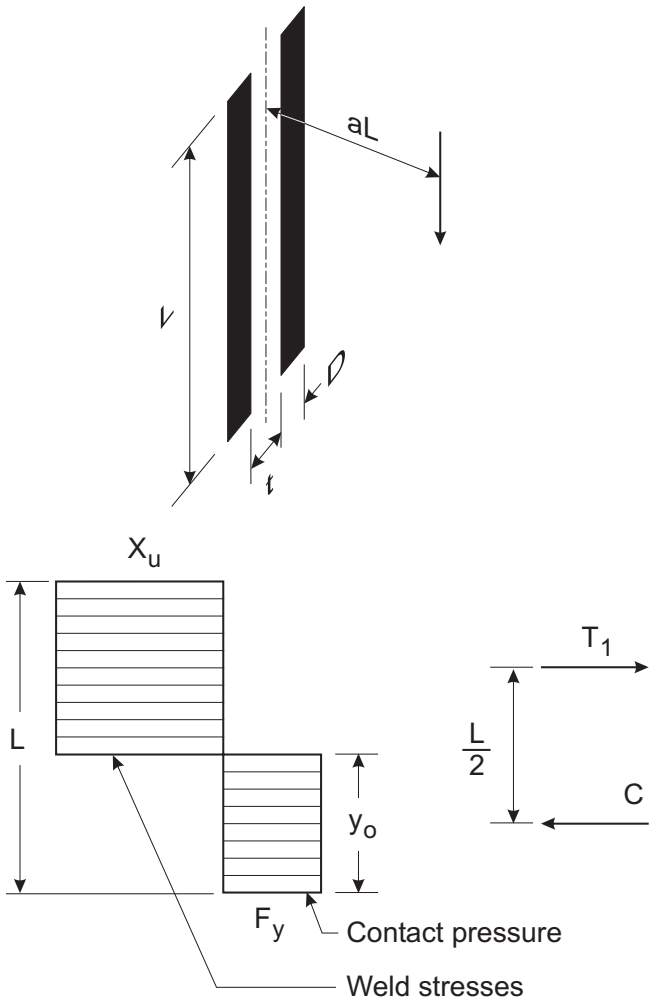

Figure 4.6 – Stress distribution assumed by Picard and Beaulieu (1991)

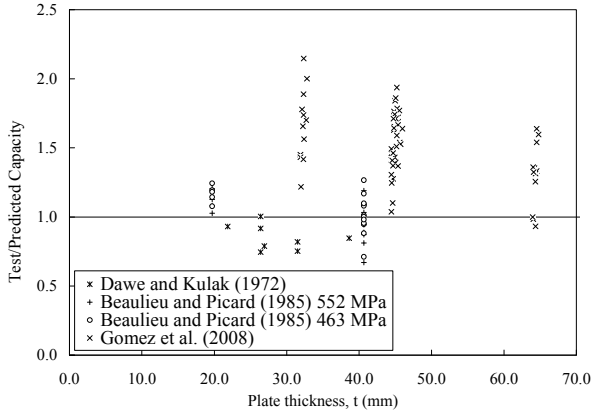

a) Test-to-predicted ratio versus plate thickness

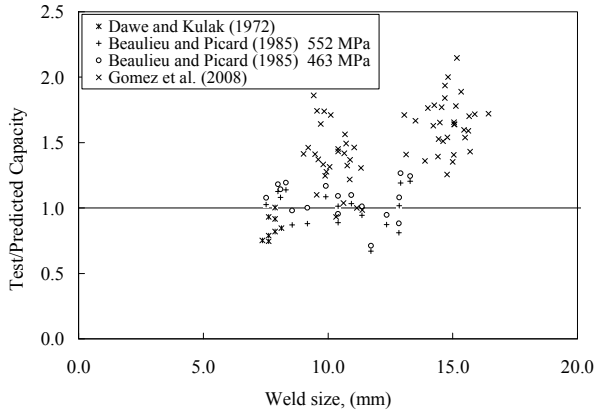

b) Test-to-predicted ratio versus weld size

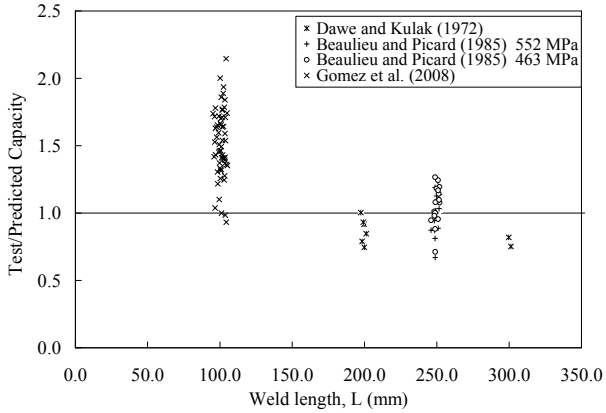

c) Test-to-predicted ratio versus weld length

Figure 4.7 – Model 1 - Test Parameters vs. Test-to-Predicted Ratios

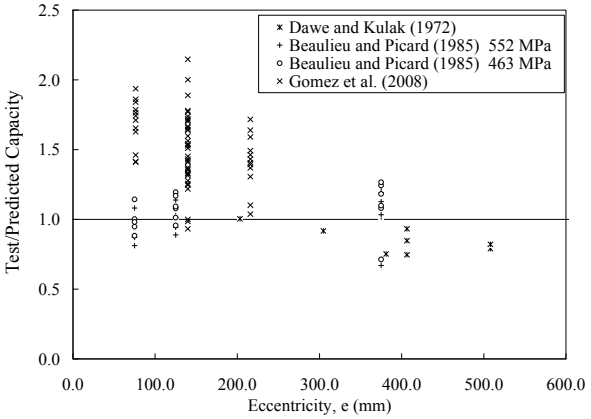

d) Test-to-predicted ratio versus eccentricity

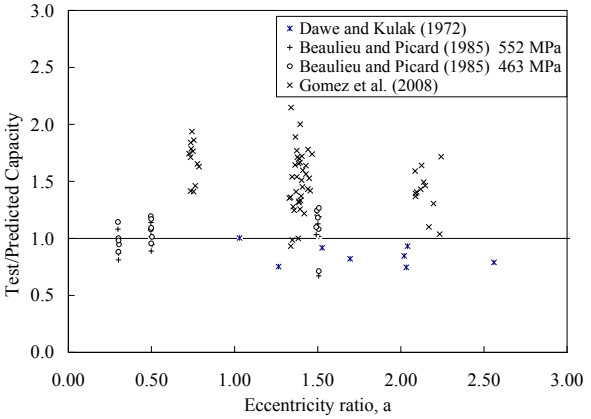

e) Test-to-predicted ratio versus eccentricity ratio

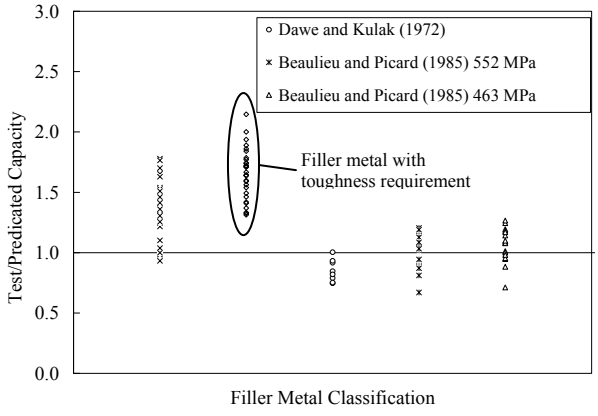

f) Test-to-predicted ratio versus filler metal classification

Figure 4.7 – (cont'd)

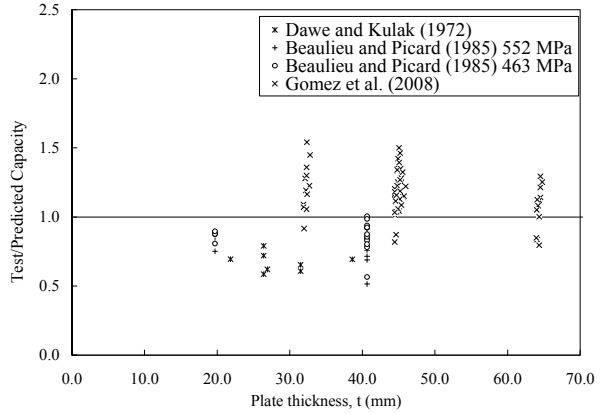

a) Test-to-predicted ratio versus plate thickness

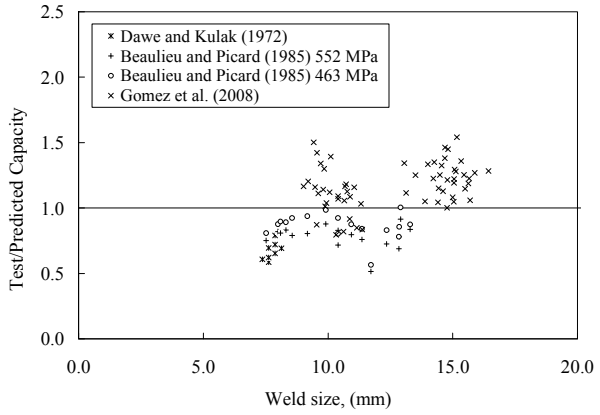

b) Test-to-predicted ratio versus weld size

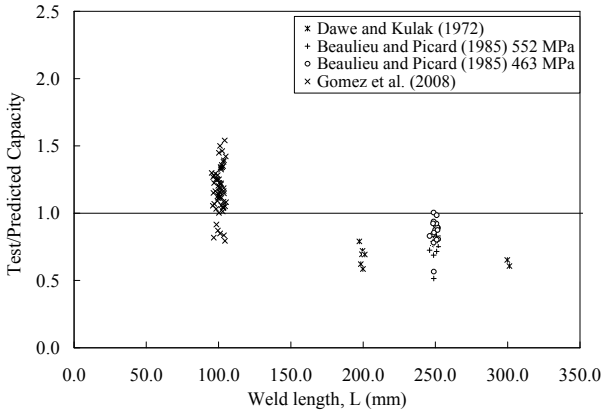

c) Test-to-predicted ratio versus weld length

Figure 4.8 – Model 2 - Test Parameters vs. Test-to-Predicted Ratios

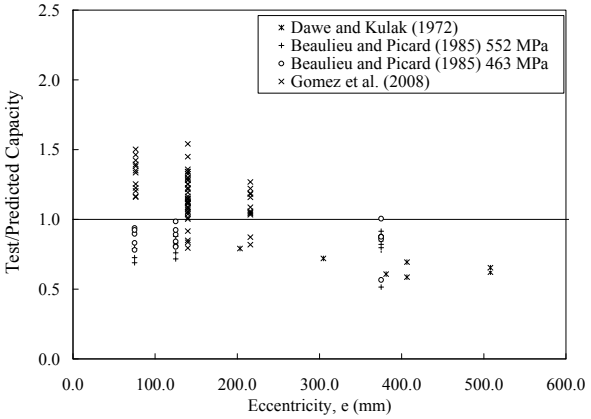

d) Test-to-predicted ratio versus eccentricity

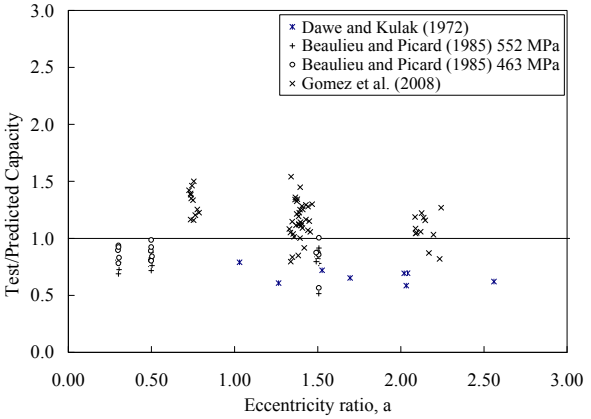

e) Test-to-predicted ratio versus eccentricity ratio

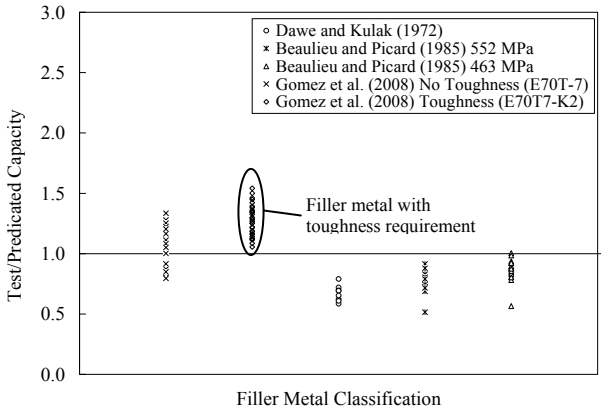

f) Test-to-predicted ratio versus filler metal classification

Figure 4.8 – (cont'd)

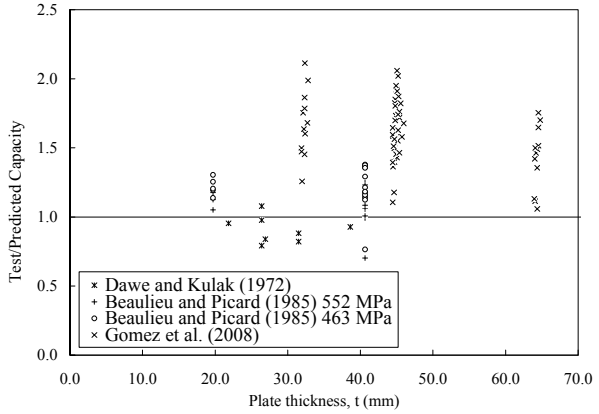

a) Test-to-predicted ratio versus plate thickness

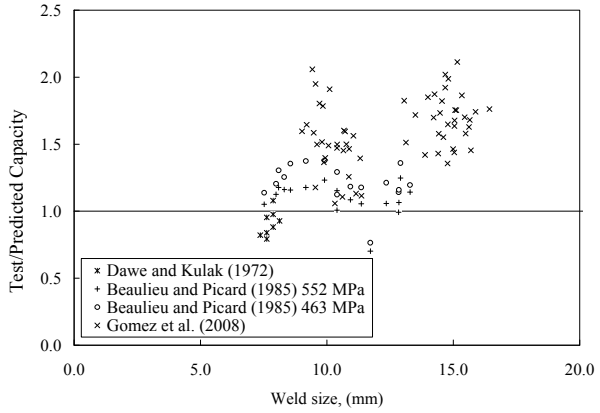

b) Test-to-predicted ratio versus weld size

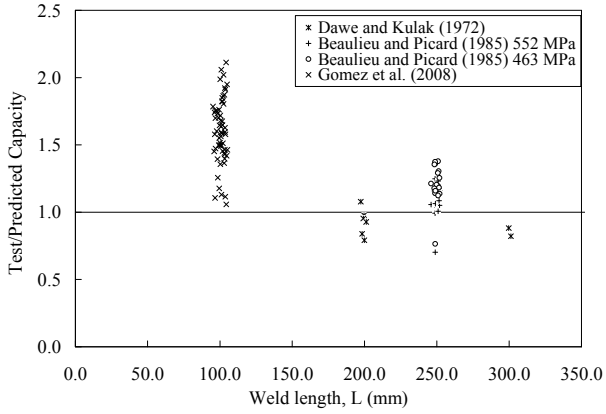

c) Test-to-predicted ratio versus weld length

Figure 4.9 – Model 3 - Test Parameters vs. Test-to-Predicted Ratios

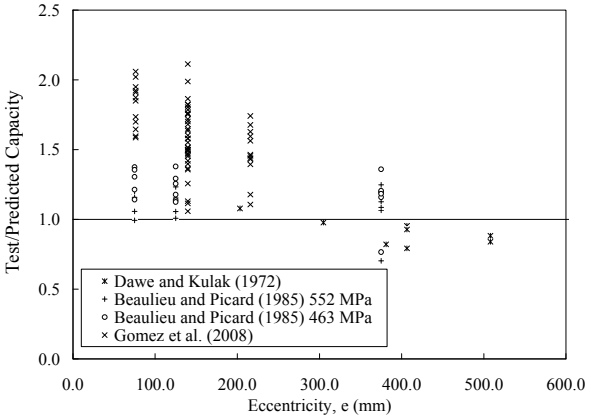

d) Test-to-predicted ratio versus eccentricity

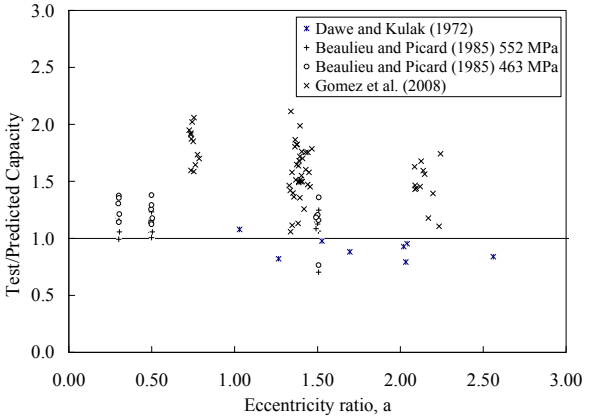

e) Test-to-predicted ratio versus eccentricity ratio

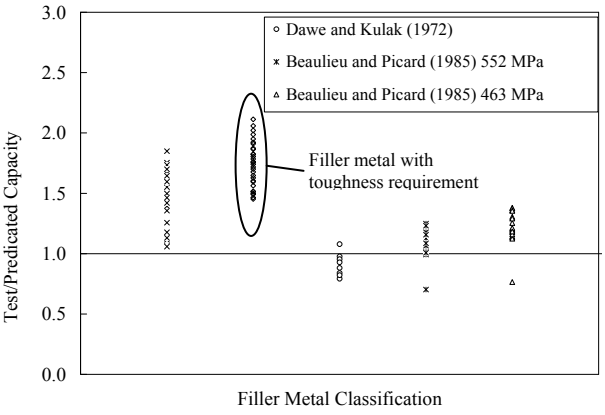

f) Test-to-predicted ratio versus filler metal classification

Figure 4.9 – (cont'd)

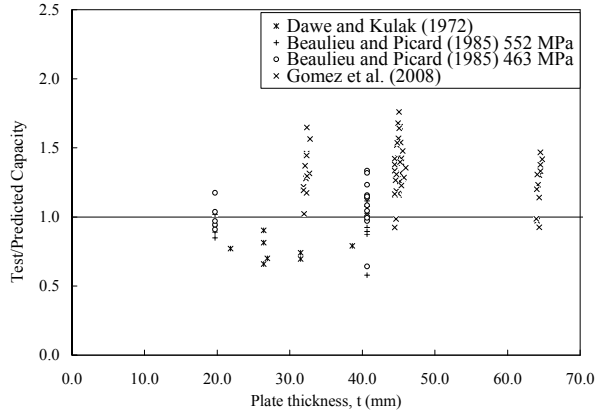

a) Test-to-predicted ratio versus plate thickness

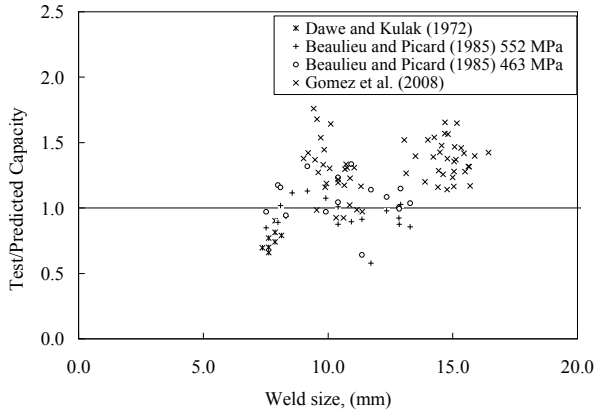

b) Test-to-predicted ratio versus weld size

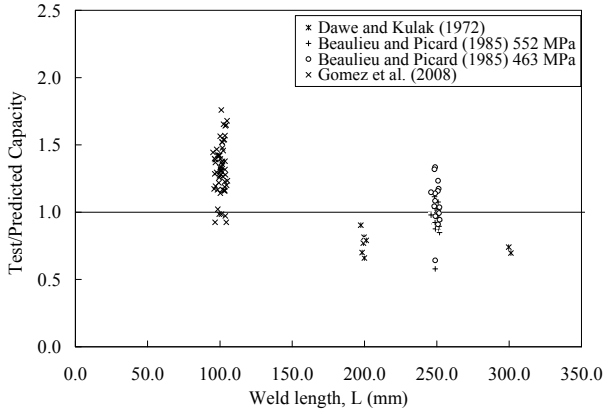

c) Test-to-predicted ratio versus weld length

Figure 4.10 – Model 4 - Test Parameters vs. Test-to-Predicted Ratios

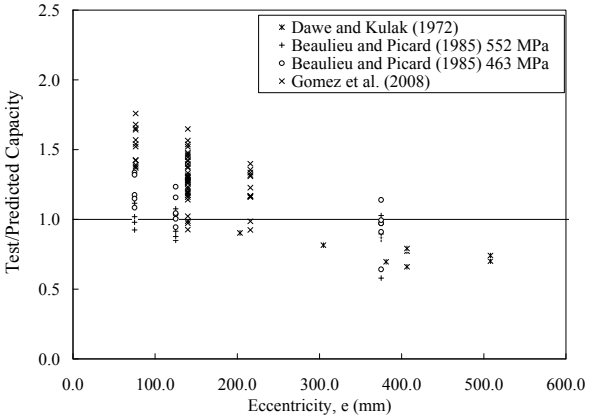

d) Test-to-predicted ratio versus eccentricity

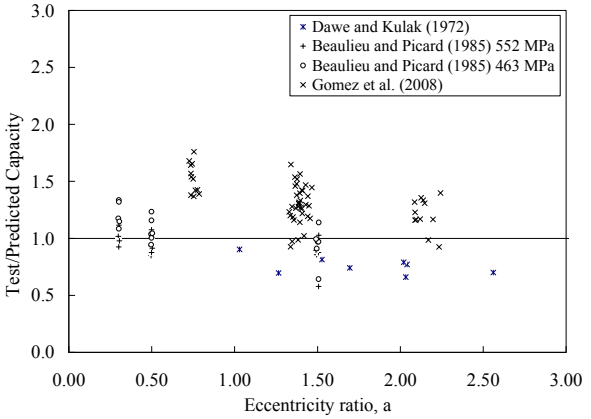

e) Test-to-predicted ratio versus eccentricity ratio

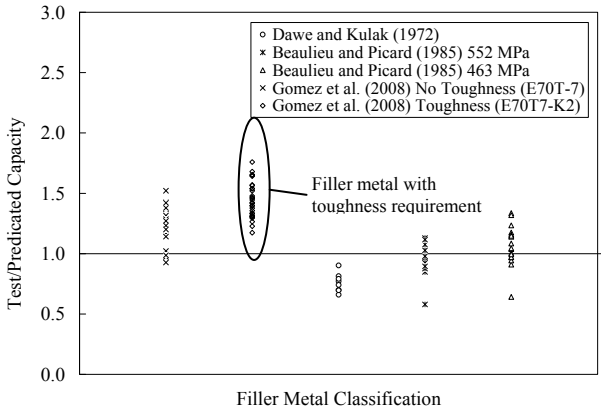

f) Test-to-predicted ratio versus filler metal classification

Figure 4.10 – (cont'd)

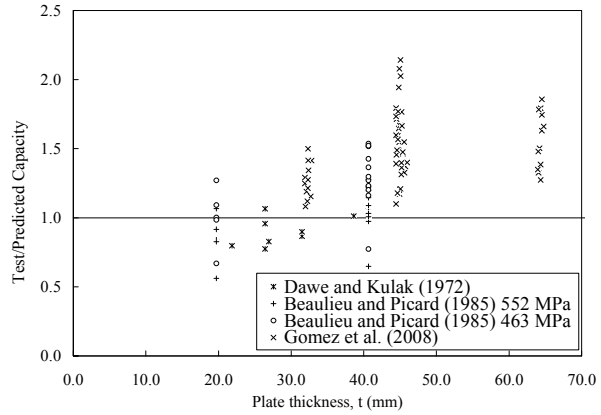

a) Test-to-predicted ratio versus plate thickness

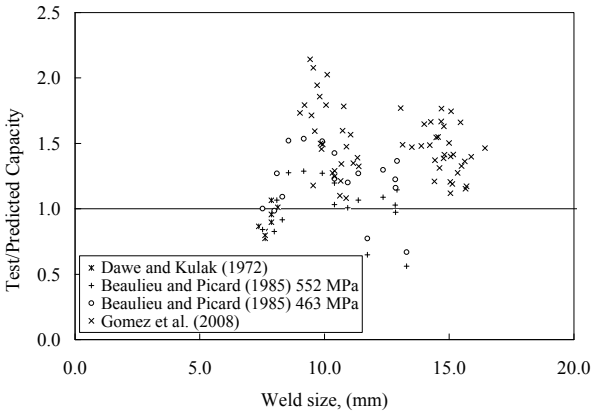

b) Test-to-predicted ratio versus weld size

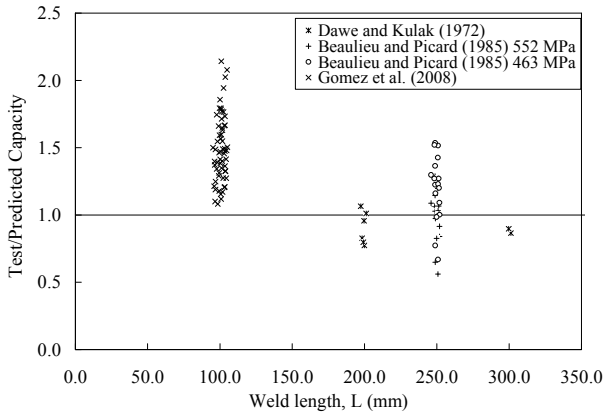

c) Test-to-predicted ratio versus weld length

Figure 4.11 – Model 5 - Test Parameters vs. Test-to-Predicted Ratios

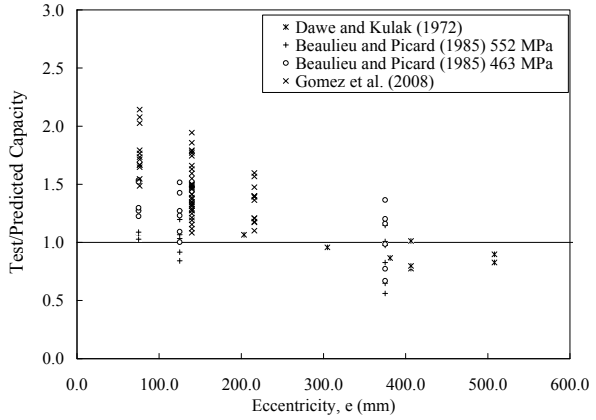

d) Test-to-predicted ratio versus eccentricity

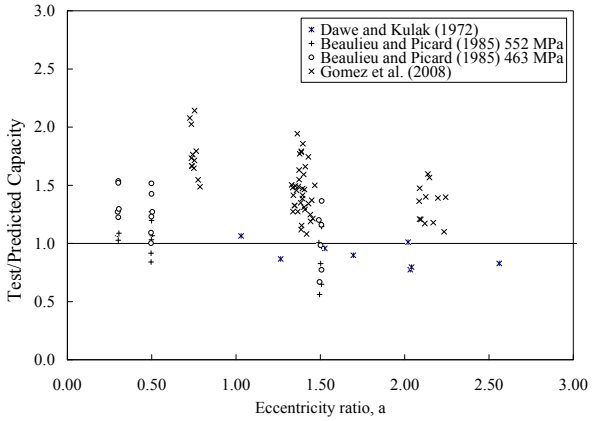

e) Test-to-predicted ratio versus eccentricity ratio

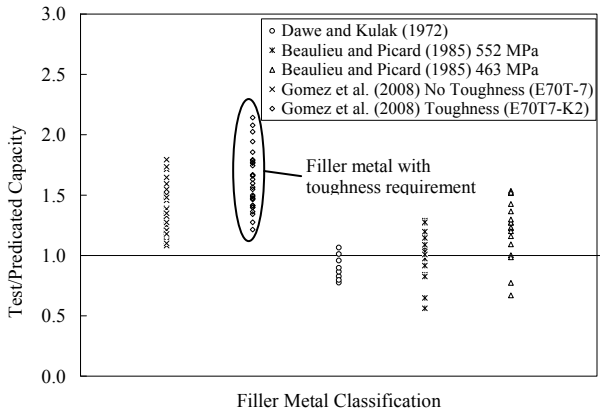

f) Test-to-predicted ratio versus filler metal classification

Figure 4.11 – (cont'd)

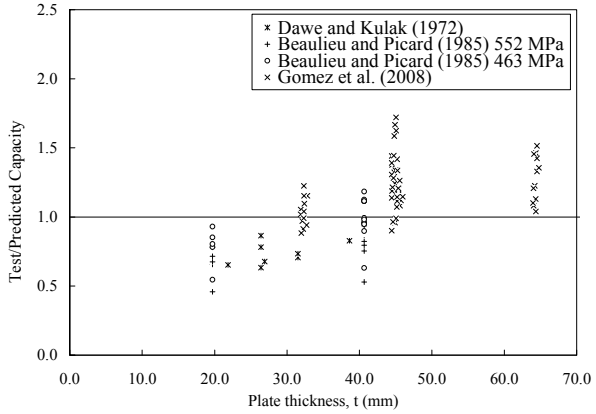

a) Test-to-predicted ratio versus plate thickness

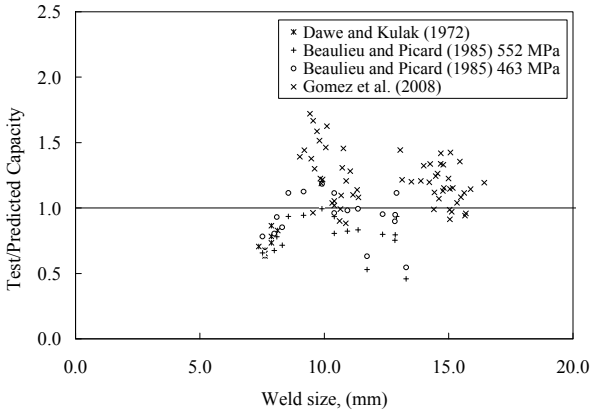

b) Test-to-predicted ratio versus weld size

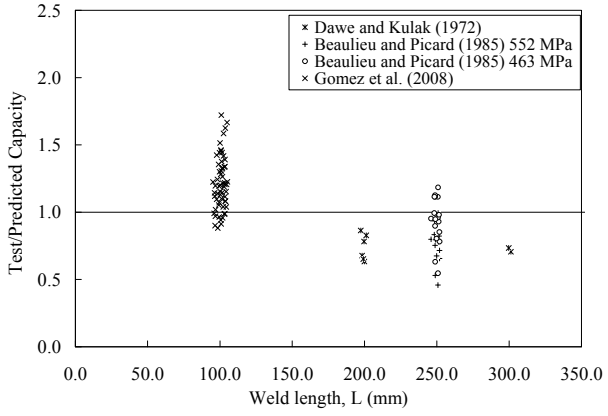

c) Test-to-predicted ratio versus weld length

Figure 4.12 – Model 6 - Test Parameters vs. Test-to-Predicted Ratios

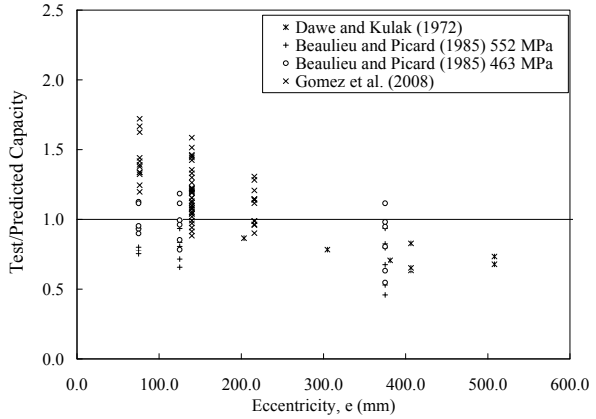

d) Test-to-predicted ratio versus eccentricity

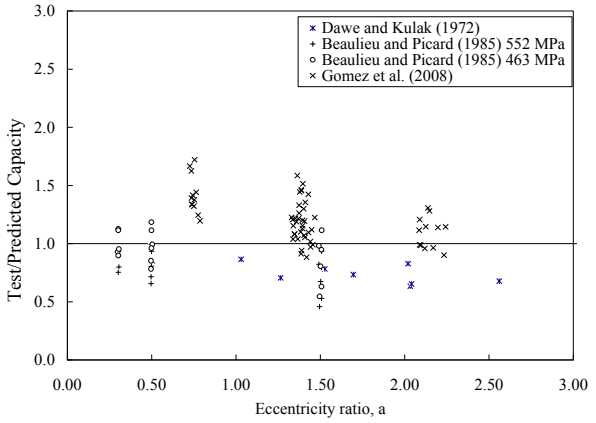

e) Test-to-predicted ratio versus eccentricity ratio

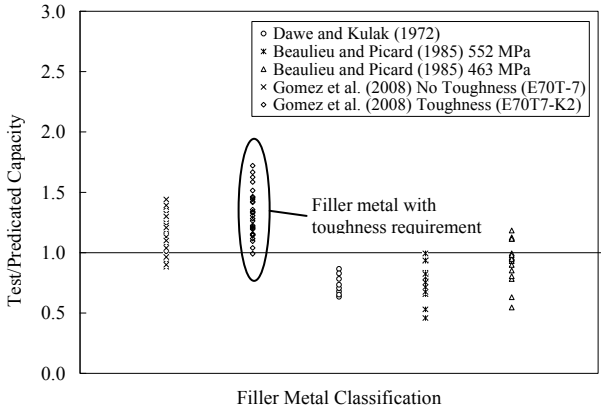

f) Test-to-predicted ratio versus filler metal classification

Figure 4.12 – (cont'd)

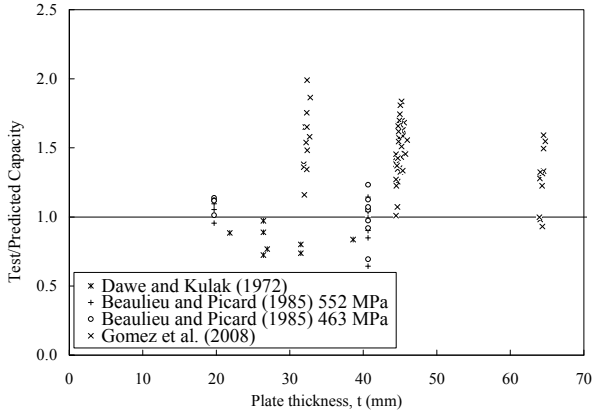

a) Test-to-predicted ratio versus plate thickness

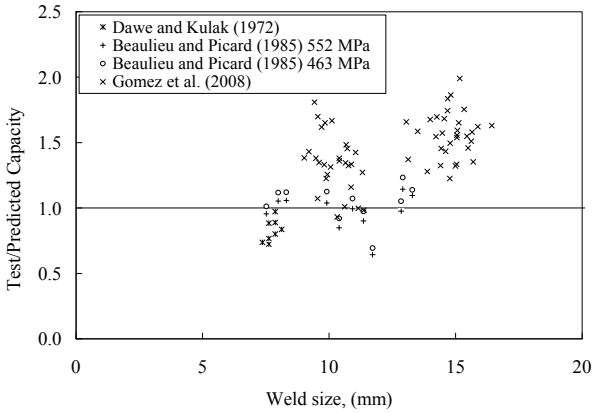

b) Test-to-predicted ratio versus weld size

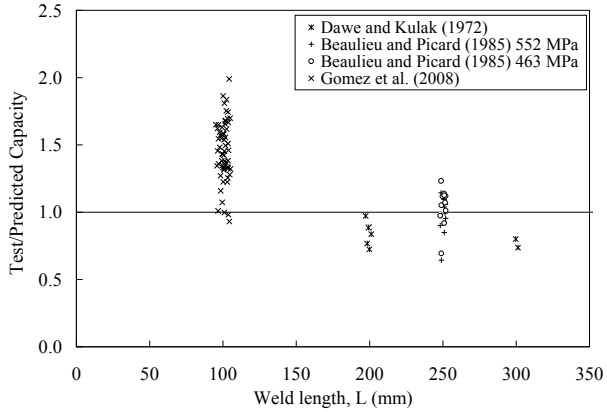

c) Test-to-predicted ratio versus weld length

Figure 4.13 – Model 7 Case 1 - Test Parameters vs. Test-to-Predicted Ratios

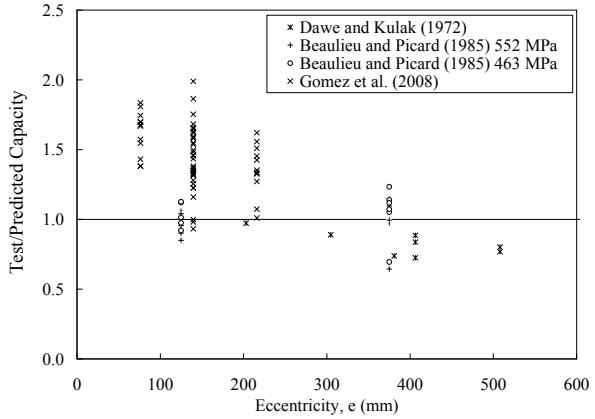

d) Test-to-predicted ratio versus eccentricity

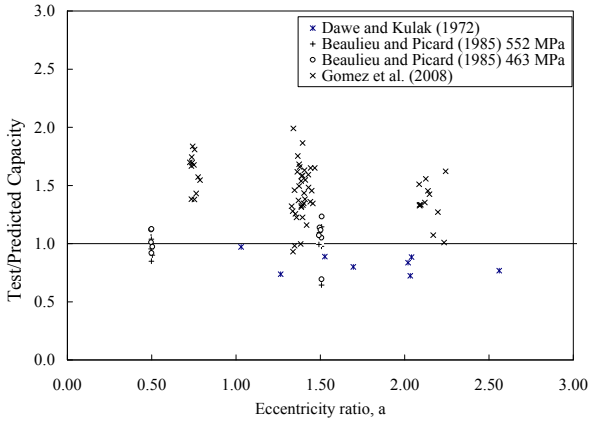

e) Test-to-predicted ratio versus eccentricity ratio

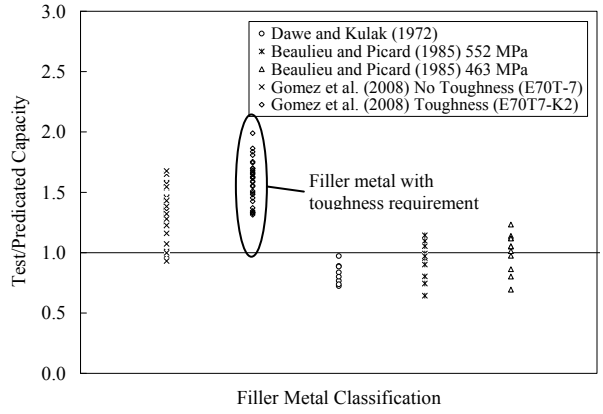

f) Test-to-predicted ratio versus filler metal classification

Figure 4.13 – (cont'd)

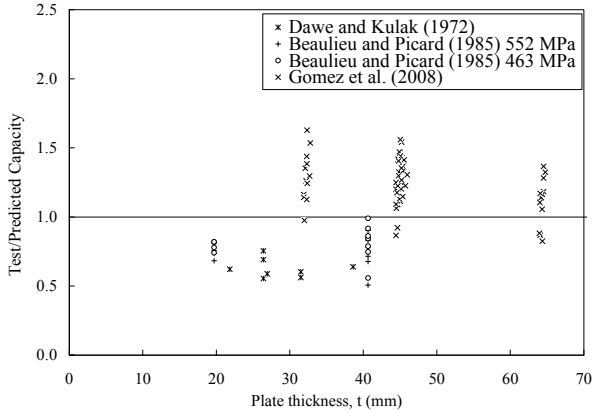

a) Test-to-predicted ratio versus plate thickness

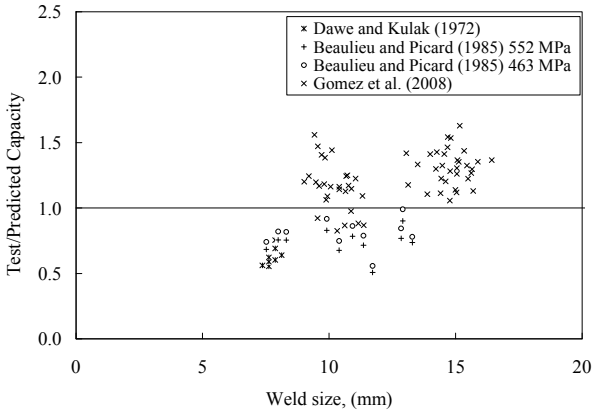

b) Test-to-predicted ratio versus weld size

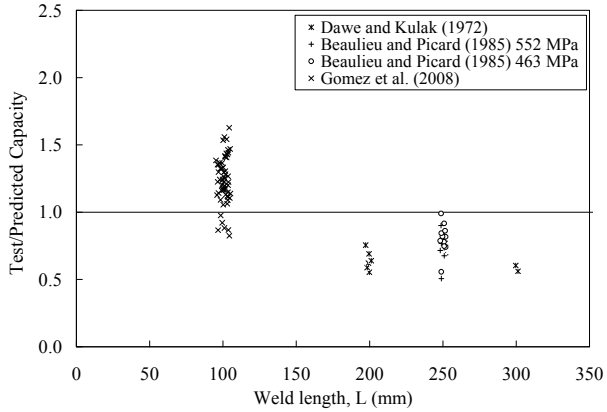

c) Test-to-predicted ratio versus weld length

Figure 4.14 – Model 7 Case 2 - Test Parameters vs. Test-to-Predicted Ratios

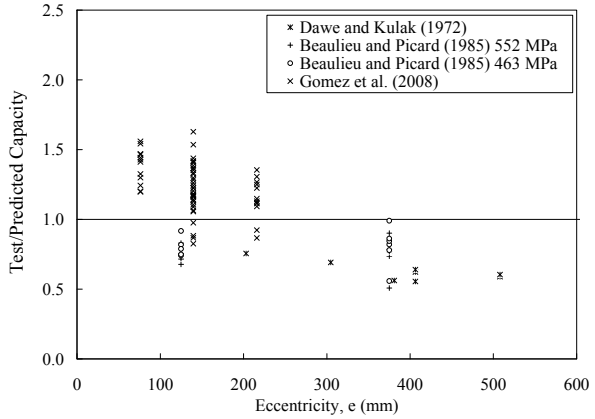

d) Test-to-predicted ratio versus eccentricity

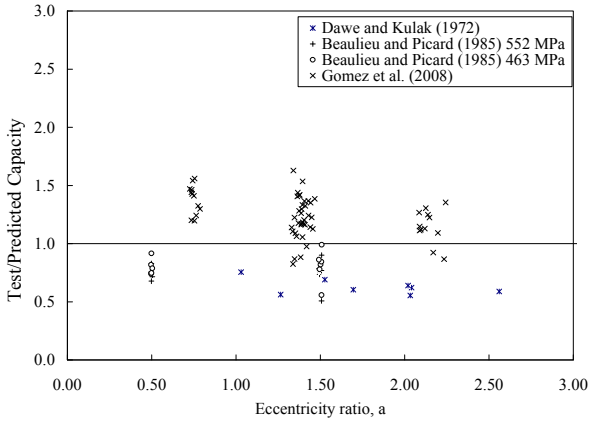

e) Test-to-predicted ratio versus eccentricity ratio

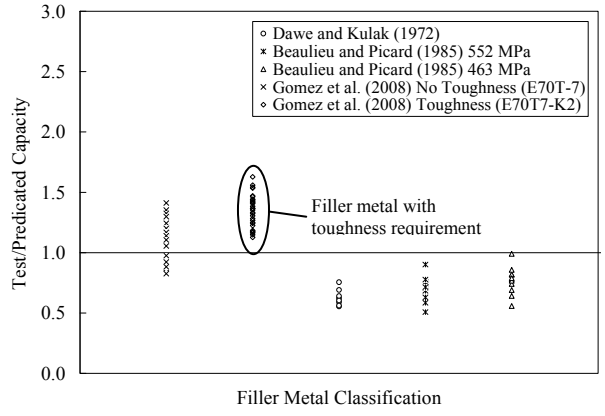

f) Test-to-predicted ratio versus filler metal classification

Figure 4.14 – (cont'd)

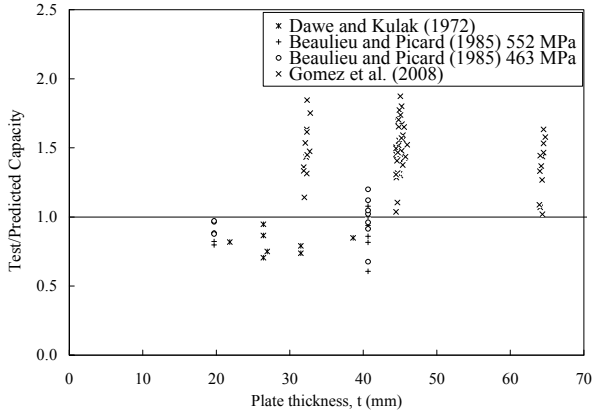

a) Test-to-predicted ratio versus plate thickness

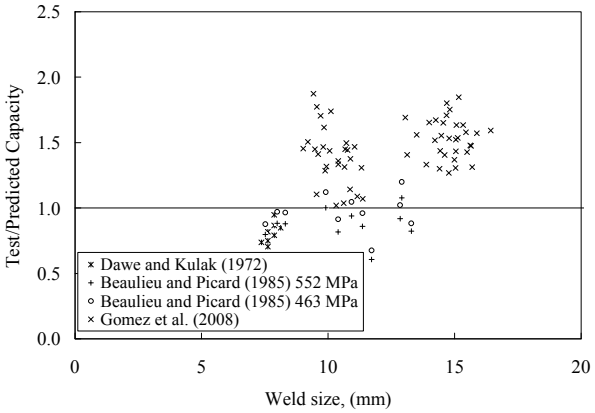

b) Test-to-predicted ratio versus weld size

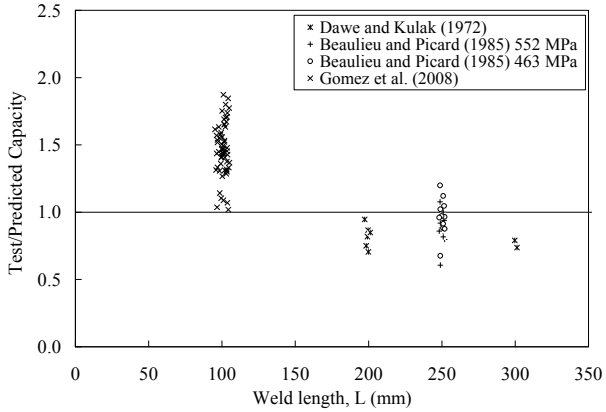

c) Test-to-predicted ratio versus weld length

Figure 4.15 – Model 7 Case 3 - Test Parameters vs. Test-to-Predicted Ratios

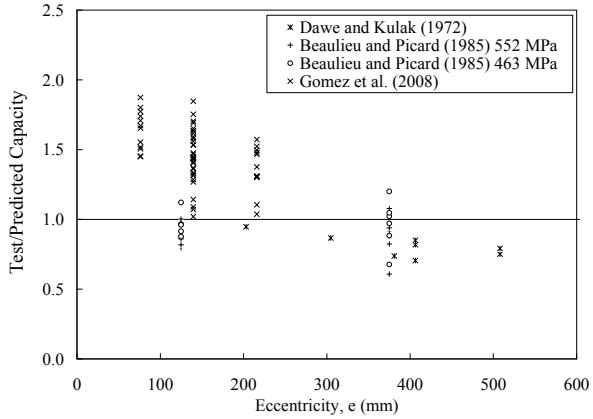

d) Test-to-predicted ratio versus eccentricity

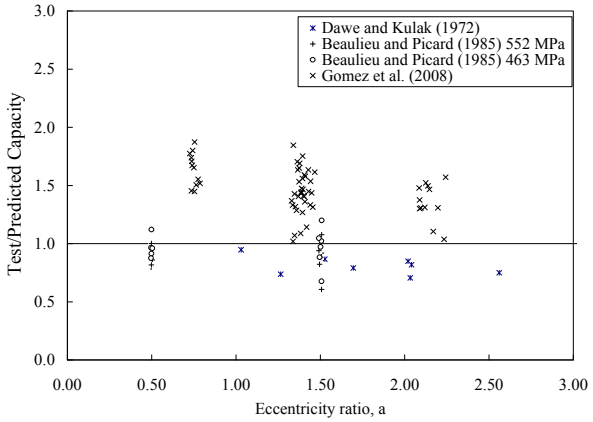

e) Test-to-predicted ratio versus eccentricity ratio

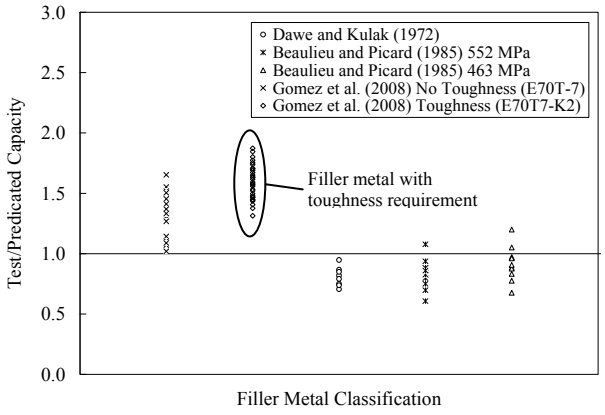

f) Test-to-predicted ratio versus filler metal classification

Figure 4.15 – (cont'd)

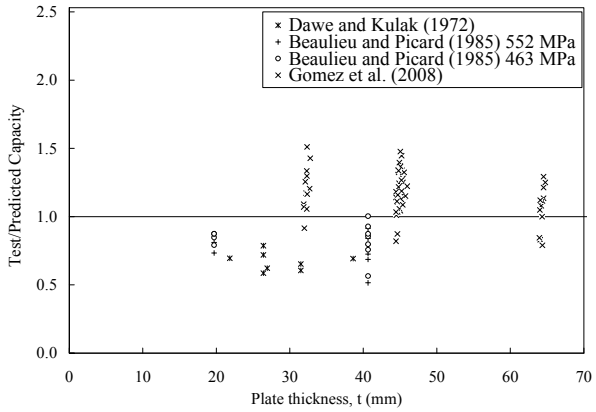

a) Test-to-predicted ratio versus plate thickness

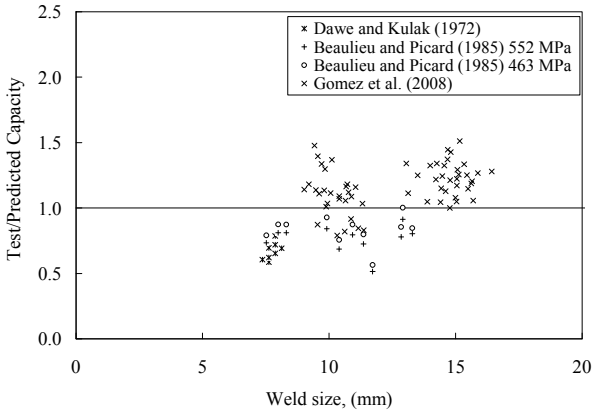

b) Test-to-predicted ratio versus weld size

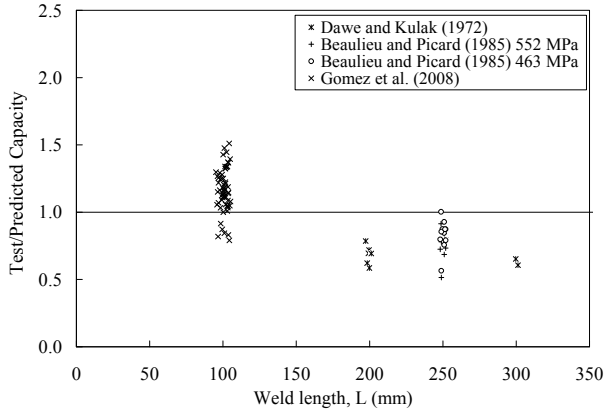

c) Test-to-predicted ratio versus weld length

Figure 4.16 – Model 7 Case 4 - Test Parameters vs. Test-to-Predicted Ratios

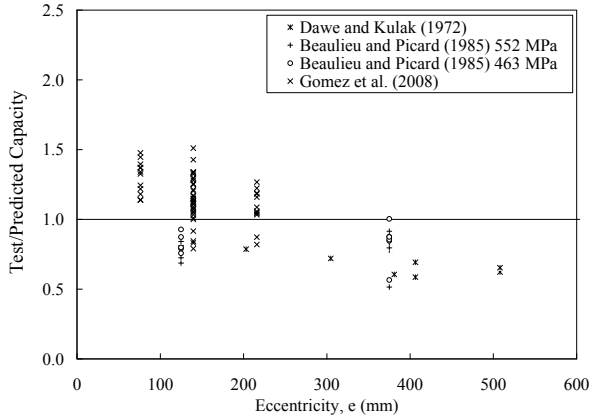

d) Test-to-predicted ratio versus eccentricity

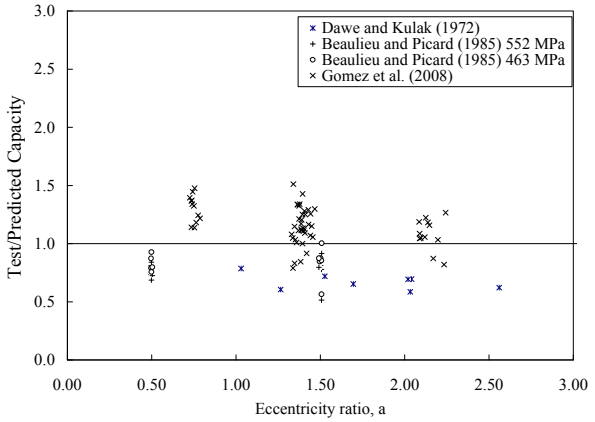

e) Test-to-predicted ratio versus eccentricity ratio

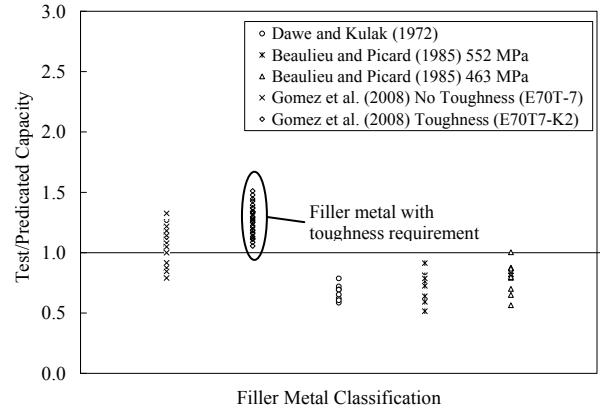

f) Test-to-predicted ratio versus filler metal classification

Figure 4.16 – (cont'd)

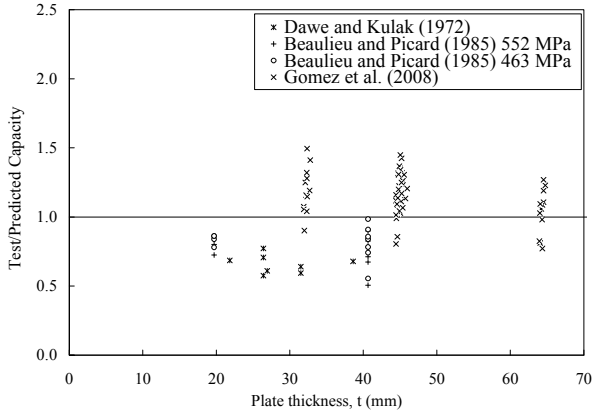

a) Test-to-predicted ratio versus plate thickness

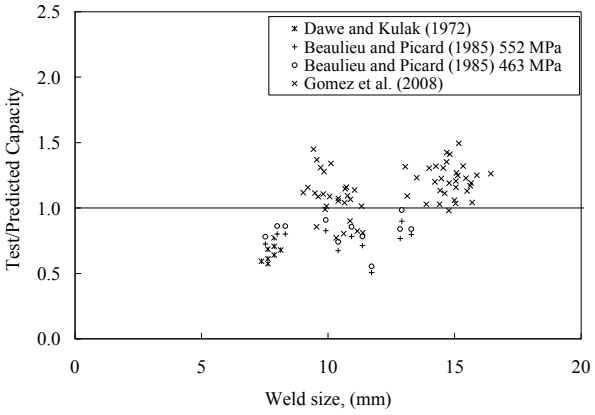

b) Test-to-predicted ratio versus weld size

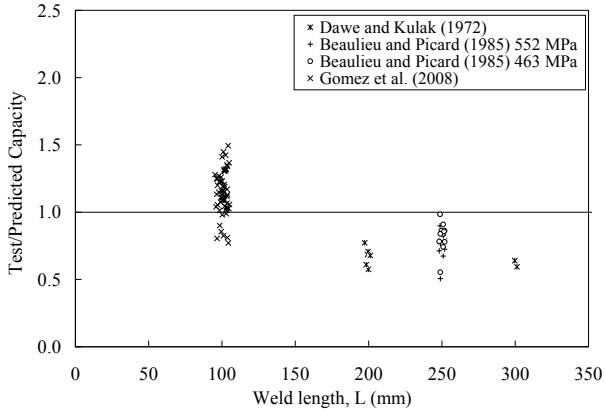

c) Test-to-predicted ratio versus weld length

Figure 4.17 – Model 7 Case 5 - Test Parameters vs. Test-to-Predicted Ratios

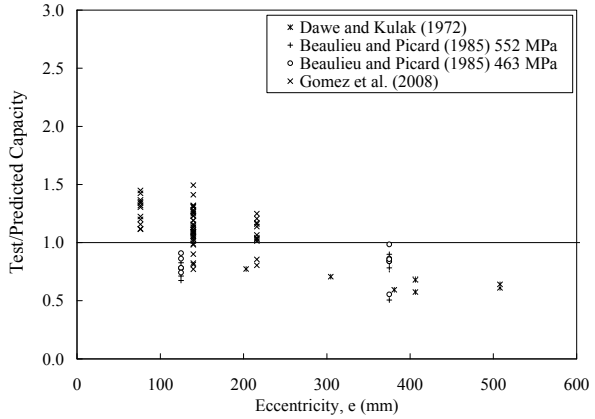

d) Test-to-predicted ratio versus eccentricity

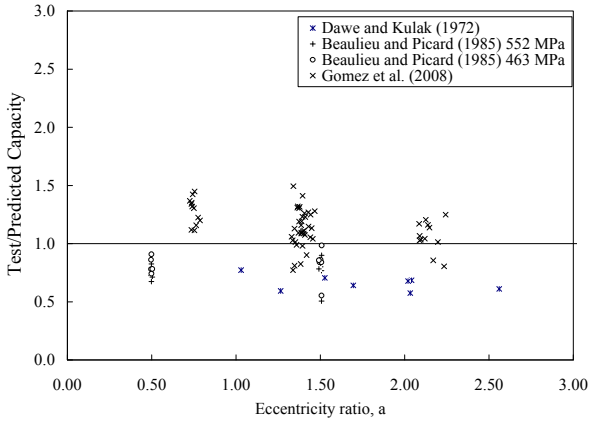

e) Test-to-predicted ratio versus eccentricity ratio

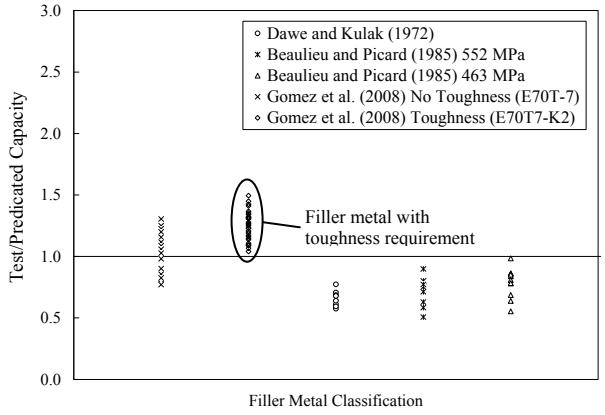

f) Test-to-predicted ratio versus filler metal classification

Figure 4.17 – (cont'd)

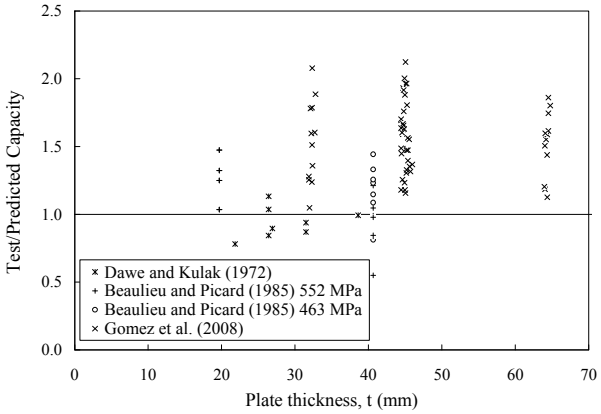

a) Test-to-predicted ratio versus plate thickness

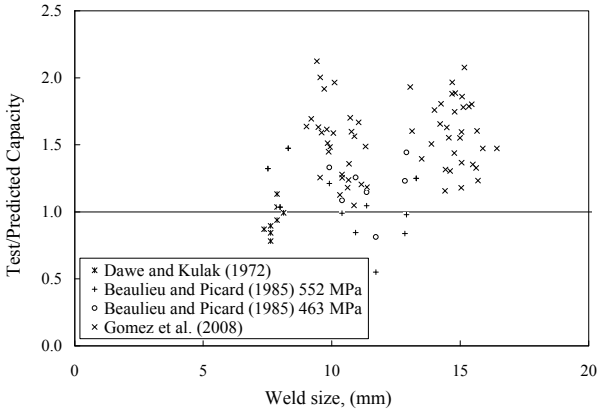

b) Test-to-predicted ratio versus weld size

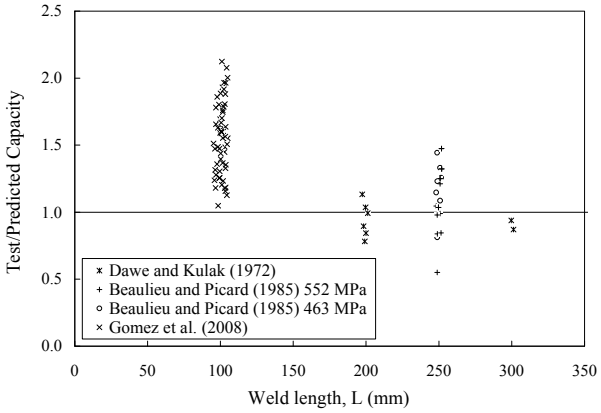

c) Test-to-predicted ratio versus weld length

Figure 4.18 – Model 7 Case 6/7 - Test Parameters vs. Test-to-Predicted Ratios

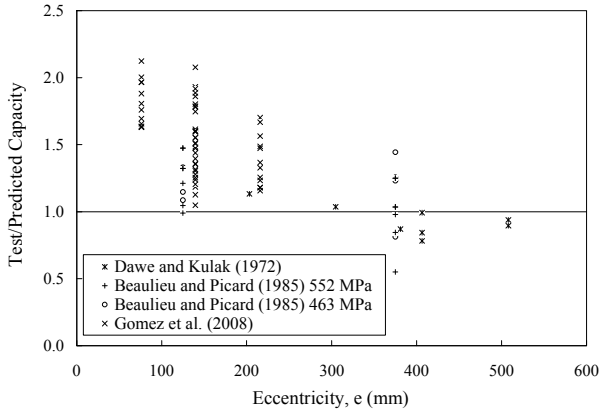

d) Test-to-predicted ratio versus eccentricity

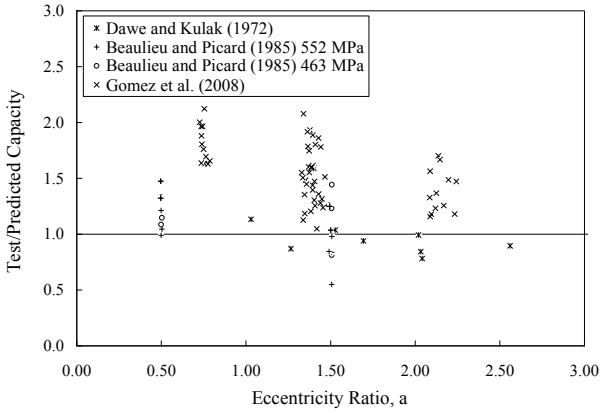

e) Test-to-predicted ratio versus eccentricity ratio

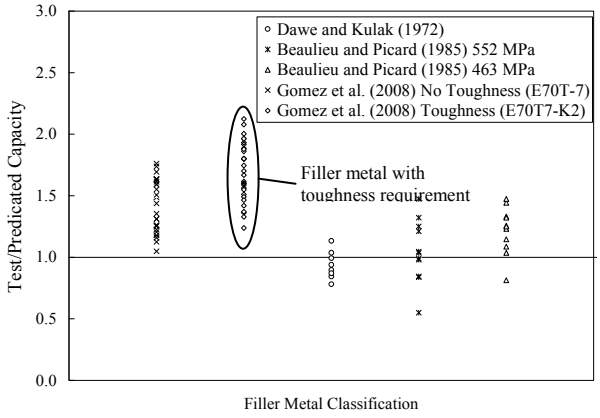

f) Test-to-predicted ratio versus filler metal classification

Figure 4.18 – (cont'd)

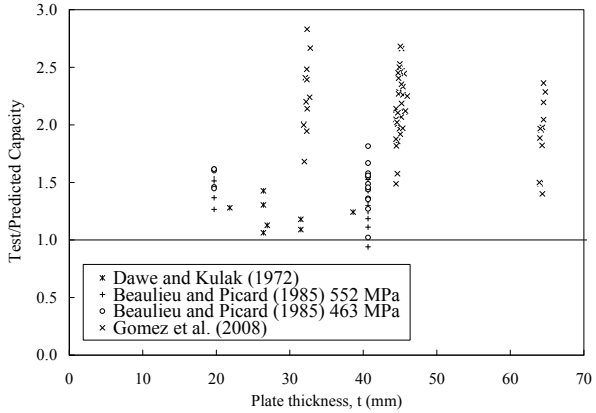

a) Test-to-predicted ratio versus plate thickness

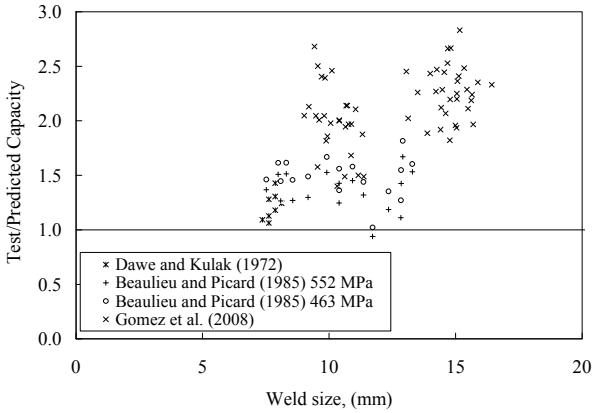

b) Test-to-predicted ratio versus weld size

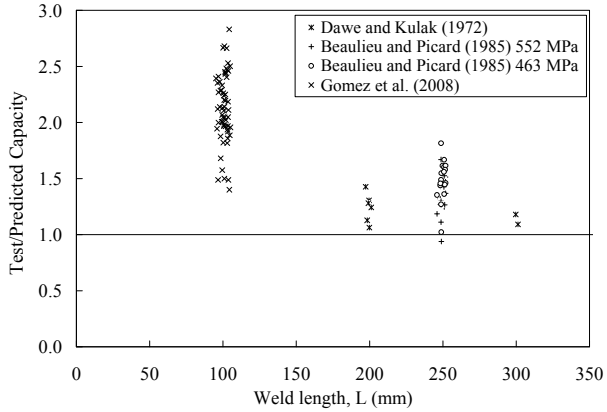

c) Test-to-predicted ratio versus weld length

Figure 4.19 – Model 8 - Test Parameters vs. Test-to-Predicted Ratios

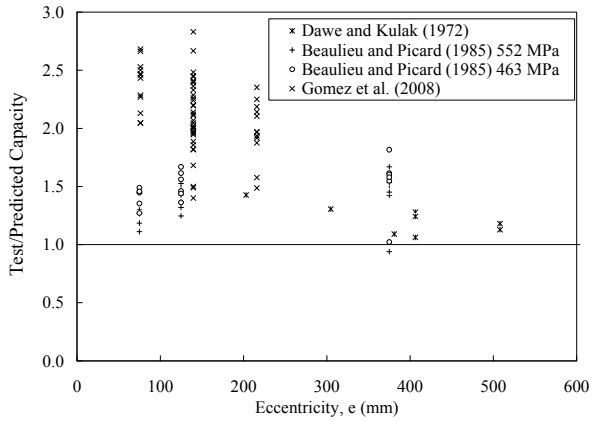

d) Test-to-predicted ratio versus eccentricity

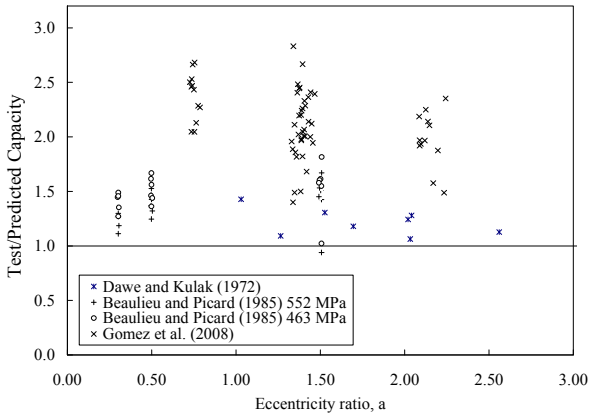

e) Test-to-predicted ratio versus eccentricity ratio

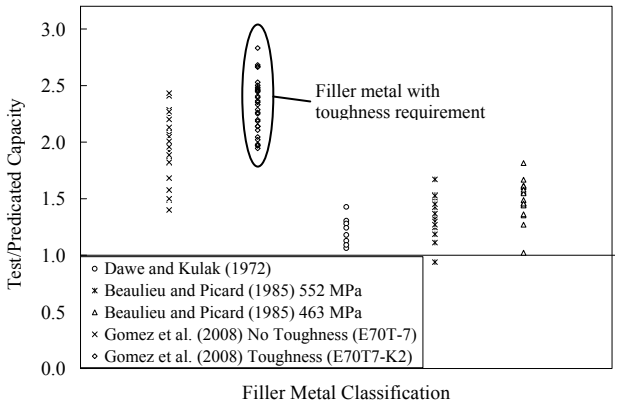

f) Test-to-predicted ratio versus filler metal classification

Figure 4.19 – (cont'd)

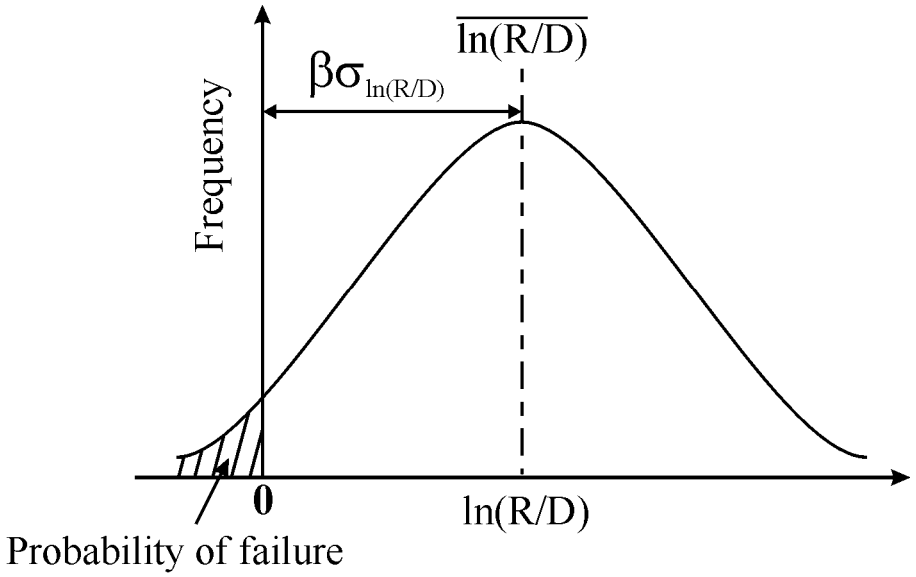

Figure 4.20 – Normal distribution curve

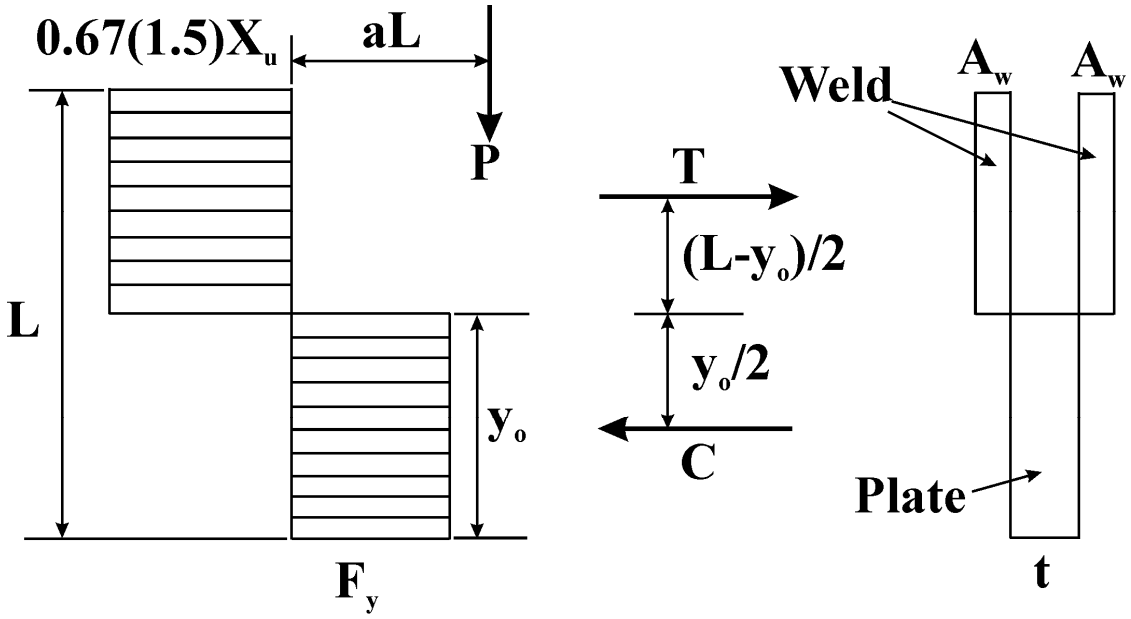

Figure 4.21 – Proposed Model for Large Load Eccentricity

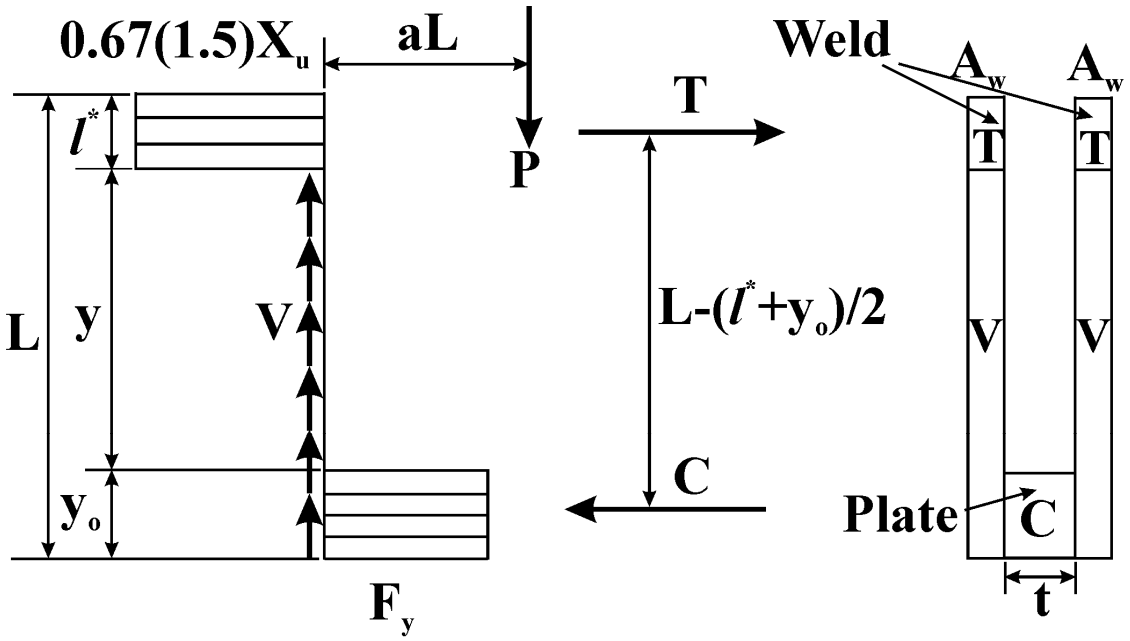

Figure 4.22 – Proposed Model for Small Load Eccentricity

Chapter 5

Summary and Conclusions

5.1 SUMMARY

The current design tables for the strength of fillet welded joints under combined shear and out-of-plane bending were derived from a closed form model proposed by Beaulieu and Picard (1985). This model is in excellent agreement with the earlier design tables that were based on the method of instantaneous centre of rotation proposed by Dawe and Kulak (1972). Both research programs preceded the work of Lesik and Kennedy (1990), which lead to the development of a load versus deformation model for fillet welds significantly different from the model used by Dawe and Kulak (1972). Although the joint strength prediction models account for plate thickness as it affects the bearing resistance of the welded joint, they do not account for a possible reduction in the tensile strength due to an increase in root notch size as the plate thickness is increased. A reliability analysis of the current design approach for welded joints under combined shear and out-of-plane bending was therefore conducted to determine the level of safety offered by current design approaches.

Test results from earlier test programs on joints under combined shear and bending were collected. Three test programs have been conducted, with the latest one conducted in 2008 as a collaborative research program between the University of Alberta and the University of California, Davis. The three test programs provide a total of 92 test results. From the two earlier test programs of Dawe and Kulak (1972) and Beaulieu and Picard (1985), strength prediction models were proposed; one using an extension of the instantaneous centre of rotation previously used for bolted connections, and the other a closed form solution proposed as an alternative to the more complex instantaneous center method. The test results cover a wide range of parameters, including plate thickness (root notch size), base metal grade, weld metal strength, weld metal classification (with and without toughness requirement), weld size and load eccentricity.

The database of available test results was used to evaluate 14 different prediction models, some of which proposed by earlier researchers and some developed in this research project. Four of these models consisted of the instantaneous centre of rotation proposed by Dawe and Kulak, but modified to consider both triangular and rectangular stress distribution in the compression zone of the connection where stresses are developed by bearing of the connected plates and incorporating load versus deformation models for fillet welds proposed by Butler and Kulak (1972) and by Lesik and Kennedy (1990). Two other models based on the method of instantaneous center, without moment transfer by bearing of the connected plates in the compression zone, were also investigated. One of these models is based on the load versus deformation model for fillet welds proposed by Lesik and Kennedy and corresponds to the model used to derive the AISC (2005) design

table and the other model made use of the load versus deformation model for fillet welds proposed by Butler and Kulak (1972). Finally, seven closed form models proposed by Neis (1980) and one closed form model proposed by Beaulieu and Picard (1985) were also evaluated.

A reliability analysis was conducted on the three most promising models to determine the level of safety offered by each models.

5.2 CONCLUSIONS

Strain gauged test specimens from the test program conducted at UC Davis indicated that the bearing region of the connecting plate reached strains large enough to justify a uniform stress distribution over the entire compression region. A prediction model based on the instantaneous centre of rotation on the tension side of the joint and a rectangular stress block on the compression side of the joint was therefore developed. A comparison of the test results with predicted capacity using this model indicated that, for welds with no toughness requirement, the value of deformation at the extreme tension end of the weld compares well with expected values, and that the presence of the root notch does not have a detrimental effect on weld strength and ductility. For weld metal with toughness requirement, the tension end weld deformation at peak load was found to be greater than for non-toughness rated welds, resulting in higher joint strength than for filler metal with no toughness requirement.

The existing CISC design approach shows a good correlation with the test data from Dawe and Kulak (1972) and Beaulieu and Picard (1985). However, the test results obtained in the UC Davis test program are much higher than the predicted capacities using the current CISC approach. For that reason, the test data from UC Davis was compared to the test data from Ng *et al.* (2002).

High values of coefficient of variation (COV) were found when the test results from three test programs were pooled together. The values of COV reduced considerably when the test-to-predicted values were grouped by test program. Other parameters such as plate thickness, load eccentricity, weld length, weld size and eccentricity ratio were found to have negligible effect on the variability of the test-to-predicted value. Weld metal toughness was found to have an effect on the test-to-predicted values. Therefore, in order to reduce the variability in test-to-predicted value, the test data were separated into two groups: test specimens prepared with toughness rated filler metal and test specimens prepared with filler metal with no toughness requirement.

Although 14 strength prediction models were evaluated by comparison of predicted strength with the test results, a detailed assessment of the models was conducted on only the three most promising models. These models are Model 4 (modified Dawe and Kulak approach to incorporate a rectangular stress block in the compression zone and the load versus deformation relationship for welds suggested by Lesik and Kennedy (1990)), Model 5 (the current AISC approach) and Model 8 (a closed form model proposed by Beaulieu and Picard and used as the current CISC approach).

An inconsistency was identified in the current CISC model proposed by Beaulieu and Picard since it takes the transverse weld area as the leg area rather than the throat area. This assumption is not in agreement with current practice of using the weld throat area to calculate the strength of a transverse weld. In addition, Beaulieu and Picard used a factor of 0.5 in their equation to obtain predictions that matched the predicted capacities in the previous edition of CISC Handbook, which was based on the Dawe and Kulak model. In addition to a resistance factor, a further reduction factor of 0.67 was added to Dawe and Kulak model in the previous edition of CISC Handbook, making the strength prediction model very conservative.

The experimental results of all documented tests on fillet welded joints indicate that the current American design approach used in the Manual of Steel Construction (AISC, 2005) is conservative. A closer analysis of the data indicated that this conservatism may be attributed to the bearing mechanism between the connected plates, which is not incorporated in the approach used for the development of the AISC design table.

Based on a reliability analysis, the safety index provided by Models 5 (current AISC approach) and 8 (current CISC approach) are significantly higher than the target value of 4.0. Although Model 4 (modified Dawe and Kulak approach) provides an acceptable level of safety, the computation procedure is complicated and time consuming. Moreover, none of the existing models with the Lesik and Kennedy load versus deformation relationship consider plate fracture, which could become critical as the plate thickness is reduced. Therefore, a simpler, closed form, model that is applicable to both weld and plate failure modes was proposed. This model provides reliable prediction and satisfactory safety index ($\beta = 4.0$) for a resistance factor of 0.67. The new proposed model consists of three equations, namely, Equation 4.27 for weld failure with large eccentricity ($a/Q > 0.53$), Equation 4.28 for weld failure under small load eccentricity, and Equation 4.34 for plate failure.

5.3 RECOMMENDATIONS FOR FUTURE RESEARCH

A closed form model for predicting the capacity of welded joints under combined shear and out-of-plane bending was proposed for joint failure in the plate rather than in the weld. The test data collected contain only five thin plate specimens that were tested in 1985. Additional test data on thin plate connections are desirable to verify the accuracy of the design model for connections with thin plates.

The test data indicated that the effect of root notch size was not significant. The strength and ductility of the weld on the tension did not seem to be reduced sufficiently to affect the strength of the welded joints. However, it is possible that as the toughness of the filler metal drops, the loss of ductility or strength of the weld metal on the tension side will be sufficient to reduce the capacity of the joint. Since all the testing to date was conducted at room temperature, tests conducted at low temperature may demonstrate an effect of root notch size (plate thickness). Low temperature tests are therefore recommended.

References

AISC (2005), "Steel Construction Manual," 13th Edition, American Institute of Steel Construction, Chicago, IL.

AWS (2005), "Specification for Carbon Steel Electrodes for Flux Cored Arc Welding," ANSI/AWS A5.20-05, American Welding Society, Miami, FL.

AWS (2005), "Specification for Low Alloy Steel Electrodes for Flux Cored Arc Welding," ANSI/AWS A5.29-2005. American Welding Society, Miami, FL.

Beaulieu, D., and Picard, A. (1985). "Résultats d'essais sur des assemblages soudés excentriques en flexion," Canadian Journal of Civil Engineering, Vol. 12, pp. 494-506.

Bornscheuer, F. W., and Feder, D. (1966). "Tests on Welded Connections with Long or Thick Fillet Welds, IIW Doc. XV-214-66," International Institute of Welding, pp. 1-10.

Bowman, M. D., and Quinn, B. P. (1994). "Examination of Fillet Weld Strength," Engineering Journal, AISC, Vol. 31, No. 3, pp. 98-108.

Butler, L. J., and Kulak, G. L. (1969). "Behaviour of Eccentrically Loaded Welded Connection," Studies in Structural Engineering No. 7, Nova Scotia Technical College, Halifax, Canada.

Butler, L. J., and Kulak, G. L. (1971). "Strength of Fillet Welds as a Function of Direction of Load," Welding Journal, Welding Research Supplement, Vol. 36, No. 5, pp. 231s-234s.

Butler, L. J., Pal, S., and Kulak, G. L. (1972). "Eccentrically Loaded Welded Connections," Journal of the Structural Division, ASCE, Vol. 98, ST5, May, pp. 989-1005.

Callele, L. J., Grondin, G. Y., and Driver, R. G. (2005). "Strength and Behaviour of Multi-Orentation Fillet Weld Connections," Structural Engineering Report 225, Department of Civil and Environmental Engineering, University of Alberta, Edmonton, AB.

Canadian Institute of Steel Construction (2004): Handbook of Steel Construction. Eighth Edition., Toronto, Ontario.

Canadian Institute of Steel Construction (2006): Handbook of Steel Construction. Ninth Edition., Toronto, Ontario.

Chen, W. F., and Han, D. J. (1988). “Plasticity for Structural Engineers,” Springer-Verlag, N.Y.

Clark, P. J. (1971). “Basis of Design for Fillet-Welded Joints under Static Loading,” Proceedings of Conference on Improving Welded Product Design,” The Welding Institute, Cambridge, England, Vol. 1, pp. 85-96.

Crawford, S.F., and G.L. Kulak (1971) "Eccentrically Loaded Bolted Connections," Journal of the Structural Division, ASCE, Vol. 97, No. ST3, pp. 765-783.

CSA, (2001). “Limit States Design of Steel Structures,” CSA S16-01, Canadian Standards Association, Toronto, ON.

Dawe, J. L., and Kulak, G. L. (1972). “Behaviour of Welded connections under combined shear and moment,” Structural Engineering Report 40, Department of Civil Engineering, University of Alberta, Edmonton, AB.

Dawe, J.L., and Kulak, G.L., (1974), “Welded connections under combined shear and moment,” Journal of the Structural Division, Proceedings of the ASCE, Vol. 100, No. ST4, pp. 727-741

Deng, K., Driver, R. G., and Grondin, G. Y. (2003). “Effect of Loading Angle on the Behaviour of Fillet Welds,” Structural Engineering Report 251, Department of Civil and Environmental Engineering, University of Alberta, Edmonton, AB.

Fisher, J. W., Galambos, T. V., Kulak, G. L., and Ravindra, M. K. (1978). “Load and Resistance Factor Design Criteria for Connectors,” Journal of the Structural Division, ASCE, Vol. 104, No. ST9, Sept., pp. 1427-1441.

Gagnon, D. P., and Kennedy, D. J. L. (1987). “Behaviour and Ultimate Strength of Partial Joint Penetration Groove Welds,” Structural Engineering Report 151, Department of Civil and Environmental Engineering, University of Alberta, Edmonton, AB.

Galambos, T. V., and M. K. Ravindra, (1978). “Load and Resistance Factor Design for Steel,” Journal of the Structural Division, ASCE, Vol. 104, No. ST9, Sept., pp. 1337-1353.

Gomez, I. R., Kwan, Y. K., Kanvinde, A. M., and Grondin, G. Y. (2008). “Strength and Ductility of Welded Joints Subjected to Out-of-Plane Bending,” Report to American Institute of Steel Construction, July, 2008.

Higgins, T.R., and Preece, F. R. (1969). “Proposed Working Stresses for Fillet Welds in Building Construction,” Engineering Journal, AISC, Vol. 6, No. 1, pp. 16-20.

Kato, B., and Morita, K. (1969). “The Strength of Fillet Welded Joints, IIW Doc. XV-267-69,” International Institute of Welding.

Lesik, D. F., and D. J. L. Kennedy, (1988). "Ultimate Strength of Eccentrically Loaded Fillet Welded Connections," Structural Engineering Report 159, Department of Civil Engineering, University of Alberta, Edmonton, AB.

Lesik, D. F., and D. J. L. Kennedy, (1990). "Ultimate Strength of Fillet Welded Connections Loaded in Plane," Canadian Journal of Civil Engineering, Vol. 17, No. 1, pp. 55-67.

Li, C., (2007), "Reliability Analysis of Concentrically Loaded Fillet Welds," MSc thesis, Department of Civil and Environmental Engineering, University of Alberta, Edmonton, Alberta, October.

Li, C., Grondin, G. Y., and Driver, R. G. (2007). "Reliability Analysis of Concentrically Loaded Fillet Welds," Structural Engineering Report 271, Department of Civil and Environmental Engineering, University of Alberta, Edmonton, AB.

Ligtenberg, F. K. (1968). "International Test Series Final Report, IIW Doc. XV-242-68," International Institute of Welding.

Mansell, D. S., and Yadav, A. R. (1982). "Failure Mechanisms in Fillet Welds," ACMSM 8: Proceedings of Eighth Australasian Conference on Mechanics of Structures and Materials, University of Newcastle, Newcastle, Australia, pp. 25.1-25.6.

Miazga, G.S., and Kennedy, D. J. L. (1986). "Behaviour of Fillet Welds as a Function of the Angle of Loading," Structural Engineering Report 133, Department of Civil Engineering, University of Alberta, Edmonton, AB.

Miazga, G. S., and Kennedy, D. J. L. (1989). "Behaviour of Fillet Welds as a Function of the Angle of Loading," Canadian Journal of Civil Engineering, Vol. 16, No. 4, pp. 583-599.

Neis, V.V. (1980). "Factored Resistance of Welded Connections Subject to Shear and Moment," Canadian Journal of Civil Engineering, Vol. 7, No. 1, pp. 84-92.

Ng, A. K. F., Driver, R. G., and Grondin, G. Y. (2002). "Behaviour of Transverse Fillet Welds," Structural Engineering Report 245, Department of Civil and Environmental Engineering, University of Alberta, Edmonton, AB.

Pham, L. (1981). "Effect of Size on the Static Strength of Fillet Welds," CSIRO Division of Building Research Technical Publication, Melbourne, Victoria, Australia.

Pham, L. (1983a). "Co-ordinated Testing of Fillet Welds Part 1-Cruciform Specimens-AWRA Contract 94, AWRA Document P6-35-82," Australian Welding Research, Vol. 12, pp. 16-25.

Pham, L. (1983b). "Co-ordinated Testing of Fillet Welds Part 2-Werner Specimens-AWRA Report P6-35-82," Australian Welding Research, Vol. 12, pp. 54-60.

Picard, A., and D. Beaulieu, (1991). “Calcul des charpentes d’acier (*Design of steel structures*),” Canadian Institute of Steel Construction, Toronto, Ont.

Schmidt, B. J., and Bartlett, F. M. (2002). “Review of resistance factor for steel: Data Collection,” Canadian Journal of Civil Engineering, Vol. 29, pp. 98-108.

Swannell, P., and Skewes, I. C. (1979a). “The Design of Welded Brackets Loaded In-Plane: Elastic and Ultimate Load Techniques-AWRA Report P6-8-77,” Australian Welding Research, Vol. 7, Jan., pp. 28-59.

Swannell, P., and Skewes, I. C. (1979b). “The Design of Welded Brackets Loaded In-Plane: General Theoretical Ultimate Load Techniques and Experimental Programme,” Australian Welding Research, Vol. 7, Apr., pp. 55-70.

Tide, R.H.R, (1980), “Eccentrically loaded weld groups – AISC Design Tables,” Engineering Journal, AISC, 17(4), 90-95.

Werren, A. (1984), "Comportement Expérimental et Calcul des Assemblages Soudés Excentriques en Flexion" (*Test behavior and design of welded joints with out-of-plane bending*), MSc Thesis, Faculty of Sciences and Engineering, University Laval, Ste-Foy, Quebec.

Appendix A

Instantaneous Centre of Rotation Approach

Appendix A

Instantaneous Centre of Rotation Approach

Dawe and Kulak developed an iterative procedure for welded joints loaded out-of-plane by modeling the plate bearing in the compression zone using a triangular stress block, combined with the instantaneous centre of rotation approach in the tension zone. The instantaneous centre of rotation approach requires that the weld on the tension side of the joint be modeled by discrete weld segments. To obtain a solution, initial values for r_o and y_o (see Figure A.1) are assumed, which establishes the location of the instantaneous centre. Each weld element has it own resisting force oriented in a direction perpendicular to the radial distance to the instantaneous centre. The force in each weld segment has vertical and horizontal components $(R_i)_v$ and $(R_i)_h$. In the compression zone the normal force H_b represents the resultant of the triangular stress block and the vertical force V_b represents the strength of the weld in the compression zone loaded at an angle $\theta = 0°$.

$$V_b = \frac{y_o}{(L - y_o)} \sum_1^n (R_i)_v \qquad [A.1]$$

The resultant force of the triangular stress distribution as shown in Figure A.1 acts at $\frac{2}{3}\,y_o$ below the neutral axis and is expressed as:

$$H_b = \frac{y_o \sigma_y t}{2} \qquad [A.2]$$

where σ_y is the maximum stress in the compression zone, taken as the yield strength of the plate material, and *t* is the plate thickness. The sum of the moments created by all the forces about the instantaneous centre is equal to

$$P(e + r_o) - \sum_1^n (R_i r_i) - r_o V_b - \left(\frac{2}{3}\right) y_o H_b = 0 \qquad [A.3]$$

Similarly, the sum of the vertical forces on the connection is equal to:

$$\sum_1^n (R_i)_v + V_b - P = 0 \qquad [A.4]$$

Substituting *P* from Equation A.3 into Equation A.4, gives:

$$\sum_1^n (R_i)_v + V_b = \left[\frac{\sum_1^n (R_i r_i) + r_o V_b + \left(\frac{2}{3}\right) y_o H_b}{e + r_o} \right] \qquad [A.5]$$

The sum of the horizontal forces gives:

$$H_b - \sum_{1}^{n} (R_i)_h = 0 \qquad \text{[A.6]}$$

Once the values r_o and y_o satisfy Equation A.5, it can be used to evaluate the terms in Equation A.6. If both equations are satisfied, the ultimate load has been determined and it can be computed by using Equation A.4. If the pair of values does not satisfied in Equation A.6, then the procedure is need to repeat by choosing another values of r_o and y_o.

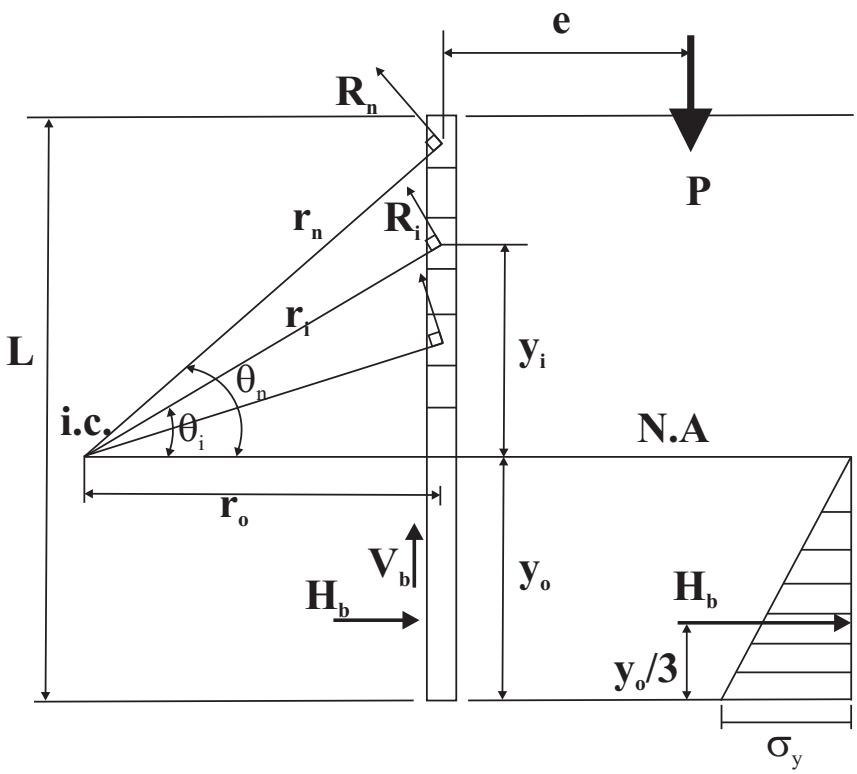

Figure A.1 – Force distribution in weld loaded in shear and bending

Sample Calculations

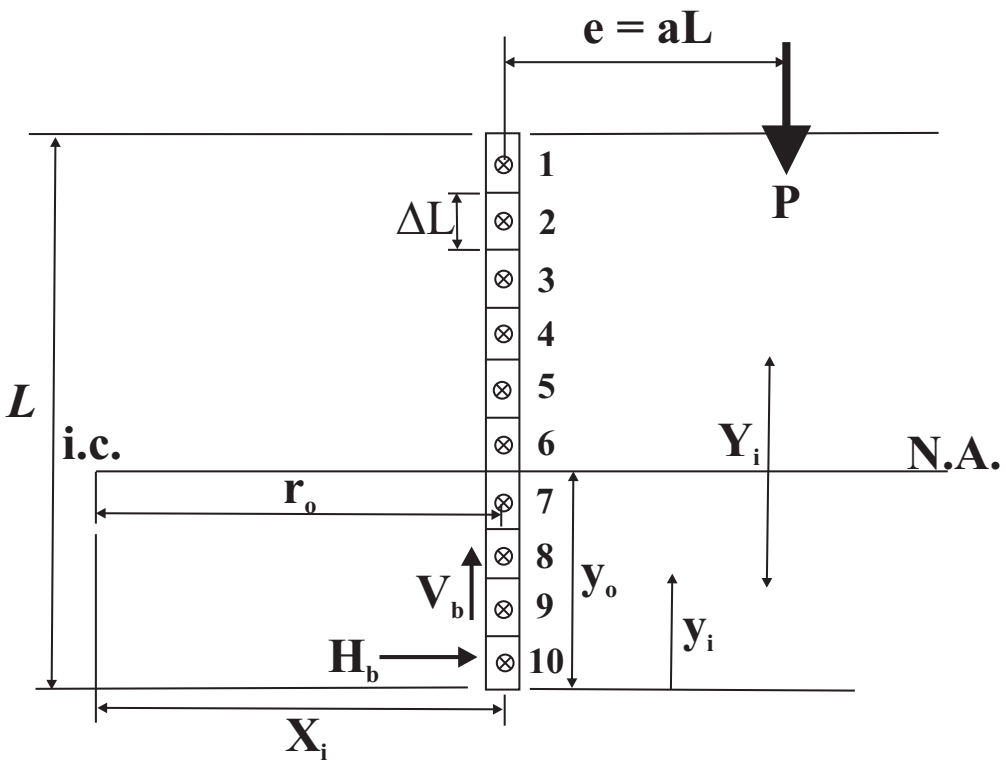

Figure A.2 – Data for sample calculation

Given,

L = 100 mm, D (weld size) = 10 mm, e = 200 mm, t = 40 mm, X_u = 490 MPa,

F_y = 300 MPa,

Assume:

ΔL = 10 mm

r_o = 2.22 mm

y_o = 55.82 mm

Solution

Calculation of geometry

In order to perform the calculation, the weld is divided into 10 elements. Together with the configuration presented in Figure A.2 and the assumed position of the instantaneous centre, the coordinates of each element of the weld group according to $X_i = x_i + r_o$ and Y_i

$= y_i - y_o$ can be computed. The detailed calculations for the geometry of the weld group are presented in Table A.1. It is noted that, when $Y_i = y_i - y_o$ becomes negative, the weld segment is below the neutral axis. Therefore, the load is transferred through the bearing plate with a triangular stress block.

Table A.1 Summary of example calculations

Elements	x_i	y_i	$X_i = x_i + r_o$	$Y_i = y_i - y_o$	$r_i = \sqrt{X_i^2 + Y_i^2}$	$\lvert\tan\theta_i\rvert$	θ_i
	(mm)	(mm)	(mm)	(mm)	(mm)		
1	0	95	2.22	39.18	39.24	17.657	86.76
2	0	85	2.22	29.18	29.26	13.150	85.65
3	0	75	2.22	19.18	19.31	8.643	83.40
4	0	65	2.22	9.18	9.44	4.136	76.41
5	0	55	2.22	-0.82	2.37		
6	0	45	2.22	-10.82	11.05		
7	0	35	2.22	-20.82	20.94		
8	0	25	2.22	-30.82	30.90		
9	0	15	2.22	-40.82	40.88		
10	0	5	2.22	-50.82	50.87		

Elements	Δ_{max}	Δ_i	μ_i	λ_i	$R_{ult,i}$	R_i	$(R_i)_v$	$(R_i)_h$	$R_i r_i$
	(mm)	(mm)			(kN)	(kN)	(kN)	(kN)	(kN mm)
1	0.69	0.53	201.7	1.420	43.4	50.7	2.9	50.6	1990.6
2		0.39	199.1	1.397	43.4	48.5	3.7	48.4	1419.8
3		0.26	194.1	1.352	43.3	42.3	4.9	42.1	817.5
4		0.13	179.2	1.221	43.1	27.1	6.4	26.4	256.2
5									
6									
7									
8									
9									
10									
						$\sum =$	17.8	167.5	4484.1

Calculation of resisting force

Since the deformation of each weld element is assumed to be directly proportional to its distance from the instantaneous centre, the deformation of the i^{th} weld element is

$$\Delta_i = \frac{r_i}{r_n}\Delta_{max} \qquad [A.7]$$

Once the angle θ_i is obtained for all elements, the values of Δ_{max} and Δ_i are computed using Equations 2.2 and A.7, respectively. The resisting force for each weld segment

(R_i) is calculated using the Equations 2.1, and 2.3 to 2.5, with the adjustments of the weld dimensions (the equations proposed by Butler and Kulak (1971) are based on a weld size of 0.25 in. (6.35 mm)) and E60 (E41XX) electrode. The force in weld segment *i*, R_i, has vertical and horizontal force components given by

$$(R_i)_v = \frac{r_o}{r_i} \times R_i \qquad [A.8]$$

$$(R_i)_h = \frac{y_i}{r_i} \times R_i \qquad [A.9]$$

The sum of the vertical and horizontal components in each element is also presented in the last row of the table. Hence, V_b and H_b can be obtained by Equations A.1 and A.2. In this example only half of the plate thickness and one single weld are considered. Therefore, H_b should be calculated based on half of the plate thickness instead of the full plate thickness (20 mm instead of 40 mm). For a joint with two fillet welds, the load is simply twice the load presented in this example.

Lastly, Equations A.5 and A.6 are checked. For the selected position of the instantaneous centre, Equation A.6 indicates an unbalanced horizontal force 0.00748, which is considered to be negligibly small. Therefore, the assumed values of r_o and y_o represent a valid solution. The ultimate load (*P*) of the single fillet weld is obtained using Equations A.4 and A.5. It is found to be 53.4 kN. The total ultimate capacity for a joint with two fillet welds and a plate twice as thick as the one used for the calculations would be 106.8 kN.

Dawe and Kulak developed a FORTRAN program to predict the ultimate capacity of eccentrically loaded fillet welded joints. The program generates successive approximations for the location of the neutral axis, y_o, along the weld length and the distance between the weld axis and the instantaneous centre, r_o, by using the Regula Falsi iterative technique. Pairs of y_o and r_o are successively generated until the connection is in equilibrium. However, the program as written by Dawe and Kulak has a number of restrictions about the size and number of individual weld segments. In order to remove the restrictions on the number and size of weld segments and to facilitate the experimentation of the method of instantaneous centre of rotation with various loads versus deformation models for the weld and stress distributions in the compression zone, a computer generated spreadsheet was developed for all the iterative procedures described above.

Appendix B

Predicted Welded Joint Capacity for All Existing Models

Appendix B

Predicted Welded Joint Capacity for All Existing Models

The predicted welded joint capacities of tested specimens from Dawe and Kulak (1972), Beaulieu and Picard (1985) and UC Davis (Gomez *et al*., 2008) using the existing models are presented in this section. Eight existing models, described in Chapters 3 and 4, are used for the predictions. Measured and predicted test results are presented in Tables B1 to B16.

The test results presented by Dawe and Kulak are analyzed and presented in Tables B1 to B3 using Models 1 to 6, Cases 1 to 7 in Model 7 and Model 8. It should be noted Cases 6 and 7 in Model 7 are used together to cover all test specimens as Case 6 is applicable for thick plates (failure in weld) and Case 7 is applicable for thin plates (failure in plate). Model 8, presented in Table B3, separates the test specimens based on the eccentricity ratio (a) for $a < 0.4$ and $a \geq 0.4$. The specimens tested by Dawe and Kulak are subjected to higher eccentricity ratios of $a \geq 0.4$.

The measured ultimate load and test-to-predicted ratios for the specimens tested by Beaulieu and Picard are presented in Tables B4 to B9. As mentioned in Chapter 3, the measured weld tensile strength (X_u) was not reported by the researchers. Therefore, X_u was assumed to be either 552 MPa or 463 MPa. The analysis using X_u of 552 MPa are presented in Tables B4 to B6. The analysis is then repeated using X_u of 463 MPa and the results are shown in Tables B7 to B9. Only 17 specimens that failed by weld are considered for predictions using Models 1 to 6 because these models are only valid for weld failure. The test specimens that failed by plate failure are not considered for these models. Since the first six models were developed based on the method of instantaneous centre of rotation, they are applicable for any load eccentricity ratio. On the other hand, for all cases in Model 7 the specimens that were subjected to low eccentricity ratios are ignored because these models are only applicable to test specimens for which failure was governed by bending rather than shear (only 11 test specimens subjected to high eccentricity ratios are analyzed). Model 8 is applicable for the weld failure under any load eccentricity. Therefore a total of 17 specimens from the test program of Beaulieu and Picard are considered in the comparison. The test specimens that failed by plate failure, either strength or stability, are not considered with Model 8.

In Tables B10 to B12, the analyzed results for UC Davis (Gomez *et al*., 2008) specimens using the existing models are presented. Total of 60 test specimens subjected to weld failure are examined using each model. Model 8 in Table B12 contains two equations for high and low eccentricity ratios. In this set of test data, all specimens are loaded under higher eccentricity; therefore, only one equation is used.

Lastly, the proposed new model is used to analyze all the test data and the results are presented in Tables B13 to B16. In Table B13, the prediction models are compared to the eight specimens presented by Dawe and Kulak. The specimens are classified according to their failure modes; weld failure and plate failure. Under weld failure, the specimens are further classified according to the eccentricity ratio using *a/Q*. For $a/Q \leq 0.59$ (for the AISC design approach) or $a/Q \leq 0.53$ (for the CISC design approach), the eccentricity is small and shear failure of the weld is the predominant failure mode and for $a/Q > 0.59$ (for the AISC approach) and $a/Q > 0.53$ (for the CISC approach), the eccentricity is considered to be large and failure is governed by bending. The proposed new model, Model 9, considers both thick plate and thin plate behaviour. In this case the capacity was calculated based on weld failure (small or large eccentricity) or on plate failure and the smaller predicted capacity is taken as the joint capacity.

The results of the analysis of the Beaulieu and Picard test data are presented in Tables B14 and B15 for X_u = 552 MPa and X_u = 463 MPa, respectively. As opposed to the previous model, all 22 specimens, including those that failed by plate tearing, are analyzed. Since the weld metal strength X_u affects the value of Q, it directly affects the classification according to a/Q, i.e. small or large eccentricity. Table B14, based on X_u of 552 MPa, shows that four specimens should have failed by plate tearing as opposed to five specimens that actually failed by plate tearing. This discrepancy can be explained by the fact that the weld metal strength, X_u, had to be assumed, which may have affected the selection of prediction equation, leading to the prediction of the incorrect failure mode in one case. It is noted that although a small number test specimens failed in the plate rather than in the weld, thus making validation of the proposed thin plate failure model difficult, none of the specimens that failed by weld failure in the experimental program were predicted to fail by plate rupture. Since there is a discrepancy between the predicted and actual failure for one of the five specimens that failed by plate rupture (indicated in Table B14 by asterisks), the test-to-predicted ratio for this failure mode is based on the predicted capacity based on plate failure rather than the minimum predicted failure load. It should be noted that the level of confidence in the results of a reliability analysis based on only five test specimens yields a low level of confidence. The specimens indicated by asterisks in Table B14 (specimens that failed in the plate) were not included in the calculations of the mean and coefficient of variation for the weld failure model. The same procedure was used for the data presented in Table B15 for X_u = 463 MPa. The total of 60 test specimens data collected at UC Davis (Gomez *et al*., 2008) are analyzed using the proposed new model and illustrated in Table B16. The predicted failure modes for all specimens agree with the observed actual failure mode, namely, weld failure.

The professional factor and coefficient of variation for each model are summarized in Table 4.1 of Chapter 4. The predicted capacity was calculated using Equation 2.6 for models involving the Lesik and Kennedy load-deformation relationship (Models 3 to 8 and 9) and based on "measured" ultimate shear strength. As mentioned in Chapter 4, the measured weld shear strength (τ_u) was not reported by the researchers. Therefore, a ratio of shear strength to tensile strength of 0.78, obtained from test results on joints with longitudinal welds only provided by Deng *et al.* (2003) and calculated based on the

fracture surface area, was used to estimate the actual shear strength of the weld and substituted in Equation 2.6 to calculate the predicted capacity.

Table B1 – Predicted capacity for test results from University of Alberta (Dawe and Kulak, 1972) (Models 1 to 6)

Specimen number	Measured ultimate load, (kN)	Model 1	Model 2	Model 3	Model 4	Model 5	Model 6
		Test/predicted	Test/predicted	Test/predicted	Test/predicted	Test/predicted	Test/predicted
A-1	278	1.004	0.791	1.079	0.903	1.065	0.865
A-2	173	0.917	0.720	0.977	0.814	0.957	0.782
A-3	103	0.746	0.585	0.792	0.660	0.775	0.634
A-4	87	0.790	0.621	0.839	0.700	0.827	0.678
A-5	105	0.932	0.695	0.954	0.771	0.797	0.653
A-6	145	0.847	0.693	0.928	0.791	1.012	0.828
A-7	265	0.752	0.608	0.821	0.696	0.866	0.706
A-8	220	0.820	0.653	0.882	0.741	0.898	0.734
Mean		0.851	0.671	0.909	0.760	0.900	0.735
Coefficient of variation, V		0.109	0.101	0.104	0.103	0.116	0.114

Table B2 – Predicted capacity for test results from University of Alberta (Dawe and Kulak, 1972) (Model 7, Cases 1 to 7)

Specimen number	Measured ultimate load, (kN)	Case 1	Case 2	Case 3	Case 4	Case 5	Case 6 / Case 7
		Test/predicted	Test/predicted	Test/predicted	Test/predicted	Test/predicted	Test/predicted
A-1	278	0.972	0.787	0.947	0.787	0.773	1.133[1]
A-2	173	0.889	0.720	0.866	0.720	0.707	1.037[1]
A-3	103	0.724	0.586	0.705	0.586	0.575	0.844[1]
A-4	87	0.768	0.622	0.750	0.622	0.611	0.896[1]
A-5	105	0.885	0.695	0.818	0.695	0.685	0.781[2]
A-6	145	0.837	0.693	0.849	0.693	0.679	0.993[1]
A-7	265	0.738	0.606	0.738	0.606	0.594	0.870[1]
A-8	220	0.801	0.653	0.791	0.653	0.641	0.939[1]
Mean		0.827	0.627	0.808	0.670	0.658	0.937
Coefficient of variation, V		0.104	0.108	0.098	0.099	0.100	0.122

(1) Predicated capacity is based on Case 6
(2) Predicated capacity is based on Case 7

Table B3 – Predicted capacity for test results from University of Alberta (Dawe and Kulak, 1972) (Model 8)

Specimen number	Measured ultimate load, (kN)	Model 8	
		$a < 0.4$	$a \geq 0.4$
		Test/predicted	Test/predicted
A-1	278	—	1.428
A-2	173	—	1.306
A-3	103	—	1.063
A-4	87	—	1.128
A-5	105	—	1.280
A-6	145	—	1.243
A-7	265	—	1.091
A-8	220	—	1.180
Mean		—	1.215
Coefficient of variation, V		—	0.101

Table B4 – Predicted capacity for test results from Université Laval (Beaulieu and Picard,1985) using X_u = 552 MPa (Models 1 to 6)

Specimen number	Measured ultimate load (kN)	Model 1	Model 2	Model 3	Model 4	Model 5	Model 6
		Test/predicted	Test/predicted	Test/predicted	Test/predicted	Test/predicted	Test/predicted
A-12-375-1	275	1.205	0.837	1.142	0.856	0.561	0.459
A-6-125-1	702	1.139	0.831	1.161	0.936	0.916	0.715
A-6-125-2	630	1.027	0.752	1.051	0.850	0.841	0.656
A-6-375-1	226	1.127	0.820	1.126	0.891	0.826	0.675
A-6-75-2	1093	1.081	0.809	1.177	1.019	1.066	0.781
B-10-125-1	1183	1.014	0.830	1.153	1.009	1.197	0.935
B-10-125-2	1109	0.944	0.760	1.056	0.914	1.066	0.834
B-10-375-1	273	0.670	0.515	0.703	0.579	0.649	0.530
B-10-375-2	485	1.191	0.915	1.248	1.027	1.145	0.935
B-10-75-1	1696	0.874	0.726	1.057	0.979	1.089	0.799
B-10-75-2	1594	0.812	0.689	0.993	0.924	1.028	0.754
B-8-125-1	1047	0.888	0.716	1.007	0.876	1.032	0.806
B-8-125-2	1274	1.086	0.878	1.232	1.076	1.272	0.994
B-8-375-1	416	1.017	0.780	1.065	0.876	0.974	0.796
B-8-375-2	427	1.033	0.796	1.086	0.895	1.008	0.823
B-8-75-1	1487	0.880	0.804	1.177	1.130	1.288	0.945
B-8-75-2	1393	0.871	0.790	1.158	1.116	1.276	0.936
Mean		0.992	0.779	1.094	0.938	1.014	0.787
Coefficient of variation, V		0.146	0.114	0.114	0.137	0.204	0.187

Table B5 – Predicted capacity for test results from Université Laval (Beaulieu and Picard, 1985) using X_u = 552 MPa (Model 7, Cases 1 to 7)

Specimen number	Measured ultimate load (kN)	Case 1	Case 2	Case 3	Case 4	Case 5	Case 6 / Case 7
		Test/predicted	Test/predicted	Test/predicted	Test/predicted	Test/predicted	Test/predicted
A-12-375-1	275	1.096	0.736	0.823	0.803	0.798	1.250(2)
A-6-125-1	702	1.058	0.755	0.879	0.811	0.802	1.475(2)
A-6-125-2	630	0.956	0.684	0.798	0.734	0.725	1.323(2)
A-6-375-1	226	1.054	0.756	0.883	0.811	0.801	1.036(2)
B-10-125-2	1109	0.901	0.715	0.860	0.725	0.713	1.046(1)
B-10-375-1	273	0.644	0.507	0.607	0.515	0.506	0.550(2)
B-10-375-2	485	1.144	0.901	1.077	0.914	0.899	0.979(2)
B-8-125-1	1047	0.849	0.677	0.817	0.687	0.674	0.989(1)
B-8-125-2	1274	1.039	0.830	1.002	0.841	0.826	1.212(1)
B-8-375-1	416	0.977	0.769	0.918	0.780	0.767	0.839(2)
B-8-375-2	427	0.994	0.785	0.939	0.796	0.783	0.845(2)
Mean		0.974	0.738	0.873	0.765	0.754	1.049
Coefficient of variation, V		0.142	0.135	0.139	0.135	0.135	0.246

(1) Predicated capacity is based on Case 6
(2) Predicated capacity is based on Case 7

Table B6 – Predicted capacity for test results from Université Laval (Beaulieu and Picard, 1985) using X_u = 552 MPa (Model 8)

Specimen number	Measured ultimate load (kN)	Model 8	
		a < 0.4	a ≥ 0.4
		Test/predicted	Test/predicted
A-12-375-1	275	—	1.532
A-6-125-1	702	—	1.513
A-6-125-2	630	—	1.368
A-6-375-1	226	—	1.509
B-10-125-1	1183	—	1.427
B-10-125-2	1109	—	1.320
B-10-375-1	273	—	0.940
B-10-375-2	485	—	1.670
B-8-125-1	1047	—	1.247
B-8-125-2	1274	—	1.526
B-8-375-1	416	—	1.425
B-8-375-2	427	—	1.452
A-6-75-2	1093	1.266	—
B-10-75-1	1696	1.185	—
B-10-75-2	1594	1.112	—
B-8-75-1	1487	1.298	—
B-8-75-2	1393	1.270	—
Mean		1.226	1.411
Coefficient of variation, V		0.062	0.131

Table B7 – Predicted capacity for test results from Université Laval (Beaulieu and Picard, 1985) using X_u = 463 MPa (Models 1 to 6)

Specimen number	Measured ultimate load (kN)	Model 1	Model 2	Model 3	Model 4	Model 5	Model 6
		Test/predicted	Test/predicted	Test/predicted	Test/predicted	Test/predicted	Test/predicted
A-12-375-1	275	1.244	0.875	1.195	0.910	0.669	0.547
A-6-125-1	702	1.195	0.891	1.255	1.037	1.092	0.853
A-6-125-2	630	1.078	0.808	1.138	0.944	1.002	0.782
A-6-375-1	226	1.182	0.876	1.205	0.971	0.985	0.805
A-6-75-2	1093	1.143	0.896	1.305	1.175	1.271	0.931
B-10-125-1	1183	1.092	0.923	1.292	1.158	1.426	1.114
B-10-125-2	1109	1.013	0.841	1.177	1.044	1.271	0.994
B-10-375-1	273	0.712	0.566	0.765	0.642	0.773	0.632
B-10-375-2	485	1.266	1.005	1.359	1.140	1.365	1.115
B-10-75-1	1696	0.947	0.831	1.213	1.148	1.297	0.953
B-10-75-2	1594	0.882	0.781	1.142	1.084	1.225	0.898
B-8-125-1	1047	0.955	0.803	1.124	1.004	1.231	0.961
B-8-125-2	1274	1.169	0.985	1.379	1.234	1.517	1.184
B-8-375-1	416	1.081	0.856	1.159	0.971	1.161	0.948
B-8-375-2	427	1.099	0.875	1.183	0.994	1.201	0.981
B-8-75-1	1487	1.002	0.938	1.375	1.336	1.536	1.126
B-8-75-2	1393	0.981	0.924	1.355	1.319	1.521	1.115
Mean		1.061	0.863	1.213	1.065	1.208	0.938
Coefficient of variation, V		0.133	0.114	0.120	0.157	0.204	0.187

Table B8 – Predicted capacity for test results from Université Laval (Beaulieu and Picard, 1985) using X_u = 463 MPa (Model 7, Cases 1 to 7)

Specimen number	Measured ultimate load (kN)	Case 1	Case 2	Case 3	Case 4	Case 5	Case 6 / Case 7
		Test/predicted	Test/predicted	Test/predicted	Test/predicted	Test/predicted	Test/predicted
A-12-375-1	275	1.139	0.779	0.883	0.846	0.839	1.250(2)
A-6-125-1	702	1.121	0.818	0.965	0.874	0.862	1.475(2)
A-6-125-2	630	1.013	0.741	0.876	0.791	0.780	1.323(2)
A-6-375-1	226	1.118	0.820	0.972	0.875	0.863	1.036(2)
B-10-125-2	1109	0.974	0.788	0.960	0.798	0.783	1.147(1)
B-10-375-1	273	0.694	0.558	0.676	0.565	0.554	0.813(1)
B-10-375-2	485	1.233	0.990	1.200	1.003	0.985	1.444(1)
B-8-125-1	1047	0.920	0.748	0.914	0.757	0.742	1.087(1)
B-8-125-2	1274	1.126	0.917	1.121	0.928	0.909	1.331(1)
B-8-375-1	416	1.052	0.844	1.022	0.855	0.840	1.231(1)
B-8-375-2	427	1.072	0.863	1.047	0.874	0.857	1.257(1)
Mean		1.042	0.806	0.967	0.833	0.819	1.218
Coefficient of variation, V		0.138	0.137	0.143	0.134	0.134	0.156

(1) Predicated capacity is based on Case 6
(2) Predicated capacity is based on Case 7

Table B9 – Predicted capacity for test results from Université Laval (Beaulieu and Picard, 1985) using X_u = 463 MPa (Model 8)

Specimen number	Measured ultimate load (kN)	Model 8	
		$a < 0.4$	$a \geq 0.4$
		Test/predicted	Test/predicted
A-12-375-1	275	—	1.603
A-6-125-1	702	—	1.615
A-6-125-2	630	—	1.461
A-6-375-1	226	—	1.614
B-10-125-1	1183	—	1.561
B-10-125-2	1109	—	1.439
B-10-375-1	273	—	1.022
B-10-375-2	485	—	1.816
B-8-125-1	1047	—	1.362
B-8-125-2	1274	—	1.668
B-8-375-1	416	—	1.548
B-8-375-2	427	—	1.580
A-6-75-2	1093	1.447	—
B-10-75-1	1696	1.353	—
B-10-75-2	1594	1.271	—
B-8-75-1	1487	1.488	—
B-8-75-2	1393	1.457	—
Mean		1.403	1.524
Coefficient of variation, V		0.064	0.129

Table B10 – Predicted capacity for test results from UC Davis (Gomez *et al.*, 2008) (Models 1 to 6)

Specimen number	Measured ultimate load (kN)	Model 1	Model 2	Model 3	Model 4	Model 5	Model 6
		Test/predicted	Test/predicted	Test/predicted	Test/predicted	Test/predicted	Test/predicted
B_125_A12_55_1	326	1.779	1.279	1.754	1.370	1.190	0.971
B_125_A12_55_2	321	1.702	1.226	1.681	1.316	1.154	0.942
B_125_A12_55_3	316	1.656	1.192	1.636	1.279	1.119	0.913
B_125_A516_55_1	197	1.218	0.916	1.257	1.022	1.082	0.883
B_125_A516_55_2	239	1.451	1.091	1.498	1.218	1.291	1.054
B_125_A516_55_3	233	1.432	1.071	1.473	1.194	1.248	1.019
B_175_A12_3_1	682	1.654	1.253	1.734	1.426	1.547	1.244
B_175_A12_3_2	778	1.764	1.335	1.850	1.521	1.647	1.323
B_175_A12_3_3	676	1.629	1.226	1.699	1.391	1.487	1.197
B_175_A12_55_1	400	1.539	1.148	1.580	1.278	1.327	1.082
B_175_A12_55_2	341	1.527	1.151	1.579	1.286	1.372	1.120
B_175_A12_55_3	354	1.510	1.128	1.552	1.257	1.313	1.072
B_175_A12_85_1	231	1.407	1.048	1.439	1.164	1.206	0.987
B_175_A12_85_2	228	1.394	1.043	1.430	1.159	1.209	0.990
B_175_A12_85_3	236	1.432	1.059	1.455	1.169	1.172	0.959
B_175_A516_3_1	533	1.461	1.204	1.645	1.422	1.794	1.442
B_175_A516_3_2	529	1.411	1.160	1.586	1.369	1.714	1.377
B_175_A516_3_3	551	1.414	1.165	1.596	1.379	1.734	1.392
B_175_A516_55_1	274	1.277	1.038	1.398	1.188	1.493	1.218
B_175_A516_55_2	265	1.246	1.013	1.365	1.160	1.457	1.188
B_175_A516_55_3	280	1.371	1.112	1.498	1.272	1.593	1.300
B_175_A516_85_1	173	1.306	1.033	1.394	1.166	1.391	1.139
B_175_A516_85_2	134	1.038	0.819	1.106	0.924	1.101	0.901
B_175_A516_85_3	149	1.101	0.872	1.178	0.986	1.178	0.965
B_250_A12_55_1	386	1.256	1.002	1.356	1.141	1.385	1.130
B_250_A12_55_2	452	1.353	1.082	1.464	1.233	1.503	1.226
B_250_A12_55_3	420	1.361	1.051	1.420	1.201	1.480	1.207
B_250_A516_55_1	276	0.985	0.836	1.115	0.973	1.325	1.081
B_250_A516_55_2	261	1.000	0.849	1.131	0.987	1.349	1.101
B_250_A516_55_3	259	0.932	0.795	1.058	0.926	1.274	1.039
B_125_B12_55_1	364	1.889	1.360	1.865	1.459	1.275	1.040

Table B10 – Cont'd

Specimen number	Measured ultimate load (kN)	Model 1	Model 2	Model 3	Model 4	Model 5	Model 6
		Test/predicted	Test/predicted	Test/predicted	Test/predicted	Test/predicted	Test/predicted
B_125_B12_55_2	375	2.001	1.449	1.988	1.565	1.414	1.154
B_125_B12_55_3	439	2.147	1.541	2.113	1.648	1.415	1.154
B_125_B516_55_1	224	1.418	1.056	1.453	1.174	1.214	0.991
B_125_B516_55_2	255	1.563	1.165	1.602	1.296	1.343	1.096
B_125_B516_55_3	270	1.739	1.300	1.785	1.445	1.500	1.225
B_175_B12_3_1	859	1.841	1.382	1.922	1.569	1.668	1.339
B_175_B12_3_2	889	1.937	1.463	2.021	1.654	1.766	1.418
B_175_B12_3_3	824	1.785	1.350	1.873	1.539	1.665	1.336
B_175_B12_55_1	441	1.771	1.325	1.822	1.478	1.549	1.263
B_175_B12_55_2	400	1.721	1.283	1.762	1.424	1.464	1.195
B_175_B12_55_3	385	1.667	1.252	1.718	1.396	1.471	1.201
B_175_B12_85_1	263	1.591	1.187	1.628	1.317	1.363	1.115
B_175_B12_85_2	266	1.639	1.222	1.677	1.356	1.401	1.146
B_175_B12_85_3	254	1.717	1.269	1.742	1.398	1.398	1.144
B_175_B516_3_1	734	1.861	1.501	2.059	1.760	2.142	1.721
B_175_B516_3_2	713	1.743	1.423	1.950	1.679	2.078	1.667
B_175_B516_3_3	690	1.711	1.394	1.911	1.642	2.025	1.625
B_175_B516_55_1	386	1.711	1.343	1.825	1.520	1.770	1.444
B_175_B516_55_2	310	1.410	1.115	1.513	1.266	1.490	1.215
B_175_B516_55_3	347	1.643	1.341	1.805	1.537	1.944	1.586
B_175_B516_85_1	204	1.369	1.086	1.465	1.227	1.475	1.207
B_175_B516_85_2	208	1.493	1.182	1.595	1.335	1.597	1.307
B_175_B516_85_3	205	1.463	1.158	1.564	1.309	1.567	1.282
B_250_B12_55_1	491	1.540	1.215	1.648	1.378	1.631	1.330
B_250_B12_55_2	498	1.597	1.253	1.702	1.418	1.661	1.355
B_250_B12_55_3	492	1.639	1.294	1.754	1.467	1.745	1.424
B_250_B516_55_1	346	1.333	1.142	1.516	1.332	1.857	1.515
B_250_B516_55_2	342	1.314	1.120	1.491	1.303	1.793	1.463
B_250_B516_55_3	339	1.325	1.126	1.500	1.307	1.784	1.456
Mean		1.520	1.175	1.603	1.326	1.493	1.215
Coefficient of variation, V		0.167	0.144	0.150	0.142	0.167	0.162

Table B11 – Predicted capacity for test results from UC Davis (Gomez *et al.*, 2008) (Model 7, Cases 1 to 7)

Specimen number	Measured ultimate load (kN)	Case 1	Case 2	Case 3	Case 4	Case 5	Case 6 / Case 7
		Test/predicted	Test/predicted	Test/predicted	Test/predicted	Test/predicted	Test/predicted
B_125_A12_55_1	326	1.651	1.353	1.536	1.256	1.249	1.781[(2)]
B_125_A12_55_2	321	1.581	1.297	1.475	1.205	1.191	1.604[(2)]
B_125_A12_55_3	316	1.538	1.261	1.434	1.171	1.159	1.597[(2)]
B_125_A516_55_1	197	1.160	0.976	1.142	0.916	0.902	1.048[(2)]
B_125_A516_55_2	239	1.382	1.162	1.361	1.091	1.074	1.255[(2)]
B_125_A516_55_3	233	1.360	1.142	1.334	1.071	1.055	1.279[(2)]
B_175_A12_3_1	682	1.573	1.325	1.553	1.244	1.225	1.630[(2)]
B_175_A12_3_2	778	1.677	1.412	1.654	1.325	1.305	1.760[(2)]
B_175_A12_3_3	676	1.546	1.299	1.518	1.218	1.200	1.656[(2)]
B_175_A12_55_1	400	1.460	1.224	1.427	1.147	1.130	1.354[(2)]
B_175_A12_55_2	341	1.455	1.226	1.437	1.151	1.133	1.316[(2)]
B_175_A12_55_3	354	1.434	1.204	1.405	1.128	1.112	1.305[(2)]
B_175_A12_85_1	231	1.335	1.120	1.307	1.050	1.034	1.179[(2)]
B_175_A12_85_2	228	1.325	1.113	1.301	1.044	1.029	1.157[(2)]
B_175_A12_85_3	236	1.353	1.130	1.312	1.057	1.043	1.233[(2)]
B_175_A516_3_1	533	1.431	1.243	1.506	1.181	1.157	1.694[(1)]
B_175_A516_3_2	529	1.380	1.198	1.449	1.138	1.115	1.632[(1)]
B_175_A516_3_3	551	1.383	1.201	1.454	1.141	1.118	1.637[(1)]
B_175_A516_55_1	274	1.256	1.089	1.318	1.035	1.014	1.484[(1)]
B_175_A516_55_2	265	1.226	1.063	1.286	1.010	0.989	1.449[(1)]
B_175_A516_55_3	280	1.348	1.168	1.412	1.109	1.087	1.592[(1)]
B_175_A516_85_1	173	1.272	1.092	1.307	1.033	1.014	1.487[(1)]
B_175_A516_85_2	134	1.010	0.867	1.037	0.820	0.805	1.180[(1)]
B_175_A516_85_3	149	1.073	0.922	1.104	0.873	0.857	1.256[(1)]
B_250_A12_55_1	386	1.226	1.056	1.268	1.000	0.981	1.438[(1)]
B_250_A12_55_2	452	1.321	1.139	1.369	1.079	1.059	1.552[(1)]
B_250_A12_55_3	420	1.279	1.105	1.332	1.048	1.028	1.506[(1)]
B_250_A516_55_1	276	0.982	0.868	1.071	0.831	0.811	1.185[(1)]
B_250_A516_55_2	261	0.998	0.883	1.089	0.845	0.825	1.204[(1)]
B_250_A516_55_3	259	0.931	0.825	1.020	0.790	0.771	1.126[(1)]
B_125_B12_55_1	364	1.754	1.438	1.634	1.335	1.321	1.786[(2)]
B_125_B12_55_2	375	1.865	1.535	1.753	1.428	1.411	1.886[(2)]

Table B11 – Cont'd

Specimen number	Measured ultimate load (kN)	Case 1	Case 2	Case 3	Case 4	Case 5	Case 6 / Case 7
		Test/predicted	Test/predicted	Test/predicted	Test/predicted	Test/predicted	Test/predicted
B_125_B12_55_3	439	1.990	1.629	1.846	1.511	1.495	2.078[(2)]
B_125_B516_55_1	224	1.345	1.127	1.314	1.056	1.041	1.238[(2)]
B_125_B516_55_2	255	1.483	1.243	1.449	1.165	1.148	1.359[(2)]
B_125_B516_55_3	270	1.650	1.385	1.615	1.298	1.279	1.512[(2)]
B_175_B12_3_1	859	1.744	1.464	1.708	1.372	1.352	1.881[(2)]
B_175_B12_3_2	889	1.836	1.542	1.801	1.446	1.425	1.966[(2)]
B_175_B12_3_3	824	1.696	1.428	1.672	1.340	1.320	1.806[(2)]
B_175_B12_55_1	441	1.682	1.413	1.651	1.325	1.305	1.553[(2)]
B_175_B12_55_2	400	1.631	1.366	1.592	1.280	1.262	1.473[(2)]
B_175_B12_55_3	385	1.586	1.333	1.559	1.251	1.232	1.396[(2)]
B_175_B12_85_1	263	1.510	1.267	1.479	1.188	1.170	1.328[(2)]
B_175_B12_85_2	266	1.556	1.305	1.522	1.223	1.206	1.368[(2)]
B_175_B12_85_3	254	1.622	1.354	1.571	1.267	1.249	1.473[(2)]
B_175_B516_3_1	734	1.809	1.559	1.874	1.477	1.449	2.124[(1)]
B_175_B516_3_2	713	1.699	1.470	1.774	1.395	1.368	2.003[(1)]
B_175_B516_3_3	690	1.668	1.442	1.739	1.368	1.341	1.965[(1)]
B_175_B516_55_1	386	1.658	1.419	1.691	1.340	1.317	1.932[(1)]
B_175_B516_55_2	310	1.371	1.177	1.407	1.113	1.093	1.602[(1)]
B_175_B516_55_3	347	1.618	1.406	1.704	1.337	1.309	1.917[(1)]
B_175_B516_85_1	204	1.335	1.148	1.376	1.087	1.066	1.563[(1)]
B_175_B516_85_2	208	1.454	1.249	1.496	1.182	1.160	1.701[(1)]
B_175_B516_85_3	205	1.425	1.225	1.467	1.159	1.137	1.668[(1)]
B_250_B12_55_1	491	1.496	1.282	1.532	1.212	1.191	1.746[(1)]
B_250_B12_55_2	498	1.548	1.324	1.579	1.251	1.229	1.803[(1)]
B_250_B12_55_3	492	1.593	1.367	1.634	1.292	1.269	1.861[(1)]
B_250_B516_55_1	346	1.332	1.183	1.466	1.134	1.107	1.615[(1)]
B_250_B516_55_2	342	1.314	1.164	1.437	1.114	1.088	1.588[(1)]
B_250_B516_55_3	339	1.325	1.171	1.444	1.121	1.094	1.598[(1)]
Mean		1.459	1.240	1.467	1.168	1.148	1.556
Coefficient of variation, V		0.155	0.144	0.135	0.140	0.142	0.169

(1) Predicated capacity is based on Case 6
(2) Predicated capacity is based on Case 7

Table B12 – Predicted capacity for test results from UC Davis (Gomez *et al.*, 2008) (Model 8)

Specimen number	Measured ultimate load (kN)	Model 8	
		$a < 0.4$	$a \geq 0.4$
		Test/predicted	Test/predicted
B_125_A12_55_1	326	—	2.410
B_125_A12_55_2	321	—	2.240
B_125_A12_55_3	316	—	2.201
B_125_A516_55_1	197	—	1.682
B_125_A516_55_2	239	—	2.007
B_125_A516_55_3	233	—	1.999
B_125_B12_55_1	364	—	2.483
B_125_B12_55_2	375	—	2.667
B_125_B12_55_3	439	—	2.831
B_125_B516_55_1	224	—	1.945
B_125_B516_55_2	255	—	2.140
B_125_B516_55_3	270	—	2.394
B_175_A12_3_1	682	—	2.285
B_175_A12_3_2	778	—	2.433
B_175_A12_3_3	676	—	2.269
B_175_A12_55_1	400	—	2.111
B_175_A12_55_2	341	—	2.121
B_175_A12_55_3	354	—	2.068
B_175_A12_85_1	231	—	1.936
B_175_A12_85_2	228	—	1.919
B_175_A12_85_3	236	—	1.966
B_175_A516_3_1	533	—	2.130
B_175_A516_3_2	529	—	2.046
B_175_A516_3_3	551	—	2.048
B_175_A516_55_1	274	—	1.858
B_175_A516_55_2	265	—	1.817
B_175_A516_55_3	280	—	2.007
B_175_A516_85_1	173	—	1.876
B_175_A516_85_2	134	—	1.488
B_175_A516_85_3	149	—	1.576
B_175_B12_3_1	859	—	2.529

Table B12 – Cont'd

Specimen number	Measured ultimate load (kN)	Model 8	
		a < 0.4	a ≥ 0.4
		Test/predicted	Test/predicted
B_175_B12_3_2	889	—	2.663
B_175_B12_3_3	824	—	2.470
B_175_B12_55_1	441	—	2.445
B_175_B12_55_2	400	—	2.331
B_175_B12_55_3	385	—	2.261
B_175_B12_85_1	263	—	2.186
B_175_B12_85_2	266	—	2.250
B_175_B12_85_3	254	—	2.352
B_175_B516_3_1	734	—	2.681
B_175_B516_3_2	713	—	2.502
B_175_B516_3_3	690	—	2.460
B_175_B516_55_1	386	—	2.452
B_175_B516_55_2	310	—	2.022
B_175_B516_55_3	347	—	2.405
B_175_B516_85_1	204	—	1.970
B_175_B516_85_2	208	—	2.141
B_175_B516_85_3	205	—	2.106
B_250_A12_55_1	386	—	1.821
B_250_A12_55_2	452	—	1.957
B_250_A12_55_3	420	—	1.887
B_250_A516_55_1	276	—	1.489
B_250_A516_55_2	261	—	1.500
B_250_A516_55_3	259	—	1.401
B_250_B12_55_1	491	—	2.196
B_250_B12_55_2	498	—	2.286
B_250_B12_55_3	492	—	2.363
B_250_B516_55_1	346	—	2.046
B_250_B516_55_2	342	—	1.979
B_250_B516_55_3	339	—	1.968
Mean		—	2.134
Coefficient of variation, V		—	0.147

Table B13 – Predicted capacity for test results from University of Alberta, Dawe and Kulak (1972) (Model 9)

Specimen number	Measured ultimate load, (kN)	a/Q	Q	Weld Failure Test/predicted		Plate Failure Test/predicted	Predicated Failure Mode	Actual Failure Mode
				a/Q ≤ 0.53	a/Q > 0.53			
A-1	278	0.47	2.20	0.758	—	0.566	Weld Failure	Weld Failure
A-2	173	0.69	2.20	—	0.784	0.482	Weld Failure	Weld Failure
A-3	103	0.92	2.20	—	0.638	0.381	Weld Failure	Weld Failure
A-4	87	1.14	2.24	—	0.678	0.395	Weld Failure	Weld Failure
A-5	105	1.23	1.65	—	0.750	0.522	Weld Failure	Weld Failure
A-6	145	0.73	2.76	—	0.761	0.397	Weld Failure	Weld Failure
A-7	265	0.50	2.55	0.575	—	0.385	Weld Failure	Weld Failure
A-8	220	0.71	2.38	—	0.713	0.414	Weld Failure	Weld Failure
Mean				0.667	0.721	—		
Coefficient of variation, V				0.194	0.076	—		

Table B14 – Predicted capacity on test results from Université Laval (Beaulieu and Picard, 1985) using X_u = 552 MPa (Model 9)

Specimen number	Measured ultimate load, (kN)	a/Q	Q	Weld Failure Test/predicted		Plate Failure Test/predicted	Predicated Failure Mode	Actual Failure Mode
				a/Q ≤ 0.53	a/Q > 0.53			
A-12-125-1	733	0.69	0.73	—	(0.750)	0.914*	Plate Failure	Plate Failure
A-12-375-1	275	2.00	0.75	—	0.843	0.733	Weld Failure	Weld Failure
A-12-375-2	304	1.99	0.75	—	(0.933)	0.810*	Weld Failure	Plate Failure
A-12-75-1	1071	0.37	0.80	(0.800)	—	1.088*	Plate Failure	Plate Failure
A-12-75-2	1131	0.38	0.78	(0.813)	—	1.134*	Plate Failure	Plate Failure
A-6-125-1	702	0.39	1.27	0.908	—	0.865	Weld Failure	Weld Failure
A-6-125-2	630	0.38	1.30	0.825	—	0.775	Weld Failure	Weld Failure
A-6-375-1	226	1.13	1.33	—	0.868	0.608	Weld Failure	Weld Failure
A-6-75-1	1190	0.30	0.99	(1.019)	—	1.190*	Plate Failure	Plate Failure
A-6-75-2	1093	0.23	1.28	1.148	—	1.096	Weld Failure	Weld Failure
B-10-125-1	1183	0.22	2.24	0.994	—	0.705	Weld Failure	Weld Failure
B-10-125-2	1109	0.24	2.09	0.897	—	0.670	Weld Failure	Weld Failure
B-10-375-1	273	0.77	1.96	—	0.559	0.354	Weld Failure	Weld Failure
B-10-375-2	485	0.77	1.95	—	0.992	0.630	Weld Failure	Weld Failure
B-10-75-1	1696	0.16	1.86	1.095	—	0.840	Weld Failure	Weld Failure
B-10-75-2	1594	0.16	1.90	1.033	—	0.778	Weld Failure	Weld Failure
B-8-125-1	1047	0.23	2.18	0.863	—	0.623	Weld Failure	Weld Failure
B-8-125-2	1274	0.23	2.21	1.059	—	0.758	Weld Failure	Weld Failure
B-8-375-1	416	0.78	1.93	—	0.846	0.540	Weld Failure	Weld Failure
B-8-375-2	427	0.75	1.99	—	0.864	0.544	Weld Failure	Weld Failure
B-8-75-1	1487	0.12	2.55	1.244	—	0.726	Weld Failure	Weld Failure
B-8-75-2	1393	0.11	2.69	1.224	—	0.681	Weld Failure	Weld Failure
Mean				1.026	0.829	1.027		
Coefficient of variation, V				0.140	0.173	0.155		

Table B15 – Predicted capacity for test results from Université Laval (Beaulieu and Picard, 1985) using X_u = 463 MPa (Model 9)

Specimen number	Measured ultimate load, (kN)	a/Q	Q	Weld Failure Test/predicted		Plate Failure Test/predicted	Predicated Failure Mode	Actual Failure Mode
				a/Q ≤ 0.53	a/Q > 0.53			
A-12-125-1	733	0.58	0.87	(0.792)	—	0.914*	Plate Failure	Plate Failure
A-12-375-1	275	1.67	0.89	—	0.893	0.733	Weld Failure	Weld Failure
A-12-375-2	304	1.67	0.90	—	(0.989)	0.810*	Weld Failure	Plate Failure
A-12-75-1	1071	0.31	0.96	(0.910)	—	1.088*	Plate Failure	Plate Failure
A-12-75-2	1131	0.32	0.93	(0.924)	—	1.134*	Plate Failure	Plate Failure
A-6-125-1	702	0.33	1.52	1.015	—	0.865	Weld Failure	Weld Failure
A-6-125-2	630	0.32	1.55	0.924	—	0.775	Weld Failure	Weld Failure
A-6-375-1	226	0.95	1.59	—	0.942	0.608	Weld Failure	Weld Failure
A-6-75-1	1190	0.25	1.18	(1.169)	—	1.190*	Plate Failure	Plate Failure
A-6-75-2	1093	0.20	1.52	1.326	—	1.096	Weld Failure	Weld Failure
B-10-125-1	1183	0.19	2.67	1.138	—	0.705	Weld Failure	Weld Failure
B-10-125-2	1109	0.20	2.49	1.024	—	0.670	Weld Failure	Weld Failure
B-10-375-1	273	0.64	2.34	—	0.617	0.354	Weld Failure	Weld Failure
B-10-375-2	485	0.65	2.32	—	1.095	0.630	Weld Failure	Weld Failure
B-10-75-1	1696	0.14	2.22	1.273	—	0.840	Weld Failure	Weld Failure
B-10-75-2	1594	0.13	2.27	1.202	—	0.778	Weld Failure	Weld Failure
B-8-125-1	1047	0.19	2.60	0.988	—	0.623	Weld Failure	Weld Failure
B-8-125-2	1274	0.19	2.64	1.212	—	0.758	Weld Failure	Weld Failure
B-8-375-1	416	0.65	2.31	—	0.934	0.540	Weld Failure	Weld Failure
B-8-375-2	427	0.63	2.37	—	0.955	0.544	Weld Failure	Weld Failure
B-8-75-1	1487	0.10	3.04	1.454	—	0.726	Weld Failure	Weld Failure
B-8-75-2	1393	0.09	3.21	1.431	—	0.681	Weld Failure	Weld Failure
Mean				1.181	0.906	1.027		
Coefficient of variation, V				0.153	0.174	0.155		

Table B16 – Predicted capacity for test results from UC, Davis (Gomez *et al.*, 2008) (Model 9)

Specimen number	Measured ultimate load, (kN)	a/Q	Q	Weld Failure Test/predicted		Plate Failure Test/predicted	Predicated Failure Mode	Actual Failure Mode
				a/Q ≤ 0.53	a/Q > 0.53			
B 125 A12 55 1	326	1.20	1.17	—	1.339	1.271	Weld Failure	Weld Failure
B 125 A12 55 2	321	1.17	1.20	—	1.285	1.210	Weld Failure	Weld Failure
B 125 A12 55 3	316	1.16	1.19	—	1.249	1.183	Weld Failure	Weld Failure
B 125 A516 55 1	197	0.82	1.73	—	0.989	0.782	Weld Failure	Weld Failure
B 125 A516 55 2	239	0.81	1.73	—	1.179	0.934	Weld Failure	Weld Failure
B 125 A516 55 3	233	0.85	1.68	—	1.157	0.930	Weld Failure	Weld Failure
B 175 A12 3 1	682	0.44	1.76	1.259	—	1.214	Weld Failure	Weld Failure
B 175 A12 3 2	778	0.43	1.75	1.348	—	1.314	Weld Failure	Weld Failure
B 175 A12 3 3	676	0.46	1.70	1.237	—	1.210	Weld Failure	Weld Failure
B 175 A12 55 1	400	0.82	1.65	—	1.238	1.012	Weld Failure	Weld Failure
B 175 A12 55 2	341	0.82	1.75	—	1.244	0.975	Weld Failure	Weld Failure
B 175 A12 55 3	354	0.84	1.67	—	1.218	0.982	Weld Failure	Weld Failure
B 175 A12 85 1	231	1.26	1.66	—	1.133	0.878	Weld Failure	Weld Failure
B 175 A12 85 2	228	1.24	1.69	—	1.128	0.866	Weld Failure	Weld Failure
B 175 A12 85 3	236	1.35	1.56	—	1.139	0.909	Weld Failure	Weld Failure
B 175 A516 3 1	533	0.28	2.67	1.195	—	0.929	Weld Failure	Weld Failure
B 175 A516 3 2	529	0.29	2.64	1.156	—	0.905	Weld Failure	Weld Failure
B 175 A516 3 3	551	0.28	2.66	1.172	—	0.910	Weld Failure	Weld Failure
B 175 A516 55 1	274	0.52	2.63	0.992	—	0.714	Weld Failure	Weld Failure
B 175 A516 55 2	265	0.52	2.63	0.970	—	0.697	Weld Failure	Weld Failure
B 175 A516 55 3	280	0.54	2.60	—	1.215	0.767	Weld Failure	Weld Failure
B 175 A516 85 1	173	0.95	2.30	—	1.128	0.730	Weld Failure	Weld Failure
B 175 A516 85 2	134	0.98	2.28	—	0.894	0.582	Weld Failure	Weld Failure
B 175 A516 85 3	149	0.94	2.31	—	0.953	0.613	Weld Failure	Weld Failure
B 250 A12 55 1	386	0.58	2.39	—	1.093	0.727	Weld Failure	Weld Failure
B 250 A12 55 2	452	0.55	2.41	—	1.180	0.785	Weld Failure	Weld Failure
B 250 A12 55 3	420	0.54	2.49	—	1.147	0.748	Weld Failure	Weld Failure
B 250 A516 55 1	276	0.39	3.43	0.685	—	0.487	Weld Failure	Weld Failure
B 250 A516 55 2	261	0.40	3.43	0.696	—	0.493	Weld Failure	Weld Failure
B 250 A516 55 3	259	0.38	3.51	0.647	—	0.457	Weld Failure	Weld Failure

Table B16 – Cont'd

Specimen number	Measured ultimate load, (kN)	a/Q	Q	Weld Failure Test/predicted		Plate Failure Test/predicted	Predicated Failure Mode	Actual Failure Mode
				a/Q ≤ 0.53	a/Q > 0.53			
B 125 B12 55 1	364	1.16	1.19	—	1.424	1.350	Weld Failure	Weld Failure
B 125 B12 55 2	375	1.10	1.26	—	1.526	1.405	Weld Failure	Weld Failure
B 125 B12 55 3	439	1.17	1.15	—	1.610	1.551	Weld Failure	Weld Failure
B 125 B516 55 1	224	0.89	1.64	—	1.138	0.924	Weld Failure	Weld Failure
B 125 B516 55 2	255	0.87	1.64	—	1.256	1.019	Weld Failure	Weld Failure
B 125 B516 55 3	270	0.88	1.66	—	1.401	1.126	Weld Failure	Weld Failure
B 175 B12 3 1	859	0.44	1.67	1.404	—	1.399	Weld Failure	Weld Failure
B 175 B12 3 2	889	0.44	1.68	1.477	—	1.463	Weld Failure	Weld Failure
B 175 B12 3 3	824	0.42	1.74	1.368	—	1.339	Weld Failure	Weld Failure
B 175 B12 55 1	441	0.81	1.69	—	1.431	1.153	Weld Failure	Weld Failure
B 175 B12 55 2	400	0.87	1.63	—	1.381	1.125	Weld Failure	Weld Failure
B 175 B12 55 3	385	0.83	1.71	—	1.351	1.074	Weld Failure	Weld Failure
B 175 B12 85 1	263	1.25	1.66	—	1.282	0.992	Weld Failure	Weld Failure
B 175 B12 85 2	266	1.29	1.65	—	1.320	1.024	Weld Failure	Weld Failure
B 175 B12 85 3	254	1.44	1.55	—	1.363	1.089	Weld Failure	Weld Failure
B 175 B516 3 1	734	0.31	2.41	1.496	—	1.236	Weld Failure	Weld Failure
B 175 B516 3 2	713	0.29	2.54	1.437	—	1.147	Weld Failure	Weld Failure
B 175 B516 3 3	690	0.29	2.52	1.402	—	1.126	Weld Failure	Weld Failure
B 175 B516 55 1	386	0.63	2.17	—	1.459	1.020	Weld Failure	Weld Failure
B 175 B516 55 2	310	0.60	2.27	-	1.213	0.823	Weld Failure	Weld Failure
B 175 B516 55 3	347	0.51	2.69	1.263	—	0.909	Weld Failure	Weld Failure
B 175 B516 85 1	204	0.89	2.34	—	1.186	0.763	Weld Failure	Weld Failure
B 175 B516 85 2	208	0.93	2.31	—	1.291	0.835	Weld Failure	Weld Failure
B 175 B516 85 3	205	0.92	2.31	—	1.265	0.817	Weld Failure	Weld Failure
B 250 B12 55 1	491	0.61	2.25	—	1.322	0.912	Weld Failure	Weld Failure
B 250 B12 55 2	498	0.64	2.18	—	1.363	0.953	Weld Failure	Weld Failure
B 250 B12 55 3	492	0.62	2.27	—	1.410	0.964	Weld Failure	Weld Failure
B 250 B516 55 1	346	0.37	3.66	0.914	—	0.637	Weld Failure	Weld Failure
B 250 B516 55 2	342	0.40	3.49	0.914	—	0.644	Weld Failure	Weld Failure
B 250 B516 55 3	339	0.41	3.41	0.930	—	0.657	Weld Failure	Weld Failure
Mean				1.141	1.254	—		
Coefficient of variation, V				0.236	0.119	—		

Appendix C

Simplified Strength Prediction Model

Appendix C

Simplified Strength Prediction Model

C.1 INTRODUCTION

The proposed simplified model (Model 9) is represented by three equations to cover the full range of load eccentricity and relative plate strength to weld strength in welded joints under combined shear and out-of-plane bending. The joint configuration under consideration consists of a single plate bracket welded using two fillet welds oriented parallel to the line of action of the applied force. Four different possible failure conditions are identified as followed:

Weld failure:

- Under large load eccentricity, the flexural capacity of the weld governs the capacity of the joint. The flexural resistance is developed through tension in part of the weld length and bearing between the welded plates in the compression zone of the welded joint. The shear resistance of the weld located in the compression zone of the joint is sufficient to resist the applied shear force.
- Under small load eccentricity, the capacity of the joint is governed by the shear capacity of the weld. A smaller portion of the joint is required to develop the required moment resistance.

Plate failure:

- Plate failure primarily in flexure when the load eccentricity is large.
- Plate failure primarily in shear when the load eccentricity is small.

The following sections present closed form calculation procedures to determine the capacity of welded joints with combined shear and out-of-plane bending. Both weld failure and plate failure are considered.

C.2 THICK PLATE BEHAVIOUR (WELD FAILURE)

When thick plate behaviour prevails the strength of the joint is governed either by flexure or shear resistance of the weld, depending on the magnitude of the load eccentricity. The load eccentricity is commonly expressed as the product of the eccentricity ratio (a) and the weld length. For a larger eccentricity ratio, the flexural capacity of the welded joint is critical and when the value of a is small, the shear force becomes dominant. The simplified model used to calculate the flexural capacity of a welded joint with combined shear and out-of-plane bending is illustrated in Figure C.1. On the tension side of the joint the tensile stresses are carried by the two fillet welds whereas the compressive stresses on the compression side of the joint are carried by bearing of the two plates.

Since the weld on the compression side of the joint does not contribute to the flexural resistance of the joint, it carries the shear force applied on the joint.

Based on the above discussion, the value of *a* that marks the change of joint behaviour from flexure critical to shear critical can be determined by equating the maximum moment capacity of the welded joint to the shear capacity of the weld in the compression zone of the joint.

The tensile stress in the tension zone is governed by the transverse fillet weld strength, which is taken 1.5 times the shear strength of the weld metal according to the work of Lesik and Kennedy (1990). The shear strength of the weld metal is taken as either 0.6 times the tensile strength of the weld metal (as per AISC (2005)) or 0.67 times the tensile strength of the weld metal (as per CSA-S16-01). The general stress distribution for small and large eccentricity is shown in Figure C.1 and C.2, respectively. Note that the two design standards (AISC (2005) and CSA-S16-01) have adopted the same design approach, but they are using different shear coefficients and the symbol designated for the minimum specified tensile strength of the filler metal (F_{EXX} used in AISC and X_u used in CSA-S16-01). In the following section, all equations designated with *a* suffix a refer to AISC, whereas, the equations with suffix *b* refer to CSA-S16-01.

As shown in Figure C.1, when flexural behaviour dominates, the load carrying capacity of the joint, P_m, can be determined from:

$$P_m = \frac{0.637 F_y t L}{a(Q + 1.273)} \qquad \text{[C.1a]}$$

$$P_m = \frac{0.711 F_y t L}{a(Q + 1.421)} \qquad \text{[C.1b]}$$

The depth of the compression zone, y_o, can be determined from equilibrium of the compression and tension forces as follows:

$$y_o = \frac{1.273 L}{Q + 1.273} \qquad \text{[C.2a]}$$

$$y_o = \frac{1.421 L}{Q + 1.421} \qquad \text{[C.2b]}$$

The shear capacity of the fillet welds in the flexural compression zone can be obtained from:

$$P_v = 2(0.60)(0.707) D\, F_{EXX}\, y_o \qquad \text{[C.3a]}$$

$$P_v = 2(0.67)(0.707) D\, X_u\, y_o \qquad \text{[C.3b]}$$

Substituting Equation C.2 into Equation C.3 and equating the resulting equation to Equation C.1, we obtain:

$$\frac{0.637\,F_y\,t\,L}{a\,(Q+1.273)} = 2(0.60)(0.707)\,D\,F_{EXX}\,\frac{1.273L}{Q+1.273} \qquad \text{[C.4a]}$$

$$\frac{0.711\,F_y\,t\,L}{a\,(Q+1.421)} = 2(0.67)(0.707)\,D\,X_u\,\frac{1.421L}{Q+1.421} \qquad \text{[C.4b]}$$

The critical value of *a* follows as:

$$a = 0.59\,Q \qquad \text{[C.5a]}$$

$$a = 0.53\,Q \qquad \text{[C.5b]}$$

Therefore, the flexural capacity of a welded joint under combined shear and out-of-plane bending is critical when $a/Q > 0.59$ and shear dominates when $a/Q < 0.59$ when the AISC specification applies. Similarly, failure of welded joints with a/Q > 0.53 is dominated by combined shear and out-of-plane bending and a/Q < 0.53 is dominated by shear when CSA-S16-01 applies.

C.2.1 Joint Capacity when *a/Q* > 0.59 (AISC) or *a/Q* > 0.53 (CSA)

When failure is governed by flexural behaviour, the stress distribution presented in Figure C.1 can be adopted for estimating the strength of a welded joint. Except for a few minor differences, the proposed model is similar to that proposed by Beaulieu and Picard (1985). Rectangular stress blocks are assumed in both tension and compression zones. The stress in the tension zone reaches the value predicted by Lesik and Kennedy (1990) for a weld loaded at $90°$ to its axis. The stress in the compression zone is equal to the yield strength of the connected plates. In contrast to the earlier model of Beaulieu and Picard, this model uses the throat area rather than the weld leg area to calculate the distributed force on the tension side of the joint. For the stress distribution proposed, the compression force (C) and the tension force (T) are equal to:

$$C = F_y\,t\,y_o \qquad \text{[C.6]}$$

$$T = 2(0.60)(1.5)(0.707)\,D\,F_{EXX}\,(L - y_o) \qquad \text{[C.7a]}$$

$$T = 2(0.67)(1.5)(0.707)\,D\,X_u\,(L - y_o) \qquad \text{[C.7b]}$$

All the terms in these equations are as defined previously.

Upon substitution of Equation C.2 for y_o in Equations C.6 and C.7 and applying equilibrium ($C = T$) we obtain:

$$P_m = \frac{0.637\, F_y\, t\, L}{a\,(Q + 1.273)} \qquad \text{[C.8a]}$$

$$P_m = \frac{0.711\, F_y\, t\, L}{a\,(Q + 1.421)} \qquad \text{[C.8b]}$$

C.2.2 Joint Capacity when *a*/*Q* < 0.59 (AISC) or *a*/*Q* < 0.53 (CSA)

An equilibrium model suitable for estimating the joint capacity when the load eccentricity is small (the moment can be resisted without mobilizing the full depth of the joint) is illustrated in Figure C.2. Once again, rectangular stress blocks are used to represent the stress distributions in the tension and compression zones. However, because the eccentricity is small, the rectangular stress blocks do not develop over the full joint depth. As for the model used for *a*/*Q* > 0.59 with AISC (2005) or a/Q > 0.53 with CSA-S16-01, it is assumed that the tensile resistance is provided by the weld and the compressive resistance is provided by bearing of the plates. The shear resistance is provided by the entire weld length with the exclusion of the tension zone and it is denoted as $y + y_o$ in Figure C.2. The depth of the joint required to resist the applied shear force can be determined from equilibrium consideration.

$$C = F_y\, t\, (L - l^* - y) \qquad \text{[C.9]}$$

$$T = 2(0.60)(1.5)(0.707)\, D\, F_{EXX}\, (L - y_o - y) \qquad \text{[C.10a]}$$

$$T = 2(0.67)(1.5)(0.707)\, D\, X_u\, (L - y_o - y) \qquad \text{[C.10b]}$$

where,

$$l^* = (L - y_o - y) \qquad \text{[C.11]}$$

By equilibrium and solve for y_o,

$$yo = \frac{1.273(L - y)}{Q + 1.273} \qquad \text{[C.12a]}$$

$$yo = \frac{1.421(L - y)}{Q + 1.421} \qquad \text{[C.12b]}$$

The moment resistance can be obtained either from the normal stress distribution shown in Figure C.2 or as the shear resistance of the weld over the length $y + y_o$ times the load eccentricity, *aL*. The resulting expressions for moment resistance are as follows:

$$M_1 = F_y\, t\, y_o \left(\frac{L + y}{2} \right) \qquad \text{[C.13]}$$

$$M_2 = 2(0.60)(0.707)DF_{EXX}(y + y_o)aL \quad \text{[C.14a]}$$

$$M_2 = 2(0.67)(0.707)DX_u(y + y_o)aL \quad \text{[C.14b]}$$

By equating Equations C.13 and C.14 and substituting the value of y_o we obtain:

$$F_y t\left[\frac{1.273(L-y)}{Q+1.273}\right]\left(\frac{L+y}{2}\right) = 2(0.60)(0.707)DF_{EXX}\left\{y + \left[\frac{1.273(L-y)}{Q+1.273}\right]\right\}aL \quad \text{[C.15a]}$$

$$F_y t\left[\frac{1.421(L-y)}{Q+1.421}\right]\left(\frac{L+y}{2}\right) = 2(0.67)(0.707)DX_u\left\{y + \left[\frac{1.421(L-y)}{Q+1.421}\right]\right\}aL \quad \text{[C.15b]}$$

From Equation C.15 one can obtain the following expression for y:

$$y = \frac{0.6667L(\sqrt{a^2Q - 3.819a + 2.25Q} - a\sqrt{Q})}{\sqrt{Q}} \quad \text{[C.16a]}$$

$$y = \frac{0.6667L(\sqrt{a^2Q - 4.263a + 2.25Q} - a\sqrt{Q})}{\sqrt{Q}} \quad \text{[C.16b]}$$

Therefore, the portion of the joint capable of providing shear resistance ($y + y_o$) is given as:

$$y + y_o = \frac{1.273L}{Q+1.273} - \left(\frac{0.6667L(\sqrt{a^2Q - 3.819a + 2.25Q} - a\sqrt{Q})}{\sqrt{Q}}\right)\left(\frac{1.273}{Q+1.273} - 1\right) \quad \text{[C.17a]}$$

$$y + y_o = \frac{1.421L}{Q+1.421} - \left(\frac{0.6667L(\sqrt{a^2Q - 4.263a + 2.25Q} - a\sqrt{Q})}{\sqrt{Q}}\right)\left(\frac{1.421}{Q+1.421} - 1\right) \quad \text{[C.17b]}$$

By rearranging Equation [C.14], the predicted weld capacity for *a/Q* < 0.59 in AISC or a/Q < 0.53 in CSA is:

$$\mathrm{P_r} = 2(0.60)(0.707)DF_{EXX}(y + y_o) \quad \text{[C.18a]}$$

$$\mathrm{P_r} = 2(0.67)(0.707)DX_u(y + y_o) \quad \text{[C.18b]}$$

Considering the complexity of Equation C.17, which is required to solve Equation C.18, a simpler approach is desirable. In order to provide a simpler expression for the weld strength in the range of *a/Q* between 0.0 and 0.59 (AISC, 2005) or 0.0 and 0.53 (CSA-

S16-01), Beaulieu and Picard suggested either a linear interpolation or a quadratic interpolation. A linear interpolation would result in:

$$P_r = P_{ro}\left(1-1.69\left(a/Q\right)\right)+1.69\left(a/Q\right)P_{r59} \quad \text{[C.19a]}$$

$$P_r = P_{ro}\left(1-1.89\left(a/Q\right)\right)+1.89\left(a/Q\right)P_{r53} \quad \text{[C.19b]}$$

where P_{ro} is the shear strength for a joint with no eccentricity given as:

$$P_{ro} = 2(0.60)(0.707)DF_{EXX}L \quad \text{[C.20a]}$$

$$P_{ro} = 2(0.67)(0.707)DX_uL \quad \text{[C.20b]}$$

and P_{r59} or P_{r53} is obtained from Equation C.8 for *a/Q* = 0.59 or *a/Q* = 0.53 . Figures C.3 and C.4 show a comparison between the simplified Equation C.18 and Equation C.19 for values of *Q* varying from 0.615 to 4.0. The linear expression is a good representation of the more complex expression for small values of *Q*, but tends to over-estimate the capacities predicted by Equation C.18 for high values of *Q*. Since Equation C.18 tends to be conservative, the higher capacity predicted by the simpler linear equation is not expected to create a problem.

C.3 THIN PLATE BEHAVIOUR (PLATE FAILURE)

The model proposed to predict the capacity of the plate under combined bending and shear is based on a lower bound model presented by Chen and Han (1988). It assumes an elastic-plastic stress distribution as shown in Figure C.5 where the extreme fibres reached their yield strength while the middle portion reaches normal stresses below the yield level. The shear capacity is provided by the elastic portion of the cross-section. This simple lower bound model results in the following interaction equation:

$$\frac{M}{M_p} = 1-\frac{3}{4}\left(\frac{P}{V_p}\right)^2 \quad \text{[C.21]}$$

where,

$$M = PaL \quad \text{[C.22]}$$

$$M_p = \frac{1}{4}tL^2F_u \quad \text{[C.23]}$$

$$V_p = \frac{1}{2}tLF_u \quad \text{[C.24]}$$

Solving Equation C.21 for P, and substituting Equations C.23 and C.24 yields the following expression for P_r:

$$P_r = \frac{2V_p(\sqrt{a^2L^2V_P{}^2 + 3M_p{}^2} - aLV_p)}{3M_p} \qquad \text{[C.25]}$$

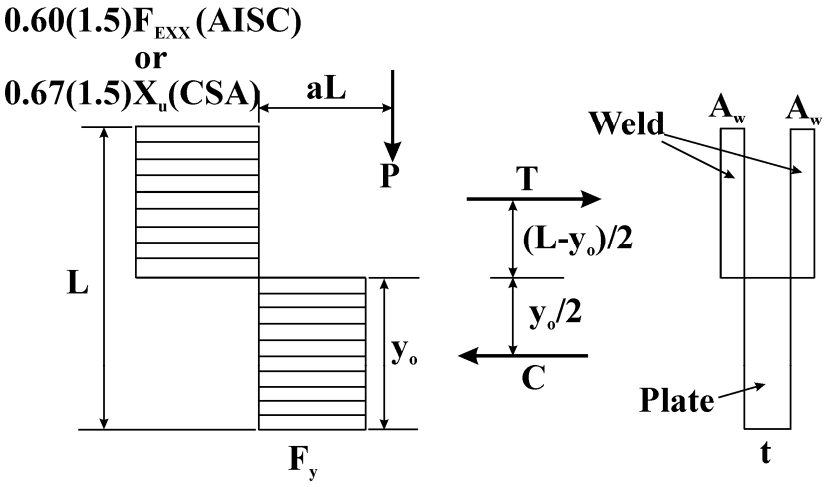

Figure C.1 – Proposed Flexure Model for Large Eccentricity

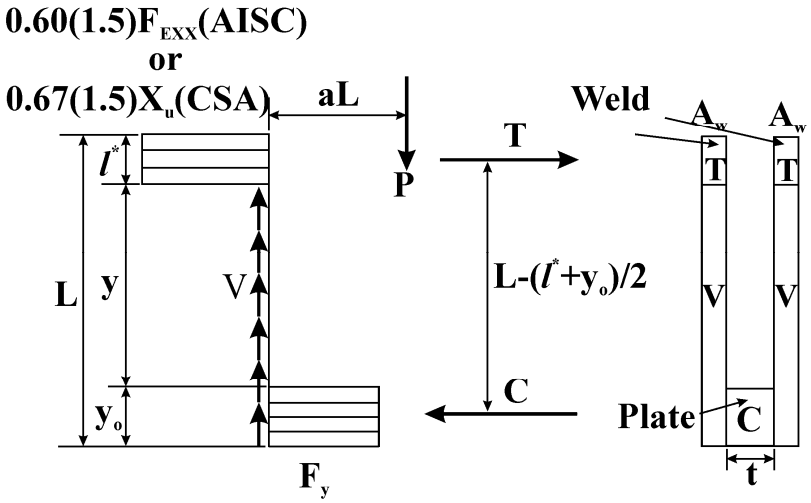

Figure C.2 – Flexure Model for Small Load Eccentricity

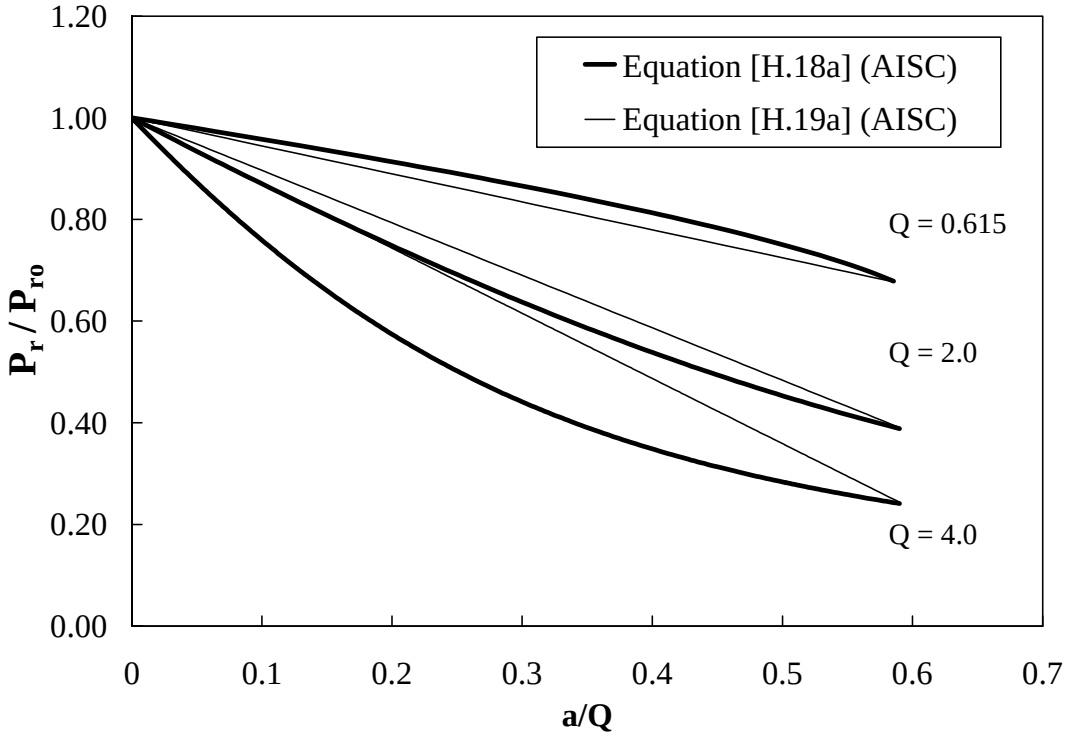

Figure C.3 – Comparison between Equations [C.18a] and [C.19a]

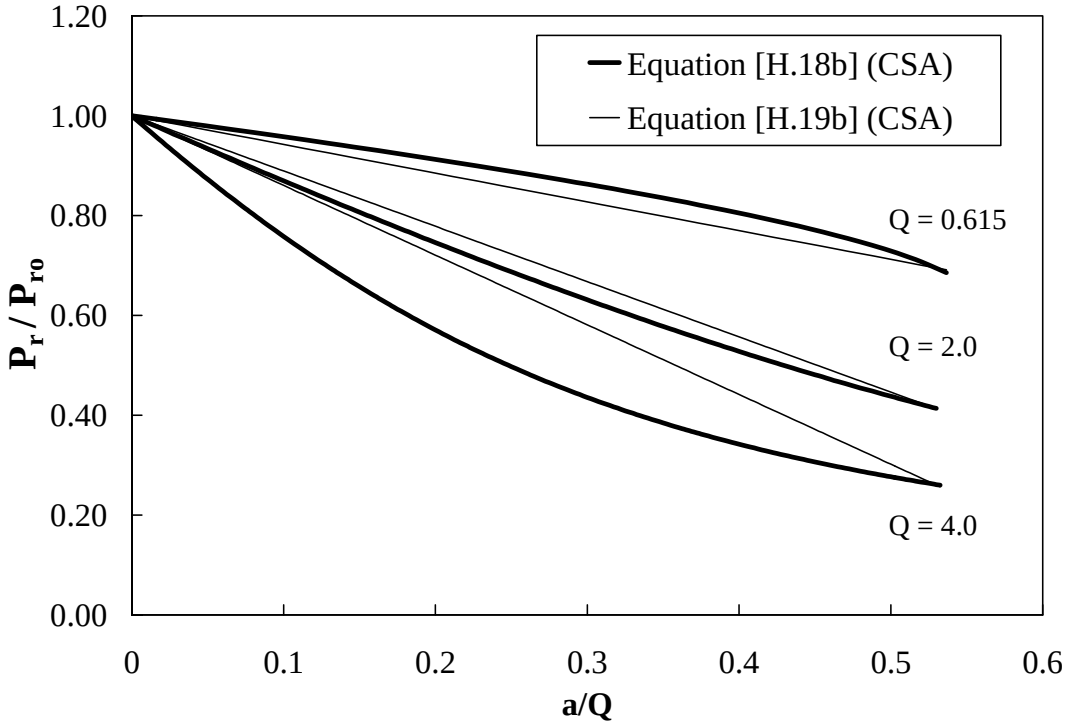

Figure C.4 – Comparison between Equations [C.18b] and [C.19b]

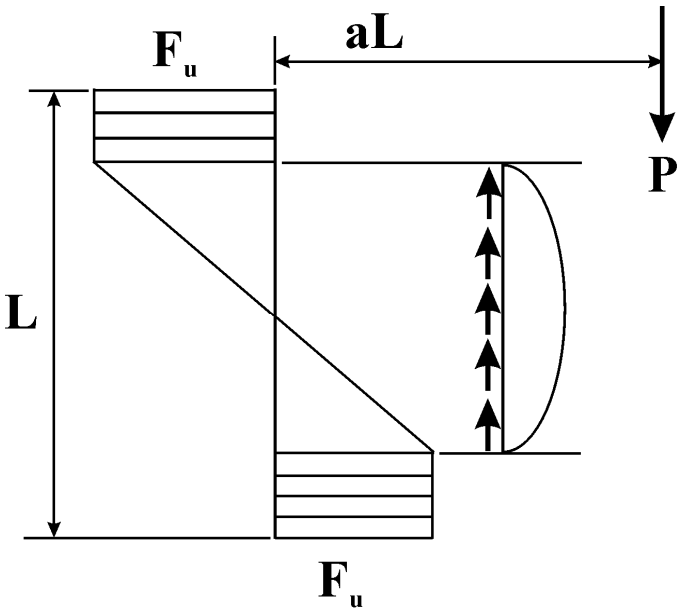

Figure C.5 – Combined Flexure and Shear Model

Appendix D

Proposed Design Tables

Appendix D

Proposed Design Tables

The welded joint strength coefficient C' given in Tables D.1 to D.6 is based on an electrode tensile strength X_u = 490 MPa, a base metal yield strength F_y = 300 MPa, a base metal tensile strength F_u = 450 MPa, and a resistance factor $\phi = 0.67$. The factored resistance P_r of an eccentrically loaded weld group is obtained from the following equation.

$$P_r = C'L \qquad [D.1]$$

where the strength coefficient C' is obtained from Tables D.1 to D.6 for a given weld size and eccentricity ratio a. The weld length L and load eccentricity are described in Figure D.1. Values of C' were calculated for a wide range of plate thickness, weld sizes, and eccentricity ratios. The required weld length is obtained by dividing the factored load, P_f, by the appropriate strength coefficient.

$$L = \frac{P_f}{C'} \qquad [D.2]$$

The shaded cells in Table D.1 represent the cases where thin plate behaviour governs the capacity of the welded joint (plate failure). All other values of C' represent thick plate connections (weld failure). Details of the models used for deriving the values presented in the design tables were presented in Appendix C.

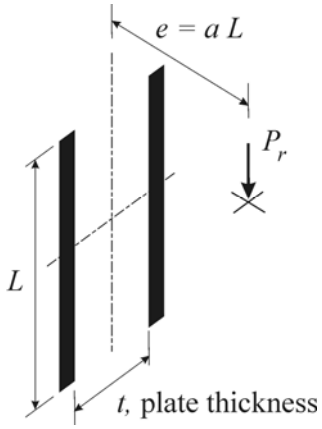

Figure D.1 Eccentrically loaded welded joint

Plots of predicted factored resistance versus eccentricity ratio are presented in Figures D.2 to D.4 for four different prediction models, namely, the modified version of the Dawe and Kulak approach presented in Chapter 5 as one providing an adequate level of safety, the model currently implemented in the CISC design tables, the instantaneous

centre of rotation approach implemented in the AISC Design manual, and the simplified approach proposed in this work (used with the design tables provided in this appendix). It is noted that, of all four models, only the proposed simplified approach accounts for thin plate behaviour.

Figure D.2 presents a comparison between the four approaches for a plate thickness of 8 mm and a weld size of 5 mm. The figure shows that the CISC approach provides the most conservative strength prediction of all four models for eccentricity ratios greater than about 0.3. As indicated earlier, this level of conservatism is the result of the addition of a reduction factor of 0.5 incorporated by Picard and Beaulieu (1991) to make their approach match the earlier CISC design tables. The other three models are in very close agreement for eccentricity ratios higher than 0.7. At smaller eccentricities, failure is found to be governed by plate failure rather than weld failure for this plate thickness. The new proposed model becomes more conservative since this is the only model that considers plate failure. Since the plate thickness used in Figure D.2 is relatively small, the contribution from the load transfer by bearing in the compression zone is expected to be minimal. This is the reason why the AISC approach is in good agreement with the modified Dawe and Kulak approach for this plate thickness.

The comparisons presented in Figure D.3 were made with a plate thickness of 40 mm and a weld size of 12 mm. For this plate thickness, the joint capacity is governed by weld failure for all eccentricity ratios. The AISC and CISC predictions are conservative compared to the modified Dawe and Kulak approach and the proposed model. This is expected since the CISC model contains the reduction factor of 0.5 and the AISC model ignores the increased contribution in the compression zone, which is significant for a 40 mm plate. The simplified design approach proposed in this work yields very similar results to the modified Dawe and Kulak approach for eccentricity ratios greater than about 0.7. At eccentricity ratios less than 0.7, the approach is more conservative than the modified Dawe and Kulak approach.

Figure D.4 presents similar comparisons for a joint with a 60 mm plate and 12 mm fillet welds. Examination of figures D.2 to D.4 indicates that the difference between the AISC approach and the CISC approach becomes smaller as the plate thickness increases. For a plate thickness of 60 mm the CISC and AISC design approaches are very close, but they are significantly more conservative than the proposed new model for eccentricity ratios greater than about 0.5.

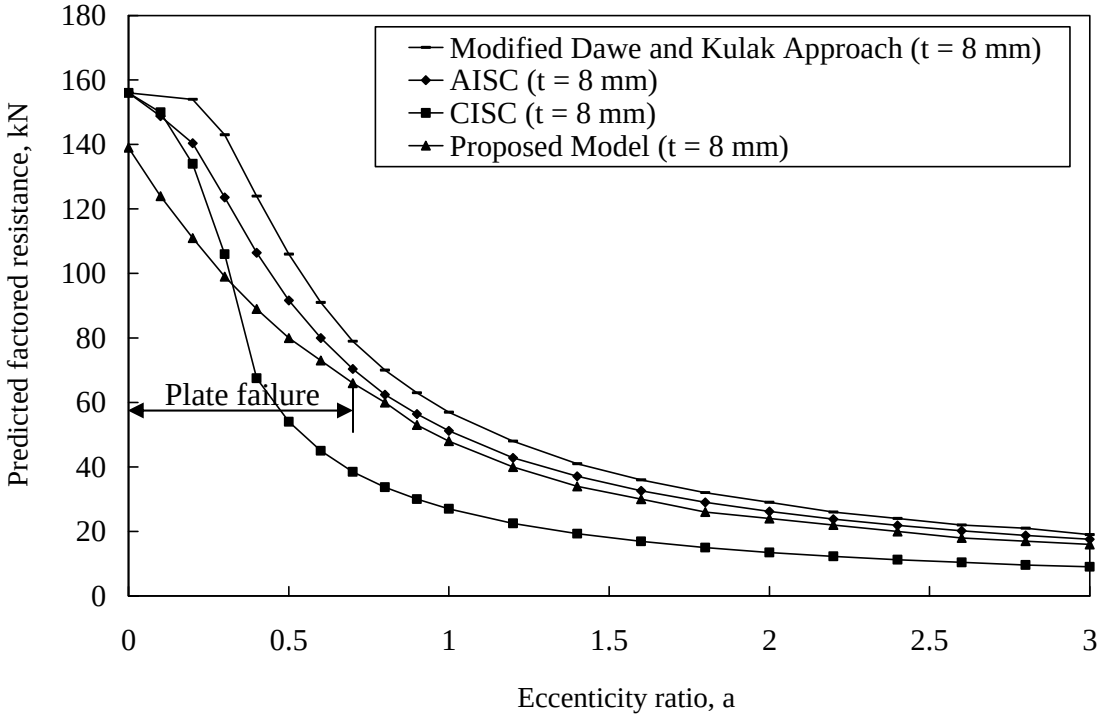

Figure D.2 Predicted capacity versus eccentricity ratio for t = 8 mm and D = 5 mm

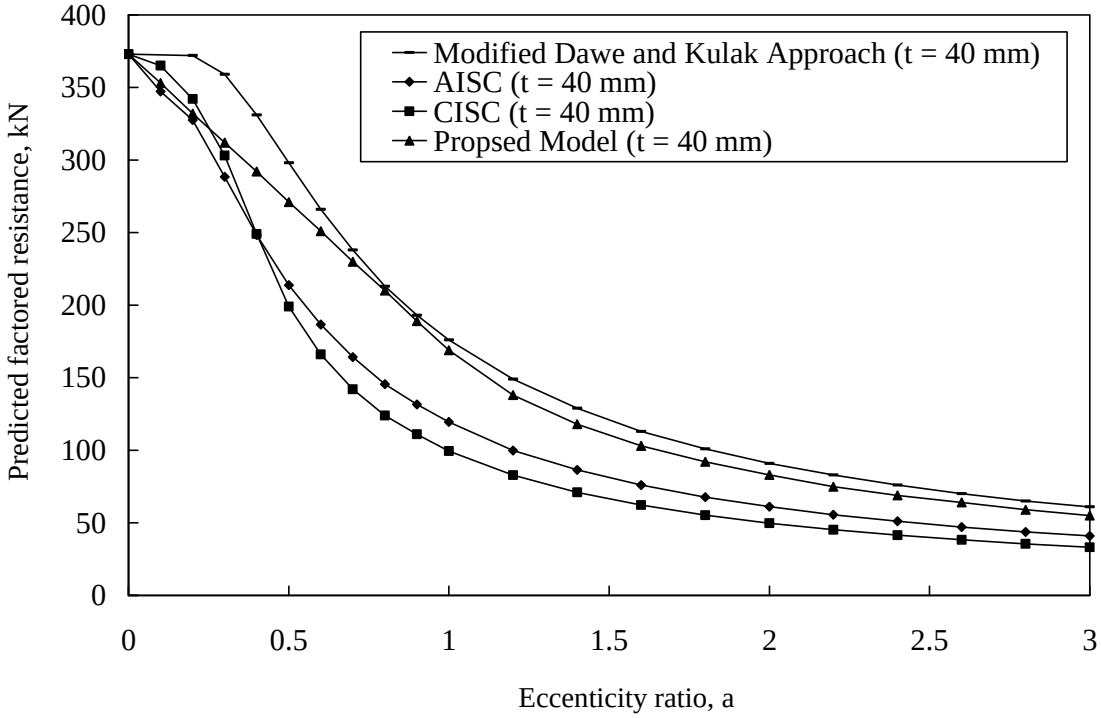

Figure D.3 Predicted capacity versus eccentricity ratio for t = 40 mm and D = 12 mm

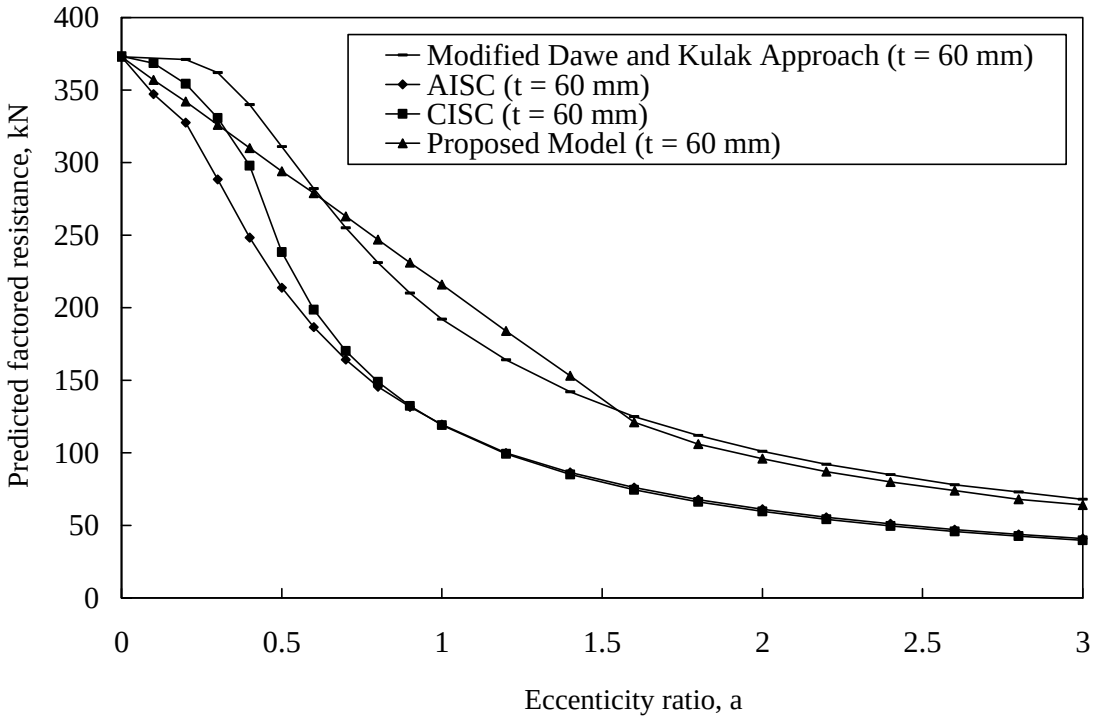

Figure D.4 Predicted capacity versus eccentricity ratio for t = 60 mm and D = 12 mm

Table D.1- Coefficients C' for plate thickness 8 to 12 mm

Plate Thickness, t		8 mm		10 mm			12 mm			
Weld Size, D (mm)		5	6	5	6	8	5	6	8	10
a	0.0	1.39	1.39	1.56	1.74	1.74	1.56	1.87	2.09	2.09
	0.1	1.24	1.24	1.43	1.55	1.55	1.45	1.73	1.86	1.86
	0.2	1.11	1.11	1.31	1.38	1.38	1.35	1.60	1.66	1.66
	0.3	0.99	0.99	1.18	1.24	1.24	1.25	1.46	1.49	1.49
	0.4	0.89	0.89	1.06	1.11	1.11	1.15	1.33	1.34	1.34
	0.5	0.80	0.80	0.93	1.01	1.01	1.04	1.20	1.21	1.21
	0.6	0.73	0.73	0.81	0.91	0.91	0.94	1.06	1.09	1.09
	0.7	0.66	0.66	0.77	0.83	0.83	0.84	0.93	1.00	1.00
	0.8	0.60	0.61	0.68	0.73	0.76	0.74	0.81	0.91	0.91
	0.9	0.53	0.56	0.60	0.65	0.70	0.66	0.72	0.81	0.84
	1.0	0.48	0.51	0.54	0.59	0.65	0.59	0.65	0.73	0.78
	1.2	0.40	0.43	0.45	0.49	0.54	0.49	0.54	0.61	0.66
	1.4	0.34	0.37	0.39	0.42	0.47	0.42	0.46	0.52	0.57
	1.6	0.30	0.32	0.34	0.37	0.41	0.37	0.41	0.46	0.50
	1.8	0.26	0.28	0.30	0.33	0.36	0.33	0.36	0.41	0.44
	2.0	0.24	0.26	0.27	0.29	0.33	0.30	0.32	0.37	0.40
	2.2	0.22	0.23	0.25	0.27	0.30	0.27	0.29	0.33	0.36
	2.4	0.20	0.21	0.23	0.24	0.27	0.25	0.27	0.31	0.33
	2.6	0.18	0.20	0.21	0.23	0.25	0.23	0.25	0.28	0.31
	2.8	0.17	0.18	0.19	0.21	0.23	0.21	0.23	0.26	0.28
	3.0	0.16	0.17	0.18	0.20	0.22	0.20	0.22	0.24	0.27

Table D.2- Coefficients C' for plate thickness 16 mm

Plate Thickness, t		16 mm					
Weld Size, D (mm)		6	8	10	12	14	16
	0.0	1.87	2.49	2.79	2.79	2.79	2.79
	0.1	1.75	2.31	2.48	2.48	2.48	2.48
	0.2	1.63	2.13	2.22	2.22	2.22	2.22
	0.3	1.52	1.95	1.98	1.98	1.98	1.98
	0.4	1.40	1.77	1.78	1.78	1.78	1.78
	0.5	1.29	1.60	1.61	1.61	1.61	1.61
	0.6	1.17	1.42	1.46	1.46	1.46	1.46
	0.7	1.06	1.23	1.33	1.33	1.33	1.33
	0.8	0.94	1.08	1.19	1.22	1.22	1.22
	0.9	0.83	0.96	1.06	1.12	1.12	1.12
a	1.0	0.75	0.86	0.95	1.02	1.04	1.04
	1.2	0.62	0.72	0.79	0.85	0.90	0.90
	1.4	0.53	0.62	0.68	0.73	0.77	0.79
	1.6	0.47	0.54	0.60	0.64	0.67	0.70
	1.8	0.42	0.48	0.53	0.57	0.60	0.62
	2.0	0.37	0.43	0.48	0.51	0.54	0.56
	2.2	0.34	0.39	0.43	0.46	0.49	0.51
	2.4	0.31	0.36	0.40	0.43	0.45	0.47
	2.6	0.29	0.33	0.37	0.39	0.41	0.43
	2.8	0.27	0.31	0.34	0.37	0.39	0.40
	3.0	0.25	0.29	0.32	0.34	0.36	0.37

Table D.3- Coefficients C' for plate thickness 20 mm

Plate Thickness, t		20 mm							
Weld Size, D (mm)		6	8	10	12	14	16	18	20
	0.0	1.87	2.49	3.11	3.48	3.48	3.48	3.48	3.48
	0.1	1.76	2.33	2.89	3.10	3.10	3.10	3.10	3.10
	0.2	1.66	2.17	2.66	2.77	2.77	2.77	2.77	2.77
	0.3	1.56	2.01	2.44	2.48	2.48	2.48	2.48	2.48
	0.4	1.46	1.85	2.22	2.23	2.23	2.23	2.23	2.23
	0.5	1.36	1.69	1.99	2.01	2.01	2.01	2.01	2.01
	0.6	1.25	1.53	1.77	1.82	1.82	1.82	1.82	1.82
	0.7	1.15	1.37	1.54	1.66	1.66	1.66	1.66	1.66
	0.8	1.05	1.21	1.35	1.46	1.52	1.52	1.52	1.52
	0.9	0.95	1.08	1.20	1.30	1.38	1.40	1.40	1.40
a	1.0	0.84	0.97	1.08	1.17	1.25	1.30	1.30	1.30
	1.2	0.69	0.81	0.90	0.98	1.04	1.09	1.13	1.13
	1.4	0.59	0.69	0.77	0.84	0.89	0.93	0.97	0.99
	1.6	0.52	0.61	0.68	0.73	0.78	0.82	0.85	0.88
	1.8	0.46	0.54	0.60	0.65	0.69	0.73	0.76	0.78
	2.0	0.41	0.48	0.54	0.59	0.62	0.65	0.68	0.70
	2.2	0.38	0.44	0.49	0.53	0.57	0.59	0.62	0.64
	2.4	0.34	0.40	0.45	0.49	0.52	0.54	0.57	0.59
	2.6	0.32	0.37	0.42	0.45	0.48	0.50	0.52	0.54
	2.8	0.29	0.35	0.39	0.42	0.44	0.47	0.49	0.50
	3.0	0.28	0.32	0.36	0.39	0.42	0.44	0.45	0.47

Table D.4- Coefficients C' for plate thickness 25 mm

Plate Thickness, t		25 mm						
Weld Size, D (mm)		8	10	12	14	16	18	20
	0.0	2.49	3.11	3.73	4.35	4.35	4.35	4.35
	0.1	2.35	2.91	3.47	3.88	3.88	3.88	3.88
	0.2	2.21	2.71	3.21	3.46	3.46	3.46	3.46
	0.3	2.06	2.51	2.94	3.10	3.10	3.10	3.10
	0.4	1.92	2.31	2.68	2.78	2.78	2.78	2.78
	0.5	1.78	2.11	2.42	2.51	2.51	2.51	2.51
	0.6	1.64	1.91	2.16	2.28	2.28	2.28	2.28
	0.7	1.50	1.71	1.89	2.03	2.08	2.08	2.08
	0.8	1.36	1.51	1.66	1.78	1.88	1.90	1.90
	0.9	1.22	1.34	1.47	1.58	1.67	1.75	1.75
a	1.0	1.07	1.21	1.32	1.42	1.50	1.57	1.62
	1.2	0.89	1.01	1.10	1.18	1.25	1.31	1.36
	1.4	0.77	0.86	0.95	1.01	1.07	1.12	1.17
	1.6	0.67	0.76	0.83	0.89	0.94	0.98	1.02
	1.8	0.60	0.67	0.74	0.79	0.83	0.87	0.91
	2.0	0.54	0.61	0.66	0.71	0.75	0.79	0.82
	2.2	0.49	0.55	0.60	0.65	0.68	0.71	0.74
	2.4	0.45	0.50	0.55	0.59	0.63	0.66	0.68
	2.6	0.41	0.47	0.51	0.55	0.58	0.60	0.63
	2.8	0.38	0.43	0.47	0.51	0.54	0.56	0.58
	3.0	0.36	0.40	0.44	0.47	0.50	0.52	0.54

Table D.5- Coefficients C' for plate thickness 40 mm

Plate Thickness, t		40 mm								
Weld Size, D (mm)		8	10	12	14	16	18	22	26	30
	0.0	2.49	3.11	3.73	4.35	4.98	5.60	6.84	6.96	6.96
	0.1	2.38	2.96	3.53	4.09	4.66	5.22	6.21	6.21	6.21
	0.2	2.28	2.81	3.32	3.83	4.34	4.83	5.54	5.54	5.54
	0.3	2.17	2.65	3.12	3.57	4.02	4.45	4.96	4.96	4.96
	0.4	2.07	2.50	2.92	3.31	3.70	4.07	4.45	4.45	4.45
	0.5	1.96	2.35	2.71	3.05	3.38	3.69	4.02	4.02	4.02
	0.6	1.86	2.20	2.51	2.79	3.06	3.31	3.65	3.65	3.65
	0.7	1.75	2.04	2.30	2.53	2.74	2.93	3.22	3.32	3.32
	0.8	1.65	1.89	2.10	2.27	2.42	2.57	2.82	3.02	3.05
	0.9	1.54	1.74	1.89	2.01	2.15	2.28	2.51	2.69	2.81
a	1.0	1.44	1.59	1.69	1.80	1.94	2.06	2.26	2.42	2.56
	1.2	1.23	1.28	1.38	1.50	1.61	1.71	1.88	2.02	2.13
	1.4	1.02	1.06	1.18	1.29	1.38	1.47	1.61	1.73	1.83
	1.6	0.81	0.92	1.03	1.13	1.21	1.28	1.41	1.51	1.60
	1.8	0.71	0.82	0.92	1.00	1.08	1.14	1.25	1.34	1.42
	2.0	0.64	0.74	0.83	0.90	0.97	1.03	1.13	1.21	1.28
	2.2	0.58	0.67	0.75	0.82	0.88	0.93	1.03	1.10	1.16
	2.4	0.53	0.62	0.69	0.75	0.81	0.86	0.94	1.01	1.06
	2.6	0.49	0.57	0.64	0.69	0.74	0.79	0.87	0.93	0.98
	2.8	0.46	0.53	0.59	0.64	0.69	0.73	0.81	0.86	0.91
	3.0	0.43	0.49	0.55	0.60	0.65	0.69	0.75	0.81	0.85

Table D.6 – Coefficients C' for plate thickness 50 mm

Plate Thickness, t		50 mm								
Weld Size, D (mm)		10	12	16	20	24	28	32	36	40
	0.0	3.11	3.73	4.98	6.22	7.46	8.70	8.70	8.70	8.70
	0.1	2.98	3.55	4.69	5.82	6.94	7.76	7.76	7.76	7.76
	0.2	2.85	3.38	4.41	5.42	6.41	6.92	6.92	6.92	6.92
	0.3	2.72	3.20	4.13	5.02	5.89	6.20	6.20	6.20	6.20
	0.4	2.58	3.02	3.85	4.62	5.36	5.57	5.57	5.57	5.57
	0.5	2.45	2.84	3.56	4.22	4.84	5.03	5.03	5.03	5.03
	0.6	2.32	2.66	3.28	3.82	4.31	4.56	4.56	4.56	4.56
	0.7	2.19	2.49	3.00	3.42	3.79	4.06	4.16	4.16	4.16
	0.8	2.06	2.31	2.71	3.02	3.31	3.55	3.76	3.81	3.81
	0.9	1.93	2.13	2.43	2.69	2.94	3.16	3.34	3.50	3.51
a	1.0	1.80	1.95	2.15	2.42	2.65	2.84	3.01	3.15	3.24
	1.2	1.53	1.60	1.79	2.02	2.21	2.37	2.50	2.62	2.72
	1.4	1.27	1.28	1.53	1.73	1.89	2.03	2.15	2.25	2.33
	1.6	1.01	1.12	1.34	1.51	1.66	1.78	1.88	1.97	2.04
	1.8	0.89	1.00	1.19	1.34	1.47	1.58	1.67	1.75	1.82
	2.0	0.80	0.90	1.07	1.21	1.32	1.42	1.50	1.57	1.63
	2.2	0.72	0.82	0.97	1.10	1.20	1.29	1.37	1.43	1.49
	2.4	0.66	0.75	0.89	1.01	1.10	1.18	1.25	1.31	1.36
	2.6	0.61	0.69	0.82	0.93	1.02	1.09	1.16	1.21	1.26
	2.8	0.57	0.64	0.77	0.86	0.95	1.01	1.07	1.12	1.17
	3.0	0.53	0.60	0.71	0.81	0.88	0.95	1.00	1.05	1.09

Table D.7 – Coefficients C' for plate thickness 60 mm

Plate Thickness, t		60 mm								
Weld Size, D (mm)		12	16	20	24	28	32	36	40	44
	0.0	3.73	4.98	6.22	7.46	8.71	9.95	10.44	10.44	10.44
	0.1	3.57	4.72	5.86	6.99	8.10	9.22	9.31	9.31	9.31
	0.2	3.42	4.47	5.50	6.51	7.50	8.31	8.31	8.31	8.31
	0.3	3.26	4.22	5.13	6.03	6.90	7.44	7.44	7.44	7.44
	0.4	3.10	3.96	4.77	5.55	6.29	6.68	6.68	6.68	6.68
	0.5	2.94	3.71	4.41	5.07	5.69	6.03	6.03	6.03	6.03
	0.6	2.79	3.45	4.05	4.59	5.08	5.47	5.47	5.47	5.47
	0.7	2.63	3.20	3.69	4.11	4.48	4.77	4.99	4.99	4.99
	0.8	2.47	2.95	3.33	3.63	3.92	4.17	4.39	4.57	4.57
	0.9	2.31	2.69	2.96	3.23	3.49	3.71	3.90	4.07	4.21
a	1.0	2.16	2.44	2.63	2.91	3.14	3.34	3.51	3.67	3.80
	1.2	1.84	1.93	2.19	2.42	2.61	2.78	2.93	3.05	3.17
	1.4	1.53	1.65	1.88	2.08	2.24	2.38	2.51	2.62	2.72
	1.6	1.21	1.44	1.65	1.82	1.96	2.09	2.20	2.29	2.38
	1.8	1.06	1.28	1.46	1.61	1.74	1.85	1.95	2.04	2.11
	2.0	0.96	1.15	1.32	1.45	1.57	1.67	1.76	1.83	1.90
	2.2	0.87	1.05	1.20	1.32	1.43	1.52	1.60	1.67	1.73
	2.4	0.80	0.96	1.10	1.21	1.31	1.39	1.46	1.53	1.58
	2.6	0.74	0.89	1.01	1.12	1.21	1.28	1.35	1.41	1.46
	2.8	0.68	0.82	0.94	1.04	1.12	1.19	1.25	1.31	1.36
	3.0	0.64	0.77	0.88	0.97	1.05	1.11	1.17	1.22	1.27